THESIS ON NATURAL AND EXACT SCIENCES B167

Pyroclastic Sanidine in the Lower Palaeozoic Bentonites – A Tool for Regional Geological Correlations

TOIVO KALLASTE

TUT PRESS

TALLINN UNIVERSITY OF TECHNOLOGY
Institute of Geology

This dissertation was accepted for the defence of the degree of Doctor of Philosophy in Natural Sciences on February 17, 2014.

Supervisor: Prof. Alvar Soesoo, Institute of Geology at Tallinn University of Technology

Co-supervisor: Dr. Tarmo Kiipli, Institute of Geology at Tallinn University of Technology

Opponents:
Prof. Kalle Kirsimäe, Institute of Ecology and Earth Sciences, Tartu University, Estonia

Dr. Ivar Murdmaa, Institute of Oceanology, Russia

Associate Prof. Piret Plink-Björklund, Department of Geology and Geological Engineering, Colorado School of Mines, USA

Defence of the thesis: March 28, 2014 at Tallinn University of Technology, Ehitajate tee 5, Tallinn, 19086, Estonia

Declaration: *Hereby I declare that this doctoral thesis, my original investigation and achievement, submitted for the doctoral degree at Tallinn University of Technology has not been submitted for doctoral or equivalent academic degree.*

Toivo Kallaste

ISSN 1406-4723
ISBN 978-9949-23-597-1 (publication)
ISBN 978-9949-23-598-8 (PDF)

LOODUS- JA TÄPPISTEADUSED B167

Püroklastiline sanidiin Alam-Paleosoikumi bentoniitides – regionaalstratigraafia uus töövahend

TOIVO KALLASTE

TTÜ KIRJASTUS

CONTENTS

LIST OF ORIGINAL PUBLICATIONS

This thesis is based on the following papers, referred to in the text with Roman numerals as listed below.

I KIIPLI, T., **KALLASTE, T**. 2002. Correlation of Telychian sections from shallow to deep sea facies in Estonia and Latvia based on the sanidine composition of bentonites. *Proceedings of the Estonian Academy of Sciences. Geology*, **51(3)**, 143–156.

II KIIPLI, T., **KALLASTE, T**. 2005. Characteristics of Ordovician volcanic ash beds. Põldvere, A. (Editor). Mehikoorma (421) drill core (27–30). Tallinn: Geological Survey of Estonia

III **KALLASTE, T**., KIIPLI, T. 2006. New correlations of Telychian (Silurian) bentonites in Estonia. *Proceedings of the Estonian Academy of Sciences. Geology*, **55(3)**, 241–251.

IV KIIPLI, T., SOESOO, A., **KALLASTE, T**., KIIPLI, E. 2008. Geochemistry of Telychian (Silurian) K-bentonites in Estonia and Latvia. *Journal of Volcanology and Geothermal Research*, **171(1-2)**, 45–58.

V KIIPLI, T., **KALLASTE, T**., NESTOR, V. 2010. Composition and correlation of volcanic ash beds of Silurian age from the eastern Baltic. *Geological Magazine*, **147(6)**, 895–909.

VI KIIPLI, T., **KALLASTE**, **T**., NESTOR, V., LOYDELL, D. K. 2010. Integrated Telychian (Silurian) K-bentonite chemostratigraphy and biostratigraphy in Estonia and Latvia. *Lethaia*, **43(1)**, 32–44.

VII KIIPLI, T., **KALLASTE**, **T**., NESTOR, V. 2012. Correlation of upper Llandovery–lower Wenlock bentonites in the När (Gotland, Sweden) and Ventspils (Latvia) drill cores: role of volcanic ash clouds and shelf sea currents in determining areal distribution of bentonite. *Estonian Journal of Earth Sciences*, **61(4)**, 295 - 306.

The co-authorship of the papers reflects that they are part of a collaborative research project. The author was responsible for all XRD and XRF analytical work and was participating in all interpretations. Geological aspects were more the topic of other members of the team.

INTRODUCTION

Altered volcanic ash interbeds (bentonites) in Lower Palaeozoic sedimentary rocks of the Baltoscandian Region are well known since the pioneer publications by Thorslund (1945) and Jaanusson (1947). Estonian bentonites were studied by Jürgenson (1958, 1964) and Vingisaar (1972), Vingisaar & Murnikova (1973). In Scandinavia the volcanic ash beds were studied by Bergström et al. (1992, 1995, 1999), Batchelor et al. (1995), Batchelor & Jeppsson (1994, 1999), Hetherington et al. (2011) and Snäll (1977).

The term "bentonite" is used in a general meaning of altered volcanic ash throughout this study, although alteration products of volcanic ashes are very variable by composition, depending on sedimentary facies and diagenetic history. Most bentonites consist dominantly of clay minerals.

The volcanic and terrigenous materials are often mixed. The term "bentonite" cannot be used for the interbeds where terrigenous material dominates, but still frequently the pyroclastic material can be extracted, analysed and correlated from this type of interbeds.

Bentonites in sedimentary sections carry information of tectonomagmatic processes in volcanic source areas (Batchelor & Evans 2000; Huff et al. 1993; Kiipli et al. 2013b), directions to volcanic sources (Bergström et al. 1995; Kiipli et al. 2013a), diagenetic environments of sedimentary rocks (Hints et al. 2006, 2008; Williams et al. 2013) and isotopic ages of rocks (Cramer et al. 2012; Bergström et al. 2008; Sell et al. 2013).

Recognizing of distinct chemical signatures of eruption layers can lead to the exceptionally precise correlation of sections (Emerson et al. 2004; Inanli et al. 2009; Kiipli et al. 2011, 2014; Ray et al. 2011; Paper V, VI, VII) which is important for proper reconstruction of the geological history of the Earth. While traditionally biostratigraphy based on the evolution of the living organisms has been used for this, in recent decades chemostratigraphy based on volcanic ash interbeds in sedimentary rocks finds extending application. Due to the affinity of life forms to specific environments it is often difficult to correlate sedimentary rocks formed in deep sea with rocks formed in shallow sea or even in continental lacustrine environment. As volcanic ashes fall and deposit equally in all environments they offer useful help to other correlation methods.

Several methods have been used for proving the correlations of Palaeozoic bentonites, e.g. immobile trace elements (Pearce 1995, Huff et al. 1998, Kiipli et al. 2001), composition of apatite phenocrysts (Batchelor & Clarkson 1993, Batchelor & Jeppsson 1994, Batchelor et al. 1995), and composition of biotite (Batchelor 2003 and Paper IV).

Main difficulties raised during these studies are: (1) Palaeozoic volcanic ashes are recrystallized and only a few elements stayed immobile; (2) Mobility-immobility of elements must be proved in every particular study case; (3) Apatite phenocrysts are present in only about 50% of volcanic ash layers; (3) Biotite phenocrysts are often sensitive to alteration agents; (4) Separation of tiny phenocrysts for analyzing is time-

consuming process; (5) Number of volcanic ash layers is often large and for reliable correlation all of them should be analysed.

A new method for proving correlations by the composition of pyroclastic sanidine – $(K,Na)AlSi_3O_8$ – has been introduced (Paper I) and applied (Papers I – VII and Kiipli et al. 2002, 2003, 2004, 2005, 2006, 2007, 2008a, 2008b, 2010, 2011, 2013a, 2014) by the author of present thesis during recent 15 years. Applying sanidine composition for proving the correlations overcomes largely the above shortcomings of other methods in the region of our study (East Baltic and Gotland). Sanidine is well preserved and present in 90% of bentonites in this region, X-ray diffraction (XRD) analysis does not require time-consuming complete extraction and purification of phenocrysts and XRD method enables good precision of analysis not accessible by other methods for the same cost.

Over 800 samples have been studied by XRD and X-ray fluorescence (XRF) methods. During the first stage (1998–2006) we studied pyroclastic material from the bentonites of drill cores from Estonia and Latvia (Aizpute core). The studies revealed that pyroclastic sanidine composition analysed by XRD can be used as a correlation criterion. During the second stage (2007–2013) the method was applied in wider area. Well-preserved sanidine was identified in sections from Gotland, Lithuania and in additional sections from Latvia, and used for correlations. Bentonite stratigraphy now serves as a useful support to biostratigraphy and sedimentary geochemistry.

Applying bentonites for the correlation of Palaeozoic sections through different palaeoenvironments is the aim of the present study.

Below, the bentonites from the region covering Estonia, Latvia, Lithuania and Gotland are described. The bentonites were mostly identified by their location (drill core name and number) and depth in metres. For the Telychian – lower Sheinwoodian of Estonia, Latvia and Gotland ID numbers are used (Paper III), which have been derived from depths in the Viki core: e.g. ID number 731 was assigned to bentonite at the depth 173.1 m. The bentonites in other cores are graphically projected to the Viki depth scale and the ID number is derived from the latter depth.

Fig. 1. Map of the studied region.

1. METHODS

XRD was used as the main analytical method. XRD measurements were performed by HZG4 diffractometer (Freiberger Präzisionmechanik, 1985) using Fe-filtered Co radiation. All samples were routinely scanned from 5 to 45° 2θ before any treatment in order to check their volcanic origin and estimate the mineralogical composition. For determination of the composition of the pyroclastic sanidine an angle range from 23.5 to 26.0 °2θ was scanned with maximum accuracy. Recent measurements were performed on D8 ADVANCE diffractometer (Bruker AXS GmbH, 2012).

Most samples were analysed also for major chemical components and trace elements by XRF method using S4 Pioneer instrument from Bruker AXS. Earlier XRF analyses before the year 2008 were performed on the VRA30 instrument produced in the former East Germany.

Grain fractions of 40 samples were analysed by the energy dispersive X-ray fluorescence (EDXRF) microanalyser at the scanning electron microscope (Zeiss EVO MA15) mostly in the Institute of Geology at Tallinn University of Technology applying low vacuum conditions.

2. BASICS ABOUT CHEMICAL COMPOSITION AND MINERAL ASSEMBLAGES OF BENTONITES

Bentonites consist mainly of authigenic minerals formed through dissolution and recrystallization of volcanic ash. Volcanic glass forming the main portion of volcanic ash has not preserved in Ordovician-Silurian bentonites. The processes of authigenic formation of minerals (absorption, hydratisation, dissolution) start already during settling of the ash (Grim & Güven 1978) and continue later with kaolinisation or chloritization of phenocrysts and chertification of host rocks (Snäll 1977, Dahlquist et al. 2012).

Resulting from different processes, bentonites of variable composition occur in the rocks. The composition of correlated bentonites largely varies areally, depending on the sedimentary-diagenetic environment and fractionation during the atmospheric transport (Kiipli et al. 2007). At the same time bentonites with different composition alternate closely in sections hinting the predetermination role of the source magma composition to the ash alteration result (Kiipli et al. 2003). Good preservation of sanidine, which is thermodynamically unstable but very slowly recrystallizing at low temperatures, excludes any role of metamorphism and strong late diagenesis involving elevated temperature in the region of Estonia–Latvia–Lithuania–Gotland. Main types of bentonites are listed below:

- Feldspathic tuffs (Fig. 2A) are distributed within shallow shelf sea facies: Ordovician in North Estonia, Silurian in northernmost sites of the areal of Silurian rocks e.g. Kirikuküla and Nurme drill cores (Fig. 1). Content of the

authigenic potassium feldspar can reach more than 80% and illite-smectite is the second main component.

- K-bentonites: illite-smectite is the dominating authigenic mineral (Fig. 2B) (Somelar et al. 2009, 2010). Rarely occur K-bentonites in which the contents of other components are so low that they cannot be seen on XRD patterns. Commonly K-feldspar and/or kaolinite accompany the main illite-smectite.
- Al-bentonites contain much of kaolinite (Fig. 2C) and are common in deep shelf sediments in Latvia and Lithuania. Content of Al_2O_3 exceeds 30% and K_2O contents are often below 3–4%. Presence of kaolinite in bentonites is easily established by the 7.15Å reflection. In the Ordovician Kinnekulle Bentonite kaolinite appears in southernmost sections of Estonia (Valga and Taagepera), (Kiipli et al. 2007, Somelar et al. 2009). In Silurian Telychian bentonites the northernmost findings of kaolinite were registered in Kaugatuma core (Fig. 1).
- Mg-bentonites contain much of corrensite (chlorite-smectite). MgO contents can exceed 12%. Other major minerals are illite-smectite and K-feldspar. This type of bentonites is distributed in the transitional zone between the shallow and deep shelf in the sediments of the Pirgu Stage (Hints et al. 2006).
- Sulphur-rich pyritic bentonites (pyrite content in a bulk sample above 30%) occur in organic-rich shales. In old cores these ash beds resemble weathered pyrite layers as the pyrite mixed with clay minerals oxidizes easily in core boxes. Pyrite-rich bentonites can be found in the Dobele Formation in Latvia and Lithuania (Fig. 2D). Bentonites in shales and marlstones are often sulphur-rich, too, concentrations reaching up to 8% (Paper V Fig. 6)
- Hematite-rich bentonites (Fe_2O_3>10%) occur in red and green coloured shaly sediments. These bentonites are characterized by dark violet colour. Other main minerals are represented by illite-smectite, K-feldspar and kaolinite assemblage. Bentonites of this type are frequent in Telychian deep shelf and transition zone sediments of South Estonia and Latvia.

The following example demonstrates how the Nurme Bentonite (ID731), a bed of particular volcanic eruption, reveals compositional changes according to the facies zone: it is feldsphatic tuff in Nurme core, Al-bentonite in Aizpute, Ohessaare and Ventspils cores, hematite-rich bentonite in Kihnu and Viki cores, K-bentonite with kaolinite and K-feldspar admixture in Ruhnu core.

The listed bentonite types form a variety of transitional compositions, only pyrite and hematite do not coexist. Sometimes the volcanic material is mixed with sedimentary terrigenous and carbonate material (quartz, illite, chlorite, calcite, dolomite). Minor authigenic components recorded in some bentonites are barite, chalcopyrite, halite, goyazite-florencite and anatase. Authigenic apatite may occur in some layers.

Authigenic formation of bentonite minerals is sensitive to the environmental conditions and carries useful information for reconstructing of sedimentary-diagenetic processes. Especially good results can be achieved by tracing compositional variations along correlated ash beds (Kiipli et al. 1997, 2007).

Bentonites contain also a small amount of pyroclastic fragments of magmatic phenocrysts (sanidine, biotite, quartz, apatite, zircon).

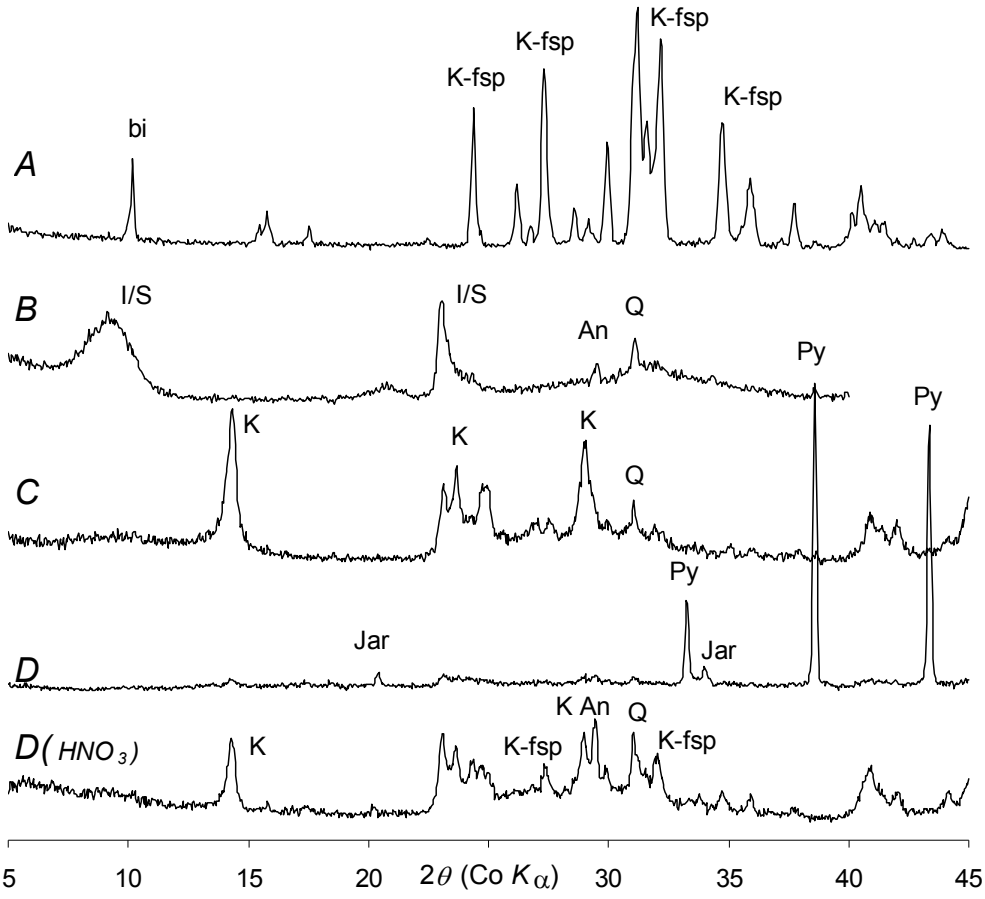

Fig. 2. XRD patterns of different bentonites. A – Osmundsberg Bentonite (Telychian) at the 88.2 m depth in the Paatsalu core. This feldspathic tuff contains 15.5% K_2O (estimated ~88% of K-feldspar) and 17.7% Al_2O_3. B – K-bentonite at the 181.4 m depth in the Soovälja-K1 core (Sandbian). Illite-smectite is the main mineral and K_2O content is 5.5%. C – Al-bentonite at the 745.0 m depth in the Vidale-263 core (Latvia, Telychian). Kaolinite dominates in this bentonite (K_2O 1.74% and Al_2O_3 34.7%). D – Pyrite-rich bentonite at the 1002.2 m depth in the Kurtuvenai-166 core (Lithuania, Telychian). D(HNO_3) – Pyrite-rich bentonite (curve D in this Fig.) after treatment with HNO_3 for removal of pyrite. Composition typical for bentonites (kaolinite and K-feldspar) is now visible.
Strong reflections are labelled as follows: K-feldspar (K-fsp), biotite (bi), illite-smectite (I/S), quartz (Q), kaolinite (K), anatase (An), pyrite (Py), jarosite (Jar).

3. PYROCLASTIC COMPONENT IN BENTONITES: SEPARATION PROCEDURE, QUANTITY, MINERAL ASSEMBLAGES AND GRAIN SIZE

XRD patterns of the bulk bentonite often reveal traces of pyroclastic minerals (biotite, quartz). Commonly pyroclastic sanidine is not visible. For more detailed study of the pyroclastic component its separation from dominating clay material is necessary. The applied procedure is described below.

Ultrasonic dispergation of two grams of sample using 0.1% Na-pyrophosphate solution in distilled water. Water suspension is poured out and the remaining fraction (grain size above ~40 μm) is treated by hot 2N HCl solution for removal of carbonates, apatite, gypsum, jarosite and Fe-sulphates. When the content of pyrite is too high in grain fraction, additional treatment with HNO_3 is applied. For dispersion of kaolinite containing bentonites ultrasonic treatment in hot 10% KOH solution is necessary but in some cases kaolinite still may not disperge completely.

The obtained grain fraction is studied and described under the microscope in reflecting light and estimates for the abundance of biotite are made. The 0.04–0.1 mm fraction forming the dominating part of the grain material is separated for XRD analysis by sieving. The grain material typically consists of pyroclastic minerals and authigenic potassium feldspar; sometimes terrigenous minerals (quartz, feldspars) and authigenic barite occur as significant components.

Authigenic K-feldspar hinders analysis of pyroclastic minerals. Portion of authigenic K-feldspar in grain material is smaller in kaolinite-containing bentonites formed in deep sea environment (Latvia, Lithuania); sometimes even only pyroclastic minerals occur. Therefore the composition of grain fraction of bentonites is characterised on an example of the Silurian of the Ventspils-D3 drill core section (Fig. 3).

Content of the >0.04 mm fraction consisting of pyroclastic, terrigenous and authigenic grains and aggregates varies mostly between 1–5%. Only in rare cases the content of pyroclastic grains exceeds 10%. The Telychian Nässumaa Bentonite (ID696) found in many sections but not in Ventspils-D3 core, is a remarkable example of the ash bed with high content of pyroclastic minerals. Such high content of pyroclastic minerals cannot be observed in any of the Ordovician bentonites.

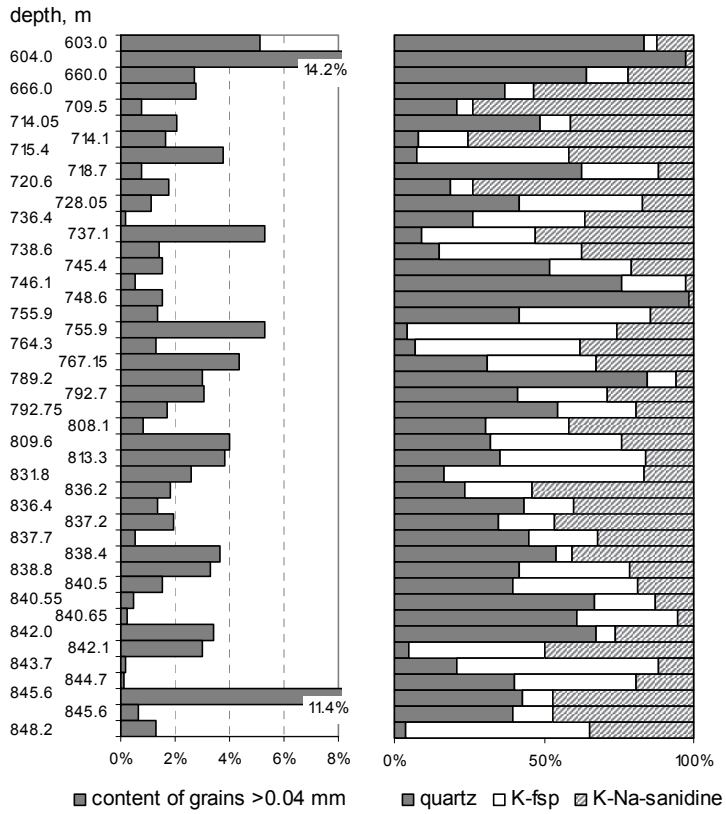

Fig. 3. Silurian bentonites and samples of terrigenous rocks with volcanic material admixture from Ventspils-D3 core. Left: Content of grains >0.04 mm. Right: Proportions of main minerals in grain fraction. Sample from depth 640.0 m was removed from the chart because of high content of barite in grains.

Pyroclastic sanidine is commonly one of the main components in grain fraction – this makes the detailed XRD analysis of sanidine possible. Still, occasionally it is difficult to collect the 10 mg of grains needed for XRD analysis. Sometimes the content of pyroclastic minerals in bentonites is low (e.g. Ventspils core at the 736.4 m depth, 0.2% of grains), while in other cases significant portion of terrigenous material which contains less coarse grains dilutes the volcanogenic component. In a sample set from the Silurian of the Ventspils core also terrigenous samples with volcanogenic admixture are present, e.g. from depth 840.65 m. Content of grains larger than 0.04 mm is only 0.26% with domination of fine quartz in it. In the East Baltic, Ordovician and Silurian pyroclastic grains are larger than the terrigenous material and such situation favours separation of pyroclastic material sometimes even from the very low contents in mixed sediments to the level measurable by XRD.

The content and grain size of pyroclastic minerals is related to the distance from the source volcano, but an example from the Osmundsberg Bentonite (ID851) indicates that the relationships are more complicated. The Osmundsberg Bentonite consists vertically of two different parts both in Estonia and Latvia. In the Ventspils

core at the 845.6 m depth the Osmundsberg Bentonite consists of grey part with 11.4% of grains >0.04 mm, including significantly also grains larger than 0.1 mm, and the red part with only 0.7% of grains which are also smaller (all less than 0.1 mm). It is not known in Ventspils which part of the above sample represents earlier and which later part of the ash layer, but in Estonian sections it has been identified that the part with larger grains forms the upper part of the ash bed, i.e. was emplaced by the later eruption. It is remarkable that sanidine composition is the same in both parts of the Osmundsberg Bentonite indicating the same source.

Grain fraction 0.04–0.1 mm has proved to be optimal for measurements of the sanidine composition in the studied region. In the fraction below 0.04 mm authigenic K-feldspar or terrigenous material often dominates, while the fraction of larger grains (>0.1 mm) is often absent or its quantity is very small. The finds of pyroclastic material with grains larger than 0.1 mm are still important, as can be considered for laser ablation ICPMS analyses or for dating. Pyroclastic grains larger than 0.25 mm have not been found over the entire studied region.

Size of biotite flakes is larger than the size of quartz and sanidine grains, and compared with the fraction 0.04–0.1 mm, biotite concentrates into the fraction >0.1 mm. In rare cases biotite flakes can reach even size of 0.25 mm. In Latvian and Lithuanian sections where bentonites contain kaolinite, the biotite flakes are often also partly or completely kaolinised. In these cases the treatment of grains ultrasonically and with reagents may disintegrate the biotite flakes and the original content may remain unnoticed. Biotite is a good indicator of volcanogenic material visually recognized easily during the fieldwork. The biotite admixture is especially valuable in terrigenous shale interbeds containing some volcanic material. Pure bentonites can be easily recognized by different colour and consistency, but volcanic material in shaly interbeds can be identified only by biotite flakes. Still, several volcanic ash beds do not contain biotite.

In addition to the sanidine, quartz and biotite in some bentonites we have found also magnetite (ID772, ID755), ilmenite (Kaugatuma core at the 267.1 m depth) and muscovite (Kiipli, Kallaste, Nestor 2010) belonging also to the magmatic phenocrysts and applicable as correlation criteria. Sometimes prismatic zircon crystals occur in remarkable amounts (Kurtuvenai-166 core at the 971.2 m depth).

When we started the study of pyroclastic minerals in bentonites of Saaremaa Island, the absence of plagioclase, the common phenocryst in recent volcanic rocks, drew attention. Later it appeared that although plagioclase is absent in shallow shelf sediments of Saaremaa, it is present in small quantities in correlative bentonites in deep shelf and especially in transition zone between the shallow and deep sea sections (Table 1). Evidently the plagioclase is unstable in shallow sea environments where intensive formation of authigenic K-feldspar proceeds and has been completely destroyed. Even the kaolinisation process in deep shelf sediments has not been aggressive enough for complete destruction of plagioclase. Plagioclase has somewhat better preserved in the bentonites of Ohesaare and Ruhnu sections located in the transition zone. EDS microanalysis of two grains from the bentonite in the När core (Gotland) at the 351.3 m depth indicated oligoclase composition suggesting magmatic origin of the plagioclase.

Table 1. Plagioclase traces in Telychian bentonites; numbers represent average plagioclase/sanidine $20\bar{1}$ intensity ratios from 0.04-0.1 mm grain fraction.

	ID311	ID494	ID696	ID731	ID776
shallow shelf (Estonia)	<0.01	<0.01	0.01	<0.01	<0.01
transition zone	0.13	0.049	0.028	0.081	0.10
deep shelf (Latvia)	0.056	0.10	<0.01	0.062	0.076

4. PYROCLASTIC SANIDINE IN BENTONITES: XRD ANALYSIS AND COMPOSITION

Authigenic K-feldspar in grain fraction complicates or even makes impossible XRD analysis of pyroclastic minerals supressing the intensity and overlapping with useful reflections. Still, the analysis of the sanidine composition (Na/K ratio) using classical method of the measurement of the $20\bar{1}$ reflection works even at the moderately high content of the authigenic K-feldspar.

In Fig. 4A, an example of the Kinnekulle Bentonite shows in main authigenic K-feldspar with relatively wide reflections a less abundant magmatic K-Na sanidine with high crystallinity (sharp reflections). Perfect peak resolution of the new D8 diffractometer enables to discriminate some reflections between these two feldspars.

Using HZG4 diffractometer detailed measurements for determination of the composition of alkali feldspars have been concentrated to the position of the $20\bar{1}$ reflection. An angle range from 23.5 to 26.0 °2θ was scanned with the step size 0.01 °2θ; the measuring time was 15 s per point. This range includes the 100 (4.255 Å) reflection of quartz, the $20\bar{1}$ reflection of various feldspar phases, and also 4.18 Å and 4.13 Å reflections of kaolinite. Therefore, the removal of kaolinite from the sample before measurements was essential.

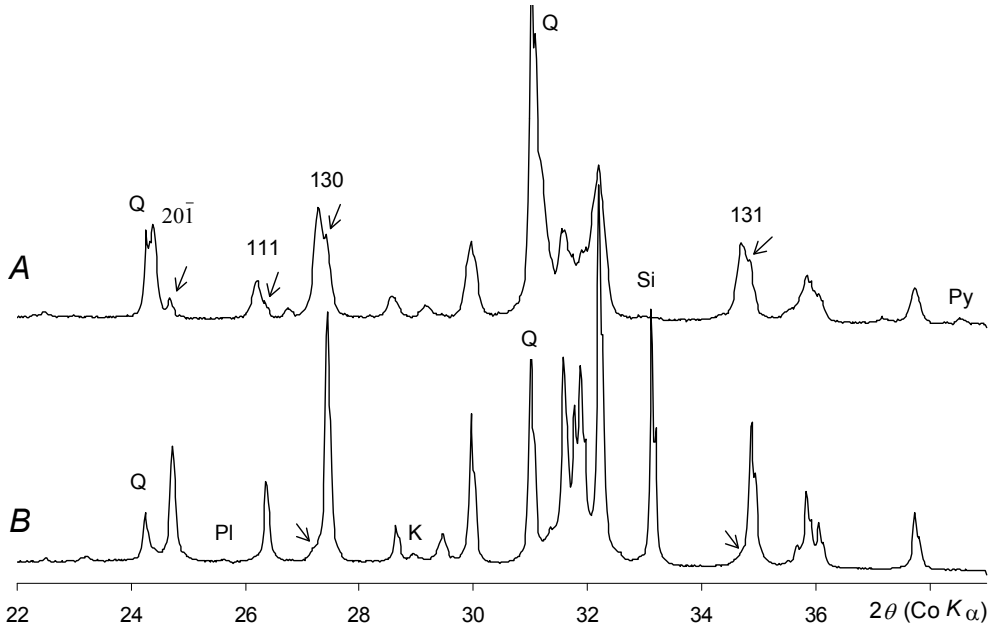

Fig. 4. XRD patterns of bentonite coarse fraction.
A – Grain fraction 0.04–0.1 mm of the Kinnekulle bentonite from Kuressaare-K3 core at depth 368.5 m. Main component is authigenic K-feldspar; arrows are pointing to the pyroclastic sanidine traces. Split reflections are labelled with indices.
B – Grain fraction 0.04–0.1 mm of the bentonite from Ventspils-D3 core at the 720.6 m depth, composed mainly of pyroclastic sanidine with quartz and K-feldspar (see arrows) admixture.
Q - quartz; Si - silicon standard added for peak shift correction; Py - pyrite; K - kaolinite; Pl - plagioclase.

Measured XRD patterns have been analysed using Mathcad 2000 application developed by the author of the present thesis (Kallaste 2002, Paper I). The convolution and curve fitting procedure revealed the XRD reflections without instrumental contribution.

http://geokogud.info/git/attachments/reference/2533/Legend_sanidine.pdf and (Paper I Fig. 3, Paper IV Fig. 3, Paper V Fig. 2) show measured curves and modelling results – true XRD reflections. The content of (Na, Ca)$AlSi_3O_8$ in mol% in K-(Na,Ca) sanidine was calculated as follows:

$(Na,Ca)_{mol\%} = (4.233 - d) / (4.233\text{-}4.033)$,

where d is d-spacing of the particular sanidine component-phase and end member values are 4.233 Å (K-sanidine) and 4.033 Å (high albite). This calculation is based on the experimental study by Orville (1967) where alkali feldspar composition was calibrated with the 20$\bar{1}$ spacings.

$CaAl_2Si_2O_8$ concentrations in studied sanidine phenocrysts rarely exceed 4 mol% (Fig. 5).

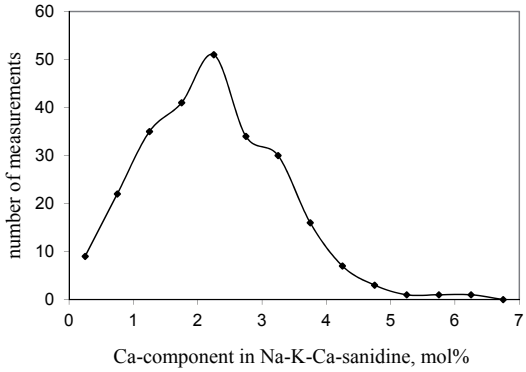

Fig. 5. Frequency of $CaAl_2Si_2O_8$ concentrations in sanidine according to the ED XRF measurements in 25 bentonite samples from the Silurian of Latvia and Gotland (Sweden).

In favourable samples, it is possible to measure crystal lattice parameters of the magmatic sanidine. Table 2 and Fig. 6 represent lattice parameters of sanidine in some samples. Although all measurements do not exhibit maximum accuracy, all sanidines can be classified as high sanidine ($2t_1$<0.66). Sanidine composition values from XRD measurements are close to the results of ED XRF microanalyses (Table 2).

From the sample SHQ4 (Sunhill Quarry, England, Ludlow age) uniquely also anorthoclase, the Na-dominating alkali feldspar, occurs together with sanidine (Table 2). In the East Baltic and Gotland sections anorthoclase has not been found.

Table 2. Cell parameters, (Si, Al) ordering parameters $2t_1$ (calculated after Kroll & Ribbe 1987) and composition of feldspars from selected bentonites.

No.	Bentonite name	*a* (Å)	*b* (Å)	*c* (Å)	α (°)	β (°)	γ (°)	$2t_1$	Na+Ca mol% XRD $(20\bar{1})$	Na+Ca mol% SEM
1	Kinnekulle	8.605	13.030	7.180	90	116.01	90	0.56		
2	Kinnekulle	8.492	13.015	7.175	90	116.02	90	0.59	24.6	
3	Osmundsberg	8.507	13.017	7.179	90	116.00	90	0.60	21.1	
4	Ventspils 720.6	8.468	13.015	7.173	90	116.02	90	0.58	29.7	31.8
5	Vidale 681.1	8.34	12.98	7.16	90	116.22	90	0.58	57.9	59.5
6	SHQ4	8.474	13.003	7.170	90	116.04	90	0.60	28.4	
7	SHQ4	8.177	12.916	7.125	93.03	116.48	90.18			

1,2 authigenic and pyroclastic sanidine, Kuressaare-K3 core, depth 368.5 m (Fig. 4A)
3 pyroclastic sanidine, Ventspils-D3 core, depth 845.6 m (grey part), Telychian
4 pyroclastic sanidine, Ventspils-D3 core, depth 720.6 m, Wenlock (Fig. 4B)
5 pyroclastic sanidine, Vidale-263 core, depth 681.1 m, Wenlock (Paper V Fig. 2.)
6,7 pyroclastic sanidine and anorthoclase, Sunhill quarry, England, Ludlow

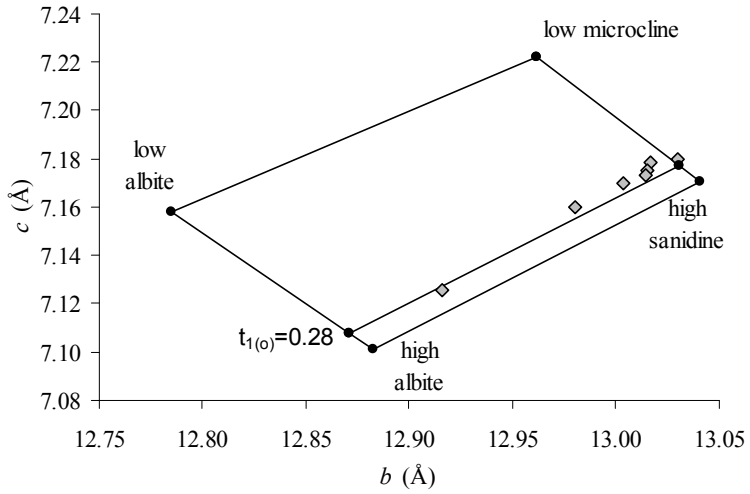

Fig. 6. Pyroclastic and authigenic feldspars in the *b*-*c* lattice parameters diagram according to the data in Table 2. Cell parameters of alkali feldspar end members (Kroll & Ribbe 1987).

Position and shape of the sanidine $20\bar{1}$ reflection varies largely. In many bentonites the reflection is sharp, its position can be measured precisely and results obtained from different samples are very close to each other. For example, calculated Na+Ca content in sanidine for ID696 bentonite varies between 22.7–23.6 mol% (analysed from 15 drill core sections), for ID494 45.5–46.6 mol% (15 sections).

Detailed XRD analysis of the sanidine crystal structure of the Osmundsberg Bentonite (ID851) from the Ventspils core section using new D8 diffractometer and TOPAS software revealed that small broadening of XRD reflections can be attributed to the strain (average strain value is 0.08%, no size related broadening). Single line fit gave maximum strain value 0.14% for the $20\bar{1}$ reflection and minimum strain value (0.055%) for the 060 reflection. Probably significant part of the strain of crystal lattice is caused by the variations in K/Na ratio due to the zonation in magmatic phenocrysts and differences between the compositions of separate grains. Therefore, probably variation in results of the SEM microanalyses of the set of sanidine grains (±2 mol%) exceeding clearly analytical uncertainty contains also some natural compositional variation even in a case of very sharp XRD reflections.

Unlike the sanidine in the Osmundsberg Bentonite, in many bentonites sanidine reveals broader $20\bar{1}$ reflection caused by the larger natural compositional variations. Sometimes also two overlapping magmatic sanidine reflections can be observed. In these cases applying of the single grain SEM analysis for obtaining the statistically representative average composition needs results from at least several tens of grains. In these samples the advantage of XRD analysis of the average sanidine composition is quite clear as XRD analyses simultaneously more than 10000 grains. SEM microanalysis is a very useful method for measuring the sanidine composition in detail.

An interesting problem is the cause of very broad XRD reflections. A saddle-like interval between $20\bar{1}$ reflections from authigenic K-sanidine and pyroclastic K-Na-sanidine needing particular component-reflection in the decomposed XRD model is common. Quite often continuous plateau-like wide composite reflection spreads from the authigenic K-sanidine $20\bar{1}$ reflection to the Na-containing sanidine (Paper V Fig. 2h). Wide tail-like reflections on the high angle side of the K-sanidine $20\bar{1}$ reflection are common, too (ID488, Paper IV Fig. 3).

Several hypotheses for the cause of this variability can be proposed: 1. Intergrowth zone between pyroclastic nucleus and authigenic feldspar cover probably exists. Part of sodium may be dissolved and replaced with potassium in the outer shell of the pyroclastic sanidine grain and feldspar of intermediate composition formed during the diagenesis. 2. Growth zonation in magmatic phenocrysts. 3. Authigenesis of Na-K-sanidine through recrystallization of the plagioclase or anorthoclase. This hypothesis is based on the observation that remarkable amount of the Na-K-sanidine of low crystallinity is present in bentonites originating from andesitic (derived from trace elements) tuffs which should contain no or very little sanidine.

The question of diagenetic distortion of the pyroclastic sanidine in bentonites or possible Na-K-sanidine authigenesis is important in using it for correlation. High resolution XRF microanalyses hopefully can answer these questions in future studies.

5. CORRELATION OF BENTONITES USING COMPOSITION OF THE PYROCLASTIC SANIDINE

Bentonites offer a unique possibility for recognition of exactly the same time levels in geological sections. This method can be used for correlation of sections from different palaeoenvironments containing various fossil assemblages. In the East Baltic and Gotland sections sanidine is one of the most abundant minerals among the pyroclastic components and XRD analysis enables to study a large number of samples within a reasonable time span and cost with perfect precision. For successful applying of bentonite correlations several prerequisites are needed:

1. Bentonites must be present in the sections under study. Constraints arise from the regional distribution of bentonites; only the most powerful volcanic eruptions spread ash over few thousands of kilometres. For deposition and preservation of bentonites calm sedimentary environment is favourable; waves and currents can wash fine ash away or mix volcanic ash with other sedimentary material.
2. Only high-quality drilling results with core containing number of bentonites. Often in drill cores rotation surfaces occur and soft bentonite interbeds are the first being lost during core rotation.
3. In some cases finding of the layers containing volcanic material can be complicated. For example, in old drill cores terrigenous clay and bentonite have often disintegrated and mixed and finding of bentonite material is often possible only with the help of the original core descriptions where bentonites have been recognised in the fresh core. Remarks of bentonites made on core

boxes are often helpful. Hard feldspathic tuffs when mixed with carbonate material hardly differ from limestone.

4. Pyroclastic component in bentonite must be possible to separate. Feldspathic tuffs, metamorphosed varieties and some kaolinised bentonites are not favourable for separation of grains. Illite-smectite-rich K-bentonites disintegrate most easily.
5. Pyroclastic component must contain enough sanidine for analysing.
6. Sanidine must have distinct composition differing clearly from the sanidine of other closely lying bentonites. Problem arises when repetitive eruptions from the same volcanic source give similar compositions according to almost all parametres.

Silurian bentonites

In the best studied Telychian sequences of the East Baltic and Gotland more than 30 eruption layers contain enough distinct sanidine enabling trustworthy correlation. Table 3 includes Telychian and lower Sheinwoodian bentonites which have wider distribution and frequent occurrence (see No of sections column). Abundance of bentonites with distinctive sanidine of good crystallinity makes correlation highly reliable, regular succession of bentonites with various distinct sanidines confirms every single correlation. For correlation of bentonites containing sanidine with broad $20\bar{1}$ reflection graphic correlation and immobile trace elements can be applied. Still, discrimination of bentonites ID518, ID520 and ID521 occurring closely in sections and characterized by similar trace element contents can be solved only provisionally.

Full table including 28 drill core sections and 63 recognized eruption layers of the correlated Telychian and lower Sheinwoodian bentonites is available at http://sarv.gi.ee/reference.php?id=2533, there are accessible measured and modelled sanidine XRD curves also.

Compared with Estonia and Latvia, in Lithuania the Telychian contains much smaller number of bentonites. In the studied sections we have found only one correlative bed with the Osmundsberg Bentonite (Kurtuvenai-161 depth 1466.7 m). Modelled sanidine XRD curves of Lithuanian bentonites of Silurian age are available at http://sarv.gi.ee/reference.php?id=2544.

From the Telychian of Gotland only the När core and Lusklint outcrop sections were studied. Study of some more sections undoubtedly would add correlative beds with East Baltic.

Table 3. Composition of sanidine in most frequent bentonites from Telychian to lower Sheinwoodian interval.

Bentonite	No of	Viki depth	Viki	Ohe-saare	När	Vents-pils	Aiz-pute-41	Pyroclastic K-Na-sanidine, main component parametres	
name	sec-tions	ID	depth, m	depth, m	depth, m	depth, m	depth, m	Na+Ca content mol%	Width of the sanidine reflection, °2θ
Ireviken	6	127		340.76	324.50	789.2	915.40		little sanidine, biotite!
Lusklint	10	150	115.02	342.08	328.1		917.10	35.2-35.8	0.19-0.34
Ohesaare	12	210	121.03	345.83		792.75	925.80	38-40	0.25-0.35
Aizpute	10	311	131.10	351.72	333.40		931.80	36.2-37.8	0.08-0.12
Kirikuküla	16	457	145.75	359.31					very wide reflection
Viki	19	475	147.50	361.30				45.2-46.3	0.12-0.20
Kaugatuma	9	480	148.00	361.70		808.1	938.60	42.0-42.8	0.18-0.27
Kuressaare	13	488	148.80	362.23			941.35		very wide reflection
Ruhnu	20	494	149.40	362.46		811.6		45.7-46.4	0.05-0.09
Viirelaid	~15	518	151.80	364.76		813.3	943.90		very wide reflection
	~10	520		365.08					very wide reflection
	~10	521	152.10						very wide reflection
	15	568	156.80	367.60			946.25		very wide reflection
Nässumaa	16	696	169.60	369.75			954.20	22.9-23.3	0.04-0.06
	14	719	171.95						little sanidine, biotite!
Nurme	18	731	173.10	369.98		837.2	957.10	38.7-40.3	0.10-0.16
Tehumardi	15	744	174.40			838.4	957.75	25.8-26.7	0.07-0.10
Paatsalu	14	755	175.55	370.09		838.8	958.25	25.5-26.2	0.25-0.30
Pahapilli	12	772		370.44				20.5-24.1	0.30-0.34
Mustjala	11	795				842.0	961.50	24.5-25.3	0.05-0.11
Osmundsberg	20	851	185.10			845.6	964.40	20.7-21.5	0.05-0.09

Correlation studies of Telychian and lower Sheinwoodian bentonites using sanidine composition after establishing of the method (Paper I) and arranging stratigraphic nomenclature of bentonites (Paper III) led to discrimination of several volcanic sources and grouping them according to bentonites (Paper IV). Residual enrichment of immobile trace elements revealed clear increase trend, up to twofold, from shallow to deep shelf facies along a correlated bentonite bed (Paper IV Fig.7). Secondly, it led to the correlation of the Ireviken Event (extinction of conodonts), well traceable in shallow water sediments, with graptolite biozonation in deep sea sediments (Kiipli et al. 2006a, Paper VI). Thirdly, the study of Lithuanian bentonites revealed that in addition to volcanic sources from the Iapetus Ocean also volcanoes from the margin of the Rheic Ocean supplied the Baltic Basin with ash (Kiipli et al. 2014). Fourthly, correlation of the Osmundsberg Bentonite from shallow water sediments in Estonia with bentonites in deep sea sediments in Latvia showed that Rumba Formation in Estonia belongs to the Lower Telychian (Kiipli et al. 2006a) differently of the former assignment to the upper Aeronian.

Silurian bentonites higher than the Telychian (up to the lower Ludlow) also can be correlated by the sanidine composition in Latvia and Estonia. Published results of these correlation studies are attached to the present thesis (Paper V).

Results of the XRD measurements are available in the collections database of the Institute of Geology at TUT: from the Ventspils-D3, Vidale-263, Ohesaare and

Ruhnu-500 core sanidine of the bentonites of the Wenlock age at http://sarv.gi.ee/reference.php?id=1203, and sanidine XRD curves from the Silurian of Lithuania at http://sarv.gi.ee/reference.php?id=2544.

The problem is that the occurrence and finding of bentonites in sections is sporadic and much more studies are needed for revealing most of the eruption layers. The sections from Latvia and Gotland are of key importance for these studies.

During the Wenlock time volcanic activity was still intense. Large number of bentonites have been found in the East Baltic sections. Number of ash beds contain distinctive sanidine suitable for proving the correlations. Still, sporadic preservation from sedimentation processes and core drilling recovery of thin ash beds limits the number of correlations. Complications for correlations arise also from the similar compositions of bentonites from closely in time successive eruptions from supposedly the same volcanic source.

Study of the upper Wenlock and lower Ludlow bentonites clarified correlation of Estonian rocks with Wenlock/Ludlow boundary (Kiipli et al. 2011). In particular, the Kuusnõmme Bentonite from drill cores in Saaremaa Island from the upper part of the Viita Beds of the Rootsiküla Stage contains sanidine identical with the bentonite from the Ventspils core between distribution intervals of graptolites *ludensis* and *nilssoni* marking the Wenlock/Ludlow boundary. This correlation is significantly more precise than previous suggestions for the position of the boundary.

Study of Lithuanian bentonites showed that in lower Homerian several bentonites correlate well with the Latvian and Estonian ones indicating that volcanoes in the collision zone between Baltica and Laurentia located relatively close to the East Baltic compared with previous periods when ashes did not reach Lithuania (Kiipli et al. 2014).

Ordovician bentonites

The data of Ordovician bentonites come mostly from Estonia (Kiipli 2001, 2002, 2003, 2005, 2006b, 2008a, 2010). The first evidence of volcanic activity is known from the Kukruse Stage. Haljala Stage contains at least 20 bentonites; the best-studied dataset comes from the Soovälja-K1 core from the centre of the Kärdla impact crater. This crater forms a unique sedimentary environment separated from the surrounding shallow sea, where large number of bentonites are well preserved, while outside the crater most of the ash beds are strongly mixed with other sedimentary material. Sanidine suitable for proving the correlations is present only in a few bentonites in the uppermost part of the Haljala Stage.

Bentonites higher in the Keila Stage (at least three layers in Estonian sections) contain little sanidine, are difficult to concentrate, but in some cases, when it was possible revealed discrete sanidine that can be used for correlations. Positive examples are the bentonites from the Taagepera core at the 481.8 and 481.2 m depths containing ca. 22 and 24 mol% of the Na+Ca component, correspondingly.

The well-known and widespread Kinnekulle Bentonite occurs at the lower boundary of the Keila Stage. Mostly in Estonia this bentonite can be easily recognised by its stratigraphic position and remarkable thickness reaching 70 cm on Hiiumaa Island. Using the sanidine method, the Kinnekulle Bentonite was proved also in the sections from South Estonia (Mehikoorma, Valga, Taagepera) where its thickness often decreases to less than 5 cm and biostratigraphic correlation is also difficult.

Correlation of the Kinnekulle Bentonite by the sanidine composition was proved to Latvia (Kandava-25 core at the 924.4 m depth and Aizpute-41 core at the 1052.5 m depth) and Lithuania (Kurtuvenai-166 core at the 1080.2 m or 1092.7 m: gamma log depth and drilling depth).

Aizpute-41 drill core contains abundant traces of volcanism in the depth interval between 1049.5 m and 1059.3 m, but the volcanic material is mixed with terrigenous material and only one ash bed forms relatively pure feldspathic tuff. In the argillaceous interbeds much of biotite can be observed and XRD analysis indicates presence of sanidine in the grain fraction. The Kinnekulle Bentonite is missing, but according to the sanidine composition (25.3 mol% Na+Ca component) correlative level is at the depth 1052.5 m. Upward in the section to the depth 1049.5 m biotite and sanidine can be found in five marl interbeds (sanidine contains 23–27 mol% Na+Ca component). Downward to the depth 1059.3 m 15 marl interbeds occur with sanidine (21–32 mol% of Na+Ca component and some with wide XRD reflection). All these layers occur in the Ordovician Adze Formation and correspond to the volcanism of the Sandbian age. Correlation with Estonian volcanic ashes of this age is uncertain (except with Kinnekulle Bentonite, Kiipli et al. 2009) as similar discrete sanidine XRD reflections in the Haljala Stage are not found in Estonia.

From the Kurtuvenai-166 core in Lithuania 1–3 m below the Kinnekulle Bentonite two marl interbeds were found containing much of pyroclastic quartz and biotite, but no sanidine. Thus, in all three Baltic States the Sandbian age volcanic ashes are different and probably point to different volcanic sources.

In the Pirgu Stage (upper Katian) five bentonites occur in the Estonian sections. One of these is relatively thick reaching 30 cm in South-West Estonia and Saaremaa; correlative beds are found in more than ten sections. Preservation conditions for volcanic ashes were variable at the Pirgu time, but mostly unfavourable causing sporadic occurrence of bentonites. From some sections (Põltsamaa-H39, Taagepera, Varbla) three ash beds have been found, from others only one or two; therefore the succession of all ash beds is not proved. Bentonites of the Pirgu Stage can be discriminated according to the sanidine composition (Kiipli et al. 2004), although the abundance of the authigenic feldspar often complicates separation of pyroclastic component.

Table 4. Sanidine data of upper Katian bentonites, Pirgu Regional Stage in Estonia. Succession of lower and upper bentonites is uncertain because bentonites occur in different sections. In the Aizpute section there are no Katian bentonites – volcanic phenocrysts including characteristic sanidine were separated from shaly interbeds.

	Estonia, average data			Aizpute core, Latvia	
Bentonite No.	No. of sections	(Na,Ca)mol% in sanidine	biotite*	depth, m	(Na,Ca)mol% in sanidine
bIV(bIII)	2	45.2; 57**	+		
bIII(bIV)	5	34.6	+		
bII	10	44.0	no	1011.0	43.9
bI(b0)	6	38.2	+	1027.5	38.8
b0(bI)	3	wide reflection	++		

* biotite +, some flakes; ++, rare
** two sanidine phases occurred in Kuressaare-K3 core at depth 302.25 m.

Area of applicability of the method

In the Estonia–Latvia–Lithuania–Gotland region almost all bentonites contain Na-K-sanidine although it has often low crystallinity.

Attempts to find sanidine in the Lower Palaeozoic bentonites from Bornholm (Denmark), Podolia (Ukraine), Oslo Region (Norway) and East Siberia (Russia) did not reveal positive results. Possible reasons are late-diagenetic elevated temperatures or chemically aggressive sedimentary-diagenetic environment causing destruction of primary pyroclastic material.

Unique find of the association of sanidine with anorthoclase in phenocrysts of bentonite from Sunhill quarry (sample SHQ4 in Table 2), Wales, indicates that the sanidine method for correlation studies of Palaeozoic bentonites may have useful applications also in other regions worldwide.

6. CONCLUSIONS

1. Pyroclastic sanidine is well preserved in Ordovician and Silurian bentonites within the Estonia–Latvia–Lithuania–Gotland region indicating low diagenetic temperatures during the whole 460 Ma long geological history.
2. Analysing of sanidine composition by XRD enables to correlate the bentonites. This new method of chemostratigraphy is simple and effective. High precision of the method is an important capability for discriminating eruption layers of quite similar compositions.
3. Good preservation of sanidine in bentonites spreading through various natural palaeo-environments adds a new possibility for correlation, which was often difficult by using only traditional biostratigraphical methods.

4. Like all other methods, correlation by the sanidine composition has its limitations. Main restrictions rise from the limited extent (from hundreds to thousands kilometres) of the volcanic ash cloud distribution. Therefore at present the method can be applied regionally. Secondly, limitations rise from the original presence and later preservation of the sanidine.
5. Integrated approach applying several correlation methods (sanidine composition, other phenocryst abundance and composition, bulk bentonite immobile elements, biostratigraphy, graphic correlation) leads to the most confident results of correlations.
6. Using the sanidine method the correlation table of the Telychian bentonites in Estonia and Latvia with some correlations to Gotland was composed enabling exceptionally detailed comparison of sections.
7. As a result, several significant refinements of stratigraphy were achieved at the level of the Aeronian/Telychian, Llandovery/Wenlock and Wenlock/Ludlow boundaries.

ACKNOWLEDGEMENTS

I thank my supervisors Prof. Alvar Soesoo and Dr. Tarmo Kiipli for their support and advice. Prof. Emer. D. Kaljo is acknowledged for reading the thesis and useful comments. I am grateful to Saima Peetermann for correcting the English.

The study was financially supported by the target financing projects of the Estonian Ministry of Education and Research Nos SF0140016s09 and SF0332652s04, and by the Estonian Science Foundation grants ETF7605, 5921 and 4070.

REFERENCES

BATCHELOR, R. A. & EVANS, J. 2000. Use of strontium isotope ratios and rare earth elements in apatite microphenocrysts for characterization and correlation of Silurian metabentonites: a Scandinavian case study. *Norsk Geologisk Tidsskrift*, **80**, 3–8.

BATCHELOR, R. A. & CLARKSON, E. N. K. 1993: Geochemistry of a Silurian metabentonite and associated apatite from the North Esk Inlier, Pentland Hills. *Scottish Journal of Geology* **29**, 123–130.

BATCHELOR, R. A. & JEPPSSON, L. 1994. Late Llandovery bentonites from Gotland, Sweden, as chemostratigraphic markers. *Journal of the Geological Society, London*, **151**, 741–746.

BATCHELOR, R. A. & JEPPSSON, L. 1999. Wenlock metabentonites from Gotland, Sweden: geochemistry, sources and potential as chemostratigraphic markers. *Geological Magazine,* **136**, 661–669.

BATCHELOR, R. A., WEIR, J. A. & SPJELDNÆS, N. 1995. Geochemistry of Telychian metabentonites from Vik, Ringerike District, Oslo region. *Norsk Geologisk Tidsskrift*, **75**, 219–228.

BATCHELOR, R. A. 2003. Geochemistry of biotite in metabentonites as an age discriminant, indicator of regional magma sources and potential correlating tool. *Mineralogical Magazine*, **67**, 807–817.

BERGSTRÖM, S. M., HUFF, W. D., KOLATA, D. R. & KALJO, D. 1992. Silurian K-bentonites in the Iapetus Region: a preliminary event-stratigraphic and tectonomagmatic assessment. *GFF*, **114**, 327–334.

BERGSTRÖM, S. M., HUFF, W. D., KOLATA, D. R. & BAUERT, H. 1995. Nomenclature, stratigraphy, chemical fingerprinting, and areal distribution of some Middle Ordovician K-bentonites in Baltoscandia. *GFF*, **117**, 1–13.

BERGSTRÖM, S.M., HUFF, W.D., KOREN, T., LARSSON, K., AHLBERG, P. & KOLATA, D. R. 1999. The 1997 core drilling through Ordovician and Silurian strata at Röstånga, S. Sweden: preliminary stratigraphic assessment and regional comparison. *GFF*, **121**, 127–135.

BERGSTRÖM, S. M., TOPRAK, F. Ö., HUFF, W. D. & MUNDIL, R. 2008. Implications of a new, biostratigraphically well-controlled, radio-isotopic age for the lower Telychian Stage of the Llandovery Series (Lower Silurian, Sweden). *Episodes* **31***,* 309–314.

CRAMER, B. D., CONDON, D. J., SÖDERLUND, U., MARSHALL, C., WORTON, G. J., THOMAS, A. T., CALNER, M., RAY, D. C., PERRIER, V., BOOMER, I., PATCHETT, P. J. & JEPPSSON, L. 2012. U-Pb (zircon) age constraints on the timing and duration of Wenlock (Silurian) paleocommunity collapse and recovery during the "Big Crisis". *Geological Society of America Bulletin*, **124**, 1841–1857.

DAHLQUIST, P., CALNER, M., KALLASTE, T., KIIPLI, T. & SIIR, S. 2012. Geochemical variations within the mid-Silurian Grötlingbo Bentonite of Sweden and the East Baltic area – discriminating between magmatic composition, ash transport fractionation and diagenetic effects. *GFF* **134**, 273–282.

EMERSON, N. R., SIMO, J. A., BYERS, C. W. & FOURNELLE, J. 2004. Correlation of (Ordovician, Mohawkian) K-bentonites in the upper Mississippi valley using apatite chemistry: implications for stratigraphic interpretation of the mixed carbonate-siliciclastic Decorah Formation. *Palaeogeography, Palaeoclimatology, Palaeoecology*, **210**, 215–233.

GRIM, R. E. & GÜVEN, N. 1978. Bentonites, Geology, Mineralogy, Properties and Uses. *Developments in Sedimentology* **24**, Elsevier, Amsterdam, 256 pp.

HETHERINGTON, C. J., NAKREM, H. A. & POTEL, S. 2011. Note on the composition and mineralogy of Wenlock Silurian bentonites from the Ringerike District: implications for local and regional stratigraphic correlation and sedimentary environments. *Norwegian Journal of Geology*, **91**, 181–192.

HINTS, R.; KIRSIMÄE, K.; SOMELAR, P.; KALLASTE, T.; KIIPLI, T. 2006. Chloritization of Late Ordovician K-bentonites from the northern Baltic Palaeobasin– influence from source material or diagenetic environment? *Sedimentary Geology*, **191**, 55–66.

HINTS, R., KIRSIMÄE, K., SOMELAR, P., KALLASTE, T. & KIIPLI, T. 2008. Multiphase Silurian bentonites in the Baltic Palaeobasin. *Sedimentary Geology,* **209**, 69–79.

HUFF, W. D., MERRIMAN, R. J., MORGAN, D. J., ROBERTS, B. 1993. Distribution and tectonic setting of Ordovician K-bentonites in the United Kingdom. *Geological Magazine*, **130**, 93–100.

HUFF, W. D., BERGSTRÖM, S. M., KOLATA, D. R. & SUN, H. 1998. The Lower Silurian Osmundsberg K-bentonite. Part II: mineralogy, geochemistry, chemostratigraphy and tectonomagmatic significance. *Geological Magazine*, **135**, 15–26.

INANLI, F. Ö., HUFF, W. D. & BERGSTRÖM, S. M. 2009. The Lower Silurian (Llandovery) Osmundsberg K-bentonite in Baltoscandia and the British Isles: Chemical fingerprinting and regional correlation. *GFF,* **131**, 269–279.

JAANUSSON, V. 1948. Vulkaanilise tegevuse jälgi Lääne-Baltoskandia ordoviitsiumi settekivimeis. Estonia, Eesti üliõpilaskonna neljas väljaanne Saksamaal, Karlsruhe, 50–52 (in Estonian).

JÜRGENSON, E. 1958. Metabentonites in Estonian SSR. Institute of Geology, studies II, Academy of Sciences of the Estonian SSR, Tallinn, 73–85 (in Russian).

JÜRGENSON, E. 1964. Silurian metabentonites of Estonian SSR. In *Litologiya Paleozojskikh otlozhenij Éstonii*, 87–100. Institute of Geology, Tallinn (in Russian).

KALLASTE, T. 2002. Eesti ja Läti paleosoilistest metabentoniitidest pärineva sanidiini mineraloogilised uuringud. TTÜ magistritöö.

KIIPLI, T., KIIPLI, E. & KALLASTE, T. 1997. Metabentonite composition related to sedimentary facies in the Lower Silurian of Estonia. *Proc. Estonian Acad. Sci. Geol.*, **46**, 93–104.

KIIPLI, T., MÄNNIK, P., BATCHELOR, R. A., KIIPLI, E., KALLASTE, T. & PERENS, H. 2001. Correlation of Telychian (Silurian) altered volcanic ash beds in Estonia, Sweden and Norway. *Norwegian Journal of Geology,* **81***,* 179–194.

KIIPLI, E., KALLASTE, T., KIIPLI, T. 2004. Metabentonites of the Pirgu Stage (Ashgill, Upper Ordovician) of the East Baltic. In conference materials: abstracts and field guidebook: WOGOGOB-2004: 8th Meeting of the Working Group on the Ordovician Geology of Baltoscandia: 13-18 May 2004, Tallinn and Tartu, Estonia. Editors: Hints, O., Ainsaar, L., Tartu University Press, 53–54.

Kiipli, T., Kallaste, T. 2006a. Wenlock and uppermost Llandovery bentonites as stratigraphic markers in Estonia, Latvia and Sweden. *GFF*, **128**, 139 - 146.

KIIPLI, T., KIIPLI, E., KALLASTE, T., HINTS, R., SOMELAR, P., KIRSIMÄE, K. 2007. Altered volcanic ash as an indicator of marine environment, reflecting pH and sedimentation rate - example from the Ordovician Kinnekulle bed of Baltoscandia. *Clays and Clay Minerals*, **55**, 177–188.

KIIPLI, T., KALLASTE, T. 2001. Volcanogenic interbed. Põldvere, A. (Editor). Estonian Geological Sections: Bulletin 3. Valga (10) drill core (16–17). Tallinn: Geological Survey of Estonia

KIIPLI, T., KALLASTE, T. 2002. Characteristics of volcanism. Põldvere, A. (Editor). Soovälja (K-1) drill core (17–21). Tallinn: Geological Survey of Estonia

KIIPLI, T., KALLASTE, T. 2003. Altered volcanic ash beds. Põldvere, A. (Editor). Ruhnu (500) drill core (31–33). Tallinn: Geological Survey of Estonia

KIIPLI, T., KALLASTE, T. 2005. Characteristics of Ordovician volcanic ash beds. Põldvere, A. (Editor). Mehikoorma (421) drill core (27–30). Tallinn: Geological Survey of Estonia

KIIPLI, T., KALLASTE, T., KIIPLI, E., ORLOVA, K. 2006b. Upper Ordovician volcanic ash beds. Põldvere, A. (Editor). Kerguta (565) drill core (15–18). Tallinn: Geological Survey of Estonia

KIIPLI, T., ORLOVA, K., KALLASTE, T. 2008a. Upper Ordovician altered volcanic ash beds. In: Männamaa (F-367) drill core (Põldvere, A., ed.). Estonian Geological Sections, 9, 29–32.

KIIPLI, T., JEPPSSON, L., KALLASTE, T., SÖDERLUND, U. 2008b. Correlation of Silurian bentonites from Gotland and the eastern Baltic using sanidine phenocryst composition and biostratigraphical consequences. *Journal of the Geological Society*, **165**, 211 - 220.

KIIPLI, T., KALLASTE, T., KLEESMENT, A., NIELSEN, A. 2009. Corroded hydrothermal quartz in Ordovician altered volcanic ash beds of the Baltoscandian Region. *Estonian Journal of Earth Sciences*, **58**, 268 - 272.

KIIPLI, T., KALLASTE, T., VOOLMA, M. 2010. Volcanic ash beds. Põldvere, A. (Editor). Estonian Geological Sections. Viki drill core. (26–27). Tallinn: Geological Survey of Estonia

KIIPLI, T., EINASTO, R., KALLASTE, T., NESTOR, V., PERENS, H., SIIR, S. 2011. Geochemistry and correlation of volcanic ash beds from Rootsiküla Stage (Wenlock-Ludlow) in the eastern Baltic. *Estonian Journal of Earth Sciences*, **60**, 207–219.

KIIPLI, T., KALLASTE, T., KIIPLI, E. & RADZEVIČIUS, S. 2013a. Correlation of Silurian bentonites based on the immobile elements in the East Baltic and Scandinavia. *GFF*, **135**, 152–161.

KIIPLI, T., SOESOO, A. & KALLASTE, T. 2013b in press. Geochemical evolution of Caledonian volcanism recorded in the sedimentary rocks of the eastern Baltic region. From: Corfu, F., Gasser, D. & Chew, D. M. (eds) New Perspectives on the Caledonides of Scandinavia and Related Areas. Geological Society, London, Special Publications, **390**.

KIIPLI, T., RADZEVIČIUS, S & KALLASTE, T. 2014. Silurian bentonites in Lithuania: correlations based on sanidine phenocryst composition and graptolite biozonation – interpretation of volcanic source regions. *Estonian J. of Earth Sciences*, **63**, 18-29.

KROLL, H., RIBBE P. H. 1987. Determining (Al,Si) distribution and strain in alkali feldspars using lattice parameters and diffraction-peak positions: A review, *Amer. Mineral*., **72**

ORVILLE, P. M. 1967. Unit-cell parameters of the microcline-low albite and the sanidine-high albite solid solution series. *American Mineralogist,* **52***,* 55–86.

PEARCE, R. B. 1995. The geochemistry of Llandovery and Wenlock age K-bentonites in the Southern Uplands. *Scottish Journal of Geology*, **31**, 23–28.

RAY, D.C., COLLINGS, A.J., WORTON, G.J. & JONES, G. 2011. Upper Wenlock bentonites from Wren's Nest Hill, Dudley: comparisons with prominent bentonites along Wenlock Edge, Shropshire, England. *Geological Magazine*, **148**, 670–681.

SELL, B., AINSAAR, L. & LESLIE, S. 2013. Precise timing of the Late Ordovician (Sandbian) super-eruptions and associated environmental, biological, and climatological events. *Journal of the Geological Society*, **170**, 711–714.

SNÄLL, S. 1977. Silurian and Ordovician bentonites of Gotland (Sweden). *Stockholm Contrib. Geol.*, **31**.

SOMELAR, P., KIRSIMÄE, K., ŚRODOŃ, J. 2009. Mixed-layer illite-smectite in the Kinnekulle K-bentonite, northern Baltic Basin. *Clay Minerals*, **44**, 455 - 468.

SOMELAR, P., KIRSIMÄE, K., HINTS, R., KIRS, J. 2010. Illitization of early Paleozoic K-bentonites in the baltic basin: decoupling of burial- and fluid-driven processes. *Clays and Clay Minerals*, **58** , 388-398.

THORSLUND, P. 1945. Om bentonitlager i Sveriges kambrosilur. *Geologiska Föreningens i Stockholm Förhandlingar*, **67**, 286–288 (in Swedish).

VINGISAAR, P. 1972. On the distribution of the main metabentonite stratum (d; XXII) in the Middle Ordovician of Baltoscandia. *Proceedings of the Academy of Sciences of the Estonian SSR, Chemistry, Geology*, **21**, 62–70 (in Russian).

VINGISAAR, P. MURNIKOVA, T. 1973. New data on the mineralogy of some Estonian Lower Caradocian metabentonites. *Proceedings of the Academy of Sciences of the Estonian SSR, Chemistry, Geology*, **22**, 149–158 (in Russian).

WILLIAMS, L. B., SRODON, J., HUFF, W. D., CLAUER, N., HERVIG, R. L. 2013. Light element distributions (N, B, Li) in Baltic Basin bentonites record organic sources. *Geochimica et Cosmochimica Acta*, **120**, 582–599.

ABSTRACT

Pyroclastic sanidine in the Lower Palaeozoic bentonites – a tool for regional geological correlations

Around 800 samples of Ordovician and Silurian bentonites were studied by X-ray diffractometry (XRD) and X-ray fluorescence method. Major part of samples was collected from the Estonia–Latvia–Lithuania–Gotland (Sweden) region. In grain fractions separated from the clay-rich bentonites pyroclastic sanidine often occurs as one of the major components. Composition of the sanidine was analysed by the precise measurements of the $20\bar{1}$ reflection. Content of $(Na,Ca)Si_3O_8$ in sanidine in different bentonites varies between 20 and 58 mol%. The composition of the sanidine is typical for a particular eruption and enables to prove the correlations between sections. In the best studied Telychian Stage over 20 well characterized correlative bentonites were established in Estonia and Latvia. Some correlations were extended also to Lithuania and Gotland. Correlation of bentonites enabled to trace changes of bentonite composition through different facies – from feldspathic tuffs in shallow water facies through illite smectite domination in transition zone to the kaolinite-rich bentonites in deep-sea environments. Accordingly, concentrations of immobile elements also change being the highest in deep-sea facies due to the highest residual enrichment. Several significant refinements of stratigraphy were achieved at the level of the Aeronian/Telychian, Llandovery/Wenlock and Wenlock/Ludlow boundaries. Applicability of the method is restricted to the bentonites where sanidine is present and by the regional distribution of bentonites. Currently, the method is successfully used in the East Baltic and Gotland. Sanidine was not found in bentonites from Bornholm, Oslo Region, Ukraine and Siberia.

KOKKUVÕTE

Püroklastiline sanidiin Alam-Paleosoikumi bentoniitides – regionaalstratigraafia uus töövahend

Röntgendifraktomeetria- (XRD) ja röntgenfluorestsentsmeetoditega uuriti ~800 Ordoviitsiumi ja Siluri bentoniidiproovi. Põhiosa proovidest oli pärit Eesti–Läti–Leedu–Gotlandi regioonist, kus bentoniidid sisaldavad püroklastilist sanidiini. Savikatest bentoniitidest separeeritud terafraktsioonis on püroklastiline sanidiin sageli üheks põhikomponentidest. Sanidiini koostis määrati XRD meetodil $20\bar{1}$ refleksi asukoha täpse mõõtmisega. $(Na,Ca)Si_3O_8$ komponendi osa erinevate bentoniitide sanidiinis varieerub 20–58 mol%, see on konkreetse vulkaanipurske iseloomulik tunnus ja annab võimaluse bentoniitide rööbistamiseks. Sanidiini analüüside baasil koostati Telychi bentoniitide tabel, mis sisaldab üle 20 usaldusväärse korrelatsiooni Eestist Lätisse, lisaks mõned ka Leetu ja Gotlandile. Bentoniitide korreleerimine võimaldas jälgida ühele vulkaanipurskele vastava kihi koostise muutumist läbi erinevate settefaatsieste – madalaveelisest päevakivitufist sügavaveelise kaoliniidirikkani, üleminekuvööndis domineerib illiit-smektiit. Bentoniitide koostise muutumisega kaasneb ka immobiilsete mikroelementide kontsentratsioonide suurenemine sügavaveelises faatsieses, mis on põhjustatud suuremast jääkrikastuse efektist seal. Bentoniitide abil saavutati olulisi täpsustusi läbilõigete korreleerimisel Aeronian/Telychian, Llandovery/Wenlock ja Wenlock/Ludlow piiride tasemel. Kirjeldatud meetodi kasutusvõimalused on siiski piiratud tuhapilvede regionaalse levikuga ja püroklastilise sanidiini olemasoluga bentoniitides. Seni on meetodit edukalt kasutatud Ida-Baltikumis ja Gotlandil. Sanidiini otsingud Bornholmi, Oslo piirkonna, Ukraina ja Siberi Ordoviitsiumi-Siluri bentoniitidest ei andnud positiivset tulemust.

ELULOOKIRJELDUS

Isikuandmed

Ees- ja perekonnanimi: Toivo Kallaste
Sünniaeg ja -koht: 19.03.1956 Eestis
Kodakondsus: Eesti
E-posti aadress: Toivo.Kallaste@ttu.ee

Hariduskäik

Tallinna Tehnikaülikool, 2002, magistrikraad (teaduskraad)
Tartu Riiklik Ülikool, 1979, füüsika

Keelteoskus

Inglise keel	algtase
Vene keel	kesktase
Saksa keel	algtase

Teenistuskäik

Alates 1979 TA Geoloogia Instituut (praegu TTÜ Geoloogia Instituut) – insener, vaneminsener, teadur

Teadustegevus ja juhendatud lõputööd

Teadustegevuse valdkonnaks on geokeemia ja röntgendifraktomeetria meetod mineraloogias.
Juhendatud TTÜ bakalaureusetöö: Siim Pajusaar, 2014

CURRICULUM VITAE

Personal data

Name: Toivo Kallaste
Date and place of birth: 19.03.1956 Estonia
E-mail address: Toivo.Kallaste@ttu.ee

Education

Tallinn University of Technology, 2002, Master of Science
University of Tartu, 1979, physics

Language competence

English	basic skills
Russian	average
German	basic skills

Professional employment

Since 1979 Institute of Geology (now Institute of Geology at TUT) – engineer, senior engineer, scientist

Research activity and thesis supervised

Main scientific interest: geochemistry and XRD mineralogy
TUT bachelor thesis supervised: Siim Pajusaar, 2014

PAPER I

KIIPLI, T., KALLASTE, T. 2002. Correlation of Telychian sections from shallow to deep sea facies in Estonia and Latvia based on the sanidine composition of bentonites. Proceedings of the Estonian Academy of Sciences. Geology, 51(3), 143–156.

Proc. Estonian Acad. Sci. Geol., 2002, **51**, 3, 143–156

Correlation of Telychian sections from shallow to deep sea facies in Estonia and Latvia based on the sanidine composition of bentonites

Tarmo Kiipli[a] and Toivo Kallaste[b]

[a] Mining Institute, Tallinn Technical University, Kopli 82, 10142 Tallinn, Estonia; tarmo.kiipli@egk.ee
[b] Institute of Geology, Tallinn Technical University, Estonia pst. 7, 10143 Tallinn, Estonia; kallaste@egk.ee

Received 22 October 2001, in revised form 23 January 2002

Abstract. Sanidine composition of 130 samples of bentonites from 12 sections of Telychian (some possibly Sheinwoodian) age was analysed by X-ray diffractometry for correlation purposes. Solid solution of magmatic sanidine contained 20–47% $NaAlSi_3O_8$ molecules. The sanidine composition is very individual for many beds and can be used successfully for correlations.

Key words: sanidine, bentonites, correlation, Silurian.

INTRODUCTION

The idea that volcanic ash beds in sedimentary sections can be used as perfect time markers for correlations was proposed long ago (e.g. Spjeldnæs 1959). Although now tephrochronology is used successfully in Quaternary geology and archaeology, identification of coeval ash beds in the Palaeozoic rocks appears to be more complicated. The reason is that the ash consists mainly of unstable amorphous material which recrystallizes easily in exogenic environments. As a result, various clay minerals and other authigenic silicates form (Ross & Shannon 1926; Grim & Güven 1978; Altaner et al. 1984; Caballero et al. 1992; Huff et al. 1996; Kiipli et al. 1997). Therefore, main chemical components and minerals cannot be used directly for correlation of ancient volcanic beds. Some elements exhibit low mobility in exogenic environments and can be used for restoring source magma in altered volcanic rocks (Winchester & Floyd 1977). Correlation on the basis of immobile trace elements has been successfully used in many works (Huff & Kolata 1989; Batchelor & Jeppsson 1994; Bergström et al. 1995; Kiipli et al. 2001). Attempts to correlate ash beds from different facies may still

fail due to the variable degree of residual enrichment of material with immobile elements in different environments. Also, no element can be strictly defined as immobile – even the low mobility elements can move to some extent. The study of trace magmatic minerals allows us to overcome these problems and to identify the bentonites. In the present study we used the composition of magmatic sanidine to recognize coeval volcanic beds in different sections.

TELYCHIAN SECTIONS IN ESTONIA AND LATVIA

The Llandovery–Wenlock boundary interval in Estonia, corresponding to a relatively high sea level period (Johnson et al. 1991), is represented by up to 95 m thick claystones and marlstones lying between nodular limestones (Rumba Formation) and reef and lagoonal dolostones (Jaagarahu and Muhu formations). In these rocks the Adavere and Jaani regional stages are distinguished (Fig. 1). The former has been correlated with the Upper Llandovery and the latter with the Lower Wenlock (Aaloe 1960; Kaljo 1962; Nestor 1997). In a relatively homogeneous claystone–marlstone sequence the boundary of these regional stages is often placed at different levels in different sections, and even in one section. For example, in the Viki core this boundary has been established at the following depths: 153.8 m (Jeppsson & Männik 1993), 135 m (Nestor 1994, fig. 14), 145.8 m (Nestor 1994, table 4 combined with fig. 3; Nestor 1997, fig. 65), 133.5 m (Nestor 1997, fig. 69). The cause of such indistinctness is different palaeontological or lithological criteria used by different authors. The original criterion for this boundary used by Aaloe (1960) was the uppermost one of the volcanic ash beds in the interval of their frequent occurrence. In the Viki core, it lies at 145.7 m, close to the beginning of the *Pterospathodus amorphognathoides amorphognathoides* conodont Zone (Kiipli et al. 2001).

In the Ohesaare core, represented by the graptolite facies, the Llandovery–Wenlock boundary was placed at the volcanic ash bed at a depth of 345.8 m. *Cyrtograptus murchisoni* occurs 0.7 m above this ash bed (Kaljo 1962). Later,

INTERNATIONAL SERIES	ESTONIA		LATVIA
	REGIONAL STAGES	FORMATIONS	FORMATIONS
Wenlock	Jaagarahu	Jaagarahu	Riga
	Jaani	Jaani	
Llandovery	Adavere	Velise	Jurmala
		Rumba	Dobele
	Raikküla	Raikküla	

Fig. 1. Stratigraphic chart according to Nestor (1997) and Kaljo et al. (1998).

the lowermost findings of this graptolite have been identified as *Cyrtograptus centrifugus* (Loydell et al. 1998). This level lies in the middle of the *Pterospathodus amorphognathoides amorphognathoides* Zone (Loydell et al. 1998, and correlation of bentonites in the present study), therefore clearly higher than the Adavere–Jaani boundary in the northern, shallower palaeoshelf sections.

In Latvia, Telychian sections are represented by red, grey, and variegated claystones above dark organic-rich argillites of the Dobele Formation. The upper boundary is not marked lithologically and can be established only by the appearance of Wenlock graptolites.

MATERIAL AND METHODS

A total of 130 samples from 12 cores were studied from volcanic beds with a thickness between 0.2 and 25 cm (Fig. 2). The same samples from six cores, representing relatively shallow palaeosea facies, were formerly used in Kiipli et al. (2001) for correlating sections on the basis of immobile trace elements. Two

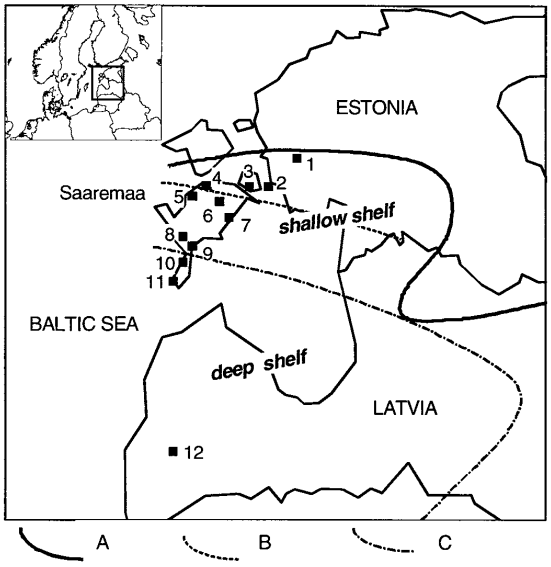

Fig. 2. Location of the studied sections and distribution of Velise sediments. A, erosional margin of Velise sediments; B, boundary between calcareous marlstones and carbonate claystones; C, boundary between carbonate claystones and claystones. 1, Kirikuküla; 2, Viirelaid; 3, Lõetsa; 4, Pahapilli; 5, Mustjala; 6, Valjala; 7, Nässumaa; 8, Viki; 9, Tehumardi; 10, Kaugatuma; 11, Ohesaare; 12, Aizpute.

sections of the present study (Aizpute and Ohesaare) are located in the deep shelf facies and one (Kaugatuma) lies near the boundary between the deep and shallow shelf facies. Mineralogy of volcanic beds is different from that of host rock. In the volcanic beds illite-smectite, kaolinite, and potassium feldspar (authigenic K-sanidine) dominate. The host rock is composed mainly of illite, potassium feldspar (orthoclase), and terrigenous quartz. Coarse fractions contain euhedral and broken magmatic quartz, biotite, and K–Na sanidine. The estimated content of magmatic phenocrysts was 1–10% of the bulk sediment. According to Kastner (1971) and Kastner & Siever (1979), sedimentary authigenic feldspars have a pure end member composition. Sanidine formation in magmatic processes, on the contrary, is characterized by a variable K to Na ratio in solid solution. Therefore, for correlation purposes we studied magmatic K–Na sanidine. The presence of sanidine of variable composition in Silurian bentonites of Gotland was established by Snäll (1977), but was not used for correlation of sections.

Sample preparation

About 1–5 g of a sample was suspended ultrasonically in distilled water and after 20 s the clay suspension was poured out. If kaolinite was still present in coarse fraction, it was disperged ultrasonically in 20% KOH solution and poured out. The residue was treated by hot 2N HCl solution, to clean the sample of hematite, calcite, apatite, and products of pyrite oxidation (gypsum, Fe-sulphates). The cleaned coarse fraction still contained, besides magmatic minerals (K–Na sanidine, quartz, biotite, zircon), also authigenic K-sanidine, pyrite or chalcopyrite. In a few samples barite occurred. The content of these minerals varied largely. Sulphides were removed by nitric acid. If the sample was large enough, the 0.04–0.1 mm and 0.1–0.25 mm fractions were separated by sieving. Pyroclastic grains larger than 0.25 mm were not found. The 0.1–0.25 mm fraction was present only in some beds, 0.04–0.1 mm fraction was established in all beds and therefore suits best for correlation studies. The fine (<0.04 mm) fraction is not suitable for the study of magmatic sanidine due to a higher content of authigenic K-sanidine, which complicates also analysis of coarser fractions. In the case of feldspathites (volcanogenic interbeds consisting mostly of authigenic potassium feldspar), it is impossible to achieve the concentration of magmatic phenocrysts sufficient for detailed study. For XRD analysis the sample was ground by hand in an agate mortar and a slurry mount was prepared using ethyl alcohol and glass slide.

Measurements

Measurements were performed on the HZG-4 diffractometer (Freiberger Präzisionmechanik) using Fe-filtered Co-radiation. All samples were routinely scanned from 5 to 45° 2θ before any treatment in order to check their volcanic origin and estimate the mineralogical composition. From the separated fraction

the $20\bar{1}$ reflection of sanidine was measured with maximum accuracy. An angle range from 23.5 to 26.0° 2θ was scanned with the step size 0.01° 2θ; the measuring time was 15 s per point. This range includes the 100 reflection of quartz, the $20\bar{1}$ reflection of various feldspar phases, and also 4.18 and 4.13 Å reflections of kaolinite. Therefore, removal of kaolinite from the sample before measurements is essential.

Calculation of the sanidine composition

A curve-fitting programme performed in MathCad 2000 was applied for calculating the exact peak position, half-width, and intensity. The measured X-ray pattern was fitted with convolution of mineral reflection and instrumental profile. The profile of quartz heated for 7 h at 800 °C was used as instrumental profile. The peak position, half-width, and intensity were calculated for four components: quartz, K-sanidine, and two K–Na sanidines. The K–Na sanidine peak position was calculated in relation to quartz or K-sanidine, depending on which of these minerals dominated in a specimen. The angle distance between quartz and K-sanidine reflections appeared to be constant, pointing to the stable composition of both minerals. Only rare traces of plagioclase were detected and therefore plagioclase reflection was not included in curve-fitting. Examples of the measured diffractograms are shown in Fig. 3.

The content of $NaAlSi_3O_8$ in mol% in K–Na sanidine was calculated according to Orville (1967), who established that the position of the $20\bar{1}$ reflection almost linearly depends on the composition of sanidine solid solution. Fast cooling of volcanic ash avoids exsolution of feldspar and favours the preservation of magmatic sanidine; therefore calculation of the feldspar composition according to the method proposed by Orville can be estimated as accurate. In perthites, calculation of the sanidine composition on the basis of only the $20\bar{1}$ reflection can lead to imprecise results because of the strain between two feldspar phases (Stewart & Wright 1974). Late recrystallization of magmatic sanidine resulting in perthite formation supposedly did not take place because the rocks have not been heated more than 50–100 °C during the geological history, as indicated by the alteration index of conodonts, which varies between 1 and 2 in the Silurian and Ordovician rocks of Estonia (Männik & Viira 1990). The precision of the analysis of the K–Na sanidine composition is ±1% in favourable cases (low intensity of authigenic feldspar reflection, no kaolinite, high intensity of the magmatic sanidine reflection) and ±2% in less favourable cases.

RESULTS

K–Na sanidine of various composition was found, containing 20–47 mol% $NaAlSi_3O_8$. In a few bentonite samples magmatic sanidine was at the level of the detection limit. Magmatic sanidine was not found in terrigenous samples. The

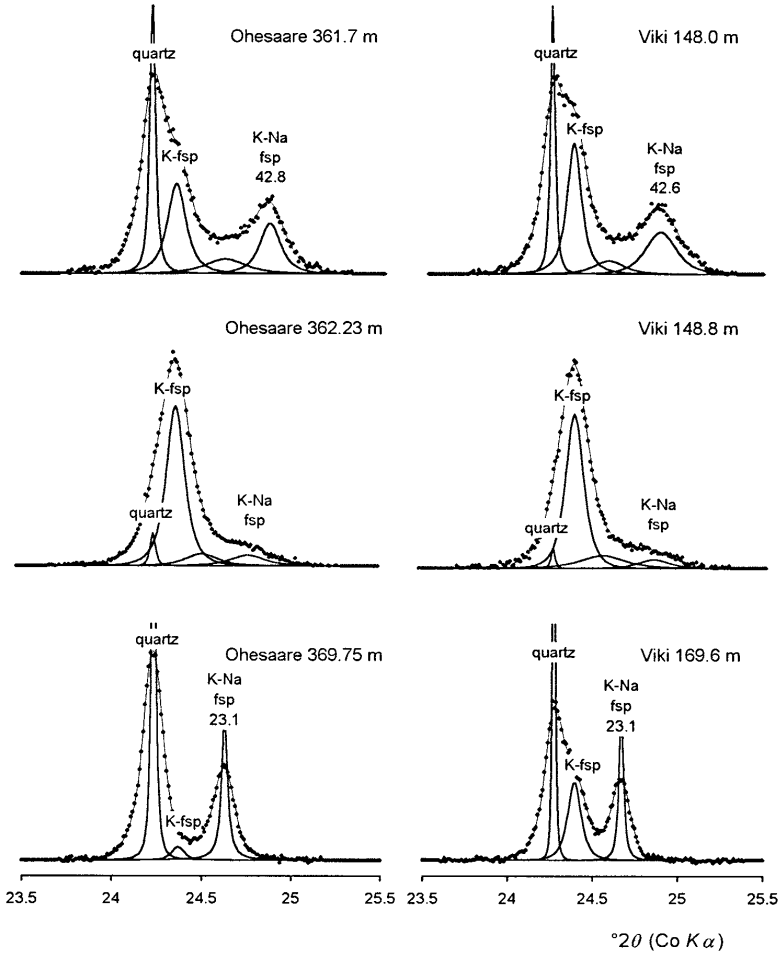

Fig. 3. Examples of measured X-ray diffraction patterns from 23.5 to 25.5 deg 2θ (Fe-filtered Co-radiation). The measured curve is marked with dots. Solid curves represent the result of curve-fitting. The uppermost and lowermost examples represent K–Na sanidine with sharp reflection, allowing good correlations. The intermediate examples represent K–Na sanidine with wide reflection impossible to use for correlation. K-fsp = K-feldspar; K–Na fsp = K–Na feldspar; the number shows the content of $NaAlSi_3O_8$ in mol% in sanidine.

rest of the volcanic samples contained a measurable amount of K–Na sanidine. Two groups of samples can be distinguished: (1) The samples exhibiting a wide elevated interval in XRD spectra without a specific well distinguishable reflection. This type can be interpreted as containing a mixture of K–Na sanidine of variable composition. Correlation of this type is not certain and can be done with some probability between beds with signs allowing better identification. Twelve of the studied beds show this type of sanidine pattern. (2) The samples exhibiting well measurable reflections and allowing calculations of the K–Na sanidine composition. These beds can be found and correlated in the studied sections with a high level of probability. Twenty-three of the studied beds revealed well measurable sanidine reflections. The reflection width varied largely and in case of wide reflections the XRD pattern was transitional between two types. Commonly, even in the presence of a sharp K–Na sanidine peak, a wide elevated region in spectra was observed. Therefore, curve-fitting with three components (quartz, K-sanidine, and one K–Na sanidine) was only rarely satisfactory, but four-component fitting revealed good results in all cases (Fig. 3). Twenty-nine volcanic beds are correlated in at least two core sections; 18 of these can be identified in four or more sections. Eight volcanic beds were identified only in one section (Table 2). A total of 37 volcanic beds were established in the Telychian sequence of Estonia and Latvia. The maximum number of volcanic beds in a single section is 23 (Ohesaare). In Table 1 two formerly published numbering systems are presented (Kiipli 1998; Kiipli et al. 2001), both beginning with zero (0) which designates the bentonite well known in Estonia as “O”. This bed was named Osmundsberg K-bentonite by Bergström et al. (1998). With only a few corrections correlations by sanidine compositions well correspond to the correlations formerly performed by trace elements (Kiipli et al. 2001). Present correlations well concord with biostratigraphy (Jeppsson & Männik 1993; Loydell et al. 1998) but allow also some refinements in the correlation of graptolite and conodont biozones. More detailed biostratigraphical analysis is currently under preparation.

SOME PROBLEMS

Until the bed has been identified in at least two sections, its stratigraphic position cannot be considered as proved. For example, in the Mustjala core two beds, at 115.87 and 117.80 m, can be well characterized by their sanidine compositions, but in other cores beds with a similar composition have opposite succession. The bed at 115.87 m in Mustjala can be correlated with the bed at 191.95 m in Tehumardi and the bed at 117.80 m in Mustjala with the bed at 190.30 m in Tehumardi. Thus, this part of the Mustjala core is possibly not in right order in the core box or one of these beds is new in Mustjala, not found in other cores. Considering graphic correlations based on currently available information, we chose a preliminary correlation as presented in Tables 1 and 2.

Table 1. Correlated volcanic beds (rows) from the studied core sections (depth in metres)

Bed No. (Kiipli 1998)	Bed No. (Kiipli et al. 2001)	Kiriku-küla*	Viire-laid*	Lõetsa*	Paha-pilli*	Valjala*	Must-jala	Nässu-maa*	Viki*
25	29					**113.80**			
24	28								**115.02**
23	27				**20.85**	**119.80**			**121.03**
	new						**69.80**		**131.10**
22	26	**12.59**					**82.08**	**199.70**	**145.75**
20	23	15.80	**65.90**	**44.40**	**40.30**			**200.70**	**147.50**
19	21								**148.00**
18	22	**17.20**					**85.40**		**148.80**
17	19	**17.85**	**66.60**	**45.10**			**85.79**	**201.80**	149.40
	18		67.75						151.80
16	17		68.30	**47.20**	**45.20**				
14	16				46.20				**152.10**
	new								
12	15	**28.25**			51.50		**94.00**		**156.80**
	new								
	14		**76.45**						
11	13		**76.70**	**56.80**	**61.70**		**105.95**	**219.40**	**169.60**
9	12		**77.60**	**57.70**	64.60		**109.63**		**171.95**
8	11		**78.11**		**65.65**	153.40			**173.10**
7	10		**78.20**				**111.95**		**174.40**
6	9		**78.48**		**67.00**				**175.55**
5	7		**79.13**		**68.50**				
	6		**79.38**						
4	5								**178.80**
	new						**117.80**		
3	4								**181.80**
2	3				**72.20**				**182.30**
1	2								**184.35**
0	0	**38.16**	85.00	**66.00**	**78.35**	**165.40**	124.70	**235.10**	**185.10**

Table 1. *Continued*

Bed No. (Kiipli 1998)	Bed No. (Kiipli et al. 2001)	Tehumardi	Kaugatuma	Ohesaare	Aizpute	Main component of K–Na sanidine	
						$NaAlSi_3O_8$, mol%	Width of the reflection, deg
						Much of biotite and quartz, little sanidine	
25	29			**340.76**			
24	28		**236.90**	**342.08**	**917.10**	35.2–35.8	0.19–0.34
23	27		**243.20**	**345.83**	**925.80**	38–40	0.25–0.35
	new		**256.00**	**351.72**	**931.80**	36.2–37.8	0.08–0.12
22	26	**163.91**	258.90	359.31		Very wide reflection	
20	23			**361.30**		45.2–46.3	0.12–0.20
19	21		**261.10**	**361.70**	**938.00**	42.0–42.8	0.18–0.27
18	22	**165.90**		**362.23**	**941.35**	Very wide reflection	
17	19	**166.70**	**261.50**	**362.46**		45.7–46.4	0.05–0.09
	18		263.10	364.76	**943.90**	Very wide reflection	
16	17			365.08	**946.90**	Very wide reflection	
14	16				**950.10**	Very wide reflection	
	new		**264.80**	367.39	**951.20**	45.0–45.8	0.12–0.17
12	15	**170.30**	264.90	**367.60**	**951.70**	Very wide reflection	
	new			369.12	**953.99**	45.5	0.09
	14			369.72		22.6	0.05
11	13		**267.00**	**369.75**	**954.20**	22.9–23.3	0.04–0.06
						Much of biotite and quartz, little sanidine	
9	12		**267.10**				
8	11	**184.03**		**369.98**	**957.10**	38.7–40.3	0.10–0.16
7	10	**185.10**	**267.20**		**957.75**	25.8–26.7	0.07–0.10
6	9	**185.80**		**370.09**		25.5–26.2	0.25–0.30
5	7	**186.70**		**370.44**		20.5–24.1	0.30–0.34
	6	**187.65**		**370.63**	**960.20**	28.1–28.8	0.07–0.08
4	5	**188.10**				40.1–40.6	0.17–0.19
	new	**190.30**	**268.60**			24.5–25.3	0.05–0.11
3	4					Very wide reflection	
2	3	**191.95**		**370.77**		45.2–47.6	0.12–0.17
1	2				**963.80**	Very wide reflection	
0	0	**193.70**	**269.60**		**964.40**	20.7–21.5	0.05–0.09

Bold – volcanic beds where sanidine was studied; normal font – beds correlated by trace elements; small font – supposed correlations.

* Cores where trace elements were studied in volcanic beds (Kiipli 1998; Kiipli & Tsegelnjuk 2001).

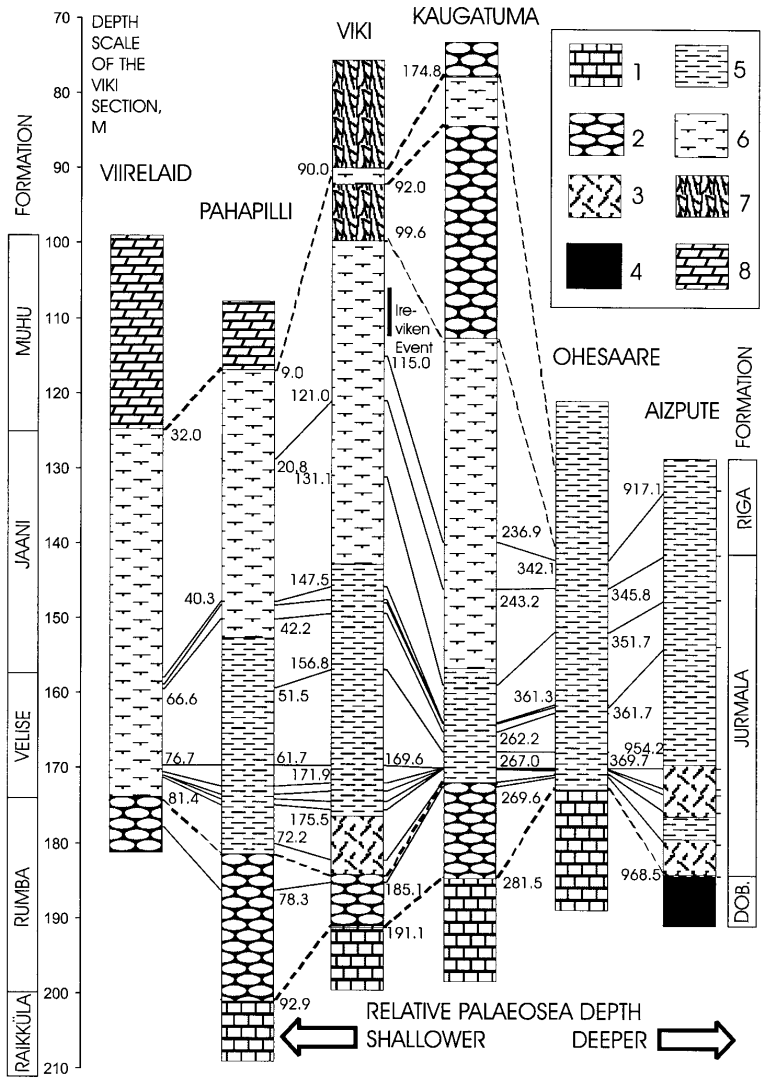

Fig. 4. Correlation of the studied sections. 1, micritic limestone; 2, nodular wackestone; 3, red and variegated shales; 4, dark organic-rich shales; 5, grey shales; 6, marlstones; 7, reef and breccia dolostones; 8, microcrystalline bedded dolostone. Solid lines show volcanic ash correlations and dashed lines show litho- and biostratigraphic correlations. DOB. = Dobele Formation.

Table 2. List of volcanic beds not correlated with other sections

Bed No. (Kiipli 1998)	Bed No. (Kiipli et al. 2001)	Core	Depth, m	Main component of K–Na sanidine	
				$NaAlSi_3O_8$, mol%	Width of the reflection, deg
21	25	Kirikuküla	15.50	Very wide reflection	
	4	Viirelaid	79.44	26.2	0.26
		Mustjala	115.87	47.3	0.12
		Tehumardi	179.90	Very wide reflection	
		Kaugatuma	262.20	46.6	0.08
		Ohesaare	370.99	35.3	0.19
		Aizpute	956.30	Very wide reflection	
–1	–1	Pahapilli	83.85	Very wide reflection	

Several volcanic beds of the Aizpute core with wide reflections are correlated only tentatively with other sections as their sanidine composition does not allow us to prove or refute correlations. Trace elements that helped correlation of these beds in Saaremaa have not been analysed in Aizpute. On the other hand, the number of beds with wide reflections at close stratigraphical levels is similar in Saaremaa and Aizpute (5 and 6, respectively). In Table 1 the supposed preliminary correlation is given with smaller font. The bed at 953.99 m in Aizpute, containing sanidine with a high sodium content, and the bed at 369.12 m in Ohesaare with high Nb and Zr (Kiipli & Kallaste 1996) were correlated by analogy with other beds with high Nb and Zr contents and sodium-rich sanidine (beds 2, 17, 19, 20, Kiipli 1998). Direct correlation using the same criterion is not possible as no more sample material for analyses is available from these beds.

Depths of volcanic beds above 940 m in the Aizpute section must be considered as conventional, as drilling depth records allow different interpretations in the range ±2–3 m. Comparison with biostratigraphic analyses is possible only by using sampling markers on core boxes.

Sanidine from 370.77 m in Ohesaare shows a somewhat different diffractogram for bed 2 compared to the others. It has a characteristic sharp peak, but also a wide tail-like reflection. It was noticed in the process of the preparation of the sample that this thin bed consisted of two visually different parts. Therefore we suppose that the sample consists of a mixture of two successive eruptions (beds 2 and 3) and sediment thickness between these beds is reduced to zero in Ohesaare (0.5 m in the Viki core).

CONCLUSIONS

1. The composition of magmatic K–Na sanidine in volcanic ash beds is a valuable tool for identification of coeval beds in sections, allowing crossing the facies boundaries.

2. Correlations of volcanic ash beds of shallow shelf sections and the deep shelf Ohesaare section generally confirm but enable also some refinements of graptolite- and conodont-based correlations by Loydell et al. (1998).

3. Correlations based on many volcanic beds reveal sedimentological features (condensation of sedimentation, facies movements) difficult to establish by other methods.

ACKNOWLEDGEMENTS

We thank the referees D. Kaljo and S. Snäll for useful remarks which considerably improved the manuscript. Financial support for this research was provided by the Estonian Science Foundation (grant No. 4070).

REFERENCES

Aaloe, A. 1960. New research into the Silurian stratigraphy of Estonia. *Eesti TA Geol. Inst. Uurimused*, **5**, 123–141 (in Russian).

Altaner, S. P., Hower, J., Whitney, G. & Aronson, J. L. 1984. Model for K-bentonite formation: evidence from zoned K-bentonites in the disturbed belt, Montana. *Geology*, **12**, 412–415.

Batchelor, R. A. & Jeppsson, L. 1994. Late Llandovery bentonites from Gotland, Sweden, as chemostratigraphic markers. *J. Geol. Soc. London*, **151**, 741–746.

Bergström, S. M., Huff, W. D., Kolata, D. R. & Bauert, H. 1995. Nomenclature, stratigraphy, chemical fingerprinting, and areal distribution of some Middle Ordovician K-bentonites in Baltoscandia. *GFF*, **117**, 1–13.

Bergström, S. M., Huff, W. D. & Kolata, D. R. 1998. The Lower Silurian Osmundsberg K-bentonite. Part I: stratigraphic position, distribution, and palaeogeographic significance. *Geol. Mag.*, **135**, 1–13.

Caballero, E., Reyes, E., Delgado, A., Huertas, F. & Linares, J. 1992. The formation of bentonite: mass balance effects. *Appl. Clay Sci.*, **6**, 265–276.

Grim, R. E. & Güven, N. 1978. Bentonites. Geology, mineralogy, properties and uses. *Developments Sedimentol.*, **24**.

Huff, W. D., & Kolata, D. R. 1989. Correlation of K-bentonite beds by chemical fingeprinting using multivariate statistics. In *Quantitative Dynamic Stratigraphy* (Cross, T. A., ed.), pp. 567–577. Prentice Hall.

Huff, W. D., Kolata, D. R., Bergström, S. M. & Zhang, Y.-S. 1996. Large-magnitude Middle Ordovician volcanic ash falls in North America and Europe: dimensions, emplacement and post emplacement characteristics. *J. Volcanol. Geothermal Res.*, **73**, 285–301.

Jeppsson, L. & Männik, P. 1993. High resolution correlations between Gotland and Estonia near the base of the Wenlock. *Terra Nova*, **5**, 348–358.

Johnson, M. E., Baarli, B. G., Nestor, H., Rubel, M., & Worsley, D. 1991. Eustatic sea level patterns from the Lower Silurian (Llandovery Series) of Southern Norway and Estonia. *Geol. Soc. Amer. Bull.*, **103**, 315–335.

Kaljo, D. 1962. On the boundary of the Llandoverian and Wenlockian in the East Baltic. *Eesti TA Geol. Inst. Uurimused*, **10**, 97–113 (in Russian).

Kaljo, D., Kiipli, T. & Martma, T. 1998. Correlation of carbon isotope events and environmental cyclicity in the East Baltic Silurian. In *Silurian Cycles* (Landing, E. & Johnson, M. E., eds.). *New York State Mus. Bull.*, 491, 297–312.

Kastner, M. 1971. Authigenic feldspars in carbonate rocks. *Amer. Mineral.*, **56**, 1403–1442.
Kastner, M. & Siever, R. 1979. Low temperature feldspars in sedimentary rocks. *Amer. J. Sci.*, **279**, 435–479.
Kiipli, E. & Kallaste, T. 1996. Geochemical characterization of some Estonian metabentonites. *Proc. Estonian Acad. Sci. Geol.*, **45**, 68–77.
Kiipli, T. 1998. Vulkanogeensed kihid Eesti settekivimites. In *60 aastat mäeinseneride õpetamist Eestis* (Reinsalu, E., ed.), pp. 9–12. Tallinna Tehnikaülikool Mäeinstituut, Tallinn.
Kiipli, T. & Tsegelnjuk, P. D. 2001. Rare metals in volcanic ash beds in Silurian sedimentary sections of Estonia, Ukraine and Moldova – application for correlations between regions. In *Rare Metals in Ukraine – View to the Future* (Galetsky, L. S., ed.), pp. 59–61. Acad. Sci. Ukraine, Kiev.
Kiipli, T., Kiipli, E. & Kallaste, T. 1997. Metabentonite composition related to sedimentary facies in the Lower Silurian of Estonia. *Proc. Estonian Acad. Sci. Geol.*, **46**, 93–104.
Kiipli, T., Männik, P., Batchelor, R. A., Kiipli, E., Kallaste, T. & Perens, H. 2001. Correlation of Telychian (Silurian) altered volcanic ash beds in Estonia, Gotland and Norway. *Norwegian J. Geol.*, **81**, 179–193.
Loydell, D. K., Kaljo, D. & Männik, P. 1998. Integrated biostratigraphy of the lower Silurian of the Ohesaare core, Saaremaa, Estonia. *Geol. Mag.*, **135**, 769–783.
Männik, P. & Viira, V. 1990. Conodonts. In *Field Meeting Estonia 1990. An Excursion Guidebook* (Kaljo, D. & Nestor, H., eds.), pp. 84–89. Inst. Geol. Estonian Acad. Sci., Tallinn.
Nestor, H. 1997. Silurian. In *Geology and Mineral Resources of Estonia* (Raukas, A. & Teedumäe, A., eds.), pp. 89–106. Estonian Acad. Publ., Tallinn.
Nestor, V. 1994. Early Silurian chitinozoans of Estonia and North Latvia. *Academia*, **4**, Estonian Acad. Publ., Tallinn.
Orville, P. M. 1967. Unit cell parameters of the microcline – low-albite and the sanidine high-albite solid solution series. *Amer. Mineral.*, **52**, 55–86.
Ross, C. S. & Shannon, E. V. 1926. Minerals of bentonite and related clays and their physical properties. *J. Amer. Ceramic Soc.*, **9**, 77–96.
Spjeldnæs, N. 1959. Silurian bentonites from Gotland, Sweden. *GFF*, **81**, 582–587.
Snäll, S. 1977. Silurian and Ordovician bentonites of Gotland (Sweden). *Stockholm Contrib. Geol.*, **31**.
Stewart, D. B. & Wright, T. L. 1974. Al/Si order and symmetry of natural alkali feldspars, and the relationship of strained cell parameters to bulk composition. *Bull. Soc. Fr. Mineral. Crystallogr.*, **97**, 336–377.
Winchester, J. A. & Floyd, P. A. 1977. Geochemical discrimination of different magma series and their differentiation products using immobile elements. *Chem. Geol.*, **20**, 325–343.

Eesti ja Läti madal- ja süvamere faatsieste Telychi läbilõigete korrelatsioon bentoniitide sanidiini koostise alusel

Tarmo Kiipli ja Toivo Kallaste

Röntgendifraktomeetriliselt on uuritud 12-st Adavere ja Jaani lademe läbilõikest kogutud 130 bentoniidiproovi sanidiini koostist. Selgus, et magmalises sanidiinis esineb 20–47 mol% $NaAlSi_3O_8$ komponenti. Sanidiini seesugune koostis on iseloomulik paljudele vulkaanilistele kihtidele ja seda saab kasutada eri läbilõigete korreleerimisel.

Корреляция теличских мелко- и глубоководных разрезов Эстонии и Латвии по составу санидина в бентонитах

Тармо Кийпли и Тойво Калласте

Методом рентгеновской дифракции изучено 130 проб бентонитов в целях определения в них состава санидина. Установлено, что содержание молекул натриевого полевого шпата в санидине варьирует от 20 до 47 мол%. Каждый вулканический слой имеет свой, только ему присущий состав санидина, а поэтому может быть успешно использован для корреляции этих слоев в отдельных разрезах.

PAPER II

KIIPLI, T., KALLASTE, T. 2005. Characteristics of Ordovician volcanic ash beds. Põldvere, A. (Editor). Mehikoorma (421) drill core (27–30). Tallinn: Geological Survey of Estonia

CHARACTERISTICS OF ORDOVICIAN VOLCANIC ASH BEDS

The Mehikoorma (421) section is located in the marginal area of the known occurrence of volcanic ashbeds (Fig. 6). The Kinnekulle K-bentonite bed, which in the West Estonian islands reaches a thickness of 50–70 cm, has been identified in the Mehikoorma section only as a 2 cm thick interbed at a depth of 306.7 m.

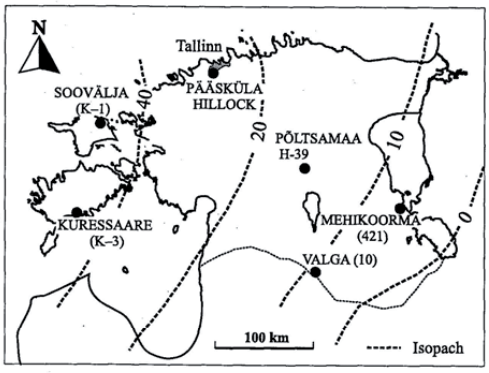

Fig. 6. Distribution of the Kinnekulle K-bentonite (isopachs given after Vingisaar 1972 and Bergström *et al.* 1995) and location of the sections mentioned in the text.

Ten argillaceous beds of suspected volcanogenic origin were sampled and analysed in the Mehikoorma (421) core. Samples were taken mostly from 0.5–15 cm thick interbeds. The chemical composition and trace elements were analysed by the XRF method (Appendix 30). Major components (in wt%) of the Kinnekulle K-bentonite bed (SiO_2 – 54.50; TiO_2 – 0.50; Al_2O_3 – 17.70; Fe_2O_3 – 3.78; MnO – 0.035; CaO – 4.62; Na_2O – 0.11; K_2O – 8.56; P_2O_5 – 0.053; LOI – 7.40) were analysed at the Laboratory of All-Union Geological Institute (VSEGEI) in St. Petersburg.

The Na content of K–Na sanidine was analysed by XRD (Table 1) as in our earlier studies (Kiipli & Kallaste 2002a, 2003). From the separated 0.04–0.1 mm fraction the $20\bar{1}$ reflection of sanidine was measured with maximum accuracy. An angular range from 23.5 to 26.0 °2θ was scanned with a step size of 0.01 °2θ; the measuring time was 15 s per point. The content of $NaAlSi_3O_8$ (in mol%) in K–Na sanidine was calculated according to Orville (1967), who established that the position of the $20\bar{1}$ reflection depends almost linearly on the composition of the sanidine solid solution. The precision of the analysis of the K–Na sanidine composition is ±1% in favourable cases (low intensity of authigenic feldspar reflection, no kaolinite, high intensity of the reflection of interest), and ±2% in less favourable cases. Correlation of separate beds over a wide area is based on the properties of magmatic K–Na sanidine and trace element distribution.

XRD and XRF analyses revealed mixed volcanogenic-terrigenous material in almost all samples. High CaO contents (Fig. 7) in these samples give evidence of the occurrence of biogenic and mechanically transported material. Pure K-bentonite was found only in a 1 cm thick bed at a depth of 311.4 m (Table 1). In most cases depositional environments and diagenetic processes caused the mixing of materials from different sources. Nevertheless, pyroclastic minerals have usually a larger grain size than terrigenous material and can be separated relatively easily.

Authigenic K-feldspar, often seriously retarding separation of pyroclastic K–Na sanidine in other regions of Estonia, can be easily disintegrated in the Mehikoorma (421) core samples after dissolution of carbonate. This compositional property enables analysis of pyroclastic sanidine even in samples with a high content of authigenic feldspar. The main obstacle for the correlation of Caradocian volcanic beds arises from the lack or low concentration of K–Na sanidine in most bentonites (Kiipli & Kallaste 2002b).

Table 1. Correlation of volcanic ash beds of the Soovälja (K–1), Mehikoorma (421) and Kuressaare (K–3) cores

Complexes by Bergström *et al*. (1995)	Regional stage	Soovälja (K–1)				Mehikoorma (421)			Kuressaare (K–3)		
		Sample depth (m)	No. of bed on core box	Biotite: – absent, (+) rare, + present, ++ abundant	$NaAlSi_3O_8$ in sanidine* (mol%), shape of the 20 Ī reflection	Sample depth (m)	Biotite: – absent, (+) rare, + present, ++ abundant	$NaAlSi_3O_8$ in sanidine* (mol%), shape of the 20 Ī reflection	Sample depth (m)	Biotite: – absent, (+) rare, + present, ++ abundant	$NaAlSi_3O_8$ in sanidine* (mol%), shape of the 20 Ī reflection
	Pirgu					251.80	+	37.6			
Grimstorp	**Keila**					**306.00**	++	–	**367.70**	++	**Weak reflection**
Kinnekulle	**Keila**	**173.10**		+	**24.5****	**306.70**	++	**25.2**	**368.50**		
Sinsen	**Haljala**								**369.20**	+	**21.6**
	Haljala	177.22	1	(+)	Weak reflection						
	Haljala	**177.45**	**2**	+	**22.1****	**310.90**	+	**22.4**	**370.50**	+	**20.8**
	Haljala	**177.62**	**3**	(+)	**Wide reflection**	**311.00**	(+)	**Wide reflection**	**370.70**	(+)	**Wide reflection**
	Haljala	178.00	4	–	Wide reflection						
	Haljala	178.83	5	not examined	–	311.15	+	Weak reflection			
	Haljala	178.90	6	–	Wide reflection						
	Haljala	179.10	7	–	Wide reflection						
	Haljala	180.32	8	–	Wide reflection	311.40	(+)	Wide reflection	372.20	–	Weak reflection
	Haljala	180.90	9	–	–						
	Haljala	181.02	10	–	Wide reflection						
Grefsen	Haljala	181.40	11	+	Wide reflection						
	Haljala	181.70	12	(+)	Wide reflection						
	Haljala	181.90	13	–	Weak reflection						
	Haljala	182.60	14	–	–	311.44	not examined	–			
	Haljala	185.32	15	–	Wide reflection						
	Haljala					311.70	–	Wide reflection			
	Haljala	186.40	16	–	Wide reflection						
	Haljala	197.21	17	(+)	Wide reflection	311.90	+	Weak reflection			
	Haljala	198.25	18	+	Wide reflection						
	Haljala	203.03	19	++	–						
	Haljala	255.98	20	–	–						

* K–Na sanidine 20 Î reflection was studied using the two-component model, only the main component is included in the table.

** in Kiipli & Kallaste (2002b) erroneously average values of the bed were published.

Well established correlations are in bold type, possible, but not proved correlations are in ordinary type. Samples collected by Tarmo Kiipli and Toivo Kallaste (Geological Survey of Estonia), analysed at the Laboratory of the Institute of Geology at Tallinn University of Technology.

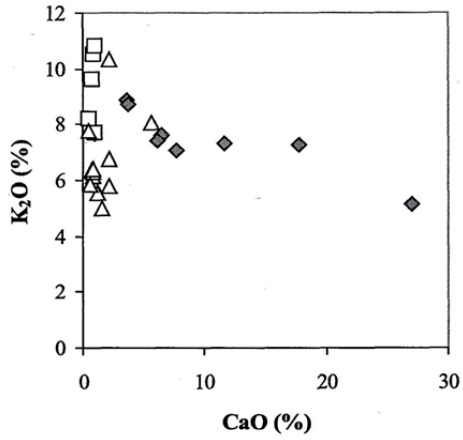

Fig. 7. CaO content versus K_2O content in studied samples.
Triangles – Soovälja (K–1), dark rhombs – Mehikoorma (421), quadrangles – Kuressaare (K–3) bentonites. High K_2O content indicates volcanic origin (typical content of terrigenous rocks is 4–5%). In the Mehikoorma (421) bentonites are rich in CaO.

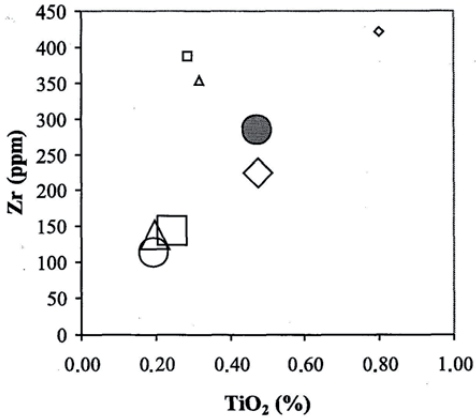

Fig. 8. TiO_2 content versus Zr content in two correlated K-bentonites.
Triangles – Soovälja (K–1), rhombs – Mehikoorma (421), quadrangles – Kuressaare (K–3), filled circle –Valga (10) cores (Kiipli & Kallaste 2001) and empty circle – Pääsküla Hillock (Hints *et al.* 1997). Large symbols – Kinnekulle K-bentonite bed. Small symbols – Grefsen K-bentonite (Soovälja (K–1) at 177.62 m, Mehikoorma (421) at 311.0 m and Kuressaare (K–3) at 370.70 m). Higher TiO_2 concentrations in Mehikoorma (421) K-bentonites are due to large amounts of terrigenous admixture. Zr content is higher in the K-bentonite from the upper part of the Grefsen complex.

Use of immobile trace elements for correlations is strongly hindered by the presence of terrigenous material in volcanogenic bentonites. For example, TiO_2 and Ba contents (Fig. 8, Appendix 30, see St. Petersburg analyses above) are much higher in the Mehikoorma (421) core bentonites than in the correlated beds of the Kuressaare (K–3) and Soovälja (K–1) cores (see Kiipli & Kallaste 2002b). This is caused by higher concentrations of Ti and Ba in terrigenous material compared to the volcanogenic material of many ash beds. Therefore concentrations of these elements should be used with some reservations. It seems that Zr and Y concentrations in the Mehikoorma bentonites (Appendix 30) are less influenced by terrigenous material, possibly due to their close concentrations in terrigenous and volcanogenic material.

A sample from the Pirgu Stage (depth 251.8 m, Appendix 1, sheet 9) was taken from a polished bedding plane, which points to an unusually soft and thin interbed lost during drilling. Provisional study showed dolomite as the main component of the sample, but the residue obtained after dissolution of carbonate material contained much authigenic K-feldspar and some biotite flakes. K–Na sanidine measurement revealed a weak, but enough distinctive 20$\bar{1}$ reflex, from which we calculated the value of 37.6 mol% sodium feldspar in sanidine solid solution. Such a K–Na-feldspar composition correlates with that of the bentonite from the lower part of the Pirgu Stage, where sanidine contains 37–39 mol% Na (e.g. Põltsamaa H–39 core, depth 177.1 m; Kiipli *et al.* 2004).

Similarly to the Soovälja (K–1) section (Kiipli & Kallaste 2002b), magmatic cycles can be recognized on the basis of the Zr/TiO_2 ratio in Caradocian volcanic beds of the Mehikoorma (421) section (Appendix 1, sheet 11; Fig. 9). In the Mehikoorma (421) core we can probably distinguish the two upper cycles identified in the Soovälja (K–1) core.

The upper cycle includes some beds from the upper part of the Grefsen complex (depths 310.9 and 311.15 m), and the Kinnekulle (306.7 m) and Grimstorp (306.0 m) beds. Bentonites in this magmatic cycle are characterized by the presence or even high content of biotite (Table 1) and often also by magmatic K–Na sanidine having a specific composition. The content of sanidine containing 22.4–25.2 mol%

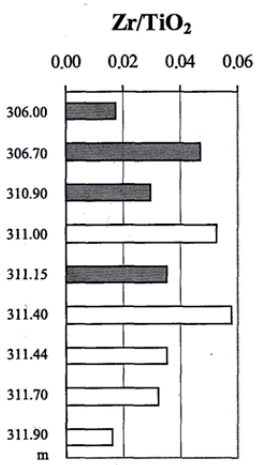

Fig. 9. Zr/TiO_2 in Mehikoorma (421) K-bentonites. Empty bars – lower cycle, filled bars – upper cycle. The upper cycle begins earlier than the lower ends, which probably indicates the formation of a new volcano.

NaAl Si_3O_8 varies largely in Caradocian volcanic ash beds, being high in Kinnekulle (depth 306.7 m) and in one of the upper Grefsen bentonites (depth 310.90 m) and only rarely detectable in other beds (Table 1). The Grimstorp bentonite can be recognized by its remarkably high biotite content and by large pyroclastic biotite and quartz grains in it. The Sinsen bentonite (not registered in the Mehikoorma (421) core) from the Kuressaare (K–3) core (depth 369.2 m; 21.6 mol% NaAl Si_3O_8) is very similar to the Upper Grefsen bentonite from the Soovälja (K–1) core (depth 177.45 m; No. 2 on the core box, Table 1) and can be identified with certainty only if both beds are present.

Bentonites of the lower magmatic cycle (medium cycle in the Soovälja (K–1) core) in the Mehikoorma (421) core are characterized by the absence or low content of biotite and a wide K–Na sanidine reflection $20\bar{1}$ (Table 1), which allows no reliable correlations on the basis of XRD patterns. In this cycle we can observe a well-developed magma differentiation cycle beginning with TiO_2-rich ash beds and ending with Zr-rich beds (see Appendix 30). An interesting new aspect is that the upper cycle begins before (volcanogenic bed at 311.15 m) the lower cycle ends (depth 311.0 m). This phenomenon needs to be checked in other sections. A preliminary conclusion is that these two cycles do not originate from the evolution of the same magma chamber inside the same volcano. Thus we can suggest the appearance of a new volcanic centre before the activity ended in the old centre.

The high content of TiO_2 (1.47%; Appendix 30) in the sample from 311.7 m indicates possible correlation with the lower part of the medium magmatic cycle in the Soovälja (K–1) section (interval 181.67–186.4 m; see Kiipli & Kallaste 2002b), but the trace element spectra of the sample do not fit with any of these beds. Thus we suppose we found a new bed, not yet registered in the Soovälja (K–1) core.

PAPER III

KALLASTE, T., KIIPLI, T. 2006. New correlations of Telychian (Silurian) bentonites in Estonia. Proceedings of the Estonian Academy of Sciences. Geology, 55(3), 241–251.

Proc. Estonian Acad. Sci. Geol., 2006, **55**, 3, 241–251

New correlations of Telychian (Silurian) bentonites in Estonia

Toivo Kallaste and Tarmo Kiipli

Institute of Geology at Tallinn University of Technology, Estonia pst. 7, 10143 Tallinn, Estonia; tarmo.kiipli@lx.egk.ee

Received 18 May 2006, in revised form 27 June 2006

Abstract. Seventy-seven Telychian bentonite samples from six drill-core sections were correlated on the basis of their sanidine composition. In total, bentonites from 43 volcanic eruptions, of which six are new discoveries, were established in the Telychian of Estonia. Names and identification (ID) codes were assigned to the bentonites. The different distribution patterns of volcanic ash thicknesses indicate different source volcanoes. Lack of several bentonites near the transition between the Rumba and Velise formations and at the Llandovery–Wenlock boundary indicates sedimentary hiatuses in the eastern part of the studied area.

Key words: bentonite, K-bentonite, Telychian, sanidine, correlation.

INTRODUCTION

The use of bentonites in the correlation of geological sections offers a unique possibility for recognition of exactly the same time levels in several outcrop and drill-core sections (e.g. Einasto et al. 1972). Limestones (Rumba Formation) and marlstones (Velise Formation) of the Adavere Stage contain a large number of thin altered volcanic ash beds – bentonites (Jürgenson 1964). These regional stratigraphic units belong to the Telychian Stage of the international stratigraphic scheme (Bergström et al. 1998; Nestor & Nestor 2002; Kiipli et al. 2006). The sanidine composition has been studied in twelve drill-cores with an aim to identify the ash beds in the Telychian of Estonia. The results show that the volcanogenic interbeds originate from at least 37 different eruptions (Kiipli et al. 2001; Kiipli & Kallaste 2002), although the greatest number of bentonite interbeds found in one section is only 22.

The aims of bentonite study are precise correlation of sections, mapping of the distribution of bentonites, and restoration of wind directions at the eruption time and locations of source volcanoes. Herein, we are going to report the results

obtained through the study of bentonites in six new sections using the same method as in Kiipli & Kallaste (2002). To bring some clarity to this rather difficult and confused subject, identification (ID) codes were assigned to all the identified bentonites. Names were given to more widespread bentonites.

MATERIAL AND METHODS

Seventy-seven bentonite samples from six drill-cores (see Fig. 1) were collected from 0.2–20 cm thick interbeds, which differed from their host marlstones and limestones in their soft clayish consistency and/or in colour. The abundance of biotite flakes was a good criterion for recognizing volcanogenic bentonites in situ. For correlation purposes, the data on bentonites studied earlier in the

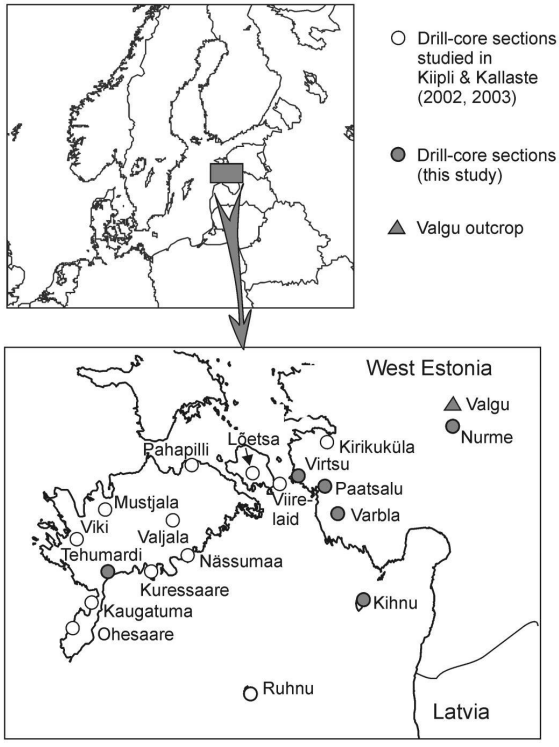

Fig. 1. Location of the studied sections.

Ohesaare, Viki, and Ruhnu sections were used (Kiipli & Kallaste 2002, 2003). The lithology and distribution of microfossils of many studied sections are discussed in Einasto et al. (1972), Jeppsson & Männik (1993), Nestor (1994), and Hints et al. (2006).

All bulk samples were scanned by X-ray diffractometry (XRD) from 5 to 45 degrees using Co Kα radiation. The occurrence of illite-smectite and/or kaolinite reflections was considered as an indication of volcanogenic material. Some volcanogenic interbeds had a high content of authigenic potassium feldspar. A low content or absence of quartz was typical of bulk volcanogenic bentonite material.

The Na content of K–Na sanidine was studied by XRD (Kiipli & Kallaste 2002). From the separated 0.04–0.1 mm fraction the range from 23.5 to 26.0 °2θ was scanned using Co Kα radiation with the step size of 0.01 °2θ; the measuring time was 15 s per point. The content of $NaAlSi_3O_8$ in K–Na sanidine (in mol %) was calculated according to Orville (1967), who established that the position of the $20\bar{1}$ reflection almost linearly depends on the composition of sanidine solid solution. The precision of the analysis of the K–Na sanidine composition was ±1% in favourable cases (low intensity of authigenic feldspar reflection, no kaolinite, high intensity of the reflection of interest) and ±2% in less favourable cases. Separate beds were correlated on the basis of the magmatic K–Na sanidine composition (Table 1). As several bentonites may have the same sanidine composition, graphic correlation between sections was applied to improve the probability of correlations.

RESULTS

The $NaAlSi_3O_8$ content of sanidine varied from 21 mol % in the Osmundsberg Bentonite to 45–48 mol % in the Valgu, Ruhnu, and Viki bentonites. The width of the sanidine reflection varied from sharp (0.05–0.15 °2θ; indicating homogeneous sanidine composition) to very wide (exceeding 0.35 °2θ). Such wide reflections were difficult to characterize in numerical values and were described as wide or very wide (Table 1). A wide sanidine reflection clearly discriminates a particular bentonite from those with sharp reflections, but is useless for discrimination between other bentonites with wide sanidine reflections. Wide reflections probably indicate heterogeneous (maybe zoned) sanidine crystals.

By combining sanidine properties and graphic correlation most of the studied bentonites can be correlated with volcanogenic interbeds established earlier in other drill-cores (Table 2). Many volcanic eruptions have been detected in more than five sections, thus their stratigraphic position among other bentonites is well proven. Compared with the earlier study (Kiipli & Kallaste 2002), six new volcanic eruptions have been established: ID 504, 720, 750, 773, 793, and 794, five of those only in one section. ID 504 was additionally found in the earlier studied Kaugatuma section at a depth of 262.2 m and possibly in the new Kihnu section in the lower part of the 10 cm thick bentonite at a depth of 211.95 m. The total number of Telychian volcanic eruptions recorded in Estonia is 43.

Table 1. Sanidine properties of Telychian bentonites

Identification numbers and names			Number of sections	Stage and formation	Pyroclastic K–Na sanidine, main component parameters	
Viki depth ID	Interpolated depth in the Viki core, m	Bentonite name			Width of the reflection (degrees) and other notes	Content of $NaAlSi_3O_8$ in sanidine, mol %
127	112.70	Ireviken	6	Jaani Stage	Much of biotite and quartz, little sanidine	
150	115.00	Lusklint	7	Mustjala	0.19–0.34	35.2–35.8
210	121.00	Ohesaare	6	Formation	0.25–0.35	38–40
311	131.10	Aizpute	6		0.08–0.12	36.2–37.8
457	145.75	Kirikuküla	10		Very wide reflection	
475	147.50	Viki	12		0.12–0.20	45.2–46.3
480	148.00	Kaugatuma	6		0.18–0.27	42.0–42.8
488	148.80	Kuressaare	8		Very wide reflection	
494	149.40	Ruhnu	14		0.05–0.09	45.7–46.4
504	150.40		2		0.08–0.20	45.6–46.6
518	151.80	Viirelaid	10		Very wide reflection	
520	152.00	Lõetsa	10		Very wide reflection	
521	152.10		8?		Very wide reflection	
564	156.40		3		0.12–0.17	45.0–45.8
568	156.80		10?		Very wide reflection	
569	156.90		1		0.07	29.0
658	165.80		2		0.09	45.5
682	168.20		2		Very wide reflection	
693	169.30		2		0.05	22.6
696	169.60	Nässumaa	13	Adavere Stage	0.04–0.06	22.9–23.3
719	171.95	Virtsu	12	Velise	Much of biotite and quartz, little sanidine	
720	172.00		1	Formation	0.085–0.122	26.5–28.0
722	172.20		2		26.5 + wide reflection	
731	173.10	Nurme	13		0.10–0.16	38.7–40.3
744	174.40	Tehumardi	11		0.07–0.10	25.8–26.7
750	175.00		1		Wide reflection	
755	175.55	Paatsalu	8		0.25–0.30	25.5–26.2
772	177.20	Pahapilli	8		0.30–0.34	20.5–24.1
773	177.30		1		Feldspathic	
774	177.40		1		0.09–0.12	46.2–48.2
776	177.60		5		0.07–0.08	28.1–28.8
777	177.70		2		0.25–0.30	22.3–26.2
788	178.80		2		0.17–0.19	40.1–40.6
793	179.30		1		Biotite flakes on bedding plane	
794	179.40		1		0.12	43.7
795	179.50	Mustjala	6		0.05–0.11	24.5–25.3
800	180.00		2		Feldspathic	
805	180.50		2	Adavere Stage	Feldspathic	
818	181.80		3	Rumba–Velise	Very wide reflection	
823	182.30	Valgu	5	transition	0.12–0.17	45.2–47.6
841	184.15		2		0.19–0.22	35.5–35.8
843	184.35		3	Adavere Stage	Very wide reflection	
851	185.10	Osmundsberg	15	Rumba	0.05–0.09	20.7–21.5
880	188.00		4	Formation	Very wide reflection	

Table 2. Correlated Telychian bentonites in the studied core sections (depth in metres). Small font indicates that sanidine was not studied – graphic correlation was used. Provisional correlation is embraced by a frame

Viki depth ID	Viki	Kures-saare	Ohe-saare	Ruhnu	Kihnu	Varbla	Paat-salu	Virtsu	Nurme
127		158.30	340.76						
150	115.00	160.00	342.08						
210	121.00		345.83			134.90			
311	131.10		351.72	459.00		137.20			
457	145.75		359.31	467.60	211.20	139.40		68.55	
475	147.50		361.30	470.80	211.70	139.85	72.50	69.20	
480	148.00		361.70	471.80					
488	148.80	184.80	362.23	473.10					
494	149.40	185.40	362.46	473.70	211.85	140.28		69.50	
504					211.95				
518	151.80	187.40	364.76	478.90	212.20		73.70		
520		188.50					74.00	71.30	
521	152.10	189.50	365.08	478.90	214.50	141.50			
564			367.39						
568	156.80	193.75	367.60		215.70	143.25			
569					215.72				
658			369.12						
682		205.20							
693			369.72						
696	169.60		369.75	488.24	220.70	146.90		79.25	
719	171.95	205.40		488.30	221.70	148.00	80.80	80.20	
720				488.30					
722				488.40					
731	173.10		369.98	489.05	222.30	148.20	81.05	80.68	17.90
744	174.40			489.05	222.70	148.60	81.09		20.10
750		209.20							
755	175.55		370.09		223.10		81.50		21.10
772		210.20	370.44				82.00	81.40	23.45
773							82.10		
774		210.30							
776			370.63				82.40		
777							82.40		
788	178.80								
793							83.75		
794		212.70							
795		212.80				150.40	83.90		
800						150.75			
805									24.50
818	181.80	214.00	370.77						24.60
823	182.30		370.77						
841			370.99						
843	184.35								
851	185.10	215.70			228.40	155.60	88.20		
880		223.80				158.30			

BENTONITE IDENTIFICATION NUMBERS AND NAMES

The former bentonite ID numbers (Kiipli et al. 2001) started from 0 (Osmundsberg Bentonite) and were assigned in stratigraphic order up- and downward from it. However, difficulties arose when new bentonites were found, because no vacant numbers were available between the earlier known and numbered bentonites. Therefore, new bentonite finds were left without an ID number in Kiipli & Kallaste (2002).

In the present study, new stratigraphic ID numbers were assigned to all established bentonites. The ID numbers were derived from the projection of the bentonite stratigraphic position to the Viki drill-core depth scale. The number marks the depth in decimetres in the Viki section. For the sake of shortness, centimetres were discarded from the end of the depth number. Besides, 1000 decimetres were subtracted from the depth, as all bentonites occur between 1000 and 2000 decimetre depth. This combination resulted in a list of three-digit ID codes for bentonites (Tables 1–3). Any new bentonite find can be easily accommodated into this list. The Viki section was selected as a basis for deriving ID numbers

Table 3. Type localities of bentonites

Viki depth ID	ID (Kiipli et al. 2001)	Bentonite name	Type locality	Thick-ness, cm	Reference
127	29	Ireviken	Ireviken section, Gotland, Sweden	10	Batchelor & Jeppsson (1994)
150	28	Lusklint	Lusklint section, Gotland, Sweden	5	Batchelor & Jeppsson (1994)
210	27	Ohesaare	Ohesaare drill-core, depth 345.8 m	2	Kiipli & Kallaste (2006)
311		Aizpute	Aizpute drill-core, depth 931.8 m	1	Kiipli & Kallaste (2006)
457	26	Kirikuküla	Kirikuküla drill-core, depth 12.59 m		
475	23	Viki	Viki drill-core, depth 147.5 m	5	
480	21	Kaugatuma	Kaugatuma drill-core, depth 261.1 m	0.5	
488	22	Kuressaare	Kuressaare drill-core, depth 184.8 m	0.5	
494	19	Ruhnu	Ruhnu drill-core, depth 473.7 m	5	
518	18	Viirelaid	Viirelaid drill-core, depth 67.75 m	1	
520	17	Lõetsa	Lõetsa drill-core, depth 47.2 m	3	
696	13	Nässumaa	Nässumaa drill-core, depth 219.4 m		
719	12	Virtsu	Virtsu drill-core, depth 80.2 m	1	
731	11	Nurme	Nurme drill-core, depth 17.9 m	6	
744	10	Tehumardi	Tehumardi drill-core, depth 185.1 m	1.2	
755	9	Paatsalu	Paatsalu drill-core, depth 81.5 m	4	
772	7	Pahapilli	Pahapilli drill-core, depth 68.5 m	5	
795		Mustjala	Mustjala drill-core, depth 117.8 m		
823	3	Valgu	Valgu trench, Rapla district	3	
851	0	Osmundsberg	Osmundsberget, Central Sweden	115	Bergström et al. (1998)

because of the great thickness of the Telychian, large number of bentonites, and a well-established conodont biostratigraphy (Jeppsson & Männik 1993; Kiipli et al. 2001).

Names were assigned to 20 widespread bentonites recognized in more than five sections in Estonia (Table 3). Most of those were named after Estonian drill-cores where they were found. The Valgu Bentonite was named after the Valgu outcrop (Klaamann 1990) in southern Rapla District. The names of Osmundsberg, Lusklint, and Ireviken were applied on the basis of correlation with the described bentonites in the literature (Batchelor & Jeppsson 1994; Bergström et al. 1998). The most frequent (found in 10–15 sections) bentonites in Estonia are as follows: Osmundsberg (851), Tehumardi (744), Nurme (731), Virtsu (719), Nässumaa (696), Lõetsa (520), Viirelaid (518), Ruhnu (494), Viki (475), and Kirikuküla (457). Correlation of these and other named bentonites forms a well-proved framework, where the stratigraphic position of rarely occurring bentonites can be established.

DISCUSSIONS ON SEDIMENTOLOGY IN THE TELYCHIAN

Bentonites were formed from very fine-grained volcanic dust and are therefore rarely preserved in shallow-water sediments from where wave activity transports fine ash material to the deeper and quieter sedimentary environments. The Telychian sediments in Estonia are represented by relatively deep-water marlstones and limestones, containing therefore a large number of bentonites. Despite a presumed quiet sedimentary environment, the record of bentonites in these sediments is still uneven. As a maximum, only 22 out of the total of 43 bentonites were found in one core (Ohesaare). Although the completeness of an established bentonite record depends partly on the quality of drilling and the experience of the sample-collecting researcher, the studied material revealed some regularities in the natural distribution of bentonites (Kiipli & Kallaste 2002 and the present study):

1. The Ireviken and Lusklint bentonites occur only in the sections of south-western Saaremaa. They are lacking in eastern Saaremaa and mainland Estonia. Often even the Ohesaare and Aizpute bentonites are absent there. This gap in the bentonite record was probably caused by a break in sedimentation near the Llandovery–Wenlock boundary, which was also proposed on the basis of biostratigraphical evidence (Nestor & Nestor 2002, 2003). Now this is also confirmed by the distribution of bentonites.
2. In many drill-cores in the eastern part of the study area several bentonites are absent in the lower part of the Velise Formation and the Velise–Rumba transition interval. The most extensive gap in the bentonite records was established in the Ruhnu section, where even the bentonites of the Rumba Formation are entirely absent. In mainland Estonia, the Paatsalu section is the

only exception with its almost full record of bentonites in the lower part of the Velise Formation. The best records of bentonites in this interval were established in the southwestern part of Saaremaa Island (Tehumardi, Viki, and Ohesaare sections). This gap in the record of bentonites was possibly caused by a major hiatus in sedimentation near the Rumba–Velise boundary.

3. Correlation of bentonites from the Nurme section is provisional as all bentonites there are very rich in authigenic feldspar, which complicates seriously the analysis of sanidine. The Nurme and Tehumardi bentonites were identified on the basis of sanidine composition, but other bentonites were correlated only graphically.
4. Correlation of bentonites 518, 520, and 521 (embraced by the frame in Table 2) is provisional as these bentonites reveal similar wide sanidine reflections and occur closely in a section. The occurrence of at least three bentonites with similar properties at this level is proved by the Kuressaare section, where all three bentonites were found.
5. In some cases an extremely low rate of sedimentation caused the deposits of two succeeding eruptions to merge. As a result, the sanidine originating from those different eruptions occurs within a single volcanic ash bed. The examples are 731 + 744 (Nurme and Tehumardi bentonites) in the Ruhnu section and 823 (Valgu) + 818 bentonites in the Ohesaare section.
6. The occurrence of a mixed (823 + 818) bentonite in the Ohesaare section at 370.77 m, which in other sections is found in the Rumba–Velise transition interval, indicates the presence of a condensed marlstone section in Ohesaare (370.9–372.6 m) corresponding to the Rumba Formation in shallow-water sections.
7. The mapped thickness of the volcanic ash layer can provide useful information on the direction of wind at the time of eruption and location of the source volcano. Up to now only the Kinnekulle eruption layer (Caradoc) is well mapped over a large area in Baltoscandia (Vingisaar 1972; Bergström et al. 1995). A number of the Osmundsberg Bentonite outcrop sites were described by Bergström et al. (1998). The thickness map of the Osmundsberg Bentonite in Estonia, presented by Kiipli et al. (2006), indicates ash transport from the northwest. The thickness of three other Telychian bentonites in Estonia shows different distribution patterns (Fig. 2). The Ruhnu Bentonite is characterized by even distribution of thickness (3–5 cm). Possibly the source volcano was located so far that no changes could be observed within the small studied area measuring 150 km × 200 km. The thickness of the Nässumaa and Nurme bentonites decreases rapidly to the southeast, probably perpendicular to the ash cloud axis. If this interpretation is correct, the Nässumaa ash was transported from the southwest and the Nurme ash from the west.
8. Restricted distribution of several bentonites, including all new discoveries, can be explained by patchy sedimentation accompanied by areas of 0-sedimentation, small thickness of many bentonites complicating their identification, and loss of soft bentonite interbeds during drilling.

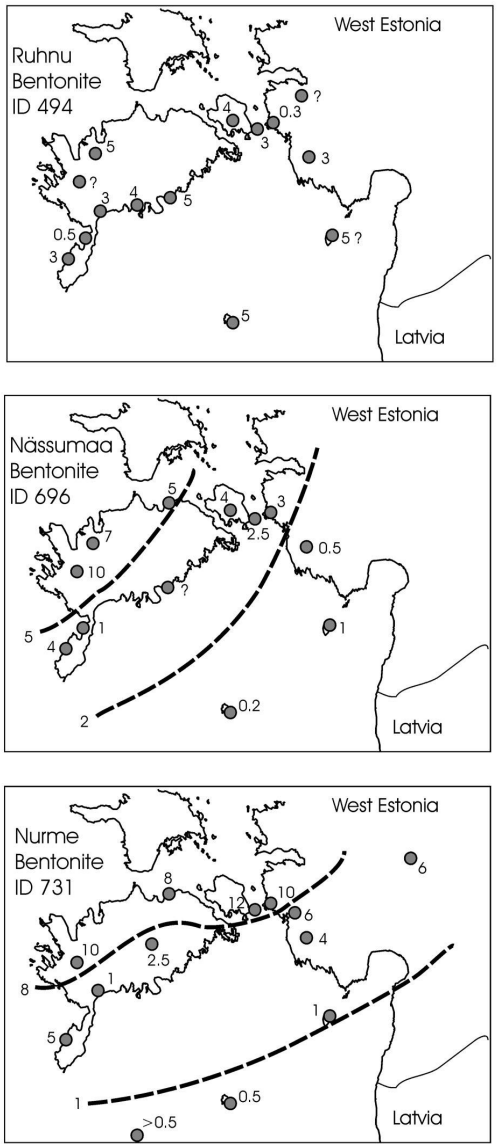

Fig. 2. Thickness (cm) distribution patterns of the Ruhnu, Nässumaa, and Nurme bentonites in Estonia.

CONCLUSIONS

The study of bentonites in new Telychian sections revealed a more complete volcanogenic record in Estonia including bentonites from 43 different volcanic eruptions. The assigned ID numbers and stratigraphic names make it easier to handle the information available on bentonites. New correlations enable us to trace gaps in the sedimentary record. Large hiatuses were confirmed at the transition of the Rumba and Velise formations and the Llandovery–Wenlock boundary. On the basis of the identification of bentonites, we assume that the deep-sea marlstone in the Ohesaare section correlates with the shallow-water Rumba Formation. Thickness distribution patterns of bentonites indicate volcanic ash transport from different directions and, correspondingly, from different sources.

ACKNOWLEDGEMENTS

This study is a contribution to IGCP project 503 and was supported by the Estonian Science Foundation (grants 5921, 6749, and target funding project 0332652s04). We are grateful to the referees D. Kaljo and R. A. Batchelor for useful comments and suggestions.

REFERENCES

Batchelor, R. A. & Jeppsson, L. 1994. Late Llandovery bentonites from Gotland, Sweden, as chemostratigraphic markers. *J. Geol. Soc. London*, **151**, 741–746.

Bergström, S. M., Huff, W. D., Kolata, D. R. & Bauert, H. 1995. Nomenclature, stratigraphy, chemical fingerprinting and areal distribution of some Middle Ordovician K-bentonites in Baltoscandia. *GFF*, **117**, 1–13.

Bergström, S. M., Huff, W. D. & Kolata, D. R. 1998. The Lower Silurian Osmundsberg K-bentonite. Part I: stratigraphic position, distribution, and palaeogeographic significance. *Geol. Mag.*, **135**, 1–13.

Einasto, R., Nestor, H., Kala, E. & Kajak, K. 1972. Correlation of the Upper Llandoverian sections in West Estonia. *Eesti NSV Tead. Akad. Toim. Keemia Geol.*, **21**, 333–343 (in Russian).

Hints, O., Killing, M., Männik, P. & Nestor, V. 2006. Frequency patterns of chitinozoans, scolecodonts, and conodonts in the upper Llandovery and lower Wenlock of the Paatsalu core, western Estonia. *Proc. Estonian Acad. Sci. Geol.*, **55**, 128–155.

Jürgenson, E. 1964. Silurian metabentonites of Estonian SSR. In *Litologiya Paleozojskikh otlozhenij Éstonii*, pp. 87–100. Institute of Geology, Tallinn (in Russian).

Jeppsson, L. & Männik, P. 1993. High resolution correlations between Gotland and Estonia near the base of the Wenlock. *Terra Nova*, **5**, 348–358.

Kiipli, E., Kiipli, T. & Kallaste, T. 2006. Identification of the O-bentonite in the deep shelf sections with implication on stratigraphy and lithofacies, East Baltic Silurian. *GFF* (submitted).

Kiipli, T. & Kallaste, T. 2002. Correlation of Telychian sections from shallow to deep sea facies in Estonia and Latvia based on the sanidine composition of bentonites. *Proc. Estonian Acad. Sci. Geol.*, **51**, 143–156.

Kiipli, T. & Kallaste, T. 2003. Altered volcanic ash beds. In *Ruhnu (500) Drill Core* (Põldvere, A., ed.), *Estonian Geol. Sections*, 5, 31–33.

Kiipli, T. & Kallaste, T. 2006. Wenlock and uppermost Llandovery bentonites as stratigraphic markers in Estonia, Latvia and Sweden. *GFF*, **128**, 139–146.
Kiipli, T., Männik, P., Batchelor, R. A., Kiipli, E., Kallaste, T. & Perens, H. 2001. Correlation of Telychian (Silurian) altered volcanic ash beds in Estonia, Sweden and Norway. *Norwegian J. Geol.*, **81**, 179–194.
Klaamann, E. 1990. Locality 8:3 Valgu outcrop. In *Field Meeting Estonia 1990* (Kaljo, D. & Nestor, H., eds), pp. 181–182. Estonian Academy of Sciences, Tallinn.
Nestor, H. & Nestor, V. 2002. Upper Llandovery to Middle Wenlock (Silurian) lithostratigraphy and chitinozoan biostratigraphy in southwestern Estonia and northernmost Latvia. *Proc. Estonian Acad. Sci. Geol.*, **51**, 67–87.
Nestor, H. & Nestor, V. 2003. Adavere lademe vanusest ja piiridest. In *Eesti Geoloogide neljas ülemaailmne kokkutulek. Eesti geoloogia uue sajandi künnisel. Konverentsi materjalid ja ekskursioonijuht* (Plado, J. & Puura, I., eds), pp. 53–55. EGS, TÜ Geoloogia Instituut.
Nestor, V. 1994. Early Silurian chitinozoans of Estonia and North Latvia. *Academia*, 4.
Orville, P. M. 1967. Unit-cell parameters of the microcline-low albite and the sanidine-high albite solid solution series. *Amer. Mineral.*, **52**, 55–86.
Vingisaar, P. 1972. On the distribution of the main metabentonite stratum (d, XXII) in the Middle Ordovician of Baltoscandia. *Eesti NSV Tead. Akad. Toim. Keemia Geol.*, **21**, 62–70 (in Russian).

Telychi (Silur) bentoniitide uued korrelatsioonid Eestis

Toivo Kallaste ja Tarmo Kiipli

Sanidiini koostise alusel on korreleeritud seitsekümmend seitse bentoniiti kuuest puursüdamikust. Kokku on kindlaks tehtud bentoniite neljakümne kolmest vulkaanipurskest. Avastatud on kuus uut bentoniiti. Bentoniitidele on omistatud stratigraafilised nimed ja ID-koodid. On diskuteeritud vulkaanilise tuha levikusuundade ja ümbriskivimi sedimentoloogia üle.

PAPER IV

KIIPLI, T., SOESOO, A., KALLASTE, T., KIIPLI, E. 2008. Geochemistry of Telychian (Silurian) K-bentonites in Estonia and Latvia. Journal of Volcanology and Geothermal Research, 171(1-2), 45–58.

Available online at www.sciencedirect.com
ScienceDirect
Journal of Volcanology and Geothermal Research 171 (2008) 45–58
Journal of volcanology and geothermal research
www.elsevier.com/locate/jvolgeores

Research paper

Geochemistry of Telichian (Silurian) K-bentonites in Estonia and Latvia

T. Kiipli *, A. Soesoo, T. Kallaste, E. Kiipli

Institute of Geology, Tallinn University of Technology, Ehitajate 5, 19086 Tallinn, Estonia

Received 4 June 2007; accepted 9 November 2007
Available online 22 November 2007

Abstract

In the Telychian section of Estonia and Latvia K-bentonites from 45 volcanic eruptions were discovered. The thickness of K-bentonite interbeds varies from a few millimetres to 20 cm. The sodium component concentration in sanidine phenocrysts measured by XRD ranges from 20 to 48 mol% and was used for establishing correlations. The Ti, Zr, Nb, Th and Sr concentrations and ratios show temporal trends indicating fractional crystallization in magma chambers. The analysis of biotite phenocrysts revealed magnesium and iron rich biotites in bentonites. Synthesis of these geochemical data enabled a classification of bentonites into seven geochemical types, which probably originate from seven different volcanic sources. Isopach schemes indicate ash transport from the west and north-west directions.

Keywords: K-bentonite; Caledonian volcanism; Silurian; Geochemistry; Sanidine; Biotite

1. Introduction

The main purpose of the article is to present results of geochemical study of altered volcanic ash beds (K-bentonites) in Telychian sections of Estonia and Latvia and to trace the geochemical history of Caledonian volcanism in northern Europe during this period. The Telychian Stage of the Silurian period covers the time interval approximately from 436 to 428 million years ago (Ogg, 2004). The Telychian sections in the Island of Saaremaa and South-West Estonia are located from 700 km to over 1000 km from active plate margins. Considering large distance to potential volcanic sources it is evident that all the ash beds recorded in Estonia and Latvia represent very large eruptions, although these beds are commonly only a few millimetres to few centimetres thick. The well-preserved Palaeozoic section in the Baltic area serves as a perfect geological note-book for reading the history of volcanism during the collisions of Avalonia, Baltica and Laurentia palaeocontinents. Previous studies of these altered ash beds included correlation and establishing the correct stratigraphic position of beds (Kiipli et al., 2001; Kiipli and Kallaste, 2002, 2006; Kallaste and Kiipli, 2006).

* Corresponding author. Tel.: +372 6203049; fax: +372 6203011.
E-mail addresses: tarmo.kiipli@gi.ee (T. Kiipli), alvar.soesoo@gi.ee (A. Soesoo), enli.kiipli@gi.ee (E. Kiipli).

0377-0273/$ - see front matter © 2007 Elsevier B.V. All rights reserved.
doi:10.1016/j.jvolgeores.2007.11.005

2. Material

Samples were collected from eighteen drill cores (226 samples) in Estonia and from the Aizpute drill core in Latvia (25 samples), (Fig. 1). For comparison, also some K-bentonite thickness data from the Ventspils and Vidale drill-cores were used. The thickness of K-bentonite interbeds varies mostly from 0.1–10 cm, reaching exceptionally 20 cm. In drill cores all interbeds with somewhat unusual consistency or colour were collected. The abundance of biotite flakes can be easily noticed during field work in many (but not in all) altered volcanic ash interbeds. Laboratory XRD study confirmed the volcanic origin showing illite–smectite, K-feldspar and/or kaolinite as the main minerals for most of samples. Samples which showed signs of terrigenous clays consisting mainly of illite, quartz and chlorite were discarded from further study.

2.1. Host rock lithology and geochemistry

In Estonia the Telychian corresponds to the Adavere Regional Stage, which consists of nodular argillaceous limestone of the Rumba Formation in the lower part and calcareous claystone of the Velise Formation in the middle and upper part. The lower part of the Jaani Stage (Mustjala Formation) consisting mostly of argillaceous marlstones belongs probably

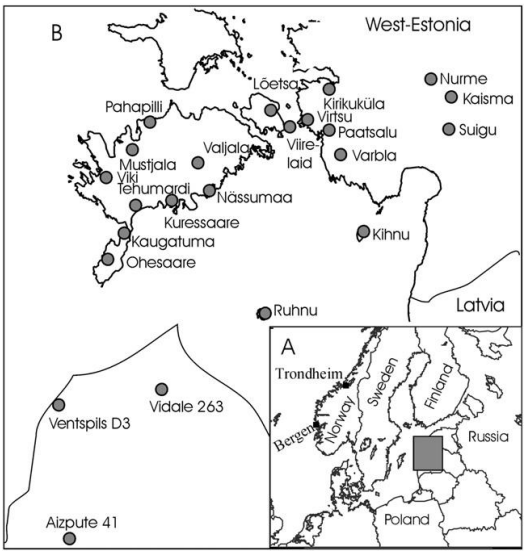

Fig. 1. Location of the studied drill-cores. A — wider area, B — study area.

also to the Telychian (Kiipli and Kallaste, 2006). The total thickness of the Telychian reaches 80 m in the Viki core. In mainland Estonia the limestone of the Rumba Formation contains brachiopods *Pentamerus oblongus*. In the offshore direction the clay content of the host rock increases. The CaO and K_2O contents in the Viki section (Fig. 2) characterise changes of the calcareous and terrigenous component ratio in the Telychian rocks in Saaremaa, west Estonia. The thick Osmundsberg K-bentonite (Bergström et al., 1998; Huff et al., 1998; Kiipli et al., 2006) which reaches 20 cm in thickness belongs to the upper part of the Rumba Formation. A large number of 0.1–10 cm thick K-bentonite layers occur in the Velise Formation. Kallaste and Kiipli (2006) counted K-bentonites from 43 different volcanic eruptions. Comparison of K-bentonite and host rock composition reveals a clear difference. The K-bentonites were Ca-poor and K-rich. A higher K_2O content of K-bentonites was characteristic of this particular lithofacies; in the deeper facies the K_2O content decreases (Kiipli et al., 1997, 2007b). In the shallow shelf (e. g. Kirikuküla section) the rocks of Adavere Stage are often dolomitised.

The Telychian rocks in the deep shelf area (Jurmala Formation in Latvia) are mainly claystones with 5 to 10% of dolomite. The carbonate content is at its lowest in the lower part of the section, but increases gradually upward. Two red-coloured intervals with an intermediate greenish-grey part have a wide distribution in West Latvia. A similar marine early diagenetic red claystone occurs also in Saaremaa. The onset of red facies in West Latvia earlier than in Saaremaa was proved by correlation of K-bentonites (Kiipli et al., 2000b). For a detailed correlation of the studied K-bentonites with graptolite biostratigraphy see Kiipli et al. (2007a).

3. Analytical methods

3.1. Standard methods

The XRD analysis of bulk samples for major mineral identification was carried out in the Institute of Geology Tallinn

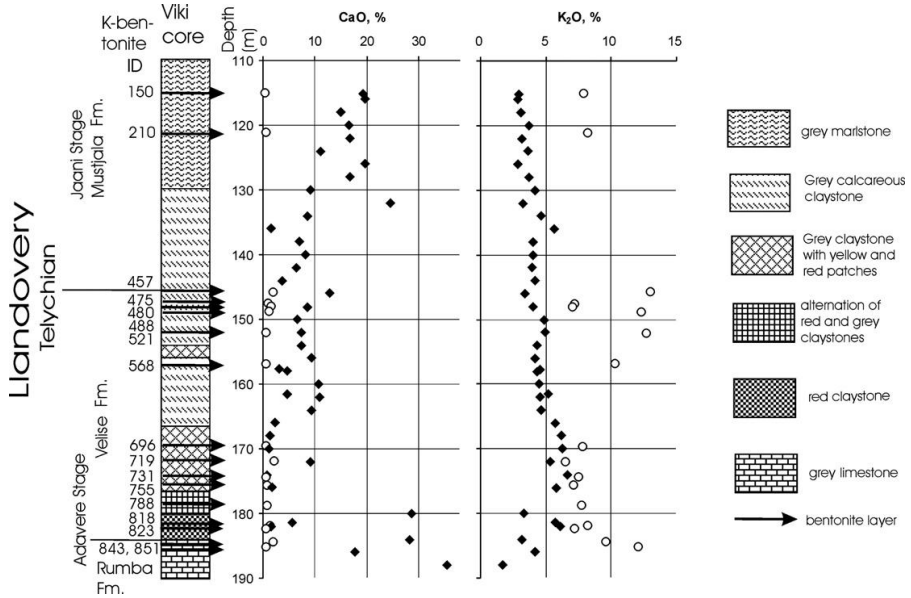

Fig. 2. CaO and K_2O content of the host rock (filled rhombs) and K-bentonites (empty circles) of the Viki core. K-bentonites differ from host rock by the low content of Ca-carbonate and by the high content of potassium.

University of Technology. In the same laboratory, standard XRF analysis was carried out for the quantitative determination of major components using traditional Li-tetraborate fusion technique. Trace elements were analysed from pressed powders. The EDXRF microprobe analysis of biotite was done in the Material Research Center of Tallinn University of Technology.

Semiquantitative estimation of biotite abundance (Table 1) under the microscope was done for the size fraction 0.04–0.1 mm separated from 2 g of bentonite sample in the following approximate ranges:+ — rare (less than 10 flakes), ++ — much (many flakes) and +++ — abundant (biotite is one of the major components in the coarse fraction).

Table 1
Composite record of Telichian volcanism in Estonia

K-bentonite name	Viki depth identificator	Bed no Kiipli et al., 2001	Thick-ness in Estonia, (cm)	Pyroclastic K–Na-sanidine, main component		Biotite abundance, and dominant cations	Trace and minor elements occurring in high concentrations	Trace and minor elements occurring in low concentrations
				Peak width, °2θ	$NaAlSi_3O_8$ (mol%)			
Mustjala formation								
Ireviken	127	29	0.2–3.0	Little sanidine		Mg+++	P,Rb	Ga,Sr
Lusklint	150	28	4.0–8.0	0.19–0.34	35.2–35.8	Mg+		Rb,Ba
Ohesaare	210	27	0.7–10.0	0.25–0.35	38–40	+	Y,Ni,Th,Ti	Ba,P
Aizpute	311		0.2–3.0	0.08–0.12	36.2–37.8	+	Nb,Zr,Th,Ba,Ti	Ga,Rb,Ni
Velise formation								
Kirikuküla	457	26	1.0–5.0	Very wide reflection		+	Ti	Nb,Zr,Ga,Th
Viki	475	23.24	2.0–5.0	0.12–0.20	45.2–46.3	Mg+	Nb,Zr,Ti	Ga,Sr,Ba
Kaugatuma	480	21	0.5–1.5	0.18–0.27	42.0–42.8	Mg++	Nb,Zr,Y,Th,Ti	Ga,Ni,P
Kuressaare	488	20.22	0.3–0.5	Very wide reflection		+	Y,Sr,Ni,Ba,Ti,P	Nb,Zr,Ga,Th
Ruhnu	494	19	0.3–5.0	0.05–0.09	45.7–46.4	Mg,Mn+	Nb,Th	Y,Sr,Ni,Ba,Ti,P
	504		<0.5	0.09	46.0	+	?	?
Viirelaid	518	18	0.3–2.0	Very wide reflection		Mg+	Sr,BaTi,P	Nb,Zr,Ga,Th
Lõetsa	520	17	0.5–3.0	very wide reflection		Mg+	Y, Sr, P	Nb,Zr,Ga
	521	16	0.5–1.0	Very wide reflection		+	Sr,Ba,Ti	Zr,Ga,Th
	564		0.2–2.5	0.12–0.17	45.0–45.8	++	Nb,Zr	Ni
	567		0.4			++	Sr,Ba,Ti	Ga,Ni
	568	15	0.4–2.5	Very wide reflection		+	Y,Ti	Nb,Zr,Ga,Rb,Th,P
	658		2	0.09	45.5	?	Nb,Zr,Y,Th	
	682		?	Very wide reflection		+	?	?
	693	14	0.1–2.0	0.05	22.6	Fe+	Rb,Ba,P	Nb,Zr,Ni,Th,Ti
Nässumaa	696	13	0.2–10.0	0.04–0.06	22.9–23.3	Fe++	Ga,Rb	Nb,Zr,Th,Ti,P
Virtsu	719	12	1.0–6.0	Little sanidine		Mg+++	Rb,P	
	720		3.0	0.085–0.122	26.5–28.0	+	Ga,Th	Zr,Sr,Ti,P
	722		1.0	Very wide reflection		+	Ti,P	Zr
Nurme	731	11	1.0–12.0	0.10–0.16	38.7–40.3	Mg+	Nb,Y,Th	Sr,Ni,Ba,Ti,P
Tehumardi	744	10	1.0–3.0	0.07–0.10	25.8–26.7	Mg+	Rb,Th	Zr,Y,Ni,Ba,Ti
	750		1.0			?	Rb	Zr,Y
Paatsalu	755	9	0.5–5.0	0.25–0.30	25.5–26.2	Mg+		Y,Sr,Ni,Ba
Pahapilli	772	7.8	1.0–5.0	0.30–0.34	20.5–24.1	Mg++	Y,Th,P	Ba
	773		1.5			+		Nb,Zr,Y,Sr,Ba,Ti
	774		2.0	0.12	46.2	?	Nb,Zr	Ni
	775		1.0	0.10	48.2	?	?	?
	776	6	0.3–6.0	0.07–0.08	28.1–28.8	Fe+	Ga,Th	Zr,Sr,Ni,Ba,Ti,P
	777	4	1.0	0.25–0.30	22.3–26.2	Mg+++		Zr,Th,P
	788	5	1.0–1.5	0.17–0.19	40.1–40.6	+++	Nb,Zr,Ti	P
	793		0.1			+++	?	?
	794		0.2	0.12	43.7	?	?	?
Mustjala	795		0.1–1.0	0.05–0.11	24.5–25.3	+++	?	?
	800		1.5			?	?	?
Rumba/Velise transition								
	805	1	0.7–3.5	Very wide reflection		Fe+		Nb,Y,Sr,Ni,Ba,Ti
	818	4	0.5–10.0	Very wide reflection		+	Rb,P	Nb,Zr,Ti
Valgu	823	3	0.1–5.0	0.12–0.17	45.2–47.6	+	Nb,Zr,Y	Rb,Sr,P
Rumba formation								
	843	2	0.5	Very wide reflection		+	Rb	Nb,Zr,Y,Th,P
	847		3	Very wide reflection		Fe+	?	?
Osmundsberg	851	0	1.5–25.0	0.05–0.09	20.7–21.5	Mg+++	Ba	Nb,Zr,Y,Ni,Ti
	880	−1	2.0–6.0	Very wide reflection		+		Nb,Zr,Sr,Ni,Th,P

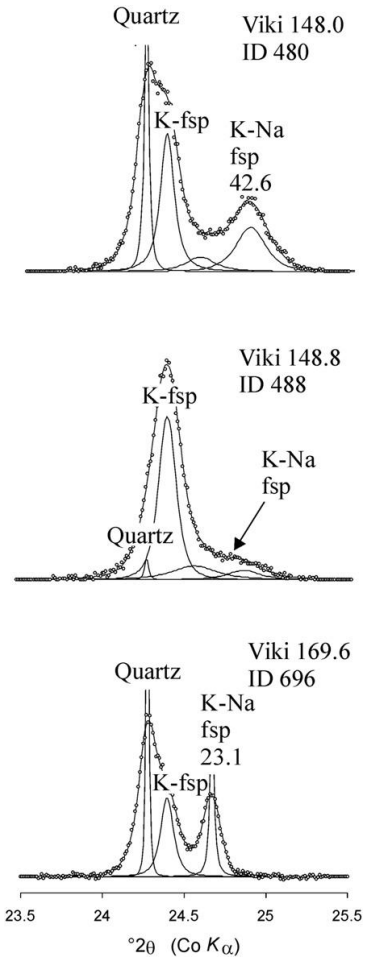

Fig. 3. XRD patterns of three K-bentonites (fraction 0.04–0.1 mm). Points mark measured curve and solid lines reflections of minerals calculated using three or four component curve fitting program — from left to right: quartz, authigenic potassium feldspar (K-fsp) and magmatic K–Na-sanidine (K–Na fsp) described by one or two components. The numbers above reflection show the calculated $NaAlSi_3O_8$ content (mol%) in the sanidine main component. Lower and upper K-bentonite can be well correlated on the basis of magmatic sanidine with a sharp $20\bar{1}$ reflection. The middle diagram reveals a wide magmatic sanidine reflection, which differentiates it clearly from the other two ones but does not enable to identify a particular eruption bed among others with a similar wide sanidine reflection.

3.2. XRD analysis of the magmatic sanidine composition

For correlation of volcanic interbeds the XRD analysis of pyroclastic K–Na sanidine composition in the coarse fraction (0.04–0.1 mm) of K-bentonites was used. XRD measurements were done using Fe-filtered Co radiation. The $20\bar{1}$ reflection of sanidine was measured in the range from 23.5 to 26.0 °2θ.

The content of $NaAlSi_3O_8$ in mol% in K–Na sanidine was calculated according to Orville (1967) who established that the position of $20\bar{1}$ reflection almost linearly depends on the composition of sanidine solid solution. Examples of measured XRD patterns are presented in Fig. 3. The method was checked by EDXRF microanalysis (Fig. 4) showing the same principal difference of sanidine composition in two analysed samples as XRD. Much larger scatter of results by EDXRF occured partly from analytical variation of sodium analyse, but maybe also from natural heterogeneity of sanidine. The precision of K–Na sanidine composition analysis using XRD is ±1% in favourable cases (low intensity of authigenic feldspar reflection, no kaolinite, high intensity and sharp reflection of interest), and in less favourable cases ±2%. The pure end members of K and Na feldspar solid solution were considered as authigenic phases (Kastner, 1971) and they were not used for correlations. The method is described in more detail in Kiipli and Kallaste (2002) and Kiipli et al. (2008).

4. Results

4.1. Sanidine composition

The sanidine $20\bar{1}$ reflection, sharp enough for characterization in numerical values was established in 25 volcanic ash interbeds (Table 1, Fig. 5). Besides the position of reflection, the width of the reflection is also a useful parameter for identification of a particular eruption layer. Twelve volcanogenic interbeds revealed a very wide sanidine reflection. Wide reflections probably indicate compositional heterogeneity of sanidine. In two bentonites only weak sanidine reflections were observed indicating a low content of sanidine. However, these weak reflections are still stronger than in terrigenous claystones. In five bentonites the magmatic K–Na sanidine was not measured, as the samples were too rich in authigenic K-feldspar complicating seriously the separation of pyroclastic minerals.

4.2. Composite record of volcanic beds in Estonia

The existence of altered volcanic ash beds in the Telychian of Estonia has been known for a long time (Jürgenson, 1964). The number of beds reaches 21 in Viki, 22 in Ohesaare and 25 in Aizpute core. In other studied sections it varies between 4 and

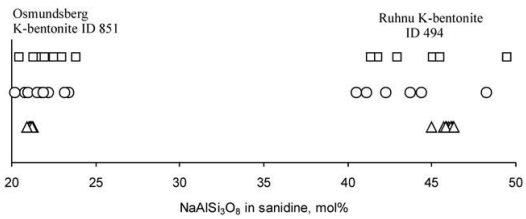

Fig. 4. Comparision of XRD analysis of sanidine (triangles) from two eruptions (ID 851 and 494, several drillcores) with EDXRF microanalyses (ID851 from Aizpute core, depth 964.4 m; ID 494 from Viirelaid core, depth 66.6 m). Both analyses discriminate clearly sanidine from these eruptions. XRD analyse represents average of many grains, therefore analyses from different cores fell very close. EDXRF analyse represents single grains, therefore scatter of these analyses is much larger, caused by natural heterogeneity and partly also by analytical variability.

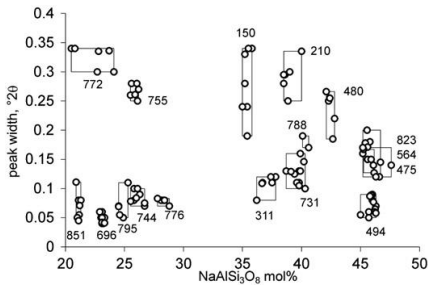

Fig. 5. Compositional variation of magmatic sanidine in the studied K-bentonites. The frame embraces correlated beds from different drill cores of the same eruption. K-bentonite identification numbers are the same used in other figures and tables. The chart demonstrates the discriminating capability of the sanidine analysis by XRD.

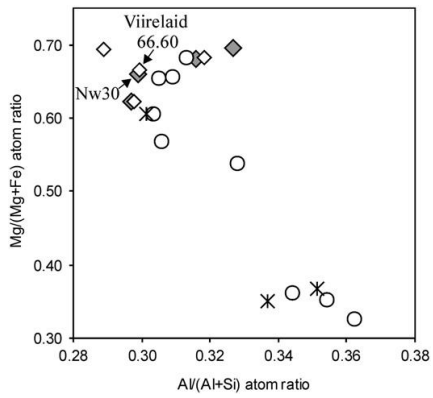

Fig. 6. Biotite composition of Telychian K-bentonites. Snowflakes — K-bentonites from the Rumba formation and Rumba/Velise transition, circles — K-bentonites from the lower part of the Velise formation and rhombs — K-bentonites from the upper part of the Velise Formation and Mustjala Formation. Grey rhombs – data from Batchelor (2003).

18. The correlation of these ash beds on the basis of the sanidine composition has revealed that none of the sections includes a complete record of ash beds, and a total of 45 K-bentonites from separate eruptions were established (Table 1). Names were assigned to the bentonites established in five or more sections (Kallaste and Kiipli, 2006). Identification numbers, derived from the depth in the Viki section, were assigned to all 45 bentonites. The ID number represents a depth in the Viki drill core in decimetres, of that 1000 decimetres was substracted as all K-bentonites occur at depths between 1000 and 2000 dm. For the sake of shortness, centimetres were discarded from the end of the depth number. For example, K-bentonite from the depth of 145.75 m in the Viki core has the ID number 457. For K-bentonites found in the Viki section, the ID number was derived from the real depth of occurrence. K-bentonites from other drill-cores were projected to the Viki depth scale graphically using correlated K-bentonites established in the Viki and other cores, and the depth in the Viki scale was used as a basis for deriving the ID number (Kallaste and Kiipli 2006). This ID number is a link between different tables and figures in the present work and was used also in Kiipli et al. (2007a). The ID number reflects also the succession of eruptions in time. Errors may occur in a succession of ash beds established only in one or a few sections and projected to the Viki section on a basis of distant neighbouring beds. The position of K-bentonites with assigned names is well proven and was used as a framework for composing the succession of less frequently found K-bentonites.

Table 2
Major components in altered volcanic ashes

Name	Kuressaare Bentonite					Nurme Bentonite					
ID	488	488	488	488	488	731	731	731	731	731	731
Core	Kirikuküla	Viki	Ruhnu	Ohesaare	Aispute	Viirelaid	Pahapilli	Valjala	Ruhnu	Ohesaare	Aispute
Depth, (m)	17.20	148.80	473.10	362.23	941.35	78.11	65.70	153.40	489.05	369.98	957.10
Thickness, (cm)	?	0.5	0.3	0.5	0.7	12.0	8.0	2.5	1.0	5.0	2.5
Lithology	Feldspathite	Feldspathite	Feldspathite	Feldspathite	K-bentonite	Feldspathite	K-bentonite	K-bentonite	K-bentonite	Tonstein	Tonstein
Facies	Shallow water		Deep water			Shallow water			Deep water		
SiO_2	62.94	58.92	59.60	60.39	47.04	59.85	57.13	55.55	52.2	51.61	50.40
TiO_2	0.86	1.15	1.32	1.55	1.42	0.41	0.56	0.53	0.575	0.75	0.75
Al_2O_3	17.80	18.65	18.39	18.21	22.95	21.13	21.38	20.77	26.7	32.29	30.56
Fe_2O_3	1.32	2.35	1.44	1.02	8.17	1.27	2.25	3.75	3.67	1.06	2.48
MnO	0.003	0.015	?	0.018	0.013	<0.002	0.024	0.010	?	<0.002	0.005
MgO	0.64	1.35	1.04	0.93	0.75	2.53	2.73	3.07	2.70	1.99	1.60
CaO	1.12	1.79	1.45	2.39	1.00	0.32	0.57	0.42	0.44	0.43	0.49
Na_2O	<0.5	<0.5	?	<0.5	?	?	?	<0.5	?	<0.5	<0.5
K_2O	14.29	11.82	12.56	13.14	5.62	11.24	9.00	8.45	4.83	4.05	2.85
P_2O_5	?	0.36	0.43	0.65	0.32	0.068	?	0.08	0.089	<0.02	0.04
LOI	1.95	2.63	2.13	2.17	12.50	2.95	4.58	4.56	7.74	8.88	9.36

4.3. Biotite composition

Biotite is a common magmatic phenocryst used widely for field identification of the volcanic origin of clay-rich interbeds. In theViirelaid core section the biotite composition of K-bentonites was studied by the EDXRF microanalyser. Seven cations (Table 3) revealed measurable reflections, which were calibrated using pure substances. The concentrations of sodium and calcium were below detection limits of the method, (<0.2 and <0.1 wt%, respectively).

Initial concentrations in weight % were converted to the atom numbers per chemical formula considering idealized biotite half-cell formula with eight cations:

$$K_1(Mg,Fe)_3Al_1Si_3O_{10}(OH,F)_2$$

Several researchers (Foster, 1960; Bailey, 1984) describe deviations from this idealized formula as a common feature of biotites. Foster (1960) suggests the following compositional ranges of natural biotites:

$$(K,Na,Ca)_{1\pm0.1}(Mg_{0.5-1.75},Fe_{0.5-1.75},R^{+3}_{0.35-1.0}) \times (Al_{1.0-1.5},Si_{2.5-3.0})O_{10}(OH,F)_2$$

The data presented in Table 3 correspond well to the natural variations established by Foster (1960). However, there are some aspects, which still need explanation. The sum of octahedral cations (adding also Al above 4 from sum of Si+Al) exceeds 3 allowed by available octahedral sites. This can be explained by part of Ti in rutile inclusions, which may be suggested from a positive correlation of Ti with the sum of the octahedral cations both in Mg- and Fe-rich biotites. Biotite from bentonite NW30 in Garntangen (Norway) analysed by Batchelor (2003) using an electron microprobe can be compared with the biotite from the Viirelaid depth 66.60 m, as these K-bentonites were previously correlated on the basis of trace element compositions (Kiipli

Table 3
Composition of biotite in Telychian K-bentonites

Sample no.	K-bentonite name	Viki depth ID	K	Mg	Fe	Ti	Mn	Al	Si	Sum
			Calculated from: Batchelor (2003) Atoms per chemical formula							
SW63	Ireviken	127	0.92	1.63	0.99	0.29	0.02	1.23	2.91	8
SW61	Lusklint	150	0.92	1.77	0.83	0.30	0.02	1.31	2.84	8
NW33	Kaugatuma?	480	0.79	1.80	0.79	0.41	0.01	1.37	2.83	8
NW30	Ruhnu	494	0.87	1.76	0.91	0.31	0.03	1.24	2.90	8
Depth, (m)			Viirelaid section, present study Atoms per chemical formula, average (upper) and standard deviation (lower)							
65.90	Viki	475	0.91	1.70	1.03	0.32	0.01	1.20	2.83	8
			0.03	0.12	0.13	0.03	0.01	0.02	0.01	
66.60	Ruhnu	494	0.88	1.83	0.92	0.33	0.04	1.20	2.80	8
			0.03	0.04	0.02	0.06	0.01	0.05	0.06	
67.75	Viirelaid	518	0.90	1.93	0.85	0.34	0.02	1.14	2.82	8
			0.01	0.02	0.02	0.02	0.00	0.02	0.03	
68.30	Lõetsa	520	0.90	1.88	0.88	0.31	0.01	1.28	2.74	8
			0.01	0.17	0.16	0.02	0.01	0.05	0.06	
76.45		693	0.93	0.88	1.60	0.26	0.01	1.53	2.79	8
			0.02	0.02	0.03	0.01	0.00	0.03	0.03	
76.70	Nässumaa	696	0.93	0.80	1.66	0.25	0.01	1.57	2.76	8
			0.02	0.01	0.02	0.03	0.01	0.04	0.03	
77.60	Virtsu	719	0.91	1.66	1.08	0.30	0.02	1.23	2.81	8
			0.02	0.03	0.01	0.01	0.01	0.01	0.01	
78.11	Nurme	731	0.84	1.89	0.88	0.40	0.02	1.24	2.73	8
			0.04	0.08	0.08	0.07	0.01	0.05	0.05	
78.20	Tehumardi	744	0.88	1.52	1.16	0.32	0.02	1.26	2.85	8
			0.03	0.09	0.08	0.00	0.01	0.03	0.01	
78.50	Paatsalu	755	0.89	1.80	0.95	0.27	0.02	1.24	2.83	8
			0.02	0.16	0.13	0.03	0.01	0.08	0.04	
79.13	Pahapilli	772	0.89	1.78	0.94	0.31	0.01	1.26	2.81	8
			0.03	0.10	0.09	0.01	0.01	0.01	0.03	
79.38		776	0.95	0.92	1.62	0.35	0.02	1.43	2.72	8
			0.01	0.02	0.02	0.02	0.00	0.01	0.01	
79.45		777	0.87	1.45	1.25	0.26	0.01	1.37	2.80	8
			0.02	0.19	0.18	0.02	0.01	0.03	0.03	
80.90		805	0.94	0.89	1.65	0.36	0.01	1.40	2.75	8
			0.02	0.03	0.04	0.02	0.00	0.02	0.03	
83.05		847	0.91	0.91	1.58	0.31	0.01	1.50	2.78	8
			0.02	0.09	0.06	0.07	0.00	0.09	0.04	
85.00	Osmundsberg	851	0.93	1.69	1.10	0.24	0.02	1.21	2.81	8
			0.01	0.03	0.03	0.01	0.00	0.02	0.01	

et al., 2001). There are small analytical differences. Our analyses show a little bit lower Si and Al and higher Mg, Fe, Ti and Mn concentrations. Using element ratios (Fig. 6.) avoids these small analytical differences and NW30 coincides exactly with Viirelaid 66.60 in this plot confirming the earlier correlation of ash beds from sections locating about 750 km apart. The correlation is also supported by a relatively high Mn content in biotites from both ash beds.

The studied biotites could be classified as iron-rich and magnesium-rich varieties. Frequently, the iron-rich biotites are characterised also by remarkably higher aluminium contents (Fig. 6). Significant variation of biotite compositions between the ash beds and relative stability within a single bed is a good basis for using it in proving correlations of ash beds from different sections.

4.4. Formation of K-bentonite from volcanic ash, gains and losses of elements

For petrogenetic interpretation of trace elements, it is important to know how element concentrations are changing during devitrification of volcanic glass and formation of authigenic minerals.

The amorphous material of volcanic ash is very sensitive to environmental chemical conditions. The main alterations took place during early diagenesis within the upper layer of sediments or even on the seafloor (Grim & Güven 1978, Kiipli et al., 1997, 2007b). The formation of the main minerals depends largely on lithofacies changes in accordance with water depth in sedimentary basin (Kiipli et al., 2006). In the deep shelf bentonites consist of association of kaolinite and illite–smectite. In shallow facies altered volcanic ashes are composed predominantly of authigenic K-feldspar. At mid-depths the illite–smectite is the major authigenic mineral (Kiipli et al., 2007b). Among the major elements sodium is lost almost completely in all facies. The greatest loss of material occurs as a result of silica removal up to 50% (Huff et al., 1996). In shallow shelf the external uptake of potassium from seawater probably promotes authigenic K-feldspar formation. Additional iron was incorporated in the form of pyrite in sulphate-reducing environments, or hematite in oxic sediments (Kiipli et al., 2000a).

Table 2 demonstrates changes in the content of major elements in two well correlated K-bentonites from shallow sea to the deep sea sections. According to the double difference in the TiO_2 content, these two bentonites originate from different source magmas: the Kuressaare Bentonite from andesitic and the Nurme Bentonite from more acidic source (Kiipli et al., 2001). In the Kuressaare Bentonite feldspar-rich varieties occur also in relatively deep sea facies, but in the Nurme Bentonite clay dominates even in shallow sea facies. Hence, the alteration of volcanic ash depends on both the facies and source magma composition (see Table 2).

4.5. Trace elements in K-bentonites

Fig. 7 shows the dynamics of immobile element (Nb Zr, Th and Ti) concentrations from shallow sea sediments in Estonia to deep sea facies in Latvia. Due to the bigger loss of silica and other major elements during the formation of kaolinite from amorphous volcanic ash, the residual enrichment with immobile elements occurs in deep sea sediments (1.5–2.5 times compared to the shallow sea facies). Use of immobile element ratios instead of element concentrations eliminates the diagenetic trends and enables better identification of beds. Useful elements are Nb, Zr, Ti, Th, Y, Sr and others.

Besides different alteration pathways in various facies some other factors may complicate correlations on the basis of trace elements. Those factors are: 1. Late diagenetic changes (mobile elements must be excluded from consideration). 2. Fractionation of ash material during air transport and sedimentation. 3. Change of source magma composition during long-lasting eruptions. These compositional trends can be studied by detailed sampling or averaged by sampling of full thickness of bed.

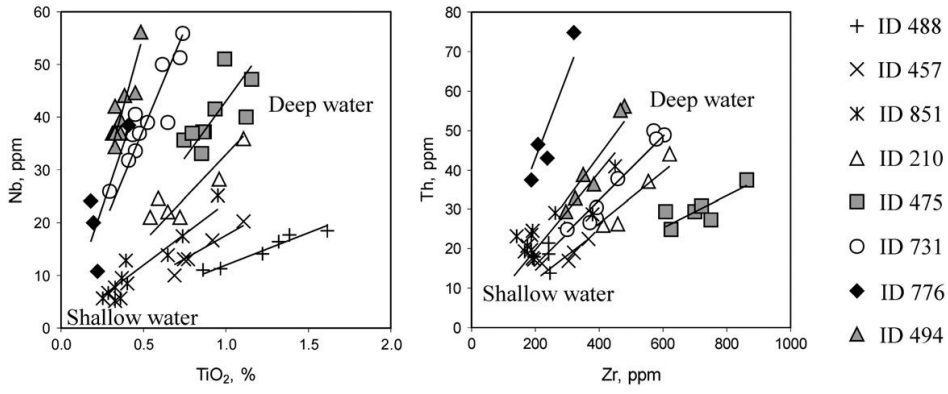

Fig. 7. Immobile trace elements in some Upper Llandovery K-bentonites, correlated using the sanidine composition, from shallow to deep water facies in Estonia and Latvia. Correlation lines indicate that element ratios are more stable than concentrations. K-bentonites in deep water sediments contain about twice higher contents of immobile trace elements compared to the same K-bentonites in shallow sea sediments. This residual enrichment effect occurs due to the bigger dissolution and removal of SiO_2 and other elements from volcanic ash during the formation of kaolinite in deep water environment.

Table 4
Trace and major element concentrations in Telychian altered volcanic ashes

K-bentonite name	Viki depth ID	Rock type	Number of analyses	Nb	Zr	Y	Ga	Rb	Sr	Ni	Th	Ba	Ti	P	K_2O	Al_2O_3
				(ppm)											(%)	(%)
Mustjala formation																
Ireviken	127	K	1	23	303	8	16	110	71	17	16	181	3557		8.2	
Ireviken	127	T	1	32	391	24	9	68	69	16	36	272	5766	1833	3.8	27.5
Lusklint	150	K	2	27	497	30	16	61	201	21	30	389	4995	262	7.4	24.3
Lusklint	150	T	1	30	476	47	17	36	171	20	32	116	5164	305	3.6	26.3
Ohesaare	210	K	3	21	422	23	21	80	149	61	26	99	3843	<130	8.1	23.3
Ohesaare	210	T	2	32	587	56	16	60	173	26	41	226	6901	524	4.4	28.5
Aizpute	311	K	1	36	474	18	14	88	117	14	40	232	4538		6.1	21.8
Aizpute	311	T	2	45	600	50	12	41	113	30	59	458	6827	631	2.5	30.9
Velise formation																
Kirikuküla	457	F	3	13	281	28	9	73	129	34	18	306	00	87	12.9	18.0
Kirikuküla	457	K	1	20	365	34	11	53	171		23		6647	800	8.2	26.3
Viki	475	F	1	35	393	36	14	76	48	16			3300		12.7	17.6
Viki	475	K	6	42	706	38	19	91	103	32	28	145	5286	326	7.9	22.2
Viki	475	T	1	47	863	47	16	56	99		37		6940	357	3.6	30.9
Kaugatuma	480	F	1	34	556	40	17	85	71	11			3940	<130		
Kaugatuma	480	K	1	41	627	35	17	99	113	26	32	201	5705	87	7.4	22.1
Kaugatuma	480	T	2	52	906	72	14	63	109	9	47	213	7384	454	4.2	31.3
Kuressaare	488	F	1	11	215	21	11	68	281	41			5139		14.3	17.8
Kuressaare	488	F	4	15	244	54	9	83	379	60	19	406	7648	2101	12.4	18.6
Kuressaare	488	K	1	18	241	23	10	61	314	24	21	335	9302	1396	5.5	23.0
Ruhnu	494	F	2	37	333	17	13	83	56	9	36	120	1967	98	12.3	18.9
Ruhnu	494	K	4	39	317	10	18	96	69	12	29	105	2087	349	9.8	21.9
Ruhnu	494	T	2	50	474	24	20	88	66	9	56	69	2901	228	4.7	29.5
Viirelaid	518	F	3	14	239	25	11	78	299	43	18	472	5784	2531	13.6	18.9
Viirelaid	518	K	1	22	364	37	12	47	315		25		8618	1173	7.0	28.6
Lõetsa	520	F	5	15	280	69	10	71	285	31	21	266	5839	5455	12.6	18.5
	521	F	2	19	298	23	11	75	323	43	16	837	7501	916	12.2	18.8
	564	K	1	45	765	39	16	80	106	7	30	163	5949		5.5	
	567	K	1	24	339	31	12	99	443	7	33	452	11738		11.6	
	568	K	3	15	267	35	17	76	208	56	15	244	4940	262	10.5	20.7
	568	K	1	21	365	56	14	50	195	8	23	226	7257	<130	5.5	31.2
	658	T	1	48	639	60		52	94	10	47		4292	698	4.2	30.9
	693	K	1	14	127	42	16	105	113	11	14	1805	1740	1702	11.0	20.6
Nässumaa	696	K	6	14	240	38	27	139	79	27	21	217	2534	220	8.5	21.8
Nässumaa	696	K	2	17	288	38	26	143	85	39	19	328	3756	830	5.1	25.8
Virtsu	719	K	4	24	432	15	22	109	87	18	27	186	3922	640	8.4	21.2
Virtsu	719	T	1	32	527	32	16	72	85		33		4370	1101	3.9	29.3
	720	T	1	24	284	22	28	82	55		63		1475	110	4.2	29.4
	722	K	1	19	261	26	18	89	134		24		6178	1009	7.8	19.7
Nurme	731	K	2	29	335	26	15	75	58	7	26	143	2115	297	11.2	21.1
Nurme	731	K	5	38	399	25	22	97	94	18	34	165	3003	240	9.2	21.5
Nurme	731	T	2	54	587	60	19	55	82	7	49	217	4900	44	3.3	31.0
Tehumardi	744	K	3	34	249	18	22	104	100	30	38	141	2428	480	7.6	21.0
Tehumardi	744	T	2	35	314	25	21	76	83	13	43	214	3645	435	4.0	26.6
	750	K	1	17	197	18	21	108	74	30	28	196	3559		8.6	
Paatsalu	755	F	1	21	446	21	12	72	38	12	28	175	5070	698	13.7	17.7
Paatsalu	755	K	4	23	482	18	21	94	98	28	23	34	5934	371	8.3	21.8
Pahapilli	772	F	1	9	163	55	10	51	122	15	23	113	1656	9819	13.1	
Pahapilli	772	K	5	28	391	31	21	97	92	21	48	171	4848	1513	7.9	23.1
	773	F	1	14	275	15	12	73	45	9	25	94	2680		12.8	
	774	K	1	42	717	44	17	81	91	10	32	122	4814		7.1	
	776	F	1	11	188	18	12	57	30	8	37	88	1173	600	12.4	15.8
	776	K	2	22	223	9	24	95	61	10	45	56	1129	70	10.0	21.0
	776	T	1	38	321	32	27	79	60	16	75	38	2648	170	4.4	27.3
	777	K		17	271	26	21	99	128	18	16	158	3097	297	9.8	
	788	K		41	657	44	20	94	112	23	33	349	7038	262	7.7	21.2

Table 4 (*continued*)

K-bentonite name	Viki depth ID	Rock type	Number of analyses	Nb	Zr	Y	Ga	Rb	Sr	Ni	Th	Ba	Ti	P	K_2O	Al_2O_3
				(ppm)											(%)	(%)
Rumba/Velise transition																
	805	K	2	12	271	18	16	73	49	8	30	95	1536	545	10.6	20.4
	818	F	2	12	208	17	16	82	54	20	16	165	2789	218	13.2	17.6
	818	K	1	15	253	21	20	104	86	34			4373	1047	8.3	19.8
Valgu	823	F	4	24	606	53		43	22	16	31	183	3456		15.1	17.5
Valgu	823	K	2	51	851	48	21	86	120	20	36	181	5186	22	7.3	22.4
Rumba formation																
	843	F	3	8	164	13	17	64	28	22	12	124	2369	393	13.0	
	843	K	2	17	187	17	15	100	83	36	14	206	3248	65	9.8	17.3
	843	K	1	22	236	33	21	161	97	40	25	382	5773	<130	5.0	
Osmundsberg	851	F	7	6	159	8	18	68	67	8	18	334	1910	415	15.3	18.2
Osmundsberg	851	F	2	9	184	5	17	91	94	8	21	397	2380		12.5	
Osmundsberg	851	T	1	14	264	5	18	94	132	11	29	716	4266	175	4.5	26.7
	880	F	2	14	269	26	14	76	52	10	17	178	5617	<130	13.9	18.7

F — feldspathite, K — K-bentonite, T — tonstein (Al-bentonite).

In Table 4 trace element data within every eruption layer are grouped by decreasing K_2O content. The first row – K_2O 16 – 11%, the main mineral is authigenic potassium feldspar. The second row – K_2O 11 – 6%, the main mineral is illite–smectite. The third row – K_2O 6 – 1.5%, bentonite contains much kaolinite besides illite–smectite. The trace element concentrations within these three groups are much different, although K-bentonites are formed from the same ash. This compositional grouping is also related to the sedimentary facies: potassium-rich K-bentonites are more common in shallow water facies and kaolinite-rich low potassium bentonites in deep sea.

An important question arises: is it possible to estimate trace element concentrations in original ash from the concentrations in K-bentonites? To find an answer to this question, trace element contents of these three groups were compared. The results showed that the concentrations of immobile elements Nb, Zr, Th and Ti are decreasing regularly from kaolinite-rich tonsteins through K-bentonites to the feldspathites giving similar ratios when calculated from these three altered volcanic ash types (Fig. 7). Taking the average Al_2O_3 content in potential felsic and intermediate source magma equal to 14% (13.6% in low Ca and 15.5% in high Ca acidic rocks according to Turekian & Wedepohl 1961) and considering Al_2O_3 immobile during conversion of ash to bentonite, coefficients for calculation of these elements in source magma can be derived. We propose approximate coefficients for calculating the concentrations of these four elements in source magma: from feldspathites (average Al_2O_3 content 18.0%) — 0.8, from K-bentonites (average Al_2O_3 content 24.6%) — 0.6 and from tonsteins containing 50% of kaolinite (average Al_2O_3 content 30.1%) — 0.5. Other trace elements are behaving more irregularly and their concentrations in source magma cannot be estimated with any probability. Although, there is no doubt that the Y, Sr, Ni, Ga and P contents in bentonites also depend largely on their concentrations in original volcanic ash as they are often characteristic of a particular K-bentonite. In the text and Table 1, the terms *high*, *average* or *low* concentration of trace elements are used relative to median ranges of concentrations in our K-bentonite database covering 33% of analysed samples: Nb 15–28, Zr 250–360, Y 21–33, Ga 14–18, Rb 73–91, Sr 80–110, Ni 12–26, Th 19–30, Ba 160–230, Ti 2900–4800 and P 260–640 ppm.

5. Discussion

5.1. Classification of ash beds according to source magma mineralogical and geochemical features

Combining sanidine, trace element and biotite data seven geochemical types of K-bentonites can be distinguished (Fig. 8):

1. *Quarz rich type*. Pyroclastic material contains abundant quartz and biotite and almost no sanidine. Most trace elements occur at the average concentration levels. Biotite is Mg-rich. Only two K-bentonites of this type occur in the sections studied in Estonia: Virtsu K-bentonite (719) and Ireviken K-bentonite (127). These eruptions were separated by a long time interval that lasted at least 2 to 3 million years. Supposedly, this volcanic center located unfavourably relative to the dominating wind direction and ash clouds rarely reached the study area.
2. *Zirconium rich type*. Pyroclastic material contains much sanidine with a high sodium (37...48 mol%) content. The quartz content is low compared to sanidine. The type is characterised by high Nb (21…54 ppm), Zr (330…900 ppm), Y (18…72 ppm) and Ti (3300…7300 ppm) contents. Biotite is Mg-rich. The Zr/Ti ratio decreases from the lowermost to the uppermost K-bentonite showing that all recorded eruptions originated from a magma chamber where fractional crystallization of zircon occurred. The Nb/Ti ratio rises in the lower part of the Velise Formation reaching maximum in the Nurme Bentonite (731) and then follows the decreasing trend of the Zr/Ti ratio. According to Pearce and Norry (1979), Nb and Zr remain in liquid magma until the latest stages of fractional crystallization; therefore, this magma belongs to the highly evolved probably alkaline type. The sharp sanidine reflection

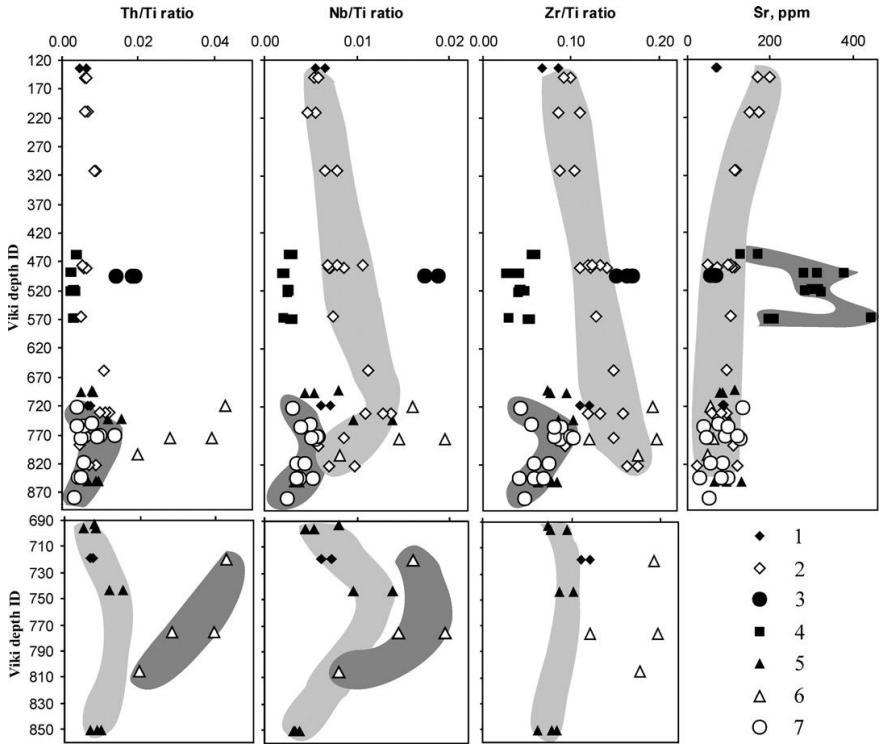

Fig. 8. Distribution of some geochemical characteristics of K-bentonites in Telychian section. Vertical scale Viki depth identificator arranges K-bentonites in order of successive eruptions. 1 — quartz rich type, 2 — zirconium rich type, 3 — niobium rich type, 4 — strontium rich type, 5 — biotite rich type, 6 — thorium rich type, 7 — variable sanidine type. Shaded areas are showing temporary geochemical trends within the same type. In upper charts most frequent geochemical types are shaded. Lower charts are an enlargements from the lower part of upper charts, where most frequent geochemical types, shaded on upper charts, are excluded for better reading.

and long-lasted activity provide evidence for a very large and slowly cooling magma chamber. This type includes the following K-bentonites: Valgu (823), 794,788, 775, 774, Nurme (731), 658, 564, 504, Kaugatuma (480), Viki (475), Aizpute (311), Ohesaare (210) and Lusklint (150). Although we assigned all these K-bentonites to the single geochemical type, it is possible, that the latter three originate from other volcanic source. This possibility can be suggested from the gap in the record of volcanic eruptions between the Viki and Aizpute K-bentonites (14.6 m in Viki depth scale) and possibly too long activity period. The Lusklint and Ireviken K-bentonites were assigned on the basis of geochemical signatures to different source volcanoes by Batchelor and Jeppsson (1994).

3. *Niobium rich type*. K-bentonites of this type are high in Nb (37…50 ppm) and Th (29…56 ppm) concentrations. The Ti, Y and P contents are low and Zr is at the average concentration level. Sanidine is Na-rich (46 mol%) with a sharp reflection. Biotite is rich in Mg and Mn. Only one bed of this type was established — the Ruhnu K-bentonite (494), but the Nurme K-bentonite (731) may also belong to this type.
4. *Strontium rich type*. K-bentonites of this geochemical type are characterised by high Sr (129…443 ppm), Ti (4700…11700 ppm), P (900…5400 ppm) and Y (23…69 ppm) contents. The Sanidine $20\bar{1}$ reflection is very wide, but clearly measurable, evidencing about a high content of heterogenous maybe not equilibrated with magma (zoned?) sanidine. The quartz/sanidine and Zr/Ti ratios are low pointing to a less evolved source magma (andesite or andesite/dacite). The biotite content is low; Lõetsa (520) and Viirelaid (518) K-bentonites contain a Mg-rich variety. Eruption beds of this type occur only in the middle part of the Telychian: 568, 567, 521, Lõetsa (520), Viirelaid (518), Kuressaare (488) and Kirikuküla (457) K-bentonites. Batchelor et al. (1995) established a principal geochemical difference between K-bentonites belonging to this type and those originating from evolved magma in Garntangen outcrop (Norway).
5. *Biotite rich type*. This type is characterised by a low content of all trace and minor elements. Sanidine is potassium-rich with sharp reflection. The biotite content is high and Fe-rich variety is common. Only the Osmundsberg K-bentonite contains Mg-rich biotite maybe suggesting other source. To this type we assigned K-bentonites in the lower part of the Telychian: Osmundsberg (851), Mustjala (795), Tehumardi (744), Nässumaa (696), 847 and 693.
6. *Thorium rich type*. Charcteristic is a high Th (30…75 ppm) and moderately high Nb (22...38 ppm) content. The Ti content is very low (1100...2600 ppm). Sanidine is rich in

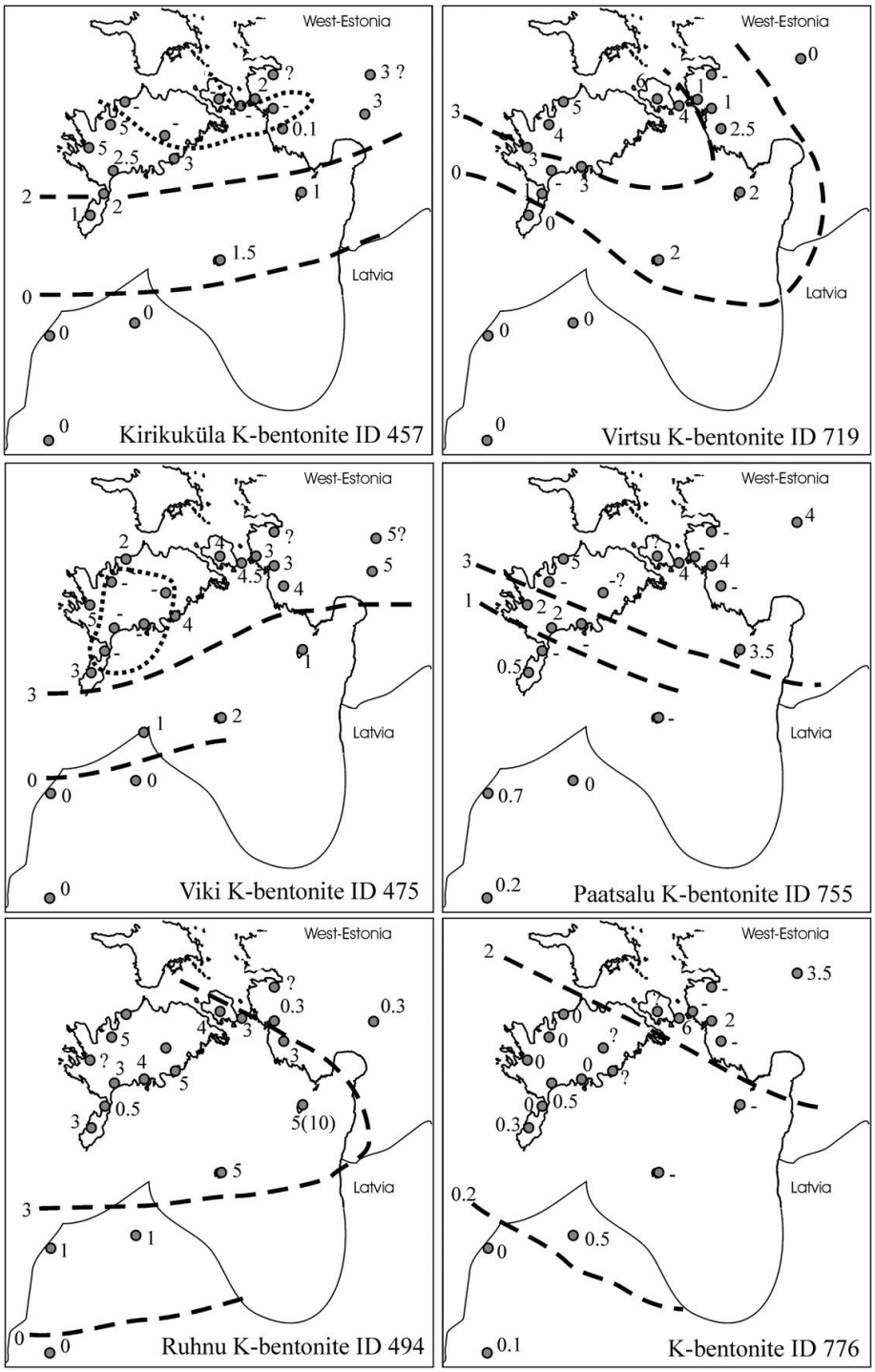

Fig. 9. Isopach schemes of some K-bentonites representing different geochemical types. Kirikuküla K-bentonite (457) — strontium rich type, Viki K-bentonite (475) — zirconium rich type, Ruhnu K-bentonite (494) — niobium rich type, Virtsu K-bentonite (719) — quartz rich type, Paatsalu K-bentonite (755) — variable sanidine type, K-bentonite ID 776 — thorium rich type.

potassium with a sharp $20\bar{1}$ reflection. Biotite is Fe-rich occurring in low contents. This type is similar to the biotite rich type, although differing significantly by the Th and Nb concentrations. Three layers were found: 805, 776 and 720.

7. *Variable sanidine type*. All trace elements occur at the average concentration levels. XRD measurements showed a wide sanidine reflection, biotite is Mg-rich. All element ratios expressed in Fig. 8 show a cycle rising in the Rumba Formation and in the lower part of the Rumba/Velise transition, then decreasing to the middle part of the Velise Formation. ID: 880, 818, 777, 773, 772, 755 and 722.

5.2. Do the geochemical types of K-bentonites originate from different volcanic sources?

1. K–Na sanidines with a sharp reflection fall into two groups: low sodium sanidines (21–28 mol% of $NaAlSi_3O_8$) and high sodium sanidines (37–48 mol% of $NaAlSi_3O_8$). Sharp XRD reflections indicate homogenous compositions of sanidine formed in equilibrium with magma. Most probably these two groups originated from different volcanic sources. The distinct sanidine composition (equilibrated with magma) provide evidence of large slowly cooling magma chambers.
2. Sanidines with wide reflections (not equilibrated with magma) refer to smaller or/and faster cooling magma chambers.
3. Geochemical changes in a magma chamber were controlled by steady long-lasting processes (magma generation by partial melting or fractional crystallization during slow cooling) over millions of years. These processes may occur in successive eruptions as geochemical trends and the step-by-step changing compositions may indicate the same volcanic source for these bentonites.
4. Gaps in the record of volcanism between the lower and middle part of the Telychian (9 m in the Viki depth scale) and also between the middle and upper part of the Telychian (14 m) indicate probably the end of the activity of some volcanic centres.

These arguments suggest that the Telychian volcanic ash beds in the East Baltic region could originate from at least 7 different volcanic sources corresponding to the geochemical and mineralogical types distinquished above.

5.3. Palaeogeography and possible locations of volcanic sources

In search of locations of volcanic sources useful suggestions can be derived from the thickness maps of correlated bentonites. Although the study area (approximately 200×200 km) is not large enough for discovering precise locations of volcanoes, the thickness schemes (Fig. 9) can help us compose isopach maps in larger areas during future studies. In general, the thicknesses of bentonites decrease to the south being often some centimetres in Estonia and only a few millimetres in Latvia. Two thickness distribution types can be distinguished:

1. Thickness decreases directly to the south or a little bit to the south-east. If this decreasing trend is perpendicular to the ash cloud axis, we can suppose source volcanoes from Southern Scandinavian Caledonides, e. g. Bergen region. In Fig. 9, K-bentonites with ID 457, 475 and 494 belong to this type. These K-bentonites represent strontium-rich, zirconium-rich and niobium-rich types. The biotite-rich type shows also a similar thickness distribution (Kallaste and Kiipli, 2006).
2. Thickness decreases to the south-west indicating a source from the middle part of the Scandinavian Caledonides, e. g. Trondheim region. K-bentonites with ID 719, 755 and 776 belong to this thickness distribution type. These bentonites reprsesent quartz-rich, variable sanidine-and thorium-rich types. The Osmundsberg K-bentonite (ID 851) showed also a similar distribution of thicknesses (Kiipli et al., 2006).

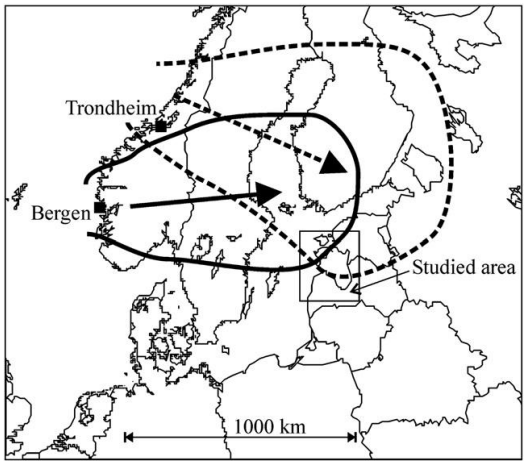

Fig. 10. Two hypothetical Telychian volcanic ash clouds explaining K-bentonite thickness trends in studied area. Dotted line — ash cloud from North-West causing decrease of thickness in studied area to South-West. Solid line — ash cloud from West causing decrease of thickness to South and South-West.

Fig. 10 illustrates two hypothetical Telychian ash clouds whose margins potentially could reach the study area. One of these hypothetical sources is located in Southern Scandinavian Caledonides, the other in the central part of Caledonides. Undoubtedly established thickness trends allow also sources from Northern Scandinavian Caledonides, although these sources located at a longer distance from Estonia being about 1400 km away. Potential sources from South-West in Central European Caledonides are only 700 km away (Beier et al., 2000; Beier and Katzung, 2001), but are not probable for most of ash beds as thicknesses decrease to the South. There is no indication also for Eastern sources where plate margin in Ural mountains is about 2000 km away from study area.

Volcanic and intrusive rocks are well known from Scandinavian Caledonides (Rutten, 1969). Isotopic ages of these rocks vary largely within the Early Palaeozoic. Telychian ages are also established for many rocks (Corfu et al., 2006): e. g. rhyolite in Solund basin, Southern Norway (Hartz et al., 2002);

trondhjemite and biotite norite plutons from Trondheim region (Nilsen et al., 2003); Ofoten felsic intrusions and trondhjemites from Niingen nappe (Steltenpohl et al., 2003) and Halti-Ridnitsokka igneous complex from Northern Caledonides (Sipilä, 1992). Identification of plutonic and massive volcanic rocks in the Caledonides as sources for K-bentonite geochemical types or particular eruption beds is a topic of future studies involving the generation of isopach maps over larger areas in Scandinavia and dating of K-bentonites and potential source rocks.

6. Conclusions

The geochemistry of immobile trace elements and the composition of sanidine and biotite phenocrysts of Telychian K-bentonites from Estonia and Latvia has enabled 45 Telychian K-bentonites to be classified into seven geochemical types. These types can indicate different magma chambers and correspondingly different source volcanoes, although this concept needs testing in future studies. At the beginning of the Telychian in the Rumba Formation only a few eruptions were recognized. The most intensive volcanism was recorded in lower part of Velise Formation where five different geochemical types occur. In upper part of Velise Formation three geochemical types were recorded and higher in section in Mustjala Formation only five K-bentonites, grouping into two types, are known. Isopach schemes suggest ash cloud transport from the west and north-west. Central European sources from the south-west are not probable for most of ash beds.

Acknowledgements

This study is a contribution of Estonian Science Foundation grants 6749, 7605, target financing project 0332652s04 and IGCP-503. We thank Valdek Mikli from Material Research Center of TUT for providing EDXRF analyses of biotite and sanidine and Kiira Orlova for XRF analyses.

Appendix A. Supplementary data

Supplementary data associated with this article can be found, in the online version, at doi:10.1016/j.jvolgeores.2007.11.005.

References

Bailey, S.W. (Ed.), 1984. Micas. Reviews in Mineralogy, Mineralogical Society of America. 584 pp.

Batchelor, R.A., 2003. Geochemistry of biotite in metabentonites as an age discriminant, indicator of regional magma sources and potential correlating tool. Mineralogical Magazine 67, 807–817.

Batchelor, R.A., Jeppsson, L., 1994. Late Llandovery bentonites from Gotland, Sweden, as chemostratigraphic markers. Journal of the Geological Society, London 151, 741–746.

Batchelor, R.A., Weir, J.A., Spjeldnaes, N., 1995. Geochemistry of Telychian metabentonites from Vik, Ringerike District, Oslo region. Norwegian Journal of Geology 75, 219–228.

Bergström, S.M., Huff, W.D., Kolata, D.R., 1998. The Lower Silurian Osmundsberg K-bentonite. Part I: stratigraphic position, distribution, and palaeogeographic significance. Geological Magazine 135, 1–13.

Beier, H., Katzung, G., 2001. The deformation history of the Rügen Caledonides (NE Germany) — implications from the structural inventory of the Rügen 5 borehole. Neues Jahrbuch für Geologie und Paläontologie, Abhandlungen 222, 269–300.

Beier, H., Maletz, J., Böhnke, A., 2000. Development of an Early Paleozoic foreland basin at the SW margin of Baltica. Neues Jahrbuch für Geologie und Paläontologie, Abhandlungen 218, 129–152.

Corfu, F., Torsvik, T.H., Andersen, T.B., Ashwal, L.D., Ramsay, D.M., Roberts, R.J., 2006. Early Silurian mafic — ultramafic and granitic plutonism in contemporaneous flysch, Magerøy, northern Norway: U–Pb ages and regional significance. Journal of Geological Society, London 163, 291–301.

Foster, M., 1960. Interpretation of the composition of Trioctahedral Micas. US Geological Survey Professional Paper 354-B, pp. 11–49.

Grim, R.E., Güven, N., 1978. Bentonites — geology, mineralogy, properties and uses. Developments in Sedimentology, vol. 24. Elsevier, Amsterdam. 256 pp.

Hartz, E.H., Martin, M.W., Andersen, A., Andersen, T.B., 2002. Volcanic rocks in the Devonian Solund Basin, Western Norway; large landslides of Silurian (439 Ma) rhyolites. Journal of the Geological Society, London 159, 121–128.

Huff, W.D., Kolata, D.R., Bergström, S.M., Zhang, Y.S., 1996. Large-magnitude Middle Ordovician volcanic ash falls in North America and Europe: dimensions, emplacement and post emplacement characteristics. Journal of Volcanology and Geothermal Research 73, 285–301.

Huff, W.D., Bergström, S.M., Kolata, D.R., Sun, H., 1998. The Lower Silurian Osmundsberg K-bentonite. Part II: mineralogy, geochemistry, chemostratigraphy and tectonomagmatic significance. Geological Magazine 135, 15–26.

Jürgenson, E., 1964. Silurian metabentonites of the Estonian SSR. In: Baukov, S. (Ed.), Lithology of Palaeozoic sediments of Estonia. Institute of Geology, Tallinn, pp. 87–100 (in Russian).

Kallaste, T., Kiipli, T., 2006. New correlations of Telychian (Silurian) bentonites in Estonia. Proceedings of the Estonian Academy of Sciences, Geology 55, 241–251.

Kastner, M., 1971. Authigenic feldspars in carbonate rocks. American Mineralogist 56, 1403–1442.

Kiipli, T., Kallaste, T., 2002. Correlation of Telychian sections from shallow to deep sea facies in Estonia and Latvia based on the sanidine composition of bentonites. Proceedings of the Estonian Academy of Sciences, Geology 51, 143–156.

Kiipli, T., Kallaste, T., 2006. Wenlock and uppermost Llandovery bentonites as stratigraphic markers in Estonia, Latvia and Sweden. GFF 128, 139–146.

Kiipli, T., Kiipli, E., Kallaste, T., 1997. Metabentonite composition related to sedimentary facies in the Lower Silurian of Estonia. Proceedings of the Estonian Academy of Sciences, Geology 46, 93–104.

Kiipli, T., Männik, P., Batchelor, R.A., Kiipli, E., Kallaste, T., Perens, H., 2001. Correlation of Telychian (Silurian) altered volcanic ash beds in Estonia, Sweden and Norway. Norwegian Journal of Geology 81, 179–193.

Kiipli, E., Kallaste, T., Kiipli, T., 2000a. Hematite and goethite in Telychian marine red beds of the East Baltic. GFF 122, 281–286.

Kiipli, E., Kiipli, T., Kallaste, T., 2000b. Early diagenetic chalcopyrite occurrences in Telychian marine red beds of West Estonia and West Latvia. Proceedings of the Estonian Academy of Sciences, Geology 49, 294–307.

Kiipli, E., Kiipli, T., Kallaste, T., 2006. Identification of O-bentonite in deep shelf sections with implication on stratigraphy and lithofacies, East baltic Silurian. GFF 128, 255–260.

Kiipli, T., Kallaste, T., Kaljo, D., Loydell, D.K., 2007a. Correlation of Telychian and lowermost Sheinwoodian K-bentonites with graptolite biozonation in the East Baltic area. Acta Palaeontologica Sinica, 46, 218–226.

Kiipli, T., Kiipli, E., Kallaste, T., Hints, R., Somelar, P., Kirsimäe, K., 2007b. Altered volcanic ash as an indicator of marine environment, reflecting pH and sedimentation rate — example from the Ordovician Kinnekulle bed of Baltoscandia. Clays and Clay Minerals 55, 177–188.

Kiipli, T., Jeppsson, L., Kallaste, T., Söderlund, U., 2008. Correlation of Silurian bentonites from Gotland and the eastern Baltic using sanidine phenocryst composition, and biostratigraphycal consequences. Journal of the Geological Society, London 165, 1–10.

Nilsen, O., Sundvoll, B., Roberts, D., Corfu, F., 2003. U–Pb geochronology and geochemistry of trondhjemites and a norite pluton from the SW Trondheim region, Central Norwegian Caledonides. Norges Geologiske Undersøkelse, Bulletin 441, 5–16.

Ogg, J.G., 2004. Status of divisions of International Geologic Time Scale. Lethaia 37, 183–199.

Orville, P.M., 1967. Unit-cell parameters of the microcline-low albite and the sanidine-high albite solid solution series. American Mineralogist 52, 55–86.

Pearce, J.A., Norry, M.J., 1979. Petrogenetic implications of Ti, Zr, Y and Nb variations in volcanic rocks. Contributions to Mineralogy and Petrology 69, 33–47.

Rutten, M.G., 1969. The Geology of Western Europe. Elsevier, Amsterdam. 520 pp.

Sipilä, P., 1992. The Caledonian Halti-Ridnitsokka igneous complex in Lapland. Geological Survey of Finland, Bulletin vol. 362 Espoo, 75 pp.

Steltenpohl, M.G., Andersen, A., Lindstrøm, M., Gromet, P., Steltenpohl, L.W., 2003. The role of felsic and mafic igneous rocks in deciphering the evolution of thrust-stacked terranes: an example from North Norwegian Caledonides. American Journal of Science 303, 149–185.

Turekian, K.K., Wedepohl, K.H., 1961. Distribution of the elements in some major units of the Earth's crust. Geological Society of America Bulletin 72, 175–191.

PAPER V

KIIPLI, T., KALLASTE, T., NESTOR, V. 2010. Composition and correlation of volcanic ash beds of Silurian age from the eastern Baltic. Geological Magazine, 147(6), 895–909.

Geol. Mag. **147** (*6*), *2010, pp. 895–909.* © *Cambridge University Press 2010*
doi:10.1017/S0016756810000294

Composition and correlation of volcanic ash beds of Silurian age from the eastern Baltic

TARMO KIIPLI*, TOIVO KALLASTE & VIIU NESTOR

Institute of Geology, Tallinn University of Technology, Ehitajate 5, 19086 Tallinn, Estonia

(*Received* 23 November 2009; *accepted* 12 February 2010; *first published online* 21 April 2010)

Abstract – Sanidine composition and bulk geochemistry of volcanic ash beds from the East Baltic indicate the subalkaline nature of the volcanism near the margins of the Baltica plate during the Silurian. Several bentonites in the Wenlock include a previously unknown sanidine with 48 to 58 mol % of the Na+Ca component. In contrast to the earlier Telychian volcanism, sodium-rich sanidine occurs in ash beds which originate from relatively moderately evolved dacitic magma. The studied material from two drill cores integrated with previous research enables production of a more complete list of 49 volcanic eruption layers for the lower to middle Wenlock in the East Baltic. This updated list of bentonites characterized by their sanidine compositions forms a good basis for future integrated bio- and chemostratigraphic correlations in northern Europe.

Keywords: K-bentonites, bentonites, geochemistry, Wenlock, Silurian, volcanism, East Baltic.

1. Introduction

Northward movement of Baltica and Avalonia continents in early Palaeozoic times reached collision stage with Laurentia in Silurian times (Cocks & Torsvik, 2005). This process caused intensive volcanism in the closing Iapetus Ocean between these continents. Silurian-age igneous rocks are known in the Norwegian Caledonides (Corfu *et al*. 2006), but also in Central Europe (Timmerman, 2008). Sedimentary rocks of Silurian age crop out in Central Estonia and the Baltic Sea islands Saaremaa and Gotland. Fragmentary outcrop areas occur throughout southern-central Sweden and the Oslo Region in Norway. A large continuous subsurface distribution area of Silurian sedimentary rocks occurs from southern Estonia through Latvia and Lithuania to the northeastern part of Poland. Overviews of the occurrence of Silurian altered volcanic ash beds (K-bentonites, bentonites) around the Iapetus palaeoocean were published in Bergström *et al*. (1992) and Huff, Bergström & Kolata (2002).

Studies so far of Wenlock bentonites in northern Europe include Cave & Loydell (1998), Batchelor & Jeppsson (1999), Kiipli & Kallaste (2006), Ray (2007) and Kiipli *et al*. (2008*a*, *c*). Due to the large number of volcanic eruption layers, and small number of studied sections, data on Wenlock bentonites are still fragmentary and far from satisfactory for reliable correlation of sections using bentonites. Here we present new results from a geochemical study of 37 bentonite layers sampled from the lower and middle Wenlock of the Ventspils D3 and Vidale 263 drill cores (Latvia) and compare these new data with earlier tephrostratigraphic and geochemical studies in the region. The aim of the present study is a geochemical characterization of lower to middle Wenlock bentonites in the East Baltic and production of a new, more complete list of volcanic ash horizons, that can be used for correlations in future studies in wider areas in northern Europe.

Aspects of the biostratigraphy the Ohesaare core have been published by Kaljo (1970) and Loydell, Kaljo & Männik (1998), the Ventspils D3 core by Gailite, Ulst & Jakovleva (1987) and the Ruhnu 500 core by Põldvere (2003). The chitinozoans of these cores have been studied by Nestor (1994). The biostratigraphy of the Vidale 263 core has not been previously published.

2. Material and methods

Thirty-seven thin bentonites varying in thickness from 0.1 to 6.0 cm (online Appendix at http//journals.cambridge.org/geo) were collected from the Ventspils D3 and Vidale 263 cores drilled in West Latvia (Fig. 1). These cores are stored in the Latvian Agency of Environment, Meteorology and Geology. While the host shales are grey, the altered volcanic ashes can be recognized by their yellowish or bluish-grey colour. Biotite phenocrysts visible to the naked eye often confirm the volcanic origin of the bentonites. Very thin volcanic ash beds were sampled together with the host shale, and separation was performed in the laboratory by picking out fragments of different colours. In these cases both volcanic ashes and host shales were analysed.

With the aim of identifying major minerals in the sampled interbeds, randomly oriented bulk samples were analysed by X-ray diffractometry (XRD). An association of illite–smectite and kaolinite as major minerals has been considered to confirm the volcanic origin of the interbeds. More rarely, volcanic ash has been altered to authigenic K-sanidine with minor

*Author for correspondence: tarmo.kiipli@gi.ee

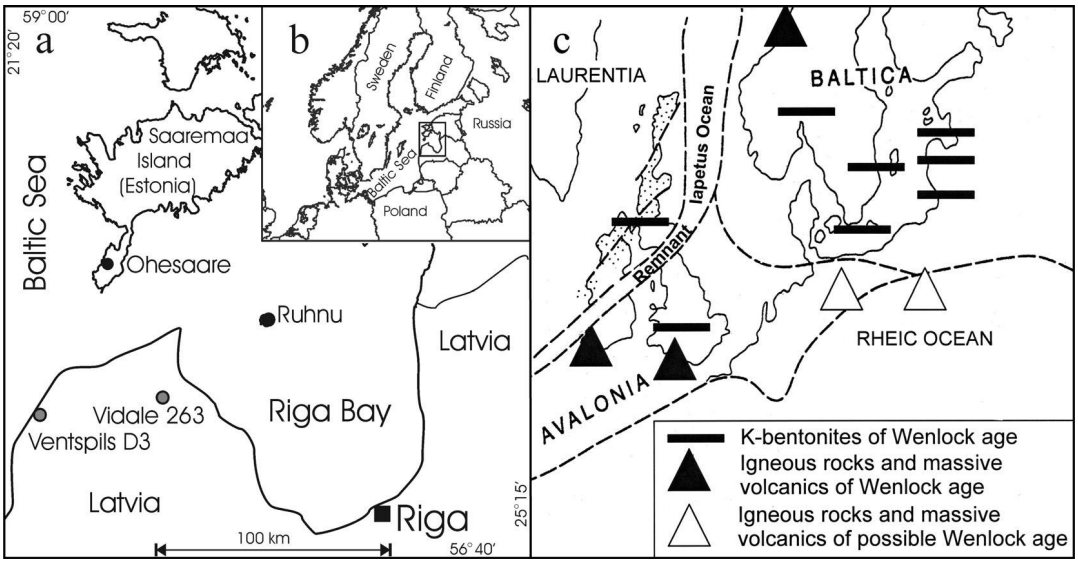

Figure 1. (a) Location of drill holes. Grey rings – sections studied in this work; black rings – sections studied in Kiipli & Kallaste (2006). Wider area (b) with location of studied region. Sketch of Wenlock palaeogeography (c) according to Cave & Loydell (1998) showing colliding Baltica and Laurentia with occurrences of Wenlock age K-bentonites, massive volcanics and igneous rocks of Wenlock age. Stippled area indicates orogenic belts.

illite–smectite and kaolinite (Hints *et al*. 2008). Host shales are composed of a different association of terrigenous minerals including illite, quartz, chlorite and minor K-feldspar.

Magmatic sanidine phenocryst (K,Na,Ca)$AlSi_3O_8$ composition has proved to be a very useful indicator of particular volcanic eruption layers (bentonites) in earlier Telychian sections from the East Baltic area (Kiipli & Kallaste, 2002; Kallaste & Kiipli, 2006; Kiipli *et al*. 2010). Kastner (1971) demonstrated that sedimentary authigenic feldspars have pure end-member compositions $KAlSi_3O_8$ or $NaAlSi_3O_8$ only. Therefore we consider intermediate compositions of the K–Na feldspar (sanidine) as an indication of magmatic origin.

A small percentage of Ca substituted for Na and minor Ba substituted for K in alkali feldspar (Ginibre, Wörner & Kronz, 2004) can influence the position of the sanidine $20\bar{1}$ reflection. Therefore numerical values of sanidine composition, calculated from that reflection, in reality show the content of the Na+Ca component in mol %. Considering this effect as minor in our previous works (Kiipli & Kallaste, 2002 and other later publications), sanidine composition was expressed in units of Na-component concentration in (K,Na)$AlSi_3O_8$. A more accurate expression, Na+Ca component in sanidine, is adopted here. Numerical values herein are still strictly comparable with those in our previous publications.

The phenocrysts were analysed from coarse fractions (0.04–0.1 mm) separated from 2 grams of bentonite. The fraction 0.04–0.1 mm constitutes a very small percentage of the bulk bentonite. Sanidine dominates among phenocrysts with less abundant biotite and quartz. While biotite occurs often as hexagonal plates, sanidine and quartz are commonly represented by irregular fragments (shards) of the original crystals. Minor apatite and zircon are observed in some layers. Plagioclase phenocrysts, which are commonly the most abundant in silicic magmas, are not preserved in the East Baltic ash beds, since they were most likely dissolved and recrystallized into clay minerals. The $20\bar{1}$ reflection was measured in a range from 23.5 to 26.0 °2θ using Fe filtered Co Kα radiation. From the position of the $20\bar{1}$ reflection, the (Na,Ca)$AlSi_3O_8$ content in (K,Na,Ca)$AlSi_3O_8$ solid solution (sanidine) was calculated according to Orville (1967). In favourable cases (sharp reflection and low content of authigenic potassium feldspar), the precision of the method was ± 1 %. In less favourable cases the precision was ± 2 %. Checking of the method by EDS microanalyses in two samples showed reasonable accordance within analytical uncertainty of both methods; in Ventspils 715.4 m EDS analysis showed $Na_{0.45}Ca_{0.03}K_{0.52}Ba_{0.00}Al_1Si_3O_8$ and XRD showed $(Na,Ca)_{0.50}(K,Ba)_{0.50}Al_1Si_3O_8$; in Ventspils 720.6 m EDS showed $Na_{0.32}Ca_{0.01}K_{0.65}Ba_{0.02}Al_1Si_3O_8$ and XRD showed $(Na,Ca)_{0.30}(K,Ba)_{0.70}Al_1Si_3O_8$. XRD analysis is performed simultaneously on 1000–2000 grains of sanidine and therefore represents average composition of the sample better than EDS microanalysis performed on only some tens of grains. All measured XRD spectra are available in the collections database of the Institute of Geology Tallinn University of Technology at http://sarv.gi.ee/reference.php?id=1203.

Many volcanic ash beds show a very wide sanidine reflection which does not permit identification of a particular bed, but nevertheless separates these beds clearly from those with a sharp reflection. Wide reflections indicate heterogeneous composition of the sanidine, caused most probably by presence of the zoned crystals in a source magma. Examples of the measured XRD profiles with curve fitting results from the Wenlock of Latvia are shown in Figure 2.

Samples of sufficient size, at least 8 g, were analysed by the standard X-ray fluorescence (XRF) method from pressed powders for major and trace elements, applying empirical correction coefficients to the measured intensities of spectral lines, at the Institute of Geology Tallinn University of Technology. Precision of the method was mostly better than ± 5 % of the concentration and for trace elements in the range 10–30 ppm better than ± 10 %. For calibration and quality control, reference materials from France (Govindaraju, 1995) and Estonia (Kiipli *et al*. 2000) were used. Long range accuracy of the method is shown in Kiipli *et al*. (2008*b*).

3. Stratigraphy

In terms of chitinozoan biozonation, the studied interval in the Ventspils D3 and Vidale 263 cores belongs to the *Margachitina margaritana* to *Conochitina subcyatha* biozones (Figs 3, 4). According to Nestor (1994), this interval comprises the lower Sheinwoodian to lower Homerian. In Vidale 263 the *Conochitina tuba, Cingulochitina cingulata, Eisenackitina spongiosa* and *Conochitina pachycephala* biozones were established (Fig. 3).

4. Results

4.a. General results

In the studied stratigraphic range (in terms of chitinozoan biozones from *M. margaritana* to *C. subcyatha*), 71 bentonite interbeds occur in four drill cores (Fig. 4). Using the chitinozoan biozonation as a framework and based on the sanidine properties, these bentonites can be grouped into 47 volcanic eruption layers (Table 1). Previously, in the Ohesaare and Ruhnu cores (Kiipli & Kallaste, 2006) only 28 eruption layers were recognized in this interval. In the Vattenfallet exposure on Gotland, a bentonite with a sharp sanidine reflection and 28.5 mol % of Na+Ca-component was found within the upper *K. ranuliformis* conodont Biozone (Kiipli *et al*. 2008*a*). In Lithuania near the *antennularius/flexilis* graptolite biozone boundary, a bentonite with a wide sanidine reflection and about 26–27 mol % of Na+Ca component was identified (Kiipli *et al*. 2008*c*). These two bentonites have not been found in Estonian and Latvian sections. Therefore the total volcanic record at the level of present knowledge comprises 49 eruption layers in the studied interval. This list is still provisional, because only eight correlations are well proved, based on sharp sanidine reflections (Table 1; Figs 4, 5), and nine correlations are less certain, characterized by wide sanidine reflections. Consequently, the larger number of eruption layers is established only in a single section.

Several bentonites are also newly recognized with a previously unknown type of sanidine XRD spectrum indicating the presence of sodium-rich, up to 58 mol %, components in alkali feldspar phenocrysts (Figs 2, 5).

4.b. *Margachitina margaritana* Biozone

This interval includes four widespread eruption layers: Aizpute (ID311), Ohesaare (ID210), Lusklint (ID150) and Ireviken (ID127). Depths of these bentonites in the Ohesaare core are 351.7 m, 345.8 m, 342.1 m and 340.8 m, respectively (Fig. 4). Bentonite names and ID numbers are those of Kallaste & Kiipli (2006) and Kiipli *et al*. (2010). The Ohesaare Bentonite and the Ireviken Bentonite are also found in the Ventspils core at depths 792.8 m and 789.2 m, respectively (Table 1; Fig. 4). Additionally, 5 cm above the Ohesaare Bentonite a new eruption layer with a sharp sanidine reflection and 37.4 mol % of Na+Ca component was found. In Vidale not one of these layers was found. A possible reason is poor core recovery in this interval causing destruction of thin soft volcanic ash beds.

4.c. *Conochitina mamilla* Biozone

Three bentonites containing sanidine with a very wide reflection occur here. Often these very wide reflections exhibit a specific plateau-like shape with a relatively abrupt fall at the Na-rich end of the spectrum (Fig. 2h). The Ohesaare 323.2 m and Ruhnu 435.84 m beds consist of two layers differing in colour. The first contains sanidine with a plateau-like spectrum and the other sanidine with a sharp reflection with 45–46 mol % of Na+Ca component. In Ventspils 767.15 m and Vidale 709.90 m, only the plateau-like type was found.

The Vidale 703.15 bed, possibly belonging to this biozone, contains sanidine with a sharp reflection.

4.d. *Conochitina tuba* Biozone

In the lower part of the biozone, two bentonites with wide sanidine reflections occur in the Ohesaare and Ruhnu sections. In the upper part of the biozone in Ohesaare, four bentonites with sharp sanidine reflections have been found. In Vidale 694.90 m a sharp sanidine reflection was also found, being very similar to the Ohesaare 301.95 m and Ohesaare 301.36 m beds. According to the sampling depth records, the Vidale 694.90 m bentonite must belong to the lower part of the *C. cingulata* Biozone, but this is only 10 cm above the first sample with *C. cingulata*, and small uncertanties in depth interpretations between bentonite researchers and biostratigraphers are possible. We consider the Vidale 694.90 m bed as belonging in the *C. tuba*

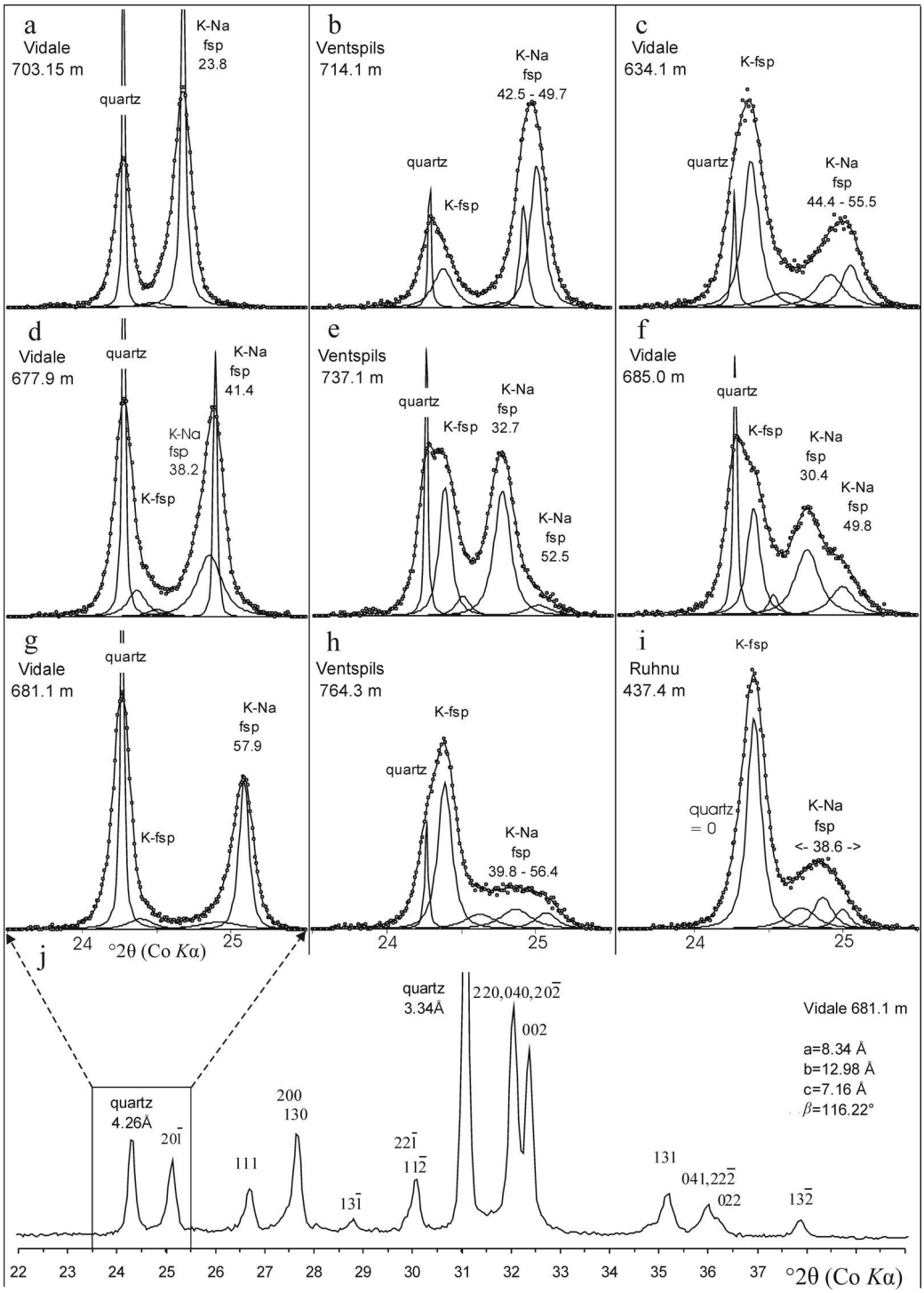

Figure 2. Selected sanidine spectra from studied bentonites. Points mark measured curve, and solid lines reflections of minerals calculated using three, four or five component curve-fitting program; from left to right: quartz, authigenic potassium feldspar (K-fsp) and magmatic K–Na-sanidine (K–Na fsp) described by one, two or three components. Numbers above reflection represent calculated $(Na,Ca)AlSi_3O_8$ content (mol %) in sanidine main component. (a–i) Various types of sanidine spectra from 23.5 to 25.5 degrees. (j) Longer XRD pattern of the sanidine from the Vidale core depth 681.1 m.

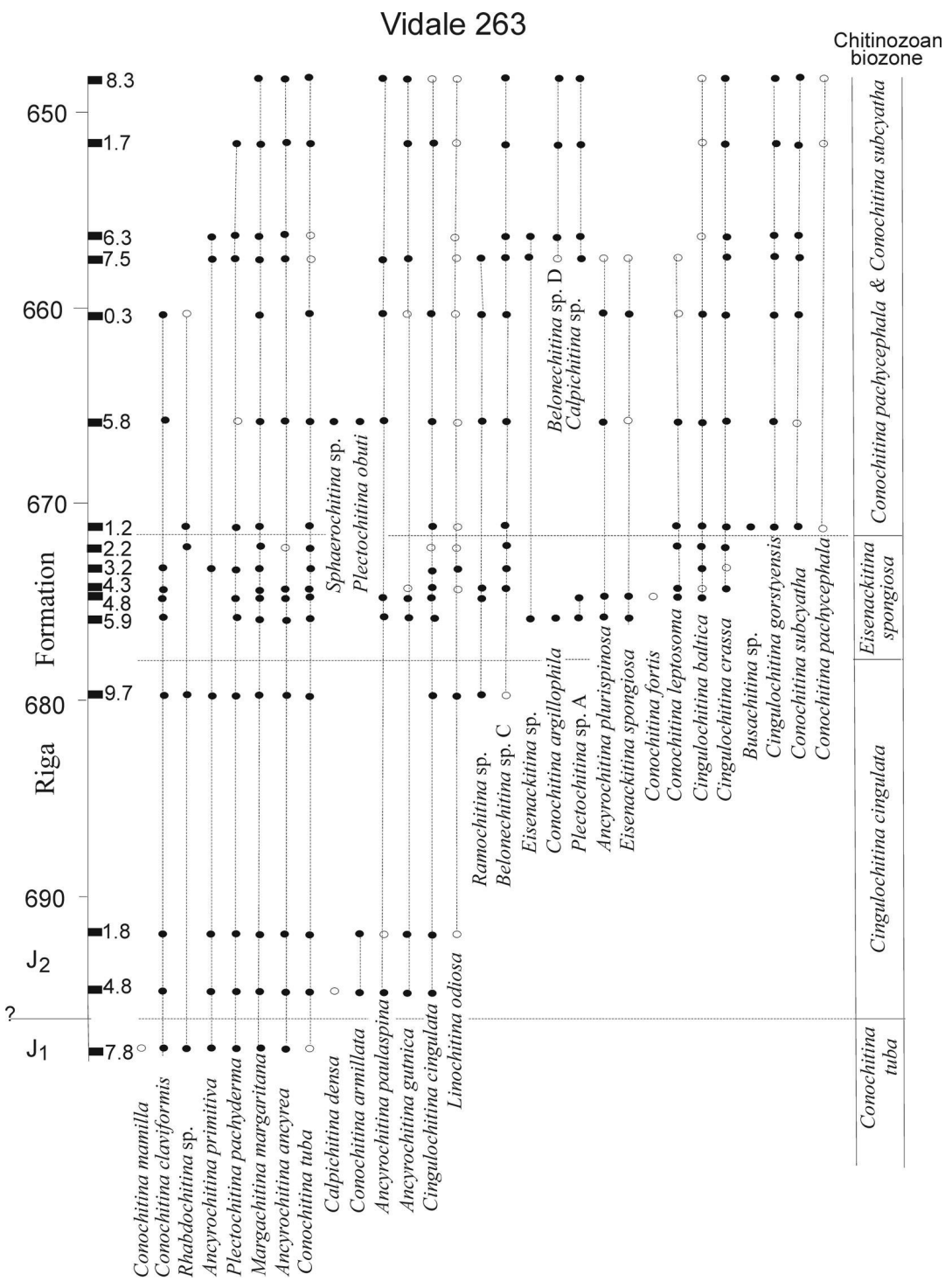

Figure 3. Distribution of chitinozoans in the Vidale 263 core.

Biozone on the basis of a very similar sanidine XRD reflection with bentonites from the upper part of *C. tuba* in Ohesaare.

The step-by-step rise of the Na+Ca-component in sanidine in closely spaced eruption layers starting from Vidale 703.15 m to Ohesaare 300.25 m is remarkable.

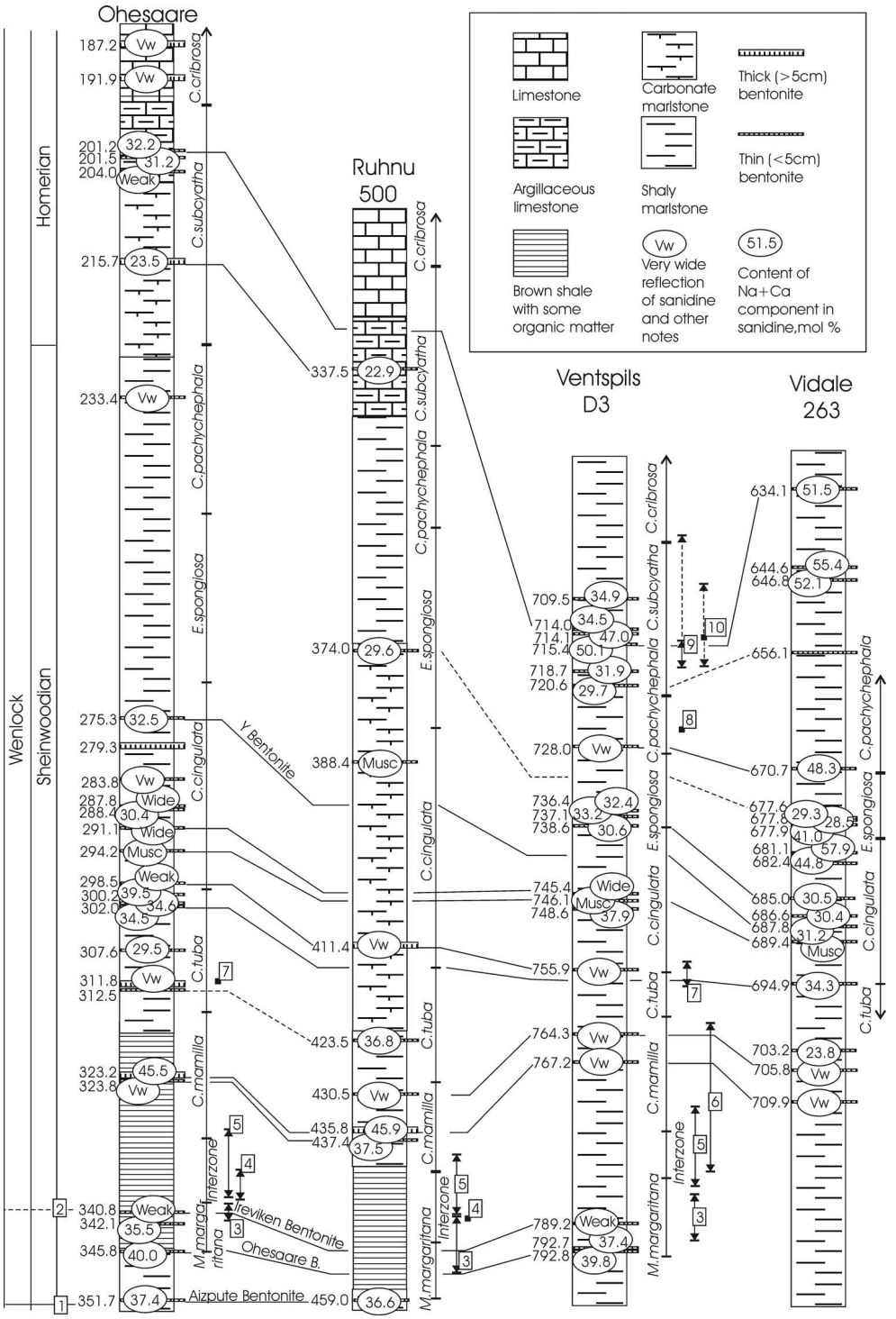

Figure 4. Geological sections of studied drill cores. 1 – traditional Llandovery/Wenlock boundary at the FAD of *Cyrtograptus centrifugus* marked by the Aizpute Bentonite (Martinsson, Bassett & Holland, 1981; Kiipli *et al*. 2010). 2 – Llandovery/Wenlock boundary proposed by Kiipli & Kallaste (2006) and Kiipli *et al*. (2008*a*) marked by the Ireviken Bentonite. 3–10 – finds of zonal graptolites (Loydell, Kaljo & Männik, 1998; Gailite, Ulst & Jakovleva, 1987; Põldvere, 2003); 3 – *Cyrtograptus murchisoni*, 4 – *Monograptus firmus*, 5 – *Monograptus riccartonensis*, 6 – *Streptograptus antennularius*, 7 – *Monograptus flexilis*, 8 – *Cyrtograptus radians*, 9 – *Testograptus testis*, 10 – *Cyrtograptus lundgreni*.

Table 1 Occurrence of Wenlock bentonites in the frame of chitinozoan biozonation

Chitinozoan biozones	Ohesaare, depth (m)	Ruhnu, depth (m)	Ventspils, depth (m)	Vidale, depth (m)	Sanidine main component: Peak width, 2 theta	Sanidine main component: $(Na,Ca)AlSi_3O_8$ mol %	Biotite
C. subcyata			709.50		0.09	34.9	++
C. subcyata	201.20		714.05		0.13–0.14	32.2–34.5	++
C. subcyata			714.10		0.18	49.8	++
C. subcyata	201.50				0.17	31.2	++
C. subcyata	203.96				Weak		+++
C. subcyata			715.40	634.10	0.23–0.25	50.1–51.5	+
C. subcyata				644.60	0.22	54.1	+
C. subcyata				646.80	0.31	51.3	++
C. subcyata			718.70		Weak		++
C. subcyata	215.70	337.50			0.06–0.07	22.9–23.5	+++
C. subcyata			720.60	656.10	0.09	29.7	++
C. pachycephala	233.44				Very wide		
C. pachycephala			728.05	670.70	Very wide		++
E. spongiosa		374.00		677.60	0.06–0.16	29.3–29.6	++
E. spongiosa				677.75	0.17	28.5	++
E. spongiosa				677.90	0.08	40.9	++
E. spongiosa			736.40		0.27	32.4	+
E. spongiosa			737.10		0.21	33.2	+
C. cingulata				681.10	0.10	57.9	no
C. cingulata				682.40	0.27	44.8	+
C. cingulata		388.40			Weak		M
C. cingulata			738.60	685.00	0.22–0.27	30.5–30.6	++
C. cingulata				686.60	0.30	30.4	+
C. cingulata	275.32			687.80	0.12–0.18	31.2–32.5	+
C. cingulata	283.78				Very wide		+++
C. cingulata	287.85				Wide		no
C. cingulata	288.44				0.11	30.4	++
C. cingulata	291.09		745.40		Wide		+
C. cingulata	294.23		746.10	689.40	Weak		M
C. cingulata			748.60		Weak		no
C. cingulata	298.51	411.45	755.90		Very wide		no
C. tuba	300.25				0.12	39.5	no
C. tuba	301.36				0.06	34.6	++
C. tuba	301.95			694.90	0.08–0.10	34.3–34.5	++
C. tuba	307.61				0.08	29.5	+++
C. tuba	311.80				Very wide		no
C. tuba	312.46	423.50			0.28	36.8	+
C. mamilla				703.15	0.07	23.8	++
C. mamilla		430.50	764.30	705.80	0.22–0.30	48.1–52.3	no
C. mamilla	323.20	435.84	767.15	709.90	0.26–0.34	46.8–47.7	+
C. mamilla	323.21	435.84			0.19–0.20	45.5–45.9	++
C. mamilla	323.85	437.40			Very wide		+
M. margaritana	340.79		789.20		Weak		+++
M. margaritana	342.08				0.24	35.5	no
M. margaritana			792.70		0.13	37.4	+
M. margaritana	345.83		792.75		0.25–0.27	39.8–40.0	+
M. margaritana	351.70				0.08–0.12	36.2–37.8	+

+++ Biotite is abundant; ++ Biotite is rare (10–100 flakes); + Less than 10 flakes; M – muscovite

This may indicate the fractional crystallization and settling of potassium-rich sanidine into the lower parts of a magma chamber.

4.e. *Cingulochitina cingulata* Biozone and lower part of *Eisenackitina spongiosa* Biozone

Most of the approximately thirteen eruption layers in the *C. cingulata* Biozone are characterized by sanidines with wide and very wide spectra, and correlations are therefore hypothetical. In the lower part of the biozone an ash bed containing muscovite can be recognized in the Ohesaare 294.23 m, Ventspils 746.10 m and Vidale 689.40 m beds. Another eruption layer containing muscovite occurs in the upper part of the biozone in the Ruhnu core at a depth of 388.40 m.

Remarkable layers occur in the middle and upper part of the *C. cingulata* Biozone with wide sanidine reflections (Figs 2e–f, 5) requiring five-component fitting of the XRD spectrum (commonly four-component fitting is sufficient). These five fitting profiles (XRD reflections) represent quartz, K-sanidine and three K–Na sanidine components. This type occurs in the Vidale core at depths of 687.80 m, 686.60 m and 685.00 m. In the Ohesaare core this type occurs at a depth 275.32 m. This layer was previously correlated with the Y Bentonite from the Slite quarry on Gotland, Sweden (Kiipli *et al*. 2008*a*). In the Ventspils core this type of sanidine occurs at a depth of 738.60 m in the *C. cingulata* Biozone and 737.10 m and 736.40 m in the lower part of the *E. spongiosa* Biozone. During sampling of the Ventspils core, we noticed that there

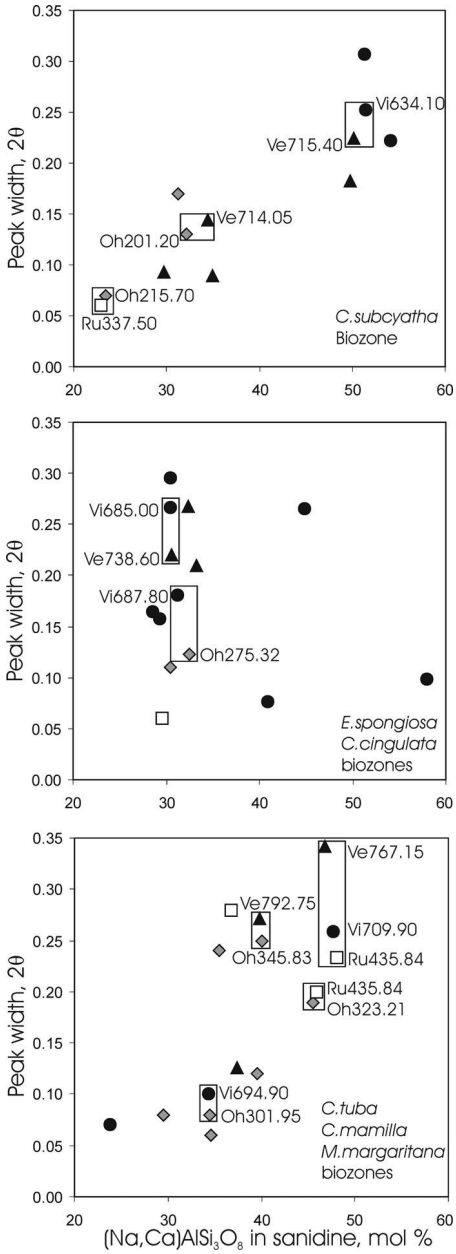

Figure 5. Sanidine composition in the lower and middle Wenlock. Frames join sanidine from correlated ash beds. Many ash beds with sanidine showing wide reflections are not represented here, because the compositions of these sanidines cannot be reliably expressed in numerical values by the method used. Black circles – Vidale (Vi); black triangles – Ventspils (Ve); grey rhombs – Ohesaare (Oh); empty squares – Ruhnu (Ru) section. Numbers represent depths of correlated bentonites (m).

was low recovery of core at this level, and no clearly understandable depth records. Therefore it cannot be excluded that occurrence of some beds of this type in the *E. spongiosa* Biozone can be considered as an artefact arising from different interpretations of depths. Future studies of more sections must make clear the real number of eruption beds of this type. In Table 1 and online Appendix Table 3, the fourth (main) component of the sanidine exhibiting 30–33 mol % of the Na+Ca-component is reported. The fifth component has lower intensity and contains about 50 mol % (± 4 mol %) of the Na+Ca-component.

In addition to the beds with wide sanidine reflections, a few with sharp reflections have also been discovered, for example, in beds from Ohesaare 288.44 m and Vidale 681.10 m. The latter is characterized by an unusually high content of the Na+Ca-component, 57.9 mol % (Fig. 2g).

4.f. *Eisenackitina spongiosa* Biozone

As well as two bentonites containing sanidine with wide reflections in the lower part (see above), we found three bentonites in this biozone in Vidale containing sharp sanidine reflections (Table 1). A bentonite from Ruhnu at 374 m also contains sanidine with a similar Na+Ca-component to that in Vidale 677.60 m, but the reflection is much sharper and this raises some doubt about the correlation of these layers.

4.g. *Conochitina pachycephala* Biozone

At the lower boundary of the biozone an ash bed containing sanidine with a very wide reflection occurs in the Ventspils (728.00 m) and Vidale (670.70 m) cores. In the upper part of the biozone in the Ohesaare (233.40 m) core, another eruption layer occurs with similar sanidine.

4.h. *Conochitina subcyatha* Biozone

In the lower and upper part of this biozone several eruption layers occur with sharp sanidine reflections and 23–35 mol % of the Na+Ca component. In the middle of the biozone in the Ventspils (715.40 m, 714.10 m) and Vidale (646.80 m, 644.60 m, 634.10 m) cores occur bentonites with a wide sanidine reflection and around 50 mol % of the Na+Ca component (Fig. 2b, c). This type of sanidine was not found in previous studies (Kiipli & Kallaste, 2006; Kiipli *et al*. 2008*a*, *c*).

4.i. Geochemistry of major components and the discrimination between volcanic ash interbeds and host rock

The host rocks in the Wenlock part of these cores are represented by shales containing 15–30 % of carbonate material. Illite, chlorite, quartz, calcite and dolomite are major minerals in the host shales. Major minerals in the bentonites are kaolinite, illite–smectite, K-feldspar and pyrite. XRF analyses (online Appendix at http://journals.cambridge.org/geo) showed unusually high contents of sulphur in bentonites reaching 9 % (Fig. 6a). Host marlstones contain on average only

0.5 % sulphur. Judging from the composition of bentonites showing low sulphur content, altered volcanic ashes contain only about 1–2 % of silicate Fe_2O_3. Host shales contain 3–5 % of silicate Fe_2O_3. A larger deviation of the bentonite regression line from the pyrite line at higher concentrations is caused by weathering of pyrite and partial removal of sulphur in drill-core boxes during the long storage time (20 years for Vidale 263 and 40 years for the Ventspils D3 core). This is confirmed by the occurrence of jarosite and gypsum reflections on XRD patterns from samples with the highest content of sulphur. The probable reason for the higher content of pyrite in bentonites compared with host shales is that the rapid accumulation of volcanic ash changes the decay of organic matter from oxic on the sea floor to sulphate reducing in the sediment.

Bentonites in the Ventspils and Vidale cores are characterized by a low (1–5 %) K_2O content in 90 % of the analysed samples and a high (24–35 %) Al_2O_3 content in 80 % of the samples. The abundance of kaolinite and consequently the low-potassium high-aluminium type of altered volcanic ash beds is typical of Palaeozoic deep shelf environments in the East Baltic (Kiipli *et al*. 2007; Hints *et al*. 2008). This composition means that in this report we favour using the term 'bentonite' instead of 'K-bentonite', the latter being characterized by much higher (5–12 %) potassium concentrations (Kiipli *et al*. 2008*b*). High-aluminium kaolinite-rich altered volcanic ash beds found in coal formations are called tonsteins (Bohor & Triplehorn, 1993). In Figure 6b the contents of Al_2O_3 and K_2O in the studied samples are recalculated to a pyrite-free composition. The background rock type fields on the chart are composed according to analytical data in Kiipli *et al*. (2008*b*, *d*). The host rocks cluster in a clearly different field caused by the higher content of quartz and carbonates. Within the central and southern part of the Baltic Basin between depths 600 and 800 m (studied depth range in Ventspils and Vidale) in bentonites, the content of smectite layers in illite–smectite ranges between 25 and 45 % (Somelar, 2009).

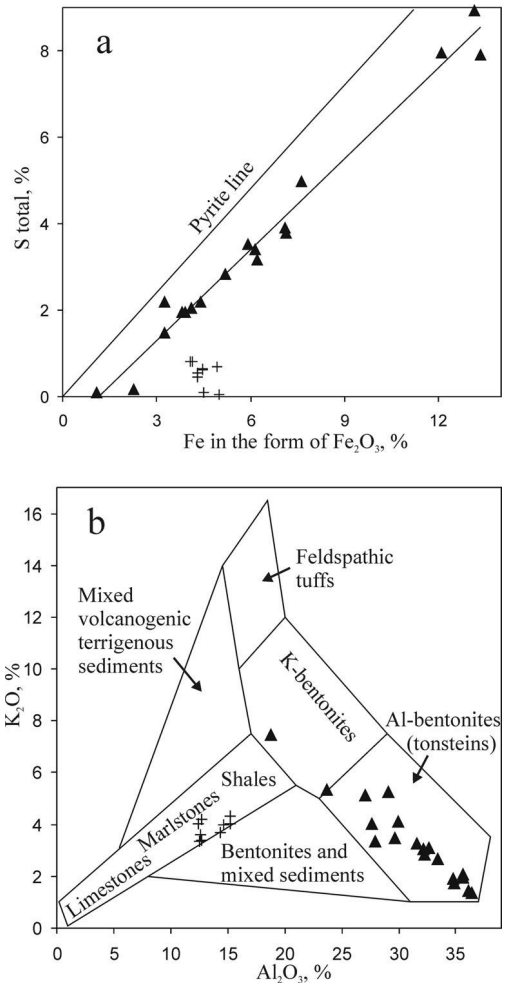

Figure 6. Comparison of major components in altered volcanic ash beds and host shales and marlstones. Black triangles – Wenlock bentonites from the Ventspils D3 and Vidale 263 drill cores. Crosses – host shales from the same cores. Rock fields on (b) are composed using analytical data from Kiipli *et al*. (2008*b*, *d*).

4.j. Geochemistry of trace elements, interpretation of source magma and tectonic setting

4.j.1. General

Volcanic ash alteration on the seafloor and in sediments leads to the formation of clay minerals. During this process 50 % or more of the original SiO_2 and cations are leached out (Huff, Kolata & Bergström, 1996; Kiipli, Kiipli & Kallaste, 2006). Therefore, easily soluble elements in bentonites cannot be used for interpreting the source magma. In contrast, concentrations of elements of low solubility increase in the forming bentonites. For example, the Al_2O_3 content in silicic magmatic rocks varies mostly between 10 and 18 %, but in altered volcanic ashes (bentonites) the Al_2O_3 content is much higher being within a range of 18–36 % (Fig. 6b). Alternatively, immobile trace elements (Ti, Zr, Y, Nb, Ce, Ga, Sc) can be used tentatively to interpret initial magma compositions (Winchester & Floyd, 1977). The problem is that concentrations of immobile elements also rise during the formation of clay from volcanic ash. In this paper, following the approach proposed by Kiipli *et al*. (2008*d*), we are using corrected values for immobile trace elements calculated as follows:

$$I_S = (14/Al_2O_3) \times I_B$$

where I_S is approximate concentration of immobile trace element in source magma; I_B is immobile trace element concentration in bentonite; 14 is average content of Al_2O_3 in silicic magmatic rocks (%),

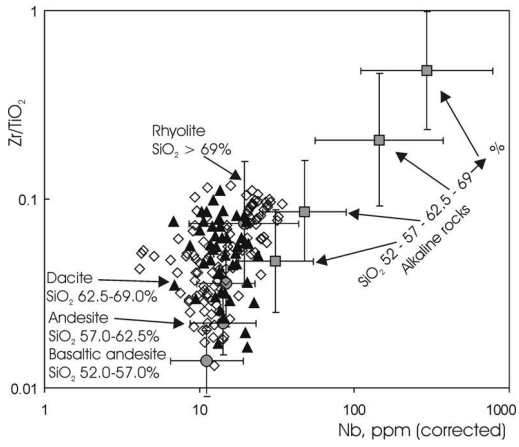

Figure 7. Comparison of Wenlock volcanism (black triangles) and earlier Telychian volcanism (empty rhombs) in the East Baltic with Pliocene to Quaternary volcanism in Italy using the Zr/TiO_2 ratio and Nb. Grey rings represent the geometric mean of the calc-alkaline rocks and grey quadrangles alkaline rocks from Italy. One standard deviation (as a coefficient) is shown by bars. Data from Italian volcanic rocks are from Peccerillo (2005), Telychian bentonites from Kiipli *et al*. (2008*d*) and Wenlock bentonites in addition to the present study are from Batchelor & Jeppson (1999) and Kiipli *et al*. (2008*a*, *c*, *d*).

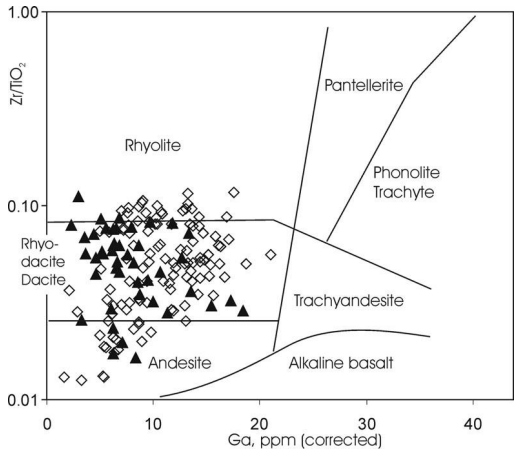

Figure 8. Comparison of Wenlock and Telychian volcanism from the East Baltic on the Zr/TiO_2–Ga chart according to Winchester & Floyd (1977). Black triangles – Wenlock bentonites; empty rhombs – Telychian bentonites.

(Turekian & Wedepohl, 1961); Al_2O_3 is content of aluminium oxide in bentonite (%).

This calculation gives values on average 50 % lower for immobile trace elements than analysed in bentonites, and these values are considered to be closer to the original concentrations. Scaling immobile trace element concentrations back to the supposed initial Al_2O_3 content enables more accurate use of many trace element diagrams. This method enables the use of element ratio diagrams as well as element concentration diagrams for altered volcanic rocks such as bentonites and K-bentonites.

4.j.2. Comparison with Pliocene to Quaternary volcanism in Italy

Intensive volcanic activity during recent geological time in Italy is represented by variable compositions of magmas forming all known volcanic rock types (Peccerillo, 2005). As a hypothesis, the tectonomagmatic environment in the Mediterranean may be considered similar to the environment in a remnant of the Iapetus Ocean between colliding Baltica and Laurentia in Wenlock times.

In Figure 7 the fractionation index, the Zr/TiO_2 ratio, is plotted against Nb concentrations interpreted as an alkalinity index (Winchester & Floyd, 1977; Pearce & Norry, 1979). Using about 1500 analyses of volcanic rocks published by Peccerillo (2005) as a framework (Fig. 7), the source magmas of Wenlock bentonites from the East Baltic can be interpreted as subalkaline, ranging from andesite to rhyolite. Overlapping of compositional ranges in Italian rocks does not exclude some mildly alkaline source magmas for East Baltic bentonites, but also does not prove it. Clearly, strongly alkaline source magmas did not provide the volcanic ash for the East Baltic bentonites. Comparison with earlier Telychian bentonites (Kiipli *et al*. 2008*d*) reveals essentially overlapping compositional ranges for both ages.

4.j.3. Zr/TiO_2–Ga chart

Winchester & Floyd (1977) proposed Ga in addition to Nb as an alkalinity index for magmatic rocks. Plotting the East Baltic bentonite data onto the framework composed by Winchester & Floyd (1977; Fig. 8) provides confirmation of the interpretation made from comparison with Italian rocks, that most source magmas of East Baltic bentonites were subalkaline. Corrected Ga concentrations are too low for alkaline magmas. Batchelor & Jeppsson (1999), based on the composition of apatite phenocrysts, proposed alkaline as well as calc-alkaline magma as a source for the some Wenlock bentonites from Gotland. Wenlock bentonites show, on average, lower corrected Ga concentrations than Telychian ones.

4.j.4. Interpretation of tectonic setting

Using corrected values of Y and Nb on the diagram for granitic rocks proposed by Pearce, Harris & Tindle (1984), these data indicate mostly volcanic arc and syn-collisional tectonic environments for the volcanic sources of the Wenlock bentonites (Fig. 9). A smaller number of points fall in the within-plate granites field.

Wenlock and earlier Telychian volcanism shows a largely overlapping distribution of concentrations with

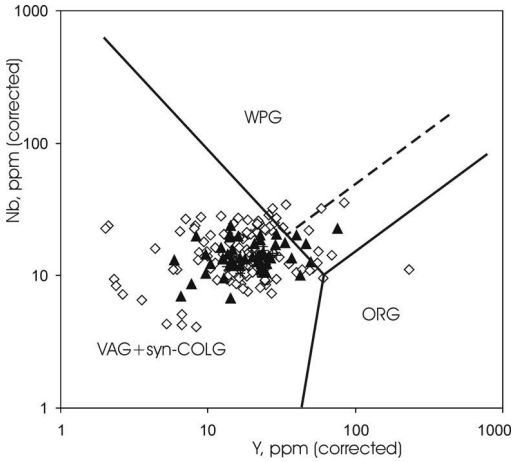

Figure 9. Comparison of Wenlock and Telychian volcanism from the East Baltic on the Y–Nb plot for granitic rocks according to Pearce, Harris & Tindle (1984). Black triangles – Wenlock bentonites; empty rhombs – Telychian bentonites. VAG+syn-COLG – volcanic arc and syn-collisional granites; WPG – within plate granites; ORG – ocean ridge granites.

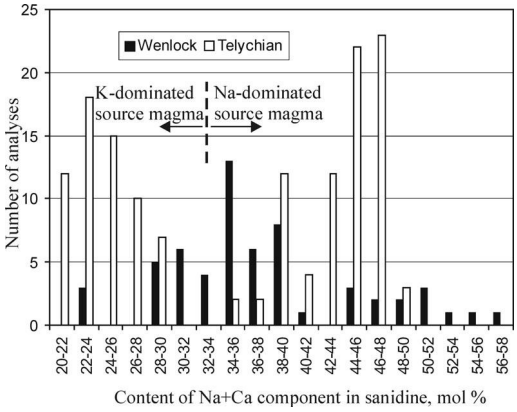

Figure 10. Frequency of the sanidine composition in the East Baltic bentonites. For explanation of separation line between K-dominated and Na-dominated source magma, see text and Figure 12.

the exception of some Telychian bentonites that reveal lower Y values.

4.j.5. Sanidine composition compared in Wenlock and Telychian bentonites

Sanidine composition in Wenlock bentonites shows a bimodal distribution clustering dominantly between 28–40 mol % and 44–58 mol % of the Na+Ca component (Fig. 10). Sanidine in Telychian bentonites also shows a bimodal distribution of composition clustering at 20–30 and 38–48 mol %. Sanidine in Wenlock bentonites is on average more sodic compared to that of Telychian bentonites.

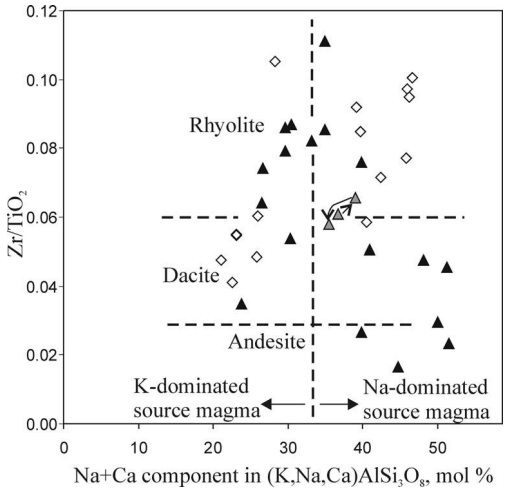

Figure 11. Sanidine composition and Zr/TiO_2 in the East Baltic bentonites with tentative interpretation of source magma. Approximate separation lines between different source magma types are according to Figures 7, 8 and 12. Grey triangles connected with arrows – the lowermost successive bentonites (Aizpute, Ohesaare and Lusklint) originated most probably from the same source. Arrows show temporal succession of eruptions.

Comparison of the sanidine compositions with the Zr/TiO_2 ratio (fractionation index) shows that the less evolved dacitic Telychian magmas had more potassic compositions of the sanidine and the highly evolved rhyolitic magmas had more sodic sanidine compositions (Fig. 11). By contrast, later in Wenlock times, less evolved magmas included more sodic sanidine phenocrysts than the highly evolved rhyolitic magmas.

5. Discussion

5.a. Use of sanidine phenocryst composition for geochemical fingerprinting of volcanic eruptions and correlation of sections

High sanidine forms in magma chambers during cooling at high temperatures and is a metastable mineral at Earth surface temperatures (Gill, 1996). After the fast cooling during volcanic eruption, recrystallization of the mineral slows down significantly and has not proceeded much in the East Baltic area, even during the 400 Ma from the Silurian to the present day. This may not be the case everywhere. For example, attempts to analyse sanidine by XRD from the Silurian bentonites of the Oslo region (Norway) correlated by trace elements with bentonites containing sanidine in Estonia (Kiipli *et al*. 2001) did not reveal measurable reflections. Evidently the rocks were heated too much during Caledonian orogenesis or Permian magmatism. Another reason for the lack of sanidine may be a highly chemically reactive environment in some organic rich black shales, for example, in Bornholm, where we also could not find sanidine by XRD. Sanidine may already have been absent in source magma. The precise

causes of a lack of sanidine in particular cases are unknown and must be the topic of future studies. Our present knowledge indicates that XRD measurements of the sanidine composition can be used successfully for geochemical fingerprinting of volcanic ash layers in Estonia, Latvia, Lithuania and Gotland (Sweden). This method can probably also be used in some areas of the mainland of Sweden, as suggested by dating of the Ordovician bentonite from Kinnekulle (southern Sweden) by the K–Ar method using sanidine (Byström-Asklund, Baadsgaard & Folinsbee, 1961).

For establishing correlations of sections by chemical and/or mineralogical fingerprinting of the volcanic ash beds in Palaeozoic sections, two approaches can be used:

(1) Analysing as many geochemical and mineralogical parameters as possible with the aim of finding the unique signature of the particular eruption layer. This approach was used by Bergström *et al*. (1995), Hetherington, Nakrem & Batchelor (2004), Batchelor (2009) and Inanli, Huff & Bergström (2009). Searching for the unique fingerprint is certainly important, but is time consuming and expensive work, and cannot be easily done for a large number of ash beds. This method is well applicable where a few eruption layers occur in sections.

(2) Another approach, analysing with maximum possible accuracy only a single significant parameter, is preferable in sections containing a large number of ash beds (Kiipli *et al*. 2010). The problem is that in this case the same composition (sanidine composition in our study) can occur repetitively in a section. For example, sharp sanidine reflections with a similar content of the Na+Ca component between 28 and 32 mol % occur in the East Baltic Silurian in 12 eruption layers (Kiipli & Kallaste, 2006; Kiipli *et al*. 2010; present study). As the East Baltic Silurian contains more than 100 established volcanic eruption layers, determination of the sanidine composition restricts possible variants for correlation considerably. Additional constraints can be obtained from the biostratigraphical information. Analysing all occurring layers for a single primary magmatic signature with very precise methods enables establishment of a unique succession of many eruptions. The unique temporal succession of several volcanic ash beds can be used, together with biostratigraphy, for correlation of sections even when the analysed parameter shows the same value in several ash beds.

5.b. Integrated petrogenetic interpretation and possible location of source volcanoes

Analysis of immobile trace elements has enabled a provisional estimate of the source magma of the Wenlock bentonites as being subalkaline, ranging from dacite to rhyolite, originating in volcanic arc and syncollisional tectonic settings. Andesite as a source magma indicated by some low Zr/TiO_2 ratios is less probable, because East Baltic Silurian volcanic ashes commonly contain sanidine as a major phenocryst. In recent andesites, sanidine occurs only rarely as a minor phenocryst (Winter, 2001, p. 303).

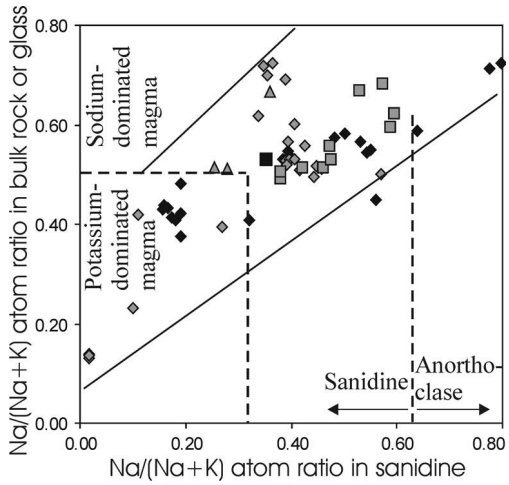

Figure 12. Comparison of the Na/(Na+K) atom ratio in sanidine and coexisting volcanic glass or whole rock. Black – comparison with glass; grey – comparison with whole rock. Rhombs – alkaline rocks; squares – rhyolites; triangles – dacites. Data sources: Anderson, Davis & Lu (2000); Basu & Vitaliano (1976); Carmichael (1967); Chesner (1998); Christiansen (2001); Gaeta (1998); Henry, Price & Smyth (1988); Landi, Bertagnini & Rosi (1999); Maughan *et al*. (2002); Macdonald, Rogers & Tindle (2007); McHenry (2009); Morgan *et al*. (2006); Pappalardo, Ottolini & Mastrolorenzo (2008); Sacchi *et al*. (2005); Smith (1974, pp. 47, 50); Zellmer & Clavero (2006).

Analysis of sanidine composition provides an additional tentative possibility of estimating the potassium/sodium ratio in source magmas. When temperature decreases in a binary $NaAlSi_3O_8$–$KAlSi_3O_8$ system, the first crystallizing phase is a potassium-rich sanidine, followed later by a more sodic one (Bowen & Tuttle, 1950). Real magmas are multicomponent systems and crystallization is more complicated. However, empirical comparison of sanidine composition with coexisting volcanic glass and whole rock shows, although strongly scattered, the same relationship (Fig. 12). Pyroclastic sanidine in the East Baltic Silurian forms commonly only a small percentage of the bentonite, indicating that eruptions occurred at the initial stages of sanidine crystallization. Therefore we may suppose higher Na/K ratios in source magma than in sanidine. Based on Figure 12, we can deduce that bentonites containing sanidine with less than approximately 33 mol % of Na+Ca component probably crystallized from potassium-dominated magma and those with more sodium-rich sanidine from the magma where sodium dominates over potassium.

Intrusive rocks of Wenlock age are known from the Scandinavian Caledonides in South Central Norway around Trondheim (Corfu *et al*. 2006). Massive metavolcanic rocks of Silurian age occur in the Northern Phyllite Zone in Germany (Timmerman, 2008) and in

the Holy Cross mountains in Poland (Krawczyk, 2008). Therefore at the level of present knowledge, volcanic sources for the East Baltic bentonites of Wenlock age could have been in a collision zone between Baltica and Laurentia or in the Central European Caledonides. Mapping of the underlying Telychian and overlying upper Wenlock volcanic ash layers indicated an origin from the Iapetus palaeo-ocean (Kiipli *et al*. 2008*a*, *b*, *c*, *d*). To enable composition of volcanic ash distribution maps, the lower–middle Wenlock bentonites need to be studied in a wider area in the future.

6. Conclusions

Study of sanidine in the lower and middle Wenlock part of the Ventspils D3 and Vidale 263 drill cores reveals about 20 previously unknown eruption layers and gives, in combination with the formerly studied Ohesaare and Ruhnu cores, the most complete list available at this time of volcanic beds for the East Baltic area constrained by the chitinozoan biozonation. XRD measurements revealed several new types of sanidine spectra, in particular, samples with a high Na+Ca (48–58 mol %) content. Sanidine in the studied part of the Wenlock in the East Baltic is of variable composition, having excellent potential for geochemical fingerprinting of volcanic eruption layers.

Immobile trace elements and the sanidine composition indicate subalkaline volcanism generated in volcanic arc and syncollisional tectonic environments. Sanidine composition suggests that both potassium- and sodium-dominated source magmas occurred in the Silurian at the margins of the Baltica plate.

Acknowledgements. This study is a contribution to the Estonian Science Foundation grant 7605 and target financing projects SF0140016s09 and SF0140020s08. We thank A. Murnieks, R. Pomeranceva and R. Einasto for kindly helping in sampling in the Latvian Agency of Environment, Meteorology and Geology, the late K. Orlova for XRF analyses, D. K. Loydell for correcting language and two anonymous referees for help.

References

ANDERSON, A. T., DAVIS, A. M. & LU, F. 2000. Evolution of Bishop Tuff rhyolitic magma based on melt and magnetite inclusions and zoned phenocrysts. *Journal of Petrology* **41**, 449–73.

BASU, A. & VITALIANO, C. J. 1976. Sanidine from the Mesa Falls Tuff, Ashton Idaho. *American Mineralogist* **61**, 405–8.

BATCHELOR, R. A. 2009 (for 2008). Geochemical "Golden Spike" for Lower Palaeozoic metabentonites. *Earth and Environmental Science Transactions of the Royal Society of Edinburgh* **99**, 177–87.

BATCHELOR, R. A. & JEPPSSON, L. 1999. Wenlock metabentonites from Gotland, Sweden: geochemistry, sources and potential as chemostratigraphic markers. *Geological Magazine* **136**, 661–9.

BERGSTRÖM, S. M., HUFF, W. D., KOLATA, D. R. & BAUERT, H. 1995. Nomenclature, stratigraphy, chemical fingerprinting and areal distribution of some Middle Ordovician K–bentonites in Baltoscandia. *GFF* **117**, 1–13.

BERGSTRÖM, S. M., HUFF, W. D., KOLATA, D. R. & KALJO, D. 1992. Silurian K-bentonites in the Iapetus Region: A preliminary event-stratigraphic and tectonomagmatic assessment. *GFF* **114**, 327–34.

BOHOR, B. F. & TRIPLEHORN, D. M. 1993. Tonsteins: altered volcanic ash layers in coal-bearing sequences. *Geological Society of America Special Paper* **285**, 1–44.

BOWEN, N. L. & TUTTLE, O. F. 1950. The system $NaAlSi_3O_8$–$KAlSi_3O_8$–H_2O. *Journal of Geology* **58**, 489–511.

BYSTRÖM-ASKLUND, A. M., BAADSGAARD, H. & FOLINSBEE, R. E. 1961. K/Ar age of biotite, sanidine and illite from Middle Ordovician bentonites at Kinnekulle Sweden. *Geologiska Föreningens i Stockholm Förhandlingar* **83**, 92–6.

CARMICHAEL, I. S. E. 1967. The mineralogy and petrology of the volcanic rocks from the Leucite Hills, Wyoming. *Contributions to Mineralogy and Petrology* **15**, 24–66.

CAVE, R. & LOYDELL, D. K. 1998. Wenlock volcanism in the Welsh Basin. *Geological Journal* **33**, 107–20.

CHESNER, C. A. 1998. Petrogenesis of the Toba Tuffs, Sumatra, Indonesia. *Journal of Petrology* **39**, 397–438.

CHRISTIANSEN, R. L. 2001. The Quaternary and Pliocene Yellowstone Plateau Volcanic Field of Wyoming, Idaho, and Montana. *US Geological Survey Professional Paper* **729-G**, 1–159.

COCKS, L. R. M. & TORSVIK, T. H. 2005. Baltica from the late Precambrian to the mid-Palaeozoic times: The gain and loss of terrain's identity. *Earth-Science Reviews* **72**, 39–66.

CORFU, F., TORSVIK, T. H., ANDERSEN, T. B., ASHWAL, L. D., RAMSAY, D. M. & ROBERTS, R. J. 2006. Early Silurian mafic–ultramafic and granitic plutonism in contemporaneous flysch, Magerøy, northern Norway: U–Pb ages and regional significance. *Journal of the Geological Society, London* **163**, 291–301.

GAETA, M. 1998. Petrogenetic implications of Ba-sanidine in the Lionato Tuff, Italy. *Mineralogical Magazine* **62**, 697–701.

GAILITE, L. K., ULST, R. J. & JAKOVLEVA, V. I. 1987. *Stratotype and type sections of the Silurian of Latvia*. Riga: Zinatne, 183 pp.

GILL, R. 1996. *Chemical Fundamentals of Geology*. London: Chapman & Hall, 290 pp.

GINIBRE, C., WÖRNER, G. & KRONZ, A. 2004. Structure and dynamics of the Laacher See magma chamber (Eifel, Germany) from major and trace element zoning in sanidine: a cathodoluminescence and electron microprobe study. *Journal of Petrology* **45**, 2197–223.

GOVINDARAJU, K. 1995. 1995 working values with confidence limits for twenty six CRPG, ANRT and IWG-GIT geostandards. *Geostandards Newsletter* **19**, Special Issue, 1–32.

HENRY, C. D., PRICE, J. G. & SMYTH, R. C. 1988. Chemical and thermal zonation in a mildly alkaline magma system Infiernito Caldera, Trans-Pecos Texas. *Contributions to Mineralogy and Petrology* **98**, 194–211.

HETHERINGTON, C. J., NAKREM, H. A., & BATCHELOR, R. A. 2004. The Bjørntvet metabentonite: A new correlation tool for the Silurian of the southwest Oslo Region. *Norwegian Journal of Geology* **84**, 239–50.

HINTS, R., KIRSIMÄE, K., SOMELAR, P., KALLASTE, T. & KIIPLI, T. 2008. Multiphase Silurian bentonites in the Baltic Palaeobasin. *Sedimentary Geology* **209**, 69–79.

HUFF, W. D., BERGSTRÖM, S. M. & KOLATA, D. R. 2002. Silurian K-bentonites of the Dnestr basin, Podolia,

Ukraine. *Journal of the Geological Society, London* **157**, 493–504.

HUFF, W. D., KOLATA, D. R. & BERGSTRÖM, S. M. 1996. Large-magnitude Middle Ordovician volcanic ash falls in North America and Europe: dimensions, emplacement and post-emplacement characteristics. *Journal of Volcanology and Geothermal Research* **73**, 285–301.

INANLI, F. Ö., HUFF, W. D. & BERGSTRÖM, S. M. 2009. The Lower Silurian (Llandovery) Osmundsberg K-bentonite in Baltoscandia and the British Isles: Chemical fingerprinting and regional correlation. *GFF* **131**, 269–79.

KALJO, D. (ed.) 1970. *Silurian of Estonia*. Tallinn: Valgus, 343 pp.

KALLASTE, T. & KIIPLI, T. 2006. New correlations of Telychian bentonites in Estonia. *Proceedings of the Estonian Academy of Sciences, Geology* **55**, 241–51.

KASTNER, M. 1971. Authigenic feldspars in carbonate rocks. *American Mineralogist* **56**, 1403–42.

KIIPLI, E., KIIPLI, T. & KALLASTE, T. 2006. Identification of the O-bentonite in the deep shelf sections with implication on stratigraphy and lithofacies, East Baltic Silurian. *GFF* **128**, 255–60.

KIIPLI, T., BATCHELOR, R. A., BERNAL, J. P., COWING, C., HAGEL-BRUNNSTROM, M., INGHAM, M. N., JOHNSON, D., KIVISILLA, J., KNAACK, C., KUMP, P., LOZANO, R., MICHIELS, D., ORLOVA, K., PIRRUS, E., ROUSSEAU, R. M., RUZICKA, J., SANDSTROM, H. & WILLIS, J. P. 2000. Seven sedimentary rock reference samples from Estonia. *Oil Shale* **17**, 215–23.

KIIPLI, T., JEPPSSON, L., KALLASTE, T. & SÖDERLUND, U. 2008*a*. Correlation of Silurian bentonites from Gotland and the East Baltic using sanidine phenocryst composition, and biostratigraphical consequences. *Journal of the Geological Society, London* **165**, 211–20.

KIIPLI, T. & KALLASTE, T. 2002. Correlation of Telychian sections from shallow to deep sea facies in Estonia and Latvia based on the sanidine composition of bentonites. *Proceedings of the Estonian Academy of Sciences, Geology* **51**, 143–56.

KIIPLI, T. & KALLASTE, T. 2006. Wenlock and uppermost Llandovery bentonites as stratigraphic markers in Estonia, Latvia and Sweden. *GFF* **128**, 139–46.

KIIPLI, T., KALLASTE, T., NESTOR, V. & LOYDELL, D. K. 2010. Integrated Telychian (Silurian) K-bentonite chemostratigraphy and biostratigraphy in Estonia and Latvia. *Lethaia* **43**, 32–44.

KIIPLI, T., KIIPLI, E., KALLASTE, T., HINTS, R., SOMELAR, P. & KIRSIMÄE, K. 2007. Altered volcanic ash as an indicator of marine environment, reflecting pH and sedimentation rate – example from the Ordovician Kinnekulle bed of Baltoscandia. *Clays and Clay Minerals* **55**, 177–88.

KIIPLI, T., MÄNNIK, P., BATCHELOR, R. A., KIIPLI, E., KALLASTE, T. & PERENS, H. 2001. Correlation of Telychian (Silurian) altered volcanic ash beds in Estonia, Sweden and Norway. *Norwegian Journal of Geology* **81**, 179–93.

KIIPLI, T., ORLOVA, K., KIIPLI, E. & KALLASTE, T. 2008*b*. Use of immobile trace elements for the correlation of Telychian bentonites on Saaremaa Island, Estonia, and mapping of volcanic ash clouds. *Estonian Journal of Earth Sciences* **57**, 39–52.

KIIPLI, T., RADZEVIČIUS, S., KALLASTE, T., MOTUZA, V., JEPPSSON, L. & WICKSRÖM, L. 2008*c*. Wenlock bentonites in Lithuania and correlation with bentonites from sections in Estonia, Sweden and Norway. *GFF* **130**, 203–10.

KIIPLI, T., SOESOO, A., KALLASTE, T. & KIIPLI, E. 2008*d*. Geochemistry of Telychian (Silurian) K-bentonites in Estonia and Latvia. *Journal of Volcanology and Geothermal Research* **171**, 45–58.

KRAWCZYK, CH. M., MCCANN, T., COCKS, L. R. M., ENGLAND, R. W., MCBRIDE, J. H. & WYBRANIEC, S. 2008. Caledonian tectonics. In *The Geology of Central Europe. Volume 1: Precambrian and Palaeozoic* (ed. T. McCann), pp. 303–81. London: Geological Society.

LANDI, P., BERTAGNINI, A. & ROSI, M. 1999. Chemical zoning and crystallization mechanisms in the magma chamber of the Pomici di Base plinian eruption of Somma-Vesuvius (Italy). *Contributions to Mineralogy and Petrology* **135**, 179–97.

LOYDELL, D. K., KALJO, D. & MÄNNIK, P. 1998. Integrated biostratigraphy of the lower Silurian of the Ohesaare core, Saaremaa, Estonia. *Geological Magazine* **135**, 769–83.

MACDONALD, R., ROGERS, N. W. & TINDLE, A. G. 2007. Distribution of germanium between phenocrysts and melt in peralkaline rhyolites from the Kenia Rift Valley. *Mineralogical Magazine* **71**, 703–13.

MARTINSSON, A., BASSETT, M. G. & HOLLAND, C. H. 1981. Ratification of Standard Chronostratigraphical Divisions and Stratotypes for the Silurian System. *Lethaia* **14**, 168.

MAUGHAN, L. L., CHRISTIANSEN, E. H., BEST, M. G., GROMME, C. S., DEINO, A. L. & TINGEY, T. G. 2002. The Oligocene Lund Tuff, Great Basin, USA: a very large volume monotonous intermediate. *Journal of Volcanology and Geothermal Research* **113**, 129–57.

MCHENRY, L. J. 2009. Element mobility during zeolitic and argillitic alteration of volcanic ash in a closed basin lacustrine environment: Case study Olduvai Gorge, Tanzania. *Chemical Geology* **265**, 540–52.

MORGAN, D. J., BLAKE, S., ROGER, N. W., DE VIVO, B., ROLANDI, G. & DAVIDSON, J. P. 2006. Magma chamber recharge at Vesuvius in the century prior to the eruption of A.D. 79. *Geology* **34**, 845–8.

NESTOR, V. 1994. Early Silurian chitinozoans in Estonia and North Latvia. *Academia* **4**, 1–163.

ORVILLE, P. M. 1967. Unit cell parameters of the microcline-low albite and the sanidine-high albite solid solution series. *American Mineralogist* **52**, 55–86.

PAPPALARDO, L., OTTOLINI, L. & MASTROLORENZO, G. 2008. The Campanian Ignimbrite (southern Italy) geochemical zoning: insight on the generation of a super-eruption from catastrophic differentiation and fast withdrawal. *Contributions to Mineralogy and Petrology* **156**, 1–26.

PEARCE, J. A., HARRIS, N. B. W. & TINDLE, A. G. 1984. Trace element discrimination diagrams for the tectonic interpretation of granitic rocks. *Journal of Petrology* **25**, 956–83.

PEARCE, J. A. & NORRY, M. J. 1979. Petrogenetic implications of Ti, Zr, Y, and Nb variations in volcanic rocks. *Contributions to Mineralogy and Petrology* **69**, 33–47.

PECCERILLO, A. 2005. *Plio-Quaternary Volcanism in Italy. Petrology, Geochemistry, Geodynamics*. Berlin, Heidelberg, New York: Springer, 365 pp.

PÕLDVERE, A. (ed.) 2003. Ruhnu (500) drill core, Estonian Geological Sections. *Geological Survey of Estonia Bulletin* **5**, 1–76.

RAY, D. C. 2007. The correlation of Lower Wenlock Series (Silurian) bentonites from the Lower Hill Farm and

Eastnor Park boreholes, Midland Platform, England. *Proceedings of the Geologists` Association* **118**, 175–85.

SACCHI, M., INSINGA, D., MILIA, A., MOLISSO, F., RASPINI, A., TORRENTE, M. M. & CONFORTI, A. 2005. Stratigraphic signature of the Vesuvius 79 AD event of the Sarno prodelta system, Naples Bay. *Marine Geology* **222–223**, 443–69.

SMITH, J. V. 1974. *Feldspar Minerals 2, Chemical and Textural Properties*. Berlin, Heidelberg, New York: Springer-Verlag, 690 pp.

SOMELAR, P. 2009. *Illitization of K-bentonites in the Baltic Basin*. Dissertationes Geologicae Universitatis Tartuensis **25**, Tartu University Press, pp. 1–118. Published thesis.

TIMMERMAN, M. J. 2008. Palaeozoic magmatism. In *The Geology of Central Europe. Volume 1: Precambrian and Palaeozoic* (ed. T. McCann), pp. 665–748. London: Geological Society.

TUREKIAN, K. K. & WEDEPOHL, K. H. 1961. Distribution of the elements in some major units of the Earth's crust. *Geological Society of America Bulletin* **72**, 175–91.

WINCHESTER, J. A. & FLOYD, P. A. 1977. Geochemical discrimination of different magma series and their differentiation products using immobile elements. *Chemical Geology* **20**, 325–43.

WINTER, J. D. 2001. *An Introduction to Igneous and Metamorphic Petrology*. Prentice Hall, 697 pp.

ZELLMER, G. F. & CLAVERO, J. E. 2006. Using trace element correlation patterns to decipher a sanidine crystal growth chronology: An example from Taapaca volcano, Central Andes. *Journal of Volcanology and Geothermal Research* **156**, 291–301.

PAPER VI

KIIPLI, T., KALLASTE, T., NESTOR, V., LOYDELL, D. K. 2010. Integrated Telychian (Silurian) K-bentonite chemostratigraphy and biostratigraphy in Estonia and Latvia. Lethaia, 43(1), 32–44.

Lethaia
AN INTERNATIONAL JOURNAL OF PALAEONTOLOGY AND STRATIGRAPHY

Integrated Telychian (Silurian) K-bentonite chemostratigraphy and biostratigraphy in Estonia and Latvia

TARMO KIIPLI, TOIVO KALLASTE, VIIU NESTOR AND DAVID K. LOYDELL

LETHAIA

Kiipli, T., Kallaste, T., Nestor, V. & Loydell, D.K. 2010: Integrated Telychian (Silurian) K-bentonite chemostratigraphy and biostratigraphy in Estonia and Latvia. *Lethaia*, Vol. 43, pp. 32–44.

The distribution of altered volcanic ash layers (K-bentonites) and Telychian chitinozoans in four East Baltic drill core sections are compared. This information is integrated with graptolite and conodont biozonations to give a precise correlation chart using four different stratigraphical tools: K-bentonite-based chemostratigraphy; chitinozoan biostratigraphy; graptolite biostratigraphy; and, conodont biostratigraphy. Thickness variations in the K-bentonites suggest that the source of the volcanic ash was to the west and northwest. □ *K-bentonites, graptolites, chitinozoans, conodonts, Silurian, Telychian.*

T. Kiipli [tarmo.kiipli@gi.ee], T. Kallaste [toivo.kallaste@gi.ee], V. Nestor [viiu.nestor@gi.ee], Institute of Geology, Tallinn University of Technology, Ehitajate 5, 19086 Tallinn, Estonia; David K. Loydell [david.loydell@port.ac.uk] School of Earth and Environmental Sciences, University of Portsmouth, Burnaby Building, Burnaby Road, Portsmouth, PO1 3QL, UK; *manuscript received on 27/12/2007; and manuscript accepted on 08/01/2009.*

Altered volcanic ash beds (K-bentonites) recognized in different facies can be used as time markers and offer the unique possibility of extremely precise correlation of sedimentary sections. Spjeldnæs (1959) was the first to use K-bentonites for correlation of Silurian strata in Scandinavia. The composition of well-preserved phenocrysts of several magmatic minerals occurring in K-bentonites is specific to each bed, and serves as a basis for reliable identification in different sections. Trace elements from apatite phenocrysts occurring in Telychian K-bentonites have been studied by Batchelor & Clarkson (1993), Batchelor & Jeppsson (1994), Batchelor *et al.* (1995), and the Sr isotopes by Batchelor & Evans (2000). Biotite phenocrysts have been studied by Batchelor (2003) and Kiipli *et al.* (2008c). Trace elements in bulk-rock samples from K-bentonites have been studied and used for correlation of these beds by Pearce (1995), Huff *et al.* (1998), Kiipli *et al.* (2001) and Batchelor *et al.* (2003). An overview of Silurian K-bentonites from the Iapetus region was published by Bergström *et al.* (1992).

The composition of sanidine has been successfully applied in correlations of Telychian K-bentonites (Kiipli & Kallaste 2002; Kiipli *et al.* 2006; Kiipli & Kallaste 2006). Kiipli *et al.* (2008c) has established a detailed Telychian K-bentonite chemostratigraphy in the East Baltic, a succession that includes K-bentonites from 44 volcanic eruptions. Identification (ID) numbers were assigned to all of these K-bentonites, and specific names were given to the most widespread ones (Kallaste & Kiipli 2006).

The main aim of the present study is to produce an integrated chemo- and biostratigraphic reference scheme based on well-studied sections. Knowledge of the biostratigraphical intervals in which K-bentonites occur will form the basis for identifying the eruption layers studied in Estonia and Latvia over a wider area (including Scandinavian sections) during future studies. Integration of K-bentonite chemostratigraphy with detailed biostratigraphy is very important for the recognition of particular eruption layers, because volcanic ash layers of similar compositions occur repetitively from the same source.

Detailed biostratigraphy of the four core sections under consideration here was published in Loydell *et al.* (1998, 2003), Põldvere (2003) and Männik (2007). The occurrence of Telychian K-bentonites with reference to the conodont biozonation was published by Kiipli *et al.* (2001). Although the conodont biozonation has been subjected to only minor changes since that time (Männik 2007), the K-bentonite chemostratigraphy has changed substantially including identification of a number of new ash layers, some revised correlations, use of sanidine as the main correlation criterion and an entirely new labelling system. Comparison of the K-bentonite-based chemostratigraphy and graptolite biozonation was presented in Kiipli *et al.* (2007a).

The large number of sections in Estonia and Latvia from which K-bentonites have been studied in the last ten years (Fig. 1) has allowed the preliminary thickness variation of several K-bentonites to be established (Kiipli *et al.* 2008a, b, c and new schemes herein) enabling us

DOI 10.1111/j.1502-3931.2009.00162.x

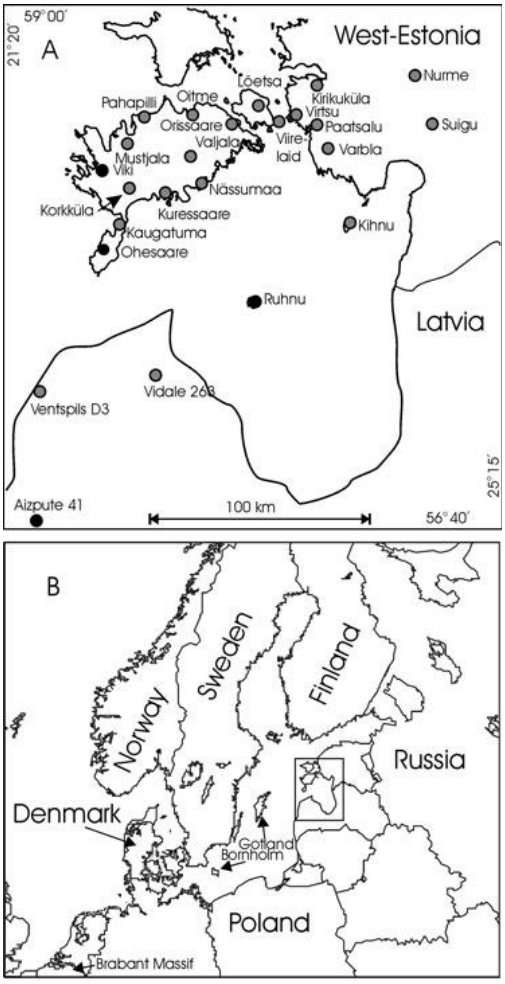

Fig. 1. Study area A, and wider geographical region with location of studied area B, black rings – sections studied in detail biostratigraphically in present work. Grey rings – all sections from which Telychian K-bentonites have been studied and used for constructing isopach maps.

to point out the potential locations of the source volcanoes, and also to predict which eruption layers we can expect to find in sections studied in the future. Future mapping of ash layers across wider areas will provide the possibility of locating the volcanic sources more precisely.

Analytical method for the study of sanidine phenocrysts

To identify particular eruption layers, the composition of magmatic sanidine phenocrysts was analysed using X-ray diffractometry (XRD). The phenocrysts were analysed from coarse fractions (0.04–0.1 mm) of the K-bentonites. The $20\bar{1}$ reflection was measured in a range from 23.5 to 26.0 °2θ. From the position of the $20\bar{1}$ reflection, the $NaAlSi_3O_8$ content in (K, Na) $AlSi_3O_8$ solid solution (sanidine) was calculated according to Orville (1967). In favourable cases (sharp reflection and low content of authigenic potassium feldspar), the precision of the method was ± 1%. In less favourable cases, the precision was ± 2%. Many volcanic ash beds show a very wide sanidine reflection, which does not permit identification of a particular bed but, nevertheless, separates these beds clearly from those with a sharp reflection (Kiipli & Kallaste 2002, 2006; Kallaste & Kiipli 2006; Kiipli *et al.* 2006, 2008a, c). The method in the previous discussion has been used effectively in studies of K-bentonites in Estonia, Latvia, Lithuania and Gotland (Sweden). In all of these regions, the Silurian rocks have not been affected by high temperatures during their geological history. Silurian K-bentonites from Bornholm and the Oslo region do not reveal XRD reflections of K-Na-sanidine, although platy feldspar phenocrysts can be observed under the microscope (personal observations). The probable cause is that rocks in these areas were heated to more than 100 °C. Elevated temperature must result in faster recrystallization of the magmatic sanidine, which is metastable below about 600 °C.

Characterization of altered volcanic ash layers

Thin (0.1–20 cm thick) volcanic ash layers in the East Baltic region have been altered to an assemblage of authigenic silicate minerals. Highly illitic illite-smectite is the dominant mineral in most altered ash beds. Chemically, these beds are characterized by high (5–12%) K_2O content and are named K-bentonites (Huff 2008). In the deep-water Aizpute-41 section, ash layers contain much kaolinite in addition to the illite-smectite and correspondingly the K_2O content in these layers is often less than in the surrounding host shales, being in the range of 1–5%. Kaolinite-rich altered volcanic ash beds have been termed tonsteins in the literature (Bohor & Triplehorn 1993). Chemically, these beds are characterized by a high-content (26–34%) of Al_2O_3 and could be called also Al-bentonites. Some altered volcanic ash layers in the relatively shallow water Viki section are composed dominantly of authigenic potassium feldspar and are characterized by an extremely high content (12–16%) of K_2O (Kiipli *et al.* 2001). These layers can be termed feldspathic tuffs or feldspathites. In the intermediate depth Ohesaare and Ruhnu sections, all three lithological

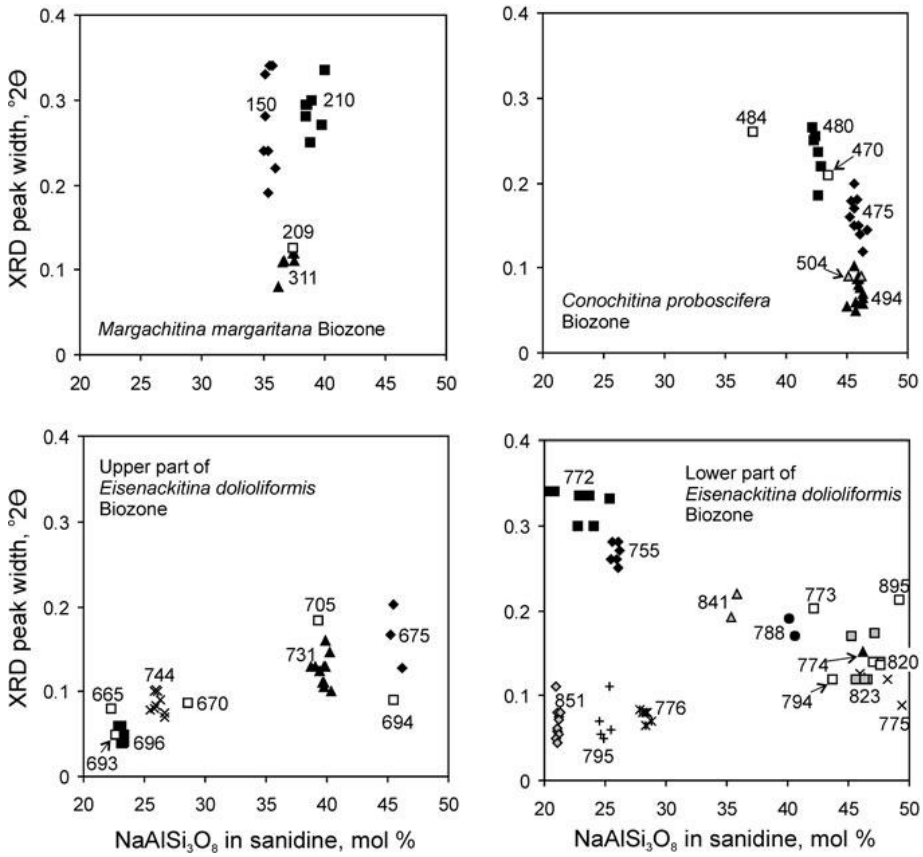

Fig. 2. Composition of sanidine from studied volcanic ash beds arranged according to chitinozoan biozones. Different symbols on each plot represent different eruption layers correlated between sections. Empty quadrangles represent volcanic eruption layers found only in a single section. ID numbers are the same as in other figures and in Table 1.

varieties of altered volcanic ashes alternate (Hints *et al.* 2008). These compositional variations have been explained by the different environments of ash alteration depending on the depth of the sea on the Palaeozoic shelf (Kiipli *et al.* 2007b). For conciseness we call all these lithological varieties K-bentonites in this study, as the K-bentonite type dominates among the studied layers.

Discrimination of particular eruption layers was achieved by analysing the composition of primary magmatic sanidine (Table 1, Fig. 2 and the section on analytical methods). Precise measurements enable discrimination even of layers with quite similar sanidine compositions in cases of sharp well-measurable reflections. For example, K-bentonites ID475 and ID480 include sanidine with 46 mol% and 42 mol% of Na-component, respectively (Table 1). Although these eruption layers occur stratigraphically very close to each other, they can be easily distinguished by XRD determinations of the sanidine composition. Within the relatively small study area (150 × 200 km), we have not observed changes in the composition of sanidine within a single eruption layer, although this can potentially occur over wider areas. For example, the Lusklint Bentonite in Gotland reveals a sharper $20\bar{1}$ sanidine reflection than it does in sections in the East Baltic region (Kiipli *et al.* 2008a). If a volcanic ash was deposited directly onto a previous eruption layer as a result of a very low background sedimentation rate and both ashes are mixed in one sample, then XRD analyses still can distinguish sanidine reflections from these separate eruption materials if the compositions are sufficiently different. This case has been observed in Ohesaare at a depth of 370.77 m, where layers ID823, with sharp sanidine reflection, and ID818, with a wide reflection, were mixed. Similarly, in the

Table 1. Sanidine properties of Telychian K-bentonites and correlation with biozones.

Bentonite ID	Bentonite name	Number of sections	Width of the sanidine reflection (degrees) and other notes	Content of $NaAlSi_3O_8$ in sanidine (mol%)	Biotite abundance	Chitinozoan biozones	Graptolite biozones	Conodont biozones
127	Ireviken	7	Much biotite & quartz, little sanidine		+++			*Ps. bicornis*
139	Storbrut	2	Little sanidine		+			
150	Lusklint	7	0.19–0.34	35.2–35.8	+	*M. margaritana*	*C. murchisoni*	
209		1	0.13	37.4	+			*P. amorphognathoides*
210	Ohesaare	7	0.25–0.35	38–40	+			
311	Aizpute	6	0.08–0.12	36.2–37.8	+			
457	Kirikuküla	11	Very wide reflection		+			
470		1	0.21	43.5	++			
475	Viki	12	0.12–0.20	45.2–46.3	+		*C. lapworthi* or *O. spiralis*	
480	Kaugatuma	7	0.18–0.27	42.0–42.8	++			
484		1	0.26	37.3	+++			
488	Kuressaare	8	Very wide reflection		+	*C. proboscifera*		*P. a. lithuanicus*
494	Ruhnu	15	0.05–0.09	45.7–46.4	+			
504		3	0.05–0.09	45.7–46.4	+			
518	Viirelaid	12?	Very wide reflection		+			
520		11?	Very wide reflection		+			
521		9?	Very wide reflection		+		*O. spiralis*	
564		4	0.12–0.17	45.0–45.8	++			
568		11?	Very wide reflection		+			
590		3	Very wide reflection		++	*A. longicollis*		
650		3	Very wide reflection		+			
658		1	0.14	40.5	++			
665		1	0.08	22.3	+++			
670		1	0.086	28.6	++		*O. spiralis* or *M. crenulata*	*P. a. angulatus*
675		2	0.127	46.2	++			
682		2	Very wide reflection		+			
693		1	0.05	22.6	+			
694		1	0.09	45.5	?			
696	Nässumaa	13	0.04–0.06	22.9–23.3	+++		*Mcl. crenulata*	
705		1	0.08–0.18	39.2–39.4	++			
719	Virtsu	12	Much biotite and quartz, little sanidine		+++			
722		3	Wide reflection + 26.5		+			
731	Nurme	14	0.10–0.16	38.7–40.3	+			
744	Tehumardi	13	0.07–0.10	25.8–26.7	++			
755	Paatsalu	9	0.25–0.30	25.5–26.2	+			
772	Pahapilli	8	0.30–0.34	20.5–24.1	+++			*P. eopennatus* ssp.n.2
773		1	0.20	42.2	+	*E. dolioliformis*	*Mcl. griestoniensis*	
774		3	0.09–0.12	46.2–48.2	++			
775		2	0.09–0.11	47.9–48.5	++			
776		6	0.07–0.08	28.1–28.8	+		*S. sartorius*	
788		2	0.17–0.19	40.1–40.6	+++			
794		1	0.12	43.7	?			
795	Mustjala	7	0.05–0.11	24.5–25.3	+++			
818		3	Very wide reflection		+			
820		1	0.14	47.6	++		*S. crispus*	
823	Valgu	6	0.12–0.17	45.2–47.6	+			*P. eopennatus* ssp.n.1
841		3	0.19–0.22	35.5–35.8	++			
843		4	Very wide reflection		+			
851	Osmundsberg	17	0.05–0.09	20.7–21.5	+++		*Sp. turriculatus*	
880		5	Very wide reflection		+			*D. staurognathoides*
895		1	0.21	49.2	++			

+++ Biotite is abundant, ++ Biotite is rare (10-100 flakes), + Only a few flakes of biotite (<10).

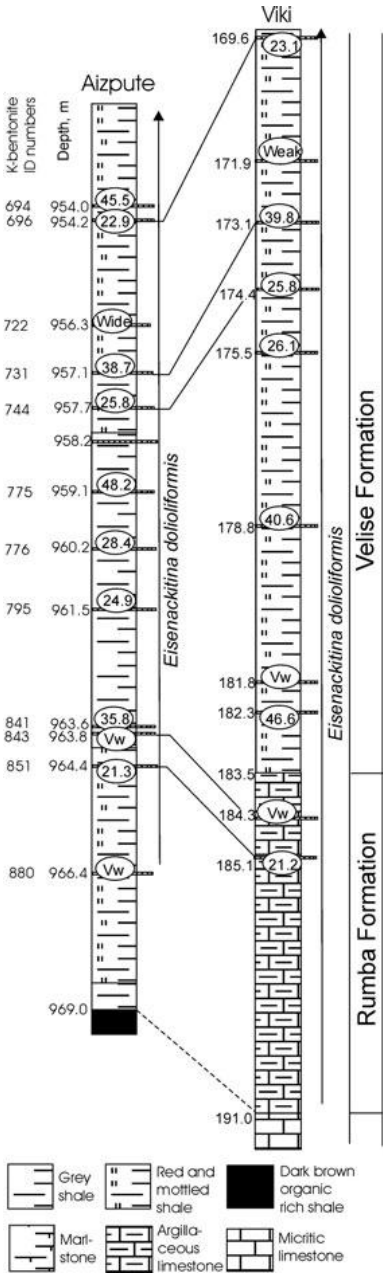

Fig. 3. Correlation of the Viki and Aizpute-41 cores using K-bentonites in the lower and middle Telychian (*Eisenackitina dolioliformis* Biozone). Despite the large number of volcanic ash beds in both cores, located about 200 km apart, only five can be correlated using their sanidine composition. In the Ruhnu core a stratigraphical gap occurs at this level and in the Ohesaare core the section is extremely condensed comprising only 2.9 m of strata. For legend see Figure 4.

Ruhnu section in the depth interval 488.24–488.40 m four different eruption layers are mixed within two samples.

Some of the eruption layers reveal unique sanidine compositions, but others include sanidines similar to those of many other layers. For example, sanidine containing 45–48 mol% of Na-component occurs in layers ID 475, 494, 504, 564, 658, 774 and 823. From this observation it follows that the identification of several eruption layers in a section is needed for establishing a unique succession of eruptions. This succession of eruptions can be identified in other sections and used for correlation. A detailed biostratigraphical framework is often essential for the reliable identification and correlation of many K-bentonite layers.

Labelling of K-bentonites

Table 1 lists K-bentonites from 51 Telychian volcanic eruptions identified in Estonia and Latvia. K-bentonite ID numbers were derived from depths in the Viki core (Kallaste & Kiipli 2006). For K-bentonites occurring in the Viki core, the ID number corresponds to the depth in decimetres from below the 100 m depth in the core: e.g. to the volcanic ash bed occurring at the depth 115.0 m was assigned the number ID 150 (Figs 3,4). Because all K-bentonites occur between 100 m and 200 m in Viki, this method gives three-digit ID numbers with 0 representing a depth of 100 m. K-bentonites occurring in other cores, but missing in the Viki core, were projected by graphic correlation to the Viki section, and this assigned formal depth in the Viki depth scale was used as the basis for derivation of the ID number (Kallaste & Kiipli 2006). The more frequently encountered and distinctive K-bentonites have been assigned names derived from the names of bore-holes and outcrops (Table 1).

The increased number of K-bentonites in Table 1 compared with earlier publications (Kallaste & Kiipli 2006, Kiipli *et al.* 2008c) is the result of the discovery of several new layers in Latvian sections.

Chitinozoan biostratigraphy and the occurrence of K-bentonites

Eisenackitina dolioliformis *Biozone*

The first appearance of *Eisenackitina dolioliformis* is in the Rumba Formation and its range corresponds to at least five graptolite biozones, including the *Spirograptus turriculatus* Biozone. The problematical identifications of *Angochitina longicollis* in the Ohesaare (Nestor 1994) and Ruhnu (Nestor 2003) cores,

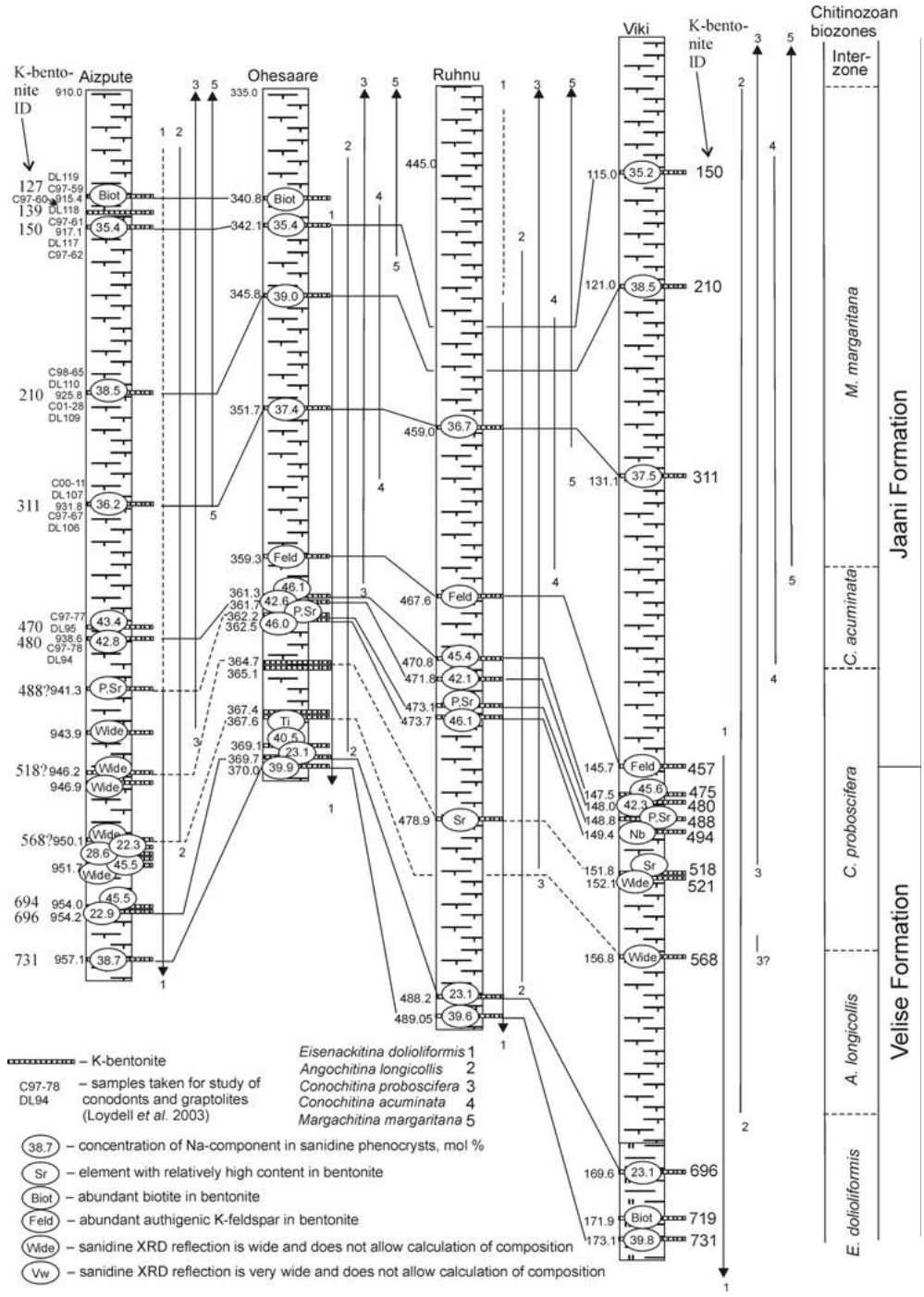

Fig. 4. Distribution of chitinozoans in four East Baltic drill-core sections and correlation of K-bentonites. For legend see Figure 3.

from the lowermost Telychian, have been re-examined and these specimens are identified now as *Angochitina* cf. *hansonica* (Soufiane & Achab 2000).

The *E. dolioliformis* Chron (early to middle Telychian) was characterized by moderately active volcanism in the closing Iapetus. Twenty-nine eruption layers are recognized in this biozone in Estonia and Latvia. Nine of them are relatively widespread and have been assigned stratigraphical names (Table 1). Twenty-three of these eruption layers include sanidine with a sufficiently distinctive composition for identification (Fig. 2). Based on geochemical data, five different volcanic sources were responsible for the deposition of these beds (Kiipli *et al.* 2008c). The best known among these K-bentonites is the Osmundsberg K-bentonite (ID 851 in this paper) studied by Bergström *et al.* (1998), Huff *et al.* (1998) and Kiipli *et al.* (2006). Bergström *et al.* (2008) recently determined the isotopic age from zircon phenocrysts of the Osmundsberg K-bentonite at Osmundsberget, Central Sweden as 438.7 ± 1.0 Ma and stated that this K-bentonite lay within the *A. longicollis* Biozone. However, given that *A. longicollis* was identified only questionably by Grahn (1998) from the Osmundsberget North section and that other early Telychian records of *A. longicollis* have proved to be misidentifications (see e.g. Loydell *et al.* 2003, p. 219), we consider that it is highly questionable that the lower Telychian of Osmundberget North belongs in the *longicollis* Biozone. More biostratigraphical research is clearly required on this very important section.

Angochitina longicollis *Biozone*

In the Viki, Ruhnu and Ohesaare cores, *A. longicollis* appears just above, and in the Aizpute-41 core a little higher above, a good marker bed, the Nässumaa K-bentonite (ID 696; Fig. 4). Based on the co-occurrences of graptolites and chitinozoans in the Aizpute-41 (Loydell *et al.* 2003) and Ventspils (Loydell & Nestor 2005) cores, *A. longicollis* appears at the base of the *Oktavites spiralis* graptolite Biozone. From the same graptolite level, *A. longicollis* has been found also in the subsurface of Gotland (Grahn 1995), in sections in the Prague Basin, Bohemia (Dufka *et al.* 1995), Girvan area, Scotland (Vandenbroucke *et al.* 2003) and Yangtze region, China (Geng *et al.* 1997). The lowest occurrence of *A. longicollis* was in the middle or upper part of the *O. spiralis* graptolite Biozone in sections in Wales (Mullins & Loydell 2001, 2002).

Five bentonites are found in this chitinozoan biozone. Most of them occur as very thin (1–5 mm thick) beds, in only a few sections in Latvia and have not been recognized in Estonia. The only widely distributed ash bed (ID 568, found in 11 sections) lies in the upper part of the *A. longicollis* biozone. This bentonite (ID 568) has a wide sanidine reflection, and can be identified in Estonian sections as the only K-bentonite occurring in this interval. Because of the indistinctive sanidine composition of this bed, its identification in Latvian sections is uncertain. For example, in Aizpute-41 three K-bentonites with wide sanidine reflections occur in this biozone.

Conochitina proboscifera *Biozone*

The *Conochitina proboscifera* Biozone was omitted from the global biozonation scheme (Verniers *et al.* 1995) because its index species was considered to appear diachronously. It is known now that this apparent diachroneity resulted from some misidentifications. In several sections, *Conochitina praeproboscifera* had been wrongly identified as *Conochitina proboscifera*. In the East Baltic, *C. praeproboscifera* appears in the lowermost part of the Rumba Formation (Nestor & Nestor 2002). In all studied sections, *C. proboscifera sensu stricto* appears above *A. longicollis* (Nestor 1994), in the upper part of the *O. spiralis* graptolite Biozone (Loydell *et al.* 2003; Loydell & Nestor 2005). From the same stratigraphical level *C. proboscifera* is known from the Banwy River section, Wales (Mullins & Loydell 2001) and from Gotland, in the Närborrningen 1 core (Grahn 1995). In the Viki core section (Fig. 4) the first specimens of *C. proboscifera* appear at the level of K-bentonite ID 568. This K-bentonite was not found in the Ruhnu core, and its location in the Aizpute-41 core is problematical. In the Ohesaare core, as indicated by several well-correlated K-bentonites, *C. proboscifera* clearly appears higher than in the Viki core. This may be because of the poor preservation of chitinozoans in the light greenish coloured shales (transitional to red coloured shales) occurring in this interval in the Ohesaare core.

Ten K-bentonites have been recognized in this biozone. Geochemical characteristics indicate three different sources for them (Kiipli *et al.* 2008c). Several K-bentonites in this interval (ID 521, 520, 518, 488, 457) are characterized by a very wide sanidine reflection indicating a heterogeneous sanidine composition. Judging from the Zr/Ti ratios, these bentonites originated from an andesitic source magma (Kiipli *et al.* 2001). A characteristic feature of these K-bentonites is a high content (200–400 ppm) of Sr.

The Ruhnu K-bentonite (ID 494) has a different composition. This distinct marker bed can be easily identified by its very sharp sanidine peak (45.7–46.3 mol% $NaAlSi_3O_8$) in 15 sections in Estonia and Latvia. This bed was recognized by its high Nb/Ti ratio also in the Garntangen section, Norway (NW30, Batchelor *et al.* 1995; Kiipli *et al.* 2001). The Viki K-bentonite

(ID 475), another geographically widely recognized ash layer in this interval, has an average $NaAlSi_3O_8$ percentage identical to that of the Ruhnu K-bentonite sanidine, but the XRD reflection is broader (Fig. 2). Sanidine in the Kaugatuma K-bentonite (ID 480) differs in the average $NaAlSi_3O_8$ percentage by only 3.5% from the sanidine in the Ruhnu and Viki K-bentonites, but this difference can be easily recognized and this ash bed identified.

Conochitina acuminata *Biozone*

Conochitina acuminata, the nominal species of the *C. acuminata* chitinozoan Biozone, has not been recorded from the East Baltic deeper-water sections (Aizpute-41, Ventspils), but it is found in many other cores (Nestor 1994, 2005). As in the Banwy River section, Wales (Mullins & Loydell 2001), in the Ohesaare core the appearance level of the species corresponds to the lower part of the *C. lapworthi* graptolite Biozone (Loydell *et al.* 1998). According to Grahn (1995), *C. acuminata* appears in the underlying *O. spiralis* graptolite Biozone in the subsurface of Gotland. In the East Baltic *C. acuminata* appears between the Kirikuküla (ID 457) and Aizpute (ID 311) K-bentonites (Fig. 4); in the Ruhnu core this species appears only 1 m above the Kirikuküla K-bentonite. No K-bentonites were found in the East Baltic in the *C. acuminata* Biozone.

Margachitina margaritana *Biozone*

Margachitina margaritana is a very widespread and distinctive chitinozoan species, but characterized by a diachronous appearance: in the *O. spiralis* graptolite Biozone (Närborrningen 1 core, Gotland, Grahn 1995; Ventspils core, Loydell & Nestor 2005), in the *insectus* Biozone (Banwy River section, Mullins & Loydell 2001; Prague Basin, Bohemia, Dufka *et al.* 1995; Mehaigne area, Belgium, Verniers 1999), in the undivided upper Telychian (Amazonas Basin and western Gondwana, Grahn 2005, 2006), and in the *centrifugus* and/or *murchisoni* biozones (Ohesaare core, Nestor 1994; see also Loydell *et al.* 1998).

It is essential to note that the early occurrences of *M. margaritana* in the Närborrningen 1 and Ventspils cores in the *spiralis* Biozone are based on the occurrence of this species in a single sample only. In both sections, *M. margaritana* has not been recorded in an interval of about 20 m above this single level, and then appears again just below the Llandovery/Wenlock boundary. No reasonable explanation for such a mode of occurrence has been proposed (Loydell & Nestor 2005). In the studied sections, *M. margaritana* appears close to the Aizpute K-bentonite (ID 311). Only in the Ohesaare section does it appear clearly higher as indicated by two well correlated K-bentonites (Fig. 4).

Six K-bentonites were found in this interval. The Aizpute K-bentonite (ID 311) yields sanidine with 36.2–37.8 mol% $NaAlSi_3O_8$ and with a sharp reflection. Both the Ohesaare (ID 210) and Lusklint (ID 150) K-bentonites are characterized by sanidines with moderately wide reflections, but the average sanidine composition in these beds is slightly different (38–40 mol% and 35–36 mol% $NaAlSi_3O_8$, respectively) allowing quite easy discrimination of these beds (Fig. 2). The Storbrut (ID 139) K-bentonite occurs as a 1-mm thick kaolinite and pyrite-rich layer only in the Aizpute-41 core. The Ireviken K-bentonite (ID 127) reveals only a weak sanidine reflection and contains abundant biotite. The Ireviken K-bentonite was found, with a thickness of 3–3.5 cm, only in cores from the western margin of the study area. The Lusklint, Storbrut and Ireviken K-bentonites are well known from Gotland (Batchelor & Jeppsson 1994; Kiipli *et al.* 2008a).

The upper boundary of the *M. margaritana* Biozone (defined by the disappearance of *A. longicollis*) was correlated by Loydell *et al.* (2003) with the *murchisoni/firmus* biozonal boundary in the Aizpute-41 core. This is in good accordance with K-bentonite-based correlations with shallower water sections. This level lies within the *Pterospathodus pennatus procerus* conodont biozone (Loydell *et al.* 2003). The Llandovery/Wenlock boundary (Hughley Brook, Shropshire, England; http://www.stratigraphy.org) has been correlated with Ireviken Event Datum 2, at the boundary between the Lower and Upper *Pseudooneotodus bicornis* conodont biozones (Jeppsson 1997). In the Lusklint 1 section in Gotland this level is 14 cm below the Ireviken K-bentonite ID 127 (Jeppsson *et al.* 2005). K-bentonite correlations suggest that this datum, and therefore also the Llandovery/Wenlock boundary, lies within the *Cyrtograptus murchisoni* graptolite biozone (Kiipli & Kallaste 2006, Kiipli *et al.* 2008a).

Interzone above the M. margaritana *Biozone*

The lower boundary of the chitinozoan interzone above the *M. margaritana* Biozone is marked by the disappearance of *A. longicollis*. The interzone corresponds to the upper part of the Ireviken Event interval (Nestor *et al.* 2002) and correlates with the *Monograptus firmus* and *Monograptus riccartonensis* graptolite biozones (Loydell *et al.* 1998, 2003). The disappearance level of *A. longicollis* (Fig. 4) occurs in all studied sections a few metres above the well-known Ireviken K-bentonite (ID 127). No volcanic ash layers were found within this interval in the East Baltic region.

Correlation of Telychian K-bentonites with the chitinozoan (this study), graptolite (Kiipli *et al.* 2007a)

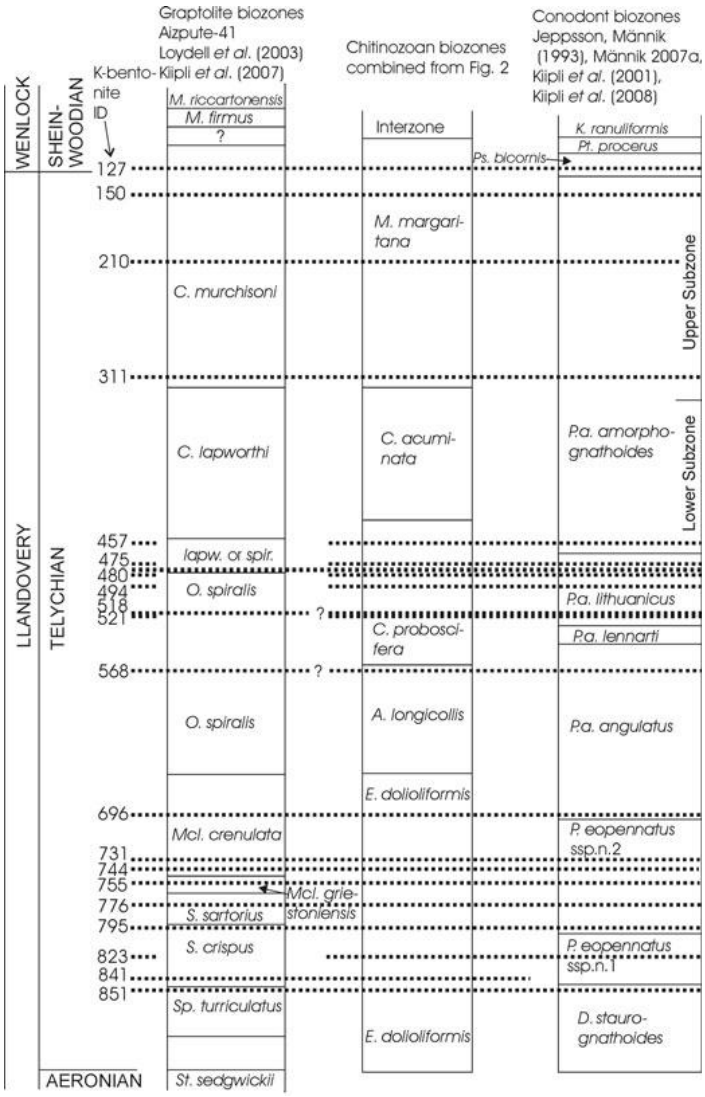

Fig. 5. Correlation chart of K-bentonite chemostratigraphy with graptolite, chitinozoan and conodont biozonations. Dotted lines represent K-bentonites. Relative thicknesses correspond to those in the Aizpute-41 core section.

and conodont (Kiipli *et al.* 2001; Männik 2007) biozonations is given in Figure 5 and Table 1.

Geographical thickness variation in K-bentonites

Plotting on maps the thicknesses of correlated K-bentonites can reveal useful information about palaeowind directions and the locations of source volcanoes. On Fig. 6 the thicknesses of six Telychian K-bentonites are shown (see also Bergström *et al.* 1998; Kiipli *et al.* 2008a,b,c).

In composing the isopach maps (Fig. 6) we encountered a dilemma: as a rule, the thickness of K-bentonites increases from south to north (i.e. the thickness of most ash beds is greater in Estonia than in Latvia), but in the northernmost part of the studied area many sections occur in which a particular K-bentonite was not found although in some closely

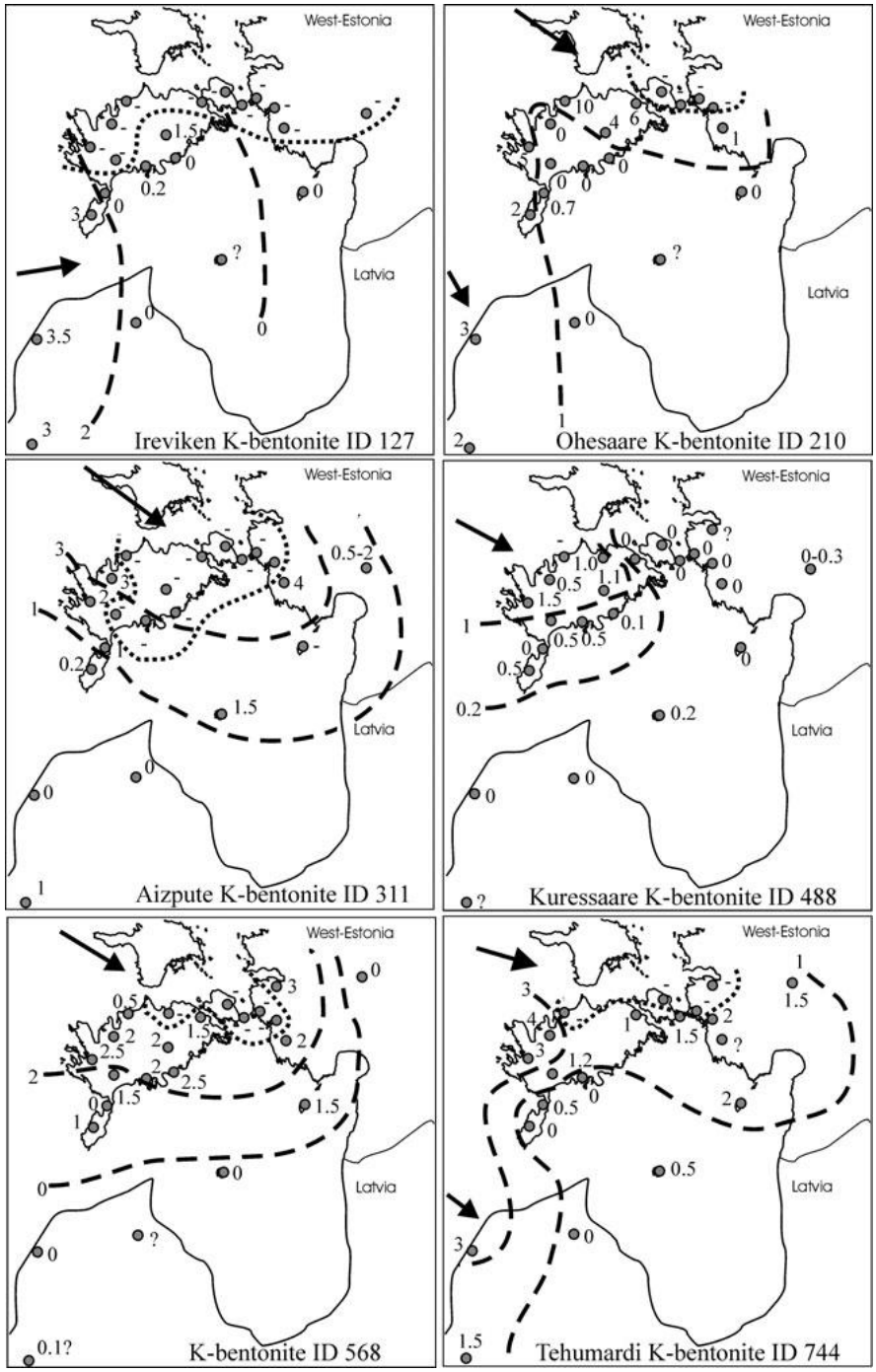

Fig. 6. Isopach schemes of six Telychian K-bentonites in Estonia and Latvia. Thicknesses are in cm. Arrows indicate suggested directions of volcanic ash cloud movement. Dashed lines – K-bentonite thickness isolines; dotted lines – border areas in shallow water regions, where a particular K-bentonite was not found.

located sections it might have the greatest thickness known. On the maps (Fig. 6) this problem is solved by considering that those beds not identified in some shallow-water regions were not deposited there most probably as a result of the environment being too hydrodynamically active, creating gaps in the K-bentonite record. Sediments in the Latvian sections formed in more stable, deeper water conditions. Therefore, the decrease in thicknesses of the K-bentonites to the south probably indicates that the marginal areas of ash clouds were located in that direction. Interestingly, some isopach maps show two distribution trends (Fig. 6), possibly indicating a change in wind direction during a long-lasting eruption. Alternatively, redistribution of the fallen ash by currents in the sea could have changed the thickness pattern. Variations in the thickness of volcanic ash layers can result also from redistribution in a highly energetic environment, amalgamating several eruptions into a single layer (multistage ash layers). Despite so many factors influencing the preserved thickness of eruption layer, all of the maps shown herein and in Kiipli *et al.* (2008a, b, c) show similar patterns, with K-bentonites being thicker in the northern and western parts of the studied area. This clearly indicates that the volcanic sources were in the closing Iapetus Ocean (Fig. 7).

Volcanic sources within Rheic Ocean have been proposed for other time intervals (Batchelor & Jeppsson 1999; Böhnke & Katzung 2001). Although volcanic rocks of Telychian age are known from the Brabant Massif, Belgium (André *et al.* 1986), the Telychian K-bentonites on Bornholm island at the southern margin of the Baltica plate have small thicknesses ranging from 0.1–2.0 cm (personal observations) contradicting the idea of volcanic ash clouds reaching Estonia from the south and southwest. Some thin ash layers found only in Latvia possibly could originate from southern sources, but more sections from the southern Baltic region need to be studied to demonstrate this.

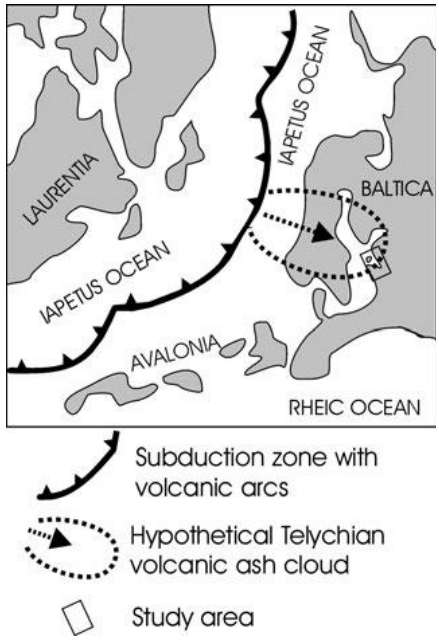

Fig. 7. Llandovery palaeogeographical map enlarged and modified from Scotese (2002). Map shows subduction of the Baltica and Avalonia plate under the Laurentia plate and the spread of the volcanic ash cloud from the subduction zone to the studied area in the East Baltic.

Conclusions

This integrated analysis of geochemical and palaeontological data has confirmed a correlation of sections along the shallower to deeper water transect in the East Baltic region based on earlier biostratigraphical studies. Synthesis of graptolite, chitinozoan and conodont biozonations with the K-bentonite-based chemostratigraphy has increased our confidence in the earlier correlations between graptolite, conodont and chitinozoan biozonations (Loydell *et al.* 1998, 2003). Integrated chemo- and biostratigraphy is a trustworthy basis for identifying and correlating volcanic ash layers in future studies.

The sources of the studied Telychian volcanic ash beds were probably located in the volcanic arcs in the Iapetus Ocean, more than 1000 km west and northwest of the study area.

Acknowledgements. – This study is a contribution to the Estonian Science Foundation projects 6749, 7138 and 7605, to the target financed projects 0140016s09, 0140020s08 and to the IGCP503. We thank A. Murnieks and R. Pomeranceva from the Latvian Agency of Environment, Meteorology and Geology for assisting us with field work on the Ventspils-D3 and Vidale-263 drillcores.

References

André, L., Hertogen, J. & Deutsch, S. 1986: Ordovician-Silurian magmatic provinces in Belgium and the Caledonian orogeny in Middle Europe. *Geology 14*, 879–882.

Batchelor, R.A. 2003: Geochemistry of biotite in metabentonites as an age discriminant, indicator of regional magma sources and potential correlating tool. *Mineralogical Magazine 67*, 807–817.

Batchelor, R.A. & Clarkson, E.N.K. 1993: Geochemistry of Silurian metabentonite and associated apatite from the North Esk Inlier, Pentland Hills. *Scottish Journal of Geology 29*, 123–130.

Batchelor, R.A. & Evans, J. 2000: Use of strontium isotope ratios and rare earth elements in apatite microphenocrysts for characterization and correlation of Silurian metabentonites: a Scandinavian case study. *Norwegian Journal of Geology 80*, 3–8.

Batchelor, R.A. & Jeppsson, L. 1994: Late Llandovery bentonites from Gotland, Sweden, as chemostratigraphic markers. *Journal of the Geological Society of London 151*, 741–746.

Batchelor, R.A. & Jeppsson, L. 1999: Wenlock metabentonites from Gotland, Sweden: geochemistry, sources and potential as chemostratigraphic markers. *Geological Magazine 136*, 661–669.

Batchelor, R.A., Weir, J.A. & Spjeldnæs, N. 1995: Geochemistry of Telychian metabentonites from Vik, Ringerike District, Oslo Region. *Norwegian Journal of Geology 75*, 219–228.

Batchelor, R.A., Harper, D.A.T. & Anderson, T.B. 2003: Geochemistry and potential correlation of Silurian (Telychian) metabentonites from Ireland and SW Scotland. *Geological Journal 38*, 161–174.

Bergström, S.M., Huff, W.D., Kolata, D.R. & Kaljo, D. 1992: Silurian K-bentonites in the Iapetus region: a preliminary event-stratigraphic and tectonomagmatic assessment. *GFF 114*, 327–334.

Bergström, S.M., Huff, W.D. & Kolata, D.R. 1998: The Lower Silurian Osmundsberg K-bentonite. Part I: stratigraphic position, distribution, and palaeogeographic significance. *Geological Magazine 135*, 1–13.

Bergström, S.M., Toprak, F.Ö., Huff, W.D. & Mundil, R. 2008: Implications of a new, biostratigraphically well-controlled, radio-isotopic age for the lower Telychian Stage of the Llandovery Series (Lower Silurian, Sweden). *Episodes 31*, 309–314.

Böhnke, A. & Katzung, G. 2001: The Middle Silurian from Bornholm (Denmark) – sedimentology, petrology and age. *Neues Jahrbuch für Geologie und Paläontologie, Abhandlungen 222*, 161–191.

Bohor, B.F. & Triplehorn, D.M. 1993: Tonsteins: Altered Volcanic-Ash Layers in Coal-Bearing Sequences. *The Geological Society of America Special Paper 285*, pp. 44.

Dufka, P., Kříž & Štorch, P. 1995: Silurian graptolites and chitinozoans from the uranium industry boreholes drilled in 1968–1971 (Prague Basin, Bohemia). *Bulletin of the Czech Geological Survey 70*, 5–14.

Geng, L.-Y., Qian, Z.-S., Ding, L.-S., Wang, Y., Wang, G.-X. & Cai, X.-Y. 1997: Silurian chitinozoans from the Yangtze region. *Palaeoworld 8*, 1–152.

Grahn, Y. 1995: Silurian Chitinozoa and biostratigraphy of subsurface Gotland. *GFF 117*, 57–65.

Grahn, Y. 1998: Lower Silurian (Llandovery- Middle Wenlock) Chitinozoa and biostratigraphy of the mainland of Sweden. *GFF 120*, 273–283.

Grahn, Y. 2005: Silurian and Lower Devonian chitinozoan taxonomy and biostratigraphy of the Trombetas Group, Amazonas Basin, northern Brazil. *Bulletin of Geosciences 80*, 245–276.

Grahn, Y. 2006: Ordovician and Silurian chitinozoan biozones of western Gondwana. *Geological Magazine 143*, 509–529.

Hints, R., Kirsimäe, K., Somelar, P., Kallaste, T. & Kiipli, T. 2008: Multiphase Silurian bentonites in the Baltic Palaeobasin. *Sedimentary Geology 209*, 69–79.

Huff, W.D. 2008: Ordovician K-bentonites: issues in interpreting and correlating ancient tephras. *Quaternary International 178*, 276–287.

Huff, W.D., Bergström, S.M., Kolata, D.R. & Sun, H. 1998: The Lower Silurian Osmundsberg K-bentonite. Part II: mineralogy, geochemistry, chemostratigraphy and tectonomagmatic significance. *Geological Magazine 135*, 15–26.

Jeppsson, L. 1997: A new latest Telychian, Sheinwoodian and Early Homerian (Early Silurian) Standard Conodont Zonation. *Transactions of the Royal Society of Edinburgh: Earth Sciences 88*, 91–114.

Jeppsson, L., Calner, M. & Eriksson, M. 2005: Locality descriptions. *In* Eriksson, M. & Calner, M. (eds): *The Dynamic Silurian Earth. Subcommission on Silurian Stratigraphy Field Meeting 2005, Field guide and Abstracts, Rapporter och meddelanden 121*, 22–56. Geological Survey of Sweden.

Kallaste, T. & Kiipli, T. 2006: New correlations of Telychian bentonites in Estonia. *Proceedings of the Estonian Academy of Sciences, Geology 55*, 241–251.

Kiipli, E., Kiipli, T. & Kallaste, T. 2006: Identification of the O-bentonite in the deep shelf sections with implication on stratigraphy and lithofacies, East Baltic Silurian. *GFF 128*, 255–260.

Kiipli, T. & Kallaste, T. 2002: Correlation of Telychian sections from shallow to deep sea facies in Estonia and Latvia based on the sanidine composition of bentonites. *Proceedings of the Estonian Academy of Sciences, Geology 51*, 143–156.

Kiipli, T. & Kallaste, T. 2006: Wenlock and uppermost Llandovery bentonites as stratigraphic markers in Estonia, Latvia and Sweden. *GFF 128*, 139–146.

Kiipli, T., Männik, P., Batchelor, R. A., Kiipli, E., Kallaste, T. & Perens, H. 2001: Correlation of Telychian (Silurian) altered volcanic ash beds in Estonia, Sweden and Norway. *Norwegian Journal of Geology 81*, 179–194.

Kiipli, T., Jeppsson, L., Kallaste, T. & Söderlund, U. 2008a: Correlation of Silurian bentonites from Gotland and the East Baltic using sanidine phenocryst composition, and biostratigraphical consequences. *Journal of the Geological Society of London 165*, 1–10.

Kiipli, T., Kallaste, T., Kaljo, D. & Loydell, D.K. 2007a: Correlation of Telychian and lowermost Sheinwoodian K-bentonites with the graptolite biozonation in the East Baltic area. *Acta Palaeontologica Sinica* (Suppl.) *46*, 218–226.

Kiipli, T., Kiipli, E., Kallaste, T., Hints, R., Somelar, P. & Kirsimäe, K. 2007b: Altered volcanic ash as an indicator of marine environment, reflecting pH and sedimentation rate – example from the Ordovician Kinnekulle bed of Baltoscandia. *Clays and Clay Minerals 55*, 177–188.

Kiipli, T., Orlova, K., Kiipli, E. & Kallaste, T. 2008b: Use of immobile trace elements for the correlation of Telychian bentonites on Saaremaa Island, Estonia, and mapping of volcanic ash clouds. *Estonian Journal of Earth Sciences 57*, 39–52.

Kiipli, T., Soesoo, A., Kallaste, T. & Kiipli, E. 2008c: Geochemistry of Telychian (Silurian) K-bentonites in Estonia and Latvia. *Journal of Volcanology and Geothermal Research 171*, 45–58.

Loydell, D.K. & Nestor, V. 2005: Integrated graptolite and chitinozoan biostratigraphy of the upper Telychian (Llandovery, Silurian) of the Ventspils D-3 core, Latvia. *Geological Magazine 142*, 369–376.

Loydell, D.K., Kaljo, D. & Männik, P. 1998: Integrated biostratigraphy of the lower Silurian of the Ohesaare core, Saaremaa, Estonia. *Geological Magazine 135*, 769–783.

Loydell, D.K., Männik, P. & Nestor, V. 2003: Integrated biostratigraphy of the lower Silurian of the Aizpute-41 core, Latvia. *Geological Magazine 140*, 205–229.

Männik, P. 2007: An updated Telychian (Late Llandovery, Silurian) conodont zonation based on Baltic faunas. *Lethaia 40*, 45–60.

Mullins, G.L. & Loydell, D.K. 2001: Integrated Silurian chitinozoan and graptolite biostratigraphy of the Banwy River section, Wales. *Palaeontology*, *44*, 731–781.

Mullins, G.L. & Loydell, D.K. 2002: Integrated lower Silurian chitinozoan and graptolite biostratigraphy of Buttington Brick Pit, Wales. *Geological Magazine 139*, 89–96.

Nestor, H. & Nestor, V. 2002: Upper Llandovery to middle Wenlock (Silurian) lithostratigraphy and chitinozoan biostratigraphy in southwestern Estonia and northernmost Latvia. *Proceedings of the Estonian Academy of Sciences, Geology 51*, 67–87.

Nestor, V. 1994: Early Silurian chitinozoans in Estonia and North Latvia. *Academia 4*, 1–163.

Nestor, V. 2003: Silurian chitinozoans. *In* Põldvere, A. (ed.): *Ruhnu (500) Drill core, Estonian Geological Sections 5*, 13–14. Geological Survey of Estonia, Tallinn.

Nestor, V. 2005: Chitinozoans of the *Margachitina margaritana* Biozone and the Llandovery-Wenlock boundary in West Estonian drill cores. *Proceedings of the Estonian Academy of Sciences, Geology 54*, 87–111.

Nestor, V., Einasto, R. & Loydell, D.K. 2002: Chitinozoan biostratigraphy and lithological characteristics of the Lower and Upper Visby boundary Beds in the Ireviken 3 section, Northwest Gotland. *Proceedings of the Estonian Academy of Sciences, Geology 51*, 215–226.

Orville, P.M. 1967: Unit cell parameters of the microcline – low-albite and the sanidine high albite solid solution series. *American Mineralogist 52*, 55–86.

Pearce, R.B. 1995: The geochemistry of Llandovery and Wenlock age K-bentonites in the Southern Uplands. *Scottish Journal of Geology 31*, 23–28.

Põldvere, A. (ed.) 2003: Ruhnu (500) drill core, Estonian Geological Sections. *Geological Survey of Estonia Bulletin 5*, 76.

Scotese C.R. 2002: http://www.scotese.com (PALEOMAP website).

Soufiane, A. & Achab, A. 2000: Upper Ordovician and Lower Silurian chitinozoans from central Nevada and Arctic Canada. *Review of Palaeobotany and Palynology 113*, 165–187.

Spjeldnæs, N. 1959: Silurian bentonites from Gotland, Sweden. *GFF 81*, 582–587.

Vandenbroucke, T., Verniers, J. & Clarkson, E.N.K. 2003: A chitinozoan biostratigraphy of the Upper Ordovician and lower Silurian strata of the Girvan area, Midland Valley, Scotland. *Transactions of the Royal Society of Edinburgh: Earth Sciences 93*, 111–134.

Verniers, J. 1999: Calibration of Chitinozoa versus graptolite biozonation in the Wenlock of Builth Wells district (Wales, U.K.), compared with other areas in Avalonia and Baltica. *Bolletino della Società Paleontologica Italiana 38*, 359–380.

Verniers, J., Nestor, V., Paris, F., Dufka, P., Sutherland, S. & Van Grootel, G. 1995: A global Chitinozoa biozonation for the Silurian. *Geological Magazine 132*, 651–666.

PAPER VII

KIIPLI, T., KALLASTE, T., NESTOR, V. 2012. Correlation of upper Llandovery–lower Wenlock bentonites in the När (Gotland, Sweden) and Ventspils (Latvia) drill cores: role of volcanic ash clouds and shelf sea currents in determining areal distribution of bentonite. Estonian Journal of Earth Sciences, 61(4), 295–306.

Correlation of upper Llandovery–lower Wenlock bentonites in the När (Gotland, Sweden) and Ventspils (Latvia) drill cores: role of volcanic ash clouds and shelf sea currents in determining areal distribution of bentonite

Tarmo Kiipli, Toivo Kallaste and Viiu Nestor

Institute of Geology at Tallinn University of Technology, Ehitajate tee 5, 19086 Tallinn, Estonia; tarmo.kiipli@gi.ee, toivo.kallaste@gi.ee, viiu.nestor@gi.ee

Received 5 February 2012, accepted 12 June 2012

Abstract. Study of volcanic ash beds using biostratigraphy, sanidine composition and immobile elements within bentonites has manifested several well-established and some provisional correlations between Gotland and East Baltic sections. Energy dispersive X-ray fluorescence microanalysis of phenocrysts has revealed bentonites containing Mg-rich or Fe-rich biotite. Sanidine phenocrysts contain, in addition to a major Na and K component, often a few per cent of Ca and Ba. On the basis of new correlations the mapping of the distribution areas of bentonites has been extended from the East Baltic to Gotland. The bentonite distribution can be separated into two parts in North Latvia–South Estonia, indicating the existence of shelf sea currents in the Baltic Silurian Basin.

Key words: correlation, bentonites, K-bentonites, sea currents, Silurian, East Baltic, Gotland.

INTRODUCTION

Volcanic ash beds in sedimentary sections have been used as time markers for refining stratigraphy (Rubel et al. 2007; Kiipli et al. 2011). Sometimes large eruptions have caused significant environmental changes followed by extinction of marine biota (Hints et al. 2003). Thin altered volcanic ashes (bentonites, K-bentonites), providing evidence for volcanism at nearby plate margins, have been detected in Baltoscandia, from the lower Silurian (e.g. Bergström et al. 1992; Batchelor et al. 1995; Batchelor & Jeppsson 1999; Hetherington et al. 2011) to the lower part of the upper Silurian (Snäll 1977). Many Silurian bentonites have been recorded also in England (e.g. Ray 2007; Ray et al. 2011) and Scotland (e.g. Batchelor & Weir 1988; Batchelor 2009). In the East Baltic area ash beds from a total of 51 volcanic eruptions have been identified in the Telychian (Kiipli et al. 2008b, 2008c, 2008d, 2010b) and 55 in the Wenlock (Kiipli et al. 2010a). Several ash beds are known in the lower Ludlow (Kiipli et al. 2011), but these are very rare in younger sedimentary rocks.

With the aim of extending the correlation of volcanic ash layers, we have studied the Llandovery–lower Wenlock of the Ventspils-D3 core section of Latvia and the När core section of Gotland (Sweden). New correlations are used for interpreting ash clouds and shelf sea currents in the Silurian Baltic Basin.

MATERIAL AND METHODS

Thirty-one bentonite samples were taken from the Llandovery and lower Wenlock of the Ventspils-D3 and När cores (Fig. 1). The thickness of the ash beds varies from 1 mm to 4 cm, which is generally less than in Estonia, where ash beds frequently reach a thickness of 5–10 cm. An additional complication with the När core was that as a result of previous studies only half of the core was preserved and we were able to find only some

Fig. 1. Location of the studied sections.

of the ash beds recorded by Snäll (1977) in the fresh core. The stratigraphical position of the ash beds was established using chitinozoan and graptolite biozonation (Gailite et al. 1987; Nestor 1994; Grahn 1995; Loydell & Nestor 2005; Fig. 2). The composition of sanidine phenocrysts in bentonites was used for correlation with the biostratigraphically well studied Aizpute-41 section (Loydell et al. 2003). The samples were analysed by X-ray diffractometry (XRD) for identifying major minerals and determination of magmatic sanidine phenocryst composition. The XRD spectra of sanidine in Telychian and lower Sheinwoodian bentonites are available online at http://sarv.gi.ee/reference.php?id=2533. The authors have applied the same methods in their previous works (Kiipli & Kallaste 2002, 2006; Kiipli et al. 2010a, 2011). The composition of volcanic phenocrysts in the bentonites of the När section was studied also by energy dispersive X-ray fluorescence (EDS) microanalysis in five samples. Samples of sufficient size (at least 2 g) were subjected to standard X-ray fluorescence (XRF) analysis for major and trace elements. The results are available in the database at http://geokogud.info/git/reference.php?id=1586 (Kiipli et al. 2011). Table 1 describes the concentrations of immobile and other useful elements for chemical fingerprinting as follows: high concentration of elements – Al_2O_3 > 26% and TiO_2 > 1.2%; Zr > 510, Nb > 37, Th > 40, Sr > 190, Ba > 320, La > 48, Ce > 140 and Y > 50 ppm; low concentrations of elements – Al_2O_3 < 20% and TiO_2 < 0.66%; Zr < 320, Nb < 22, Th < 29, Sr < 110, Ba < 190, La < 18, Ce < 35 and Y < 27 ppm. These values were derived by dividing all available analyses of bentonites from the Baltic Silurian deep shelf area into three equal groups – high, average and low concentrations for each element. Geochemical analyses were carried out in the Institute of Geology at Tallinn University of Technology.

RESULTS

Major minerals in altered volcanic ashes

Bentonites in Estonia are composed mainly of highly illitic illite-smectite and authigenic potassium feldspar (Kiipli et al. 2008b), with kaolinite present only in the sections near the southern border. In Latvia and Gotland, however, kaolinite is a common major component in addition to illite-smectite, while K-feldspar is relatively rare and occurs in lower concentrations (Table 1). This areal difference has been studied in the Ordovician Kinnekulle ash bed (Kiipli et al. 2007) and probably originates from differences in sedimentary facies. During the Early Palaeozoic Era, Latvia and Gotland were located on the deep shelf and Estonia mainly in the shallow shelf area. By contrast, Hints et al. (2008) proposed a late diagenetic origin for potassium feldspar in bentonites. Kaolinite-rich ash beds have lost much more silica and other major components during the conversion of ash to clay than illite-smectite- and feldspar-rich bentonites in Estonia (Kiipli et al. 2006). Consequently, the expected concentrations of immobile elements used for chemical fingerprinting are significantly higher in Latvia and Gotland than in the correlative beds in Estonia (Kiipli et al. 2008d). Ratios of immobile elements can still be used for chemical identification of eruption layers. Authigenic pyrite and its weathering products (gypsum and jarosite) in drill core boxes are frequent in bentonite beds. Pyroclastic quartz occurs in almost all bentonites in a concentration of ca 1%. Reflections of anatase appear on XRD patterns, starting from TiO_2 concentrations of ca 1%.

Aeronian (Llandovery) bentonites

Snäll (1977) recorded nine thin bentonites in the När core within the interval 363.0–371.8 m containing *Conochitina iklaensis*, which Grahn (1995) assigned to the lower Aeronian *Coronograptus gregarius* graptolite Biozone (= *Demirastrites triangulatus–Pribylograptus leptotheca* biozones). Due to the poor state of the core, we found material from only two bentonites. The attempts to analyse sanidine composition revealed no XRD reflection (369.8 m) or only a weak reflection (367.8 m). Wide sanidine reflections were established in two bentonites from the Dobele Formation of the Aizpute-41 section. No ash bed correlations can be suggested on the basis of the data available at present.

Bentonites in the *Spirograptus turriculatus–Streptograptus crispus* Biozone interval (Telychian, Llandovery)

In terms of chitinozoan biozonation, this interval belongs to the lower part of the *Eisenackitina dolioliformis* Biozone. Eight bentonites were found in the Ventspils

Fig. 2. Correlation of the Llandovery–lower Wenlock sections between Gotland (Sweden) and Latvia. Biostratigraphy of the När core is from Grahn (1995), Aizpute from Loydell et al. (2003) and Ventspils from Nestor (1994), Gailite et al. (1987) and Loydell & Nestor (2005). *Streptograptus wimani* in the Ventspils core indicates the lower part of the *lapworthi* Biozone. The interpretations of the depth interval ca 920–935 m of the Aizpute core by Loydell et al. (2003) differ ca 2 m from the depths used for bentonites. For the correct position of bentonites relative to samples studied by Loydell et al. (2003) see Kiipli & Kallaste (2006).

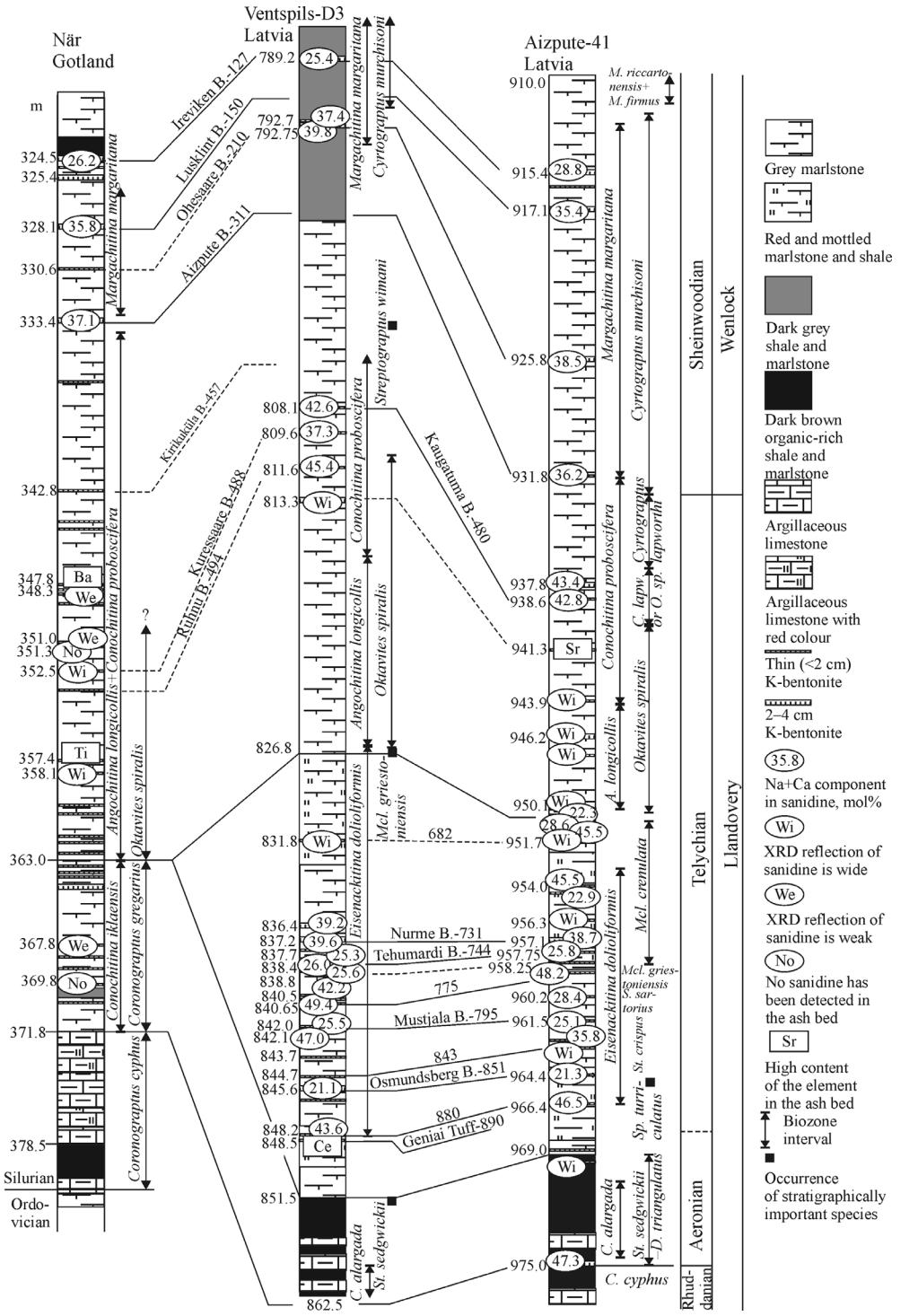
När
Gotland
Ventspils-D3
Latvia
Aizpute-41
Latvia
m
Ireviken B.-127
Lusklint B.-150
Ohessaare B.-210
Aizpute B.-311
Kirikukülla B.-457
Kuressaare B.-488
Rõhnu B.-494
Kaugatuma B.-480
Nurme B.-731
Tehumardi B.-744
775
Mustjala B.-795
843
Osmundsberg B.-851
880
Geniai Tuff-890
682
Margachitina margaritana
Cyrtograptus murchisoni
Streptograptus wimani
Conochitina proboscifera
Angochitina longicollis
Oktavites spiralis
Mcl. griesto-niensis
Eisenackitina dolioliformis
Conochitina iklaensis
Coronograptus gregarius
Coronograptus cyphus
C. alargada
St. sedgwickii
A. longicollis
Mcl. crenulata
Mcl. gries-toniensis
S. sar-torius
St. crispus
Sp. turri-culatus
D. triangulatus
C. cyphus
M. riccarto-nensis+
M. firmus
Cyrtograptus lapworthi
C. lapw. gr.
O. sp.
Grey marlstone
Red and mottled marlstone and shale
Dark grey shale and marlstone
Dark brown organic-rich shale and marlstone
Argillaceous limestone
Argillaceous limestone with red colour
Thin (<2 cm) K-bentonite
2–4 cm K-bentonite
Na+Ca component in sanidine, mol%
XRD reflection of sanidine is wide
XRD reflection of sanidine is weak
No sanidine has been detected in the ash bed
High content of the element in the ash bed
Biozone interval
Occurrence of stratigraphically important species
Silurian
Ordo-vician
Rhud-danian
Aeronian
Telychian
Sheinwoodian
Wenlock
Llandovery

Table 1. Analytical data of the studied bentonites

Depth, m	Thick-ness, cm	Stratigraphy	Sanidine properties			Biotite abun-dance	XRD mineralogy of bulk sample	XRF, trace elements		Correlations	
			Na + Ca modal component, mol%	Width of the reflection	Remarks			Low content	High content	Bento-nite ID	Bentonite name
När core											
324.5	2.0	Sheinwoodian	26.2	0.12	Weak	+++	I/S,kaol,biot	Ba,Ce,La,Sr,Y	Al	127	Ireviken
325.4	4.0	Sheinwoodian					Kaol,K-fsp,I/S,qu,gyp,pyr			139?	Storbrut?
328.1	2.0	Sheinwoodian	35.8	0.18		++	Kaol,I/S,K-fsp,goyazite/ florencite,qu		Al,Ce,La,Sr,Y,Zr	150	Lusklint
333.4	2.0	Sheinwoodian	37.1	0.09		++	I/S,kaol,K-fsp,qu,Na-K-san, biot	Ce,La	Al,Nb,Th,Zr	311	Aizpute
342.8	0.7	Telychian					K-fsp,I/S,kaol,qu,anatase		Ti,(Sr),Y,Zr	457?	Kirikuküla?
347.8	0.4	Telychian					K-fsp,I/S,kaol,anatase	Nb,Th	Ti,Ba,Ce,La,Sr,Y		New
348.3	0.5	Telychian	33.4	0.16	Weak	++	I/S,kaol,qu(traces)	Ti,Ba,	Al,Nb,Th,Zr		New
348.9	0.2	Telychian					I/S,qu(traces)				New
351.0	0.2	Telychian			Very weak	+	I/S	Ba,Ce,La	Y,Zr		New
351.3		Telychian			No	++(+)	I/S,biot,kaol(traces)	Ti,Ba,Ce,La,Nb,Th,Zr			New
352.5	0.9	Telychian			Wide	++	K-fsp,I/S,kaol,qu,anatase	La	Al,Ti,Ba,Sr	488?	Kuressaare
353.6	0.2	Telychian					K-fsp,I/S,kaol,anatase, terrig(traces)			?	
357.4	0.3	Telychian					K-fsp,I/S,kaol(traces), anatase,qu,pyr,jar,gyp	Al,La,Y	Ti,Ba,Sr		New
358.1	0.5	Telychian			Wide	–	I/S,kaol,K-fsp,anatase		Al,Ti,Ce,Th,Y,Zr		New
367.8	2.0	Aeronian	27.4	0.21	Weak	++	I/S,calcite,kaol,anatase				
369.8	1.0	Aeronian			No	++	I/S,terrig,calcite				
Ventspils-D3 core											
789.2	3.5	Sheinwoodian	25.9	0.29		+++	Kaol,I/S,biot,qu	Ti,Ba,Ce,Nb,Sr,Y	Al	127	Ireviken
792.7	0.2	Sheinwoodian	37.4	0.13		+	I/S,kaol,K-fsp,qu,gyp,pyr				New
792.75	3.0	Sheinwoodian	39.8	0.27		+	I/S,kaol,K-fsp,qu,pyr,jar,gyp	Ti,Ba	Al,Ce,La,Y	210	Ohesaare
808.1	1.0	Telychian	42.6	0.24		++	Kaol,I/S,K-fsp,qu,anatase, biot,gyp	Ba,Sr	Al,Ti,Ce,La,Nb,Th,Y, Zr	480	Kaugatuma
809.6	0.2	Telychian	37.3	0.26		?	Kaol,I/S,K-fsp,anatase,biot, qu,gyp			488?	Kuressaare?

Table 1. *Continued*

Depth, m	Thick-ness, cm	Stratigraphy	Sanidine properties			Biotite abun-dance	XRD mineralogy of bulk sample	XRF, trace elements		Correlations	
			Na + Ca modal component, mol%	Width of the reflection	Remarks			Low content	High content	Bento-nite ID	Bentonite name
811.6	1.0	Telychian	45.8	0.09		++	I/S,kaol,qu,Na-K-san?	Ti,Ba,Sr	Al,Nb,Th,Zr	494	Ruhnu
813.3	2.0	Telychian	38.2	0.32	Wide	+	K-fsp,kaol,I/S,anatase,qu,pyr	Th	Al,Ce,La	518?	Viirelaid?
831.8	0.3	Telychian	28.8	0.32	Very wide	+	K-fsp,I/S,kaol,qu,anatase, chalc?,hematite,biot			682	
836.2		Telychian					I/S,kaol,K-fsp?,qu	Ba,Sr	Al,Ce,La,Nb,Th,Zr		New
836.4	3.0	Telychian	39.3	0.08		++	I/S,kaol,K-fsp,qu,Na-K-san?	Ti	Al,Ce,La,Nb,Th,Y,Zr		New
837.2	2.0	Telychian	39.6	0.11		++	I/S,kaol,K-fsp,qu	Ti	Al,Ce,La,Nb,Th,Y,Zr	731	Nurme
837.7	1.0	Telychian	25.3	0.15		?	I/S,K-fsp,kaol,qu,Na-K-san, hematite, chalc?	Ti,Ba,Ce,La,Y,Zr			New
838.4	3.0	Telychian	26	0.10		++	I/S,kaol,K-fsp,qu,biot,Na-K-san, hematite	Ti,Ba,Sr,Y,Zr		744	Tehumardi
838.8	0.7	Telychian	25.6	0.29		+	I/S,kaol,K-fsp,qu,anatase	Ba,Sr	Al,Ti,Ce,La,Th,Y,Zr	755	Paatsalu
840.5	0.3	Telychian	42.2	0.20		+++	I/S, terrig		Ti,Ba,Nb,Y,Zr	773	
840.55	0.2	Telychian	46.2	0.15		++	I/S,kaol,K-fsp,qu			774	
840.65	0.2	Telychian	49.4	0.09		++	I/S, terrig	Al,La,Zr		775	
842.0	0.5	Telychian	25.5	0.06		+++	Kaol,I/S,K-fsp,qu,qyp,biot,pyr	Sr	Al,Th,Zr	795	Mustjala
842.1	0.2	Telychian	47	0.14		++	I/S,kaol,K-fsp,qu?,anatase,qyp		Al,Ti,Ba,Ce,La,Nb, Th,Zr	800	
843.7	0.3	Telychian	32.4	0.32	Wide	+	Terrig,I/S,gyp	Al,Nb,Th,Zr	Sr	818	
844.7	0.4	Telychian	31.2	0.34	Very wide	++	Terrig,I/S,calcite,dolomite	Al,Th		843	
845.6	3.0	Telychian	21.1	0.06		++	Grey: kaol,I/S,K-fsp,biot,qu?, Na-K-san	Ce,La,Nb,Y,Zr	Al,Ba	851	Osmundsberg
846.0	0.2	Telychian					I/S,k-fsp,kaol,qu,anatase				New
848.2	1.5	Telychian					I/S,k-fsp,kaol,apatite,anatase	Nb,Th	Ti,Ba,Ce,La,Sr,Y	880	
848.5	1.0	Telychian					K-fsp,kaol,I/S,goyazite/ florencite,apatite,anatase		Ti,Ba,Ce,La,Sr,Y	890	Geniai

Terrig = illite + chlorite + quartz, kaol = kaolinite, I/S = illite-smectite, K-fsp = potassium feldspar, qu = quartz, gyp = gypsum, pyr = pyrite, chalc = chalcopyrite, biot = biotite, san = sanidine, jar = jarosite.

core in this interval, four of which can be correlated with bentonites from the Aizpute section on the basis of sanidine composition and Ti and Nb (Figs 2 and 3). Among these, a bed at 845.6 m is correlative with the well-known and widespread Osmundsberg Bentonite (ID851) (Kiipli et al. 2006, 2008b; Inanli et al. 2009). In Ventspils the Osmundsberg Bentonite consists of a grey and a red part, both revealing identical sanidine composition, but the concentrations of immobile elements are significantly lower in the red part than in the grey part (Fig. 3). A thin bed at 842.1 m in the Ventspils core reveals very high Zr, Th, Nb and Ti concentrations (Fig. 3), excluding (together with its position in the section) correlation with ash beds known in Estonia and the Aizpute-41 section in Latvia. A unique 1 cm thick hard tuff layer (the Geniai Tuff) occurs at 848.5 m containing La, Ce, Nd, Sr and P at the level of major components. We have suggested a source magma of carbonatite composition for this bed (Kiipli et al. 2012). In the När core this interval is in a stratigraphical gap, which, according to Grahn (1995), encompasses much of the Aeronian and the Telychian up to the *Oktavites spiralis* graptolite Biozone.

Bentonites in the *Streptograptus sartorius–Monoclimacis crenulata* Biozone interval (Telychian, Llandovery)

In terms of chitinozoan biozonation, this interval belongs to the upper part of the *Eisenackitina dolioliformis* Biozone. In the Ventspils core ten bentonites have been found in this interval, two of which (at depths 840.65 m and 838.4 m) can be firmly correlated on the basis of their sanidine composition with the Aizpute section and sections in Estonia (Figs 3, 4, Table 1). The Nurme Bentonite (ID 731), which is in the *Monoclimacis crenulata* Biozone in the Aizpute core (Fig. 2), has two correlation possibilities in the Ventspils section differing by only 0.8 m in depth (836.4 m and 837.2 m). An identical composition of sanidine, immobile trace elements and close stratigraphical position in the section permit of both correlations. At the same time these compositional signatures confidently distinguish these ash beds from others in this interval. Evidently both ash layers originate from the same volcanic source and the short time span between the eruptions did not allow noticeable evolution of the magma composition. Provisionally, the Nurme Bentonite has been correlated with the bentonite at 837.2 m depth, and the bentonite at 836.4 m depth is considered as new. The bentonite at 837.7 m depth is also new, having no counterparts in previously studied sections. This bed is characterized by a low concentration of all immobile elements and potassium-rich sanidine similar to the Mustjala Bentonite occurring 2.3 m lower in the core. In the När core this interval is still within the stratigraphical gap (Fig. 2).

Bentonites in the *Oktavites spiralis–Cyrtograptus lapworthi* Biozone interval (Telychian, Llandovery)

In terms of chitinozoan biozonation, this interval belongs to the *Angochitina longicollis* and *Conochitina proboscifera* biozones. A bentonite in the Ventspils core at 808.1 m depth correlates, on the basis of its distinctive sanidine composition (42.6 mol% of $(Na + Ca)AlSi_3O_8$ in the modal component) and high content of Nb and Zr, with a bentonite at 938.6 m depth in the Aizpute core and with the Kaugatuma Bentonite (ID 480) in Estonia. Similarly, a bentonite in the Ventspils core at 811.6 m depth correlates perfectly (45.8 mol% of the $(Na + Ca)AlSi_3O_8$ in the modal component and sharp XRD reflection) with the Ruhnu Bentonite (ID 494) in Estonia. In the När core, according to Snäll (1977), 19 ash beds occur in the 334–363 m interval. From 11 of these we found some material for laboratory study. These ash beds are mostly characterized by wide or weak sanidine XRD reflections and a high content of P, Ti, Sr, Ba, La and Ce. In Estonia six ash beds have a similar geochemical type. The wide sanidine reflection does not enable unequivocal correlations. Some provisional correlations can be proposed based on the TiO_2–Nb chart (Fig. 3). One variant of these provisional correlations is expressed in Fig. 2, but clearly this is not the only one possible. According to this correlation variant, at least nine ash beds of this type occur in Latvia and Gotland and two of the Estonian ash beds (ID 520 and 521) do not extend to these areas. Two ash beds in the När section at depths of 348.3 m and 351.0 m belong to another geochemical type characterized by a high content of Nb, Zr and Th (Fig. 3). By contrast with Nb-, Zr- and Th-rich ashes in Estonia, these beds do not exhibit a strong and sharp sanidine reflection and consequently most probably are the product of other eruptions. The ash beds of these two geochemical types were first distinguished by Batchelor

Fig. 3. Sanidine composition (left column) and TiO_2/Nb ratio (right column) in the studied bentonites compared with the bentonites from Estonia (oval contours). ID numbers of Estonian bentonites are in bold font. Ve – Ventspils-D3, Ve-838.8-755 – core-depth (m)-ID number of the bentonite. A – *murchisoni* Biozone interval, B – *spiralis–lapworthi* Biozone interval, C – *sartorius–crenulata* Biozone interval, D – *turriculatus–crispus* Biozone interval. Broken lines indicate correlations.

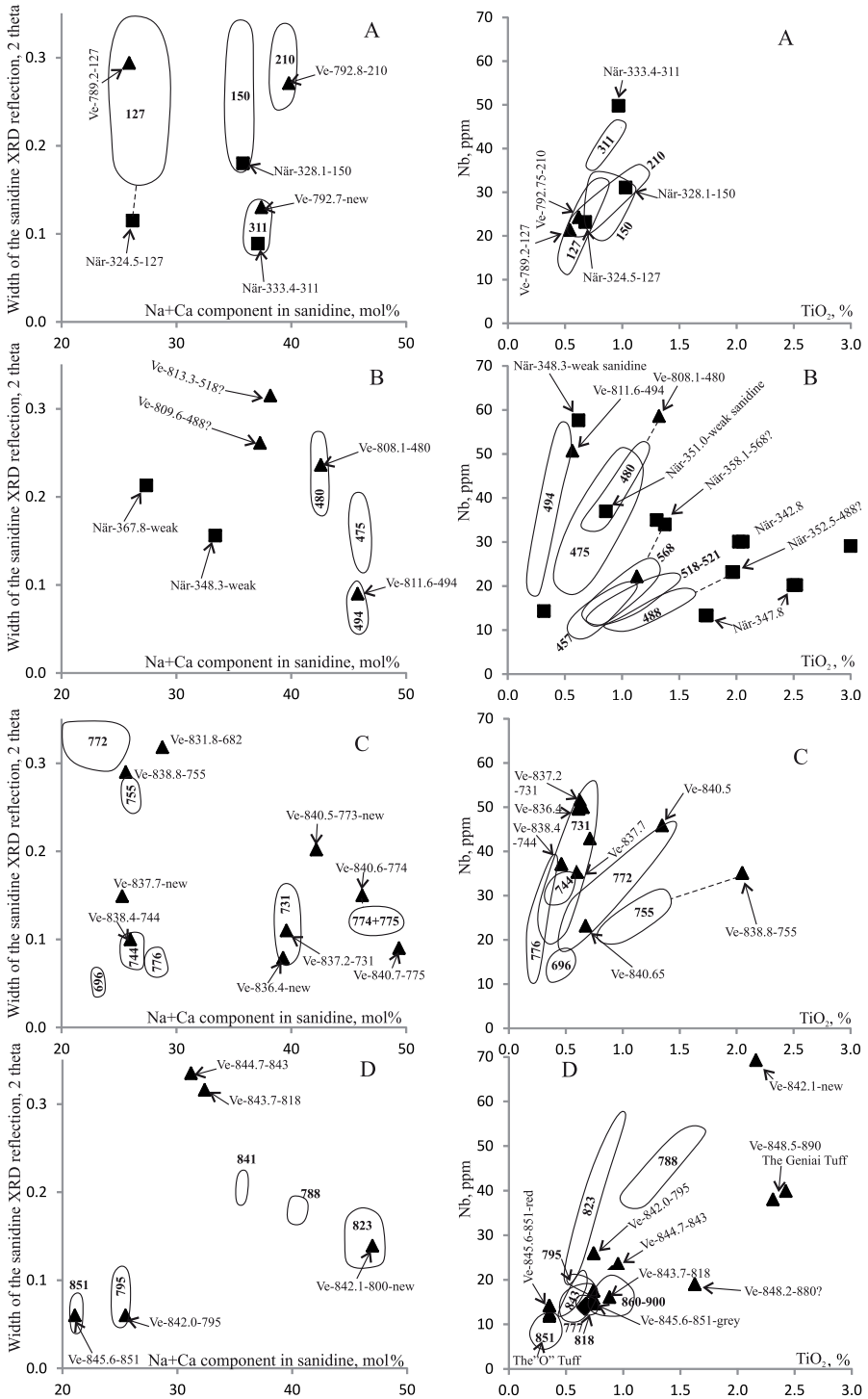
A
Ve-789.2-127
127
150
210
Ve-792.8-210
När-328.1-150
Ve-792.7-new
311
När-324.5-127
När-333.4-311
Width of the sanidine XRD reflection, 2 theta
Na+Ca component in sanidine, mol%
B
Ve-813.3-518?
Ve-809.6-488?
Ve-808.1-480
480
475
När-367.8-weak
När-348.3-weak
Ve-811.6-494
494
C
772
Ve-831.8-682
Ve-838.8-755
755
Ve-840.5-773-new
Ve-840.6-774
774+775
Ve-837.7-new
Ve-838.4-744
744
776
731
Ve-837.2-731
Ve-840.7-775
696
Ve-836.4-new
D
Ve-844.7-843
Ve-843.7-818
841
788
823
Ve-842.1-800-new
851
795
Ve-842.0-795
Ve-845.6-851
Nb, ppm
TiO2, %
A
När-333.4-311
311
210
Ve-792.75-210
När-328.1-150
Ve-789.2-127
127
150
När-324.5-127
B
När-348.3-weak sanidine
Ve-808.1-480
Ve-811.6-494
Ve-351.0-weak sanidine
480
494
475
När-358.1-568?
568
När-342.8
När-352.5-488?
518-521
488
457
När-347.8
C
Ve-837.2
-731
Ve-836.4
Ve-838.4
-744
731
Ve-840.5
Ve-837.7
744
772
755
Ve-838.8-755
776
696
Ve-840.65
D
Ve-842.1-new
Ve-848.5-890
The Geniai Tuff
788
823
Ve-842.0-795
Ve-844.7-843
Ve-845.6-851-red
795
Ve-843.7-818
Ve-848.2-880?
860-900
Ve-845.6-851-grey
851
818
The "O" Tuff

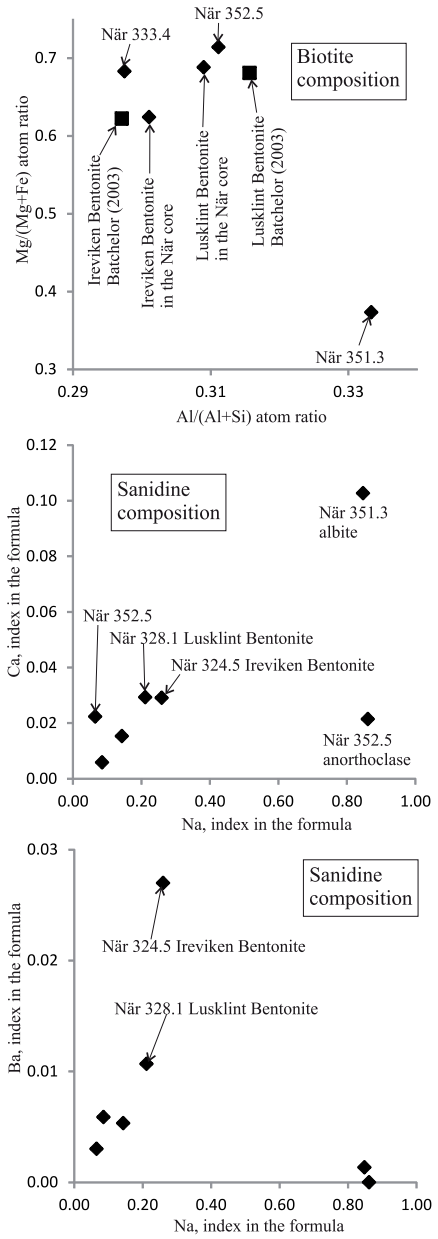

Fig. 4. Composition of biotite and sanidine phenocrysts according to the EDS microanalyses.

et al. (1995) in the Garntangen section in Norway correlating with this level (Kiipli et al. 2001). In total, probably seven studied ash beds within this interval in the När section are new (at depths 358.1, 357.4, 351.3, 351.0, 348.9, 348.3 and 347.8 m), i.e. not known from previously studied sections.

Bentonites in the *Cyrtograptus murchisoni* Biozone interval (Sheinwoodian, Wenlock)

In terms of chitinozoan biozonation, this interval belongs to the *Margachitina margaritana* Biozone (Fig. 2). The Aizpute Bentonite is distinct from others in this interval in its sharp sanidine reflection with 37 mol% of Na + Ca component and high Nb, Zr and Th contents. In the När core the Lusklint and Ireviken bentonites, in the Ventspils core the Ohesaare and Ireviken bentonites are found as well (Figs 2 and 3). The Ireviken Bentonite marks Ireviken Event Datum 2 (Jeppsson & Männik 1993). Kiipli et al. (2008a) showed that this level correlates to a level within the upper part of the *C. murchisoni* graptolite Biozone. The occurrence of the Ireviken Bentonite in the Ventspils section (Fig. 2) also within the *C. murchisoni* Biozone supports that correlation. A new ash bed occurs in the Ventspils core at a depth of 792.7 m, having a sharp sanidine reflection not found in other sections at this stratigraphical level.

Composition of volcanic phenocrysts according to EDS microanalysis

Five samples from the När core where enough grain material was available were subjected to EDS micro-analysis. In each sample 30–70 grains were measured. Reference glass material BBM-1 distributed by the International Association of Geoanalysts was analysed together with the samples under study and corrections to the results of a few per cent of the concentration were derived from the reference sample analysis. The results are presented in Table 2 and Fig. 4.

Among the phenocrysts, quartz dominates in the Ireviken, Lusklint and När-351.3 m bentonites and sanidine in the Aizpute and När-352.5 m bentonites. Biotite is present in all studied samples in variable concentrations. A few grains of authigenic kaolinite, pyrite, barite and illite are found as well. An especially rich assemblage of minerals was detected in the När-351.3 m bentonite, represented by several magmatic (magnetite, Ti-oxide, albite) and authigenic (pyrite, strontianite, goyazite-florencite, kaolinite and illite) grains.

Biotite composition was calculated according to the idealized half-cell chemical formula with eight cations: $(K,Na)_1(Mg,Fe,Ti,Mn,Ca,Sr,Ba)_3(Al,Si,P)_4O_{10}(OH,F)_2$. The average of 5–9 grains is represented in Table 2 and in Fig. 4. Four of the studied ashes contain Mg-rich biotites and one (När-351.3 m) contains Fe-rich biotite. The same two groups of biotite were found in the Telychian of the Viirelaid core (Estonia), although

Table 2. Composition of phenocrysts in ash beds of the När core

	Ireviken B. När 324.5	Lusklint B. När 328.1	Aizpute B. När 333.4	När 351.3	När 352.5
Quartz, %	63	54	17	67	7
Sanidine, %	13	35	56	19	76
Biotite, %	24	10	28	14	17
Other minerals	Kaolinite, pyrite	Kaolinite, apatite in sanidine	Kaolinite, barite, illite	Magnetite, Ti-oxide, pyrite, strontianite, goyazite-florencite, albite, kaolinite, illite	Anorthoclase, barite, illite
Composition of biotite, atoms per chemical formula					
Na	0.08	0.11	0.10	0.13	0.13
K	0.92	0.89	0.90	0.87	0.87
Mg	1.65	1.79	1.79	0.99	1.87
Fe	1.00	0.81	0.83	1.65	0.75
Ti	0.29	0.31	0.34	0.30	0.30
Mn	0.016	0.026	0.019	0.019	0.016
Ca	0.007	0.002	0.005	0.019	0.011
Sr	0.005	0.004	0.002	0.006	0.011
Ba	0.030	0.055	0.022	0.019	0.042
Al	1.20	1.24	1.19	1.33	1.24
Si	2.80	2.76	2.81	2.66	2.75
P	0.001	0.000	0.000	0.011	0.003
Composition of sanidine, atoms per chemical formula					
Na	0.26	0.21	0.14	0.09	0.06
K	0.68	0.74	0.83	0.90	0.91
Ca	0.029	0.029	0.015	0.006	0.022
Sr	0.002	0.005	0.002	0.001	0.002
Ba	0.027	0.011	0.005	0.006	0.003
Al	1.00	0.93	1.03	1.00	1.01
Si	2.93	3.05	2.94	2.99	2.96
Ti	0.011	0.005	0.021	0.003	0.006
Mn	0.000	0.002	0.001	0.001	0.001
Fe	0.065	0.008	0.014	0.004	0.023

Fe-rich biotites occurred stratigraphically at a somewhat lower level in the Telychian *crispus–crenulata* graptolite biozones (Kiipli et al. 2008d). Comparison with biotite analyses from Batchelor (2003) shows similar results for the Ireviken and Lusklint bentonites from outcrops on Gotland and from the När core (present study), confirming the correlation based on sanidine composition.

Sanidine composition was calculated according to the idealized chemical formula with five cations: $(K,Na,Ca,Ba,Sr)_1(Al,Si,Ti,Mn,Fe)_4O_8$. An average of 6–31 grains is represented in Table 2 and Fig. 4. The average content of the Na + Ca component is generally lower according to EDS analysis than the modal component according to XRD analysis. The reason is the presence of other components than modal, predominantly with a lower content of the Na + Ca component. The difference may arise in part also from the smaller number of grains, and consequently the less reliable result analysed by EDS (6–31 grains) compared to XRD (simultaneous average of ca 2000 grains). An interesting result from EDS analysis, not accessible by XRD, is the concentration of other cations than sodium and potassium in sanidine. Relatively high (2–3 mol%) content of the $CaAl_2Si_2O_8$ component in sanidine was established in the Ireviken, Lusklint and När-352.5 m bentonites. Sanidine in the Ireviken and Lusklint bentonites is remarkable for the high content (1–2.5 mol%) of $BaAl_2Si_2O_8$. The Sr, Ti, Mn and Fe concentrations in sanidine were too low for reliable calculation of the index in the chemical formula (Table 2).

Areal distribution of bentonites

The areal distribution of bentonites depends on the ancient volcanic ash clouds and the distribution maps can reveal the directions from which the ashes were transported. The distribution areas composed by Kiipli et al. (2008b, 2008c, 2008d, 2010b) for ca 20 bentonites

in the eastern Baltic indicate ash transport from the northwest in terms of the present-day orientation of Europe. Correlation with the När section enables extension of the bentonite distribution areas for the Ireviken, Lusklint, Ohesaare and Aizpute bentonites (Fig. 5). These areas confirm ash transport from the Iapetus Ocean, closing between Baltica and Laurentia. Judging from these maps, the bentonites in Jämtland and Dalarna in Sweden should be significantly thicker than in Estonia and Latvia. This conclusion is confirmed by the occurrence of the 1 m thick Osmundsberg Bentonite in Dalarna (Inanli et al. 2009). In southern Sweden and in the Oslo region we can expect these volcanic ashes to have similar thicknesses as in the eastern Baltic, e.g. in the range of milli- and centimetres.

Sea currents, too, can modify the areal extent of individual bentonites, redistributing and sorting the material by grain size. This has happened with an ash bed in recent sediments near the coast of Chile (Fisher & Schmincke 1984), where an oceanward current separates the volcanic ash area into two parts. Examining the distribution of bentonites in the Baltic Silurian (Fig. 5; Kiipli et al. 2008b, 2008c, 2008d, 2010b), we notice that the bentonite distribution areas are often similarly separated into two parts. There are two possible explanations: the influence of sea currents or a change in wind direction during a long-lasting eruption. As the separation occurs in a specific part of the Silurian basin, in present-day North Latvia and South Estonia, a sea current is a more likely reason. In the same area gaps or condensed sequences often occur in Silurian sections (Fig. 2; Loydell et al. 2003; Kiipli et al. 2011, 2012). In terms of basin depth, this area belongs to the transition between shallow shelf and deep shelf regions. An oceanic current coming from the southeast was interpreted from the kaolinite admixture in deep shelf sedimentary rocks by Kiipli et al. (2009) for Telychian time. Separation of the distribution areas of Silurian bentonites into two provides further support for the existence of this current. Figure 6 displays the shelf sea branch of the oceanic current in accordance with the bentonite distribution areas. It is not clear how closed the ocean within the Caledonian collision zone was during the Telychian–early Wenlock: possibly the shelf sea branch of the current returned to the Rheic Ocean (Fig. 6), but alternatively there could also have been a passage to a remnant of the Iapetus Ocean. Worsley et al. (2011) measured the direction of ripple and tool marks on bedding planes in the Telychian of the Oslo Region and established the dominant direction of currents from northwest to southeast, i.e. opposite to the direction we have proposed. A reasonable explanation could be that a

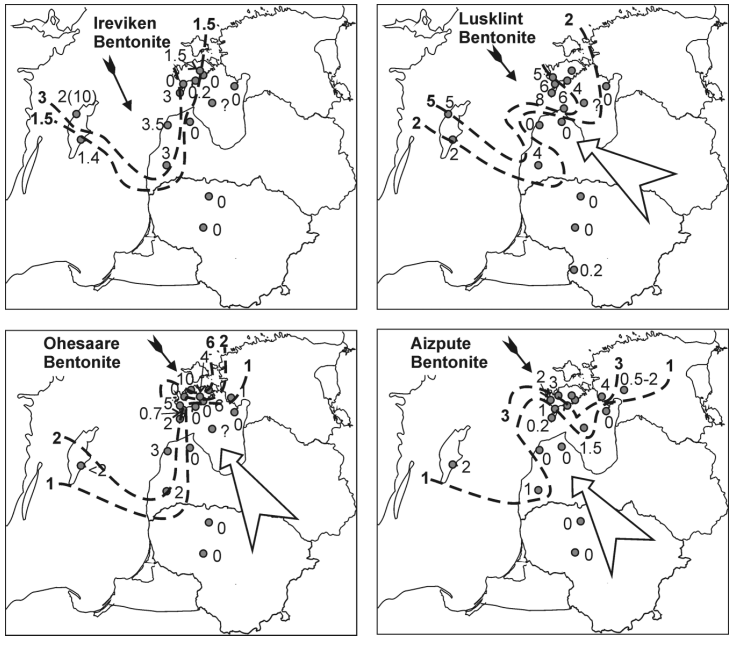

Fig. 5. Distribution maps of the four bentonites from the Sheinwoodian (lower Wenlock). Details of the distribution in Estonia and names and numbers of all drill cores can be found in Kiipli et al. (2008b, 2008d, 2010b).

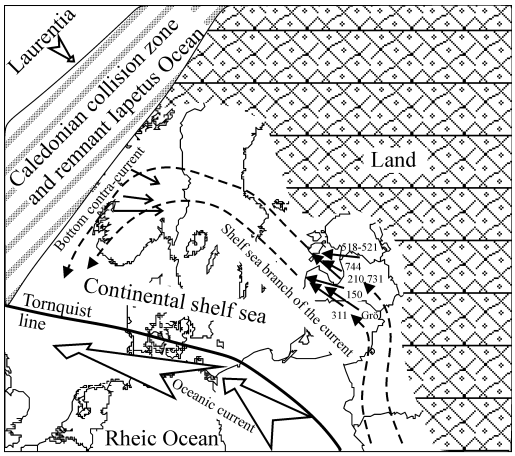

Fig. 6. Silurian shelf sea in Baltoscandia with interpreted shelf sea currents (arrows with broken lines). Arrows with solid lines indicate currents which separate the volcanic ash distribution areas into two parts. The ID numbers of the bentonite are near the arrows. The oceanic current is shown according to Kiipli et al. (2009). Arrows indicating coastal contracurrent direction are from Worsley et al. (2011).

shelf sea current flowing from the southeast and striking the coast formed by the rising Caledonian mountains rebounded as a contra-current along the sea bottom.

CONCLUSIONS

Correlation of volcanic ash beds using biostratigraphy, phenocryst composition and immobile elements within bentonites has revealed several well-established and a number of provisional correlations between the Gotland and East Baltic sections. The occurrence of the Aizpute Bentonite in the subsurface of Gotland together with the Lusklint and Ireviken bentonites increases the confidence that the correlation of exposed sections on Gotland, based on volcanic ash beds, with the graptolite biozonation at the level of the Ireviken Event (Kiipli et al. 2008a) is reliable. Approximately twelve new ash beds were discovered and geochemically characterized. These characterizations could be used for demonstrating correlations in future studies. New correlations enabled extension of the mapping of the distribution areas of bentonites from the East Baltic to Gotland. These extended maps point more reliably than previous studies to the volcanic source areas in the closing Iapetus Ocean. Separation of the bentonite distribution areas into two parts in North Latvia–South Estonia indicates the existence of a shelf sea current in the Baltic Silurian Basin coming from the southeast in terms of the present-day orientation.

Acknowledgements. The authors thank A. Murnieks and R. Pomeranceva (Latvian Agency of Environment, Meteorology and Geology) for assistance with the study of the Ventspils-D3 drill core, L. M. Wickström for her help in study of the När core and S. Peetermann for correcting the English. This study is a contribution to IGCP591, Estonian Research Council grant 8963 and project SF0140016s09. Creation and maintenance of the attached database was supported by the Estonian Research Council project KESTA.

REFERENCES

Batchelor, R. A. 2003. Geochemistry of biotite in metabentonites as an age discriminant, indicator of regional magma sources and potential correlating tool. *Mineralogical Magazine*, **67**, 807–817.

Batchelor, R. A. 2009. Geochemical 'Golden Spike' for Lower Palaeozoic metabentonites. *Earth & Environmental Science Transactions of the Royal Society of Edinburgh*, **99**, 177–187.

Batchelor, R. A. & Jeppsson, L. 1999. Wenlock metabentonites from Gotland, Sweden: geochemistry, sources and potential as chemostratigraphic markers. *Geological Magazine*, **136**, 661–669.

Batchelor, R. A. & Weir, J. A. 1988. Metabentonite geochemistry: magmatic cycles and graptolite extinctions at Dob's Linn, southern Scotland. *Transactions of the Royal Society of Edinburgh: Earth Sciences*, **79**, 19–41.

Batchelor, R. A., Weir, J. A. & Spjeldnæs, N. 1995. Geochemistry of Telychian metabentonites from Vik, Ringerike District, Oslo region. *Norsk Geologisk Tidsskrift*, **75**, 219–228.

Bergström, S. M., Huff, W. D., Kolata, D. R. & Kaljo, D. 1992. Silurian K-bentonites in the Iapetus Region: a preliminary event-stratigraphic and tectonomagmatic assessment. *GFF*, **114**, 327–334.

Fisher, R. V. & Schmincke, H. U. 1984. *Pyroclastic Rocks*. Springer-Verlag, Berlin, 472 pp.

Gailite, L. K., Ulst, R. J. & Yakovleva, V. I. 1987. *Stratotipicheskie i tipovye razrezy Silura Latvii* [*Stratotype and Type Sections of the Silurian of Latvia*]. Zinatne, Riga, 183 pp. [in Russian].

Grahn, Y. 1995. Lower Silurian Chitinozoa and biostratigraphy of subsurface Gotland. *GFF*, **117**, 57–65.

Hetherington, C. J., Nakrem, H. A. & Potel, S. 2011. Note on the composition and mineralogy of Wenlock Silurian bentonites from the Ringerike District: implications for local and regional stratigraphic correlation and sedimentary environments. *Norwegian Journal of Geology*, **91**, 181–192.

Hints, O., Hints, L., Meidla, T. & Sohar, K. 2003. Biotic effects of the Ordovician Kinnekulle ash-fall recorded in northern Estonia. *Bulletin of the Geological Society of Denmark*, **50**, 115–123.

Hints, R., Kirsimäe, K., Somelar, P., Kallaste, T. & Kiipli, T. 2008. Multiphase Silurian bentonites in the Baltic Palaeobasin. *Sedimentary Geology*, **209**, 69–79.

Inanli, F. Ö., Huff, W. D. & Bergström, S. M. 2009. The Lower Silurian (Llandovery) Osmundsberg K-bentonite in Baltoscandia and the British Isles: chemical fingerprinting and regional correlation. *GFF*, **131**, 269–279.

Jeppsson, L. & Männik, P. 1993. High resolution correlations between Gotland and Estonia near the base of Wenlock. *Terra Nova*, **5**, 348–358.

Kiipli, E., Kiipli, T. & Kallaste, T. 2006. Identification of O-bentonite in deep shelf sections with implication on stratigraphy and lithofacies, East Baltic Silurian. *GFF*, **128**, 255–260.

Kiipli, E., Kiipli, T. & Kallaste, T. 2009. Reconstruction of currents in the Mid-Ordovician–Early Silurian central Baltic Basin using geochemical and mineralogical indicators. *Geology*, **37**, 271–274.

Kiipli, T. & Kallaste, T. 2002. Correlation of Telychian sections from shallow to deep sea facies in Estonia and Latvia based on the sanidine composition of bentonites. *Proceedings of the Estonian Academy of Sciences, Geology*, **51**, 143–156.

Kiipli, T. & Kallaste, T. 2006. Wenlock and uppermost Llandovery bentonites as stratigraphic markers in Estonia, Latvia and Sweden. *GFF*, **128**, 139–146.

Kiipli, T., Männik, P., Batchelor, R. A., Kiipli, E., Kallaste, T. & Perens, H. 2001. Correlation of Telychian (Silurian) altered volcanic ash beds in Estonia, Sweden and Norway. *Norwegian Journal of Geology (Norsk Geologisk Tidskrift)*, **81**, 179–193.

Kiipli, T., Kiipli, E., Kallaste, T., Hints, R., Somelar, P. & Kirsimäe, K. 2007. Altered volcanic ash as an indicator of marine environment, reflecting pH and sedimentation rate – example from the Ordovician Kinnekulle bed of Baltoscandia. *Clays and Clay Minerals*, **55**, 177–188.

Kiipli, T., Jeppsson, L., Kallaste, T. & Söderlund, U. 2008a. Correlation of Silurian bentonites from Gotland and the eastern Baltic using sanidine phenocryst composition, and biostratigraphical consequences. *Journal of the Geological Society*, **165**, 211–220.

Kiipli, T., Orlova, K., Kiipli, E. & Kallaste, T. 2008b. Use of immobile trace elements for the correlation of Telychian bentonites on Saaremaa Island, Estonia, and mapping of volcanic ash clouds. *Estonian Journal of Earth Sciences*, **57**, 39–52.

Kiipli, T., Radzevičius, S., Kallaste, T., Motuza, V., Jeppsson, L. & Wickström, L. 2008c. Wenlock bentonites in Lithuania and correlation with bentonites from sections in Estonia, Sweden and Norway. *GFF*, **130**, 203–210.

Kiipli, T., Soesoo, A., Kallaste, T. & Kiipli, E. 2008d. Geochemistry of Telychian (Silurian) K-bentonites in Estonia and Latvia. *Journal of Volcanology and Geothermal Research*, **171**, 45–58.

Kiipli, T., Kallaste, T. & Nestor, V. 2010a. Composition and correlation of volcanic ash beds of Silurian age from the eastern Baltic. *Geological Magazine*, **147**, 895–909.

Kiipli, T., Kallaste, T., Nestor, V. & Loydell, D. K. 2010b. Integrated Telychian (Silurian) K-bentonite chemo-stratigraphy and biostratigraphy in Estonia and Latvia. *Lethaia*, **43**, 32–44.

Kiipli, T., Einasto, R., Kallaste, T., Nestor, V., Perens, H. & Siir, S. 2011. Geochemistry and correlation of volcanic ash beds from the Rootsiküla Stage (Wenlock–Ludlow) in the eastern Baltic. *Estonian Journal of Earth Sciences*, **60**, 207–219.

Kiipli, T., Radzevičius, S., Kallaste, T., Kiipli, E., Siir, S., Soesoo, A. & Voolma, M. 2012. The Geniai Tuff in the southern East Baltic area – a new correlation tool near the Aeronian/Telychian stage boundary, Llandovery, Silurian. *Bulletin of Geosciences*, **87**, 695–704.

Loydell, D. K. & Nestor, V. 2005. Integrated graptolite and chitinozoan biostratigraphy of the upper Telychian (Llandovery, Silurian) of the Ventspils D-3 core, Latvia. *Geological Magazine*, **142**, 369–376.

Loydell, D. K., Männik, P. & Nestor, V. 2003. Integrated biostratigraphy of the lower Silurian of the Aizpute-41 core, Latvia. *Geological Magazine*, **140**, 205–229.

Nestor, V. 1994. Early Silurian chitinozoans in Estonia and North Latvia. *Academia*, 4, 1–163.

Ray, D. C. 2007. The correlation of Lower Wenlock Series (Silurian) bentonites from the Lower Hill Farm and Eastnor Park boreholes, Midland Platform, England. *Proceedings of the Geologists' Association*, **118**, 175–185.

Ray, D. C., Collings, A. V. J., Worton, G. J. & Jones, G. 2011. Upper Wenlock bentonites from Wren's Nest Hill, Dudley: comparisons with prominent bentonites along Wenlock Edge, Shropshire, England. *Geological Magazine*, **148**, 670–681.

Rubel, M., Hints, O., Männik, P., Meidla, T., Nestor, V., Sarv, L. & Sibul, I. 2007. Lower Silurian biostratigraphy of the Viirelaid core, western Estonia. *Estonian Journal of Earth Sciences*, **56**, 193–204.

Snäll, S. 1977. *Silurian and Ordovician Bentonites of Gotland (Sweden)*. Stockholm Contributions in Geology XXXI:1, 80 pp.

Worsley, D., Baarli, G., Howe, M. P. A., Hjaltason, F. & Alm, D. 2011. New data on the Bruflat Formation and the Llandovery/Wenlock transition in the Oslo Region, Norway. *Norwegian Journal of Geology*, **91**, 101–120.

Ülem-Llandovery – Alam-Wenlocki bentoniitide korrelatsioon Näri (Gotland, Rootsi) ja Ventspilsi (Läti) puursüdamike vahel: vulkaanilise tuha pilvede ning merehoovuste roll bentoniidi levikuala tekkel

Tarmo Kiipli, Toivo Kallaste ja Viiu Nestor

Biostratigraafia, sanidiini koostis ja immobiilsed elemendid bentoniitides võimaldasid kindlaks teha mitu kindlat ning mõned esialgsed korrelatsioonid Gotlandi ja Ida-Baltikumi vahel. Fenokristallide mikroanalüüs näitas, et bentoniitides esineb Mg- või Fe-rikast biotiiti. Sanidiini fenokristallid sisaldavad peale K- ja Na-komponendi ka mõni protsent Ca- ning Ba-komponenti. Uued korrelatsioonid võimaldasid laiendada bentoniitide leviku skeeme Gotlandini. Bentoniitide levikualad jagunevad Põhja-Lätis – Lõuna-Eestis kaheks, osutades hoovusele Balti Siluri šelfimeres, mis jaotas vulkaanilise tuha osakesi ringi.

DISSERTATIONS DEFENDED AT
TALLINN UNIVERSITY OF TECHNOLOGY ON
NATURAL AND EXACT SCIENCES

1. **Olav Kongas**. Nonlinear Dynamics in Modeling Cardiac Arrhytmias. 1998.

2. **Kalju Vanatalu**. Optimization of Processes of Microbial Biosynthesis of Isotopically Labeled Biomolecules and Their Complexes. 1999.

3. **Ahto Buldas**. An Algebraic Approach to the Structure of Graphs. 1999.

4. **Monika Drews**. A Metabolic Study of Insect Cells in Batch and Continuous Culture: Application of Chemostat and Turbidostat to the Production of Recombinant Proteins. 1999.

5. **Eola Valdre**. Endothelial-Specific Regulation of Vessel Formation: Role of Receptor Tyrosine Kinases. 2000.

6. **Kalju Lott**. Doping and Defect Thermodynamic Equilibrium in ZnS. 2000.

7. **Reet Koljak**. Novel Fatty Acid Dioxygenases from the Corals *Plexaura homomalla* and *Gersemia fruticosa.* 2001.

8. **Anne Paju**. Asymmetric oxidation of Prochiral and Racemic Ketones by Using Sharpless Catalyst. 2001.

9. **Marko Vendelin**. Cardiac Mechanoenergetics *in silico*. 2001.

10. **Pearu Peterson**. Multi-Soliton Interactions and the Inverse Problem of Wave Crest. 2001.

11. **Anne Menert**. Microcalorimetry of Anaerobic Digestion. 2001.

12. **Toomas Tiivel**. The Role of the Mitochondrial Outer Membrane in *in vivo* Regulation of Respiration in Normal Heart and Skeletal Muscle Cell. 2002.

13. **Olle Hints**. Ordovician Scolecodonts of Estonia and Neighbouring Areas: Taxonomy, Distribution, Palaeoecology, and Application. 2002.

14. **Jaak Nõlvak**. Chitinozoan Biostratigrapy in the Ordovician of Baltoscandia. 2002.

15. **Liivi Kluge**. On Algebraic Structure of Pre-Operad. 2002.

16. **Jaanus Lass**. Biosignal Interpretation: Study of Cardiac Arrhytmias and Electromagnetic Field Effects on Human Nervous System. 2002.

17. **Janek Peterson**. Synthesis, Structural Characterization and Modification of PAMAM Dendrimers. 2002.

18. **Merike Vaher**. Room Temperature Ionic Liquids as Background Electrolyte Additives in Capillary Electrophoresis. 2002.

19. **Valdek Mikli**. Electron Microscopy and Image Analysis Study of Powdered Hardmetal Materials and Optoelectronic Thin Films. 2003.

20. **Mart Viljus**. The Microstructure and Properties of Fine-Grained Cermets. 2003.

21. **Signe Kask**. Identification and Characterization of Dairy-Related *Lactobacillus.* 2003

22. **Tiiu-Mai Laht**. Influence of Microstructure of the Curd on Enzymatic and Microbiological Processes in Swiss-Type Cheese. 2003.

23. **Anne Kuusksalu**. 2–5A Synthetase in the Marine Sponge *Geodia cydonium*. 2003.

24. **Sergei Bereznev**. Solar Cells Based on Polycristalline Copper-Indium Chalcogenides and Conductive Polymers. 2003.

25. **Kadri Kriis**. Asymmetric Synthesis of C_2-Symmetric Bimorpholines and Their Application as Chiral Ligands in the Transfer Hydrogenation of Aromatic Ketones. 2004.

26. **Jekaterina Reut**. Polypyrrole Coatings on Conducting and Insulating Substracts. 2004.

27. **Sven Nõmm**. Realization and Identification of Discrete-Time Nonlinear Systems. 2004.

28. **Olga Kijatkina**. Deposition of Copper Indium Disulphide Films by Chemical Spray Pyrolysis. 2004.

29. **Gert Tamberg**. On Sampling Operators Defined by Rogosinski, Hann and Blackman Windows. 2004.

30. **Monika Übner**. Interaction of Humic Substances with Metal Cations. 2004.

31. **Kaarel Adamberg**. Growth Characteristics of Non-Starter Lactic Acid Bacteria from Cheese. 2004.

32. **Imre Vallikivi**. Lipase-Catalysed Reactions of Prostaglandins. 2004.

33. **Merike Peld**. Substituted Apatites as Sorbents for Heavy Metals. 2005.

34. **Vitali Syritski**. Study of Synthesis and Redox Switching of Polypyrrole and Poly(3,4-ethylenedioxythiophene) by Using *in-situ* Techniques. 2004.

35. **Lee Põllumaa**. Evaluation of Ecotoxicological Effects Related to Oil Shale Industry. 2004.

36. **Riina Aav**. Synthesis of 9,11-Secosterols Intermediates. 2005.

37. **Andres Braunbrück**. Wave Interaction in Weakly Inhomogeneous Materials. 2005.

38. **Robert Kitt**. Generalised Scale-Invariance in Financial Time Series. 2005.

39. **Juss Pavelson**. Mesoscale Physical Processes and the Related Impact on the Summer Nutrient Fields and Phytoplankton Blooms in the Western Gulf of Finland. 2005.

40. **Olari Ilison**. Solitons and Solitary Waves in Media with Higher Order Dispersive and Nonlinear Effects. 2005.

41. **Maksim Säkki**. Intermittency and Long-Range Structurization of Heart Rate. 2005.

42. **Enli Kiipli**. Modelling Seawater Chemistry of the East Baltic Basin in the Late Ordovician–Early Silurian. 2005.

43. **Igor Golovtsov**. Modification of Conductive Properties and Processability of Polyparaphenylene, Polypyrrole and polyaniline. 2005.

44. **Katrin Laos**. Interaction Between Furcellaran and the Globular Proteins (Bovine Serum Albumin β-Lactoglobulin). 2005.

45. **Arvo Mere**. Structural and Electrical Properties of Spray Deposited Copper Indium Disulphide Films for Solar Cells. 2006.

46. **Sille Ehala**. Development and Application of Various On- and Off-Line Analytical Methods for the Analysis of Bioactive Compounds. 2006.

47. **Maria Kulp**. Capillary Electrophoretic Monitoring of Biochemical Reaction Kinetics. 2006.

48. **Anu Aaspõllu.** Proteinases from *Vipera lebetina* Snake Venom Affecting Hemostasis. 2006.

49. **Lyudmila Chekulayeva**. Photosensitized Inactivation of Tumor Cells by Porphyrins and Chlorins. 2006.

50. **Merle Uudsemaa**. Quantum-Chemical Modeling of Solvated First Row Transition Metal Ions. 2006.

51. **Tagli Pitsi**. Nutrition Situation of Pre-School Children in Estonia from 1995 to 2004. 2006.

52. **Angela Ivask**. Luminescent Recombinant Sensor Bacteria for the Analysis of Bioavailable Heavy Metals. 2006.

53. **Tiina Lõugas**. Study on Physico-Chemical Properties and Some Bioactive Compounds of Sea Buckthorn (*Hippophae rhamnoides* L.). 2006.

54. **Kaja Kasemets**. Effect of Changing Environmental Conditions on the Fermentative Growth of *Saccharomyces cerevisae* S288C: Auxo-accelerostat Study. 2006.

55. **Ildar Nisamedtinov**. Application of ^{13}C and Fluorescence Labeling in Metabolic Studies of *Saccharomyces* spp. 2006.

56. **Alar Leibak**. On Additive Generalisation of Voronoï's Theory of Perfect Forms over Algebraic Number Fields. 2006.

57. **Andri Jagomägi**. Photoluminescence of Chalcopyrite Tellurides. 2006.

58. **Tõnu Martma**. Application of Carbon Isotopes to the Study of the Ordovician and Silurian of the Baltic. 2006.

59. **Marit Kauk**. Chemical Composition of $CuInSe_2$ Monograin Powders for Solar Cell Application. 2006.

60. **Julia Kois**. Electrochemical Deposition of $CuInSe_2$ Thin Films for Photovoltaic Applications. 2006.

61. **Ilona Oja Açik**. Sol-Gel Deposition of Titanium Dioxide Films. 2007.

62. **Tiia Anmann**. Integrated and Organized Cellular Bioenergetic Systems in Heart and Brain. 2007.

63. **Katrin Trummal**. Purification, Characterization and Specificity Studies of Metalloproteinases from *Vipera lebetina* Snake Venom. 2007.

64. **Gennadi Lessin**. Biochemical Definition of Coastal Zone Using Numerical Modeling and Measurement Data. 2007.

65. **Enno Pais**. Inverse problems to determine non-homogeneous degenerate memory kernels in heat flow. 2007.

66. **Maria Borissova**. Capillary Electrophoresis on Alkylimidazolium Salts. 2007.

67. **Karin Valmsen**. Prostaglandin Synthesis in the Coral *Plexaura homomalla*: Control of Prostaglandin Stereochemistry at Carbon 15 by Cyclooxygenases. 2007.

68. **Kristjan Piirimäe**. Long-Term Changes of Nutrient Fluxes in the Drainage Basin of the Gulf of Finland – Application of the PolFlow Model. 2007.

69. **Tatjana Dedova**. Chemical Spray Pyrolysis Deposition of Zinc Sulfide Thin Films and Zinc Oxide Nanostructured Layers. 2007.

70. **Katrin Tomson**. Production of Labelled Recombinant Proteins in Fed-Batch Systems in *Escherichia coli*. 2007.

71. **Cecilia Sarmiento**. Suppressors of RNA Silencing in Plants. 2008.

72. **Vilja Mardla**. Inhibition of Platelet Aggregation with Combination of Antiplatelet Agents. 2008.

73. **Maie Bachmann**. Effect of Modulated Microwave Radiation on Human Resting Electroencephalographic Signal. 2008.

74. **Dan Hüvonen**. Terahertz Spectroscopy of Low-Dimensional Spin Systems. 2008.

75. **Ly Villo**. Stereoselective Chemoenzymatic Synthesis of Deoxy Sugar Esters Involving *Candida antarctica* Lipase B. 2008.

76. **Johan Anton**. Technology of Integrated Photoelasticity for Residual Stress Measurement in Glass Articles of Axisymmetric Shape. 2008.

77. **Olga Volobujeva**. SEM Study of Selenization of Different Thin Metallic Films. 2008.

78. **Artur Jõgi**. Synthesis of 4'-Substituted 2,3'-dideoxynucleoside Analogues. 2008.

79. **Mario Kadastik**. Doubly Charged Higgs Boson Decays and Implications on Neutrino Physics. 2008.

80. **Fernando Pérez-Caballero**. Carbon Aerogels from 5-Methylresorcinol-Formaldehyde Gels. 2008.

81. **Sirje Vaask**. The Comparability, Reproducibility and Validity of Estonian Food Consumption Surveys. 2008.

82. **Anna Menaker**. Electrosynthesized Conducting Polymers, Polypyrrole and Poly(3,4-ethylenedioxythiophene), for Molecular Imprinting. 2009.

83. **Lauri Ilison**. Solitons and Solitary Waves in Hierarchical Korteweg-de Vries Type Systems. 2009.

84. **Kaia Ernits**. Study of In_2S_3 and ZnS Thin Films Deposited by Ultrasonic Spray Pyrolysis and Chemical Deposition. 2009.

85. **Veljo Sinivee**. Portable Spectrometer for Ionizing Radiation "Gammamapper". 2009.

86. **Jüri Virkepu**. On Lagrange Formalism for Lie Theory and Operadic Harmonic Oscillator in Low Dimensions. 2009.

87. **Marko Piirsoo**. Deciphering Molecular Basis of Schwann Cell Development. 2009.

88. **Kati Helmja**. Determination of Phenolic Compounds and Their Antioxidative Capability in Plant Extracts. 2010.

89. **Merike Sõmera**. Sobemoviruses: Genomic Organization, Potential for Recombination and Necessity of P1 in Systemic Infection. 2010.

90. **Kristjan Laes**. Preparation and Impedance Spectroscopy of Hybrid Structures Based on $CuIn_3Se_5$ Photoabsorber. 2010.

91. **Kristin Lippur**. Asymmetric Synthesis of 2,2'-Bimorpholine and its 5,5'-Substituted Derivatives. 2010.

92. **Merike Luman**. Dialysis Dose and Nutrition Assessment by an Optical Method. 2010.

93. **Mihhail Berezovski**. Numerical Simulation of Wave Propagation in Heterogeneous and Microstructured Materials. 2010.

94. **Tamara Aid-Pavlidis**. Structure and Regulation of BDNF Gene. 2010.

95. **Olga Bragina**. The Role of Sonic Hedgehog Pathway in Neuro- and Tumorigenesis. 2010.

96. **Merle Randrüüt**. Wave Propagation in Microstructured Solids: Solitary and Periodic Waves. 2010.

97. **Marju Laars**. Asymmetric Organocatalytic Michael and Aldol Reactions Mediated by Cyclic Amines. 2010.

98. **Maarja Grossberg**. Optical Properties of Multinary Semiconductor Compounds for Photovoltaic Applications. 2010.

99. **Alla Maloverjan**. Vertebrate Homologues of Drosophila Fused Kinase and Their Role in Sonic Hedgehog Signalling Pathway. 2010.

100. **Priit Pruunsild**. Neuronal Activity-Dependent Transcription Factors and Regulation of Human *BDNF* Gene. 2010.

101. **Tatjana Knjazeva**. New Approaches in Capillary Electrophoresis for Separation and Study of Proteins. 2011.

102. **Atanas Katerski**. Chemical Composition of Sprayed Copper Indium Disulfide Films for Nanostructured Solar Cells. 2011.

103. **Kristi Timmo.** Formation of Properties of $CuInSe_2$ and $Cu_2ZnSn(S,Se)_4$ Monograin Powders Synthesized in Molten KI. 2011.

104. **Kert Tamm**. Wave Propagation and Interaction in Mindlin-Type Microstructured Solids: Numerical Simulation. 2011.

105. **Adrian Popp**. Ordovician Proetid Trilobites in Baltoscandia and Germany. 2011.

106. **Ove Pärn**. Sea Ice Deformation Events in the Gulf of Finland and This Impact on Shipping. 2011.

107. **Germo Väli**. Numerical Experiments on Matter Transport in the Baltic Sea. 2011.

108. **Andrus Seiman**. Point-of-Care Analyser Based on Capillary Electrophoresis. 2011.

109. **Olga Katargina**. Tick-Borne Pathogens Circulating in Estonia (Tick-Borne Encephalitis Virus, *Anaplasma phagocytophilum*, *Babesia* Species): Their Prevalence and Genetic Characterization. 2011.

110. **Ingrid Sumeri**. The Study of Probiotic Bacteria in Human Gastrointestinal Tract Simulator. 2011.

111. **Kairit Zovo**. Functional Characterization of Cellular Copper Proteome. 2011.

112. **Natalja Makarytsheva**. Analysis of Organic Species in Sediments and Soil by High Performance Separation Methods. 2011.

113. **Monika Mortimer**. Evaluation of the Biological Effects of Engineered Nanoparticles on Unicellular Pro- and Eukaryotic Organisms. 2011.

114. **Kersti Tepp**. Molecular System Bioenergetics of Cardiac Cells: Quantitative Analysis of Structure-Function Relationship. 2011.

115. **Anna-Liisa Peikolainen**. Organic Aerogels Based on 5-Methylresorcinol. 2011.

116. **Leeli Amon**. Palaeoecological Reconstruction of Late-Glacial Vegetation Dynamics in Eastern Baltic Area: A View Based on Plant Macrofossil Analysis. 2011.

117. **Tanel Peets**. Dispersion Analysis of Wave Motion in Microstructured Solids. 2011.
118. **Liina Kaupmees**. Selenization of Molybdenum as Contact Material in Solar Cells. 2011.
119. **Allan Olspert**. Properties of VPg and Coat Protein of Sobemoviruses. 2011.
120. **Kadri Koppel**. Food Category Appraisal Using Sensory Methods. 2011.
121. **Jelena Gorbatšova**. Development of Methods for CE Analysis of Plant Phenolics and Vitamins. 2011.
122. **Karin Viipsi**. Impact of EDTA and Humic Substances on the Removal of Cd and Zn from Aqueous Solutions by Apatite. 2012.
123. **David Schryer**. Metabolic Flux Analysis of Compartmentalized Systems Using Dynamic Isotopologue Modeling. 2012.
124. **Ardo Illaste**. Analysis of Molecular Movements in Cardiac Myocytes. 2012.
125. **Indrek Reile**. 3-Alkylcyclopentane-1,2-Diones in Asymmetric Oxidation and Alkylation Reactions. 2012.
126. **Tatjana Tamberg**. Some Classes of Finite 2-Groups and Their Endomorphism Semigroups. 2012.
127. **Taavi Liblik**. Variability of Thermohaline Structure in the Gulf of Finland in Summer. 2012.
128. **Priidik Lagemaa**. Operational Forecasting in Estonian Marine Waters. 2012.
129. **Andrei Errapart**. Photoelastic Tomography in Linear and Non-linear Approximation. 2012.
130. **Külliki Krabbi**. Biochemical Diagnosis of Classical Galactosemia and Mucopolysaccharidoses in Estonia. 2012.
131. **Kristel Kaseleht**. Identification of Aroma Compounds in Food using SPME-GC/MS and GC-Olfactometry. 2012.
132. **Kristel Kodar**. Immunoglobulin G Glycosylation Profiling in Patients with Gastric Cancer. 2012.
133. **Kai Rosin**. Solar Radiation and Wind as Agents of the Formation of the Radiation Regime in Water Bodies. 2012.
134. **Ann Tiiman**. Interactions of Alzheimer's Amyloid-Beta Peptides with Zn(II) and Cu(II) Ions. 2012.
135. **Olga Gavrilova**. Application and Elaboration of Accounting Approaches for Sustainable Development. 2012.
136. **Olesja Bondarenko**. Development of Bacterial Biosensors and Human Stem Cell-Based *In Vitro* Assays for the Toxicological Profiling of Synthetic Nanoparticles. 2012.
137. **Katri Muska**. Study of Composition and Thermal Treatments of Quaternary Compounds for Monograin Layer Solar Cells. 2012.
138. **Ranno Nahku**. Validation of Critical Factors for the Quantitative Characterization of Bacterial Physiology in Accelerostat Cultures. 2012.
139. **Petri-Jaan Lahtvee**. Quantitative Omics-level Analysis of Growth Rate Dependent Energy Metabolism in *Lactococcus lactis*. 2012.
140. **Kerti Orumets**. Molecular Mechanisms Controlling Intracellular Glutathione Levels in Baker's Yeast *Saccharomyces cerevisiae* and its Random Mutagenized Gluthatione Over-Accumulating Isolate. 2012.
141. **Loreida Timberg**. Spice-Cured Sprats Ripening, Sensory Parameters Development, and Quality Indicators. 2012.
142. **Anna Mihhalevski**. Rye Sourdough Fermentation and Bread Stability. 2012.

143. **Liisa Arike**. Quantitative Proteomics of *Escherichia coli*: From Relative to Absolute Scale. 2012.
144. **Kairi Otto**. Deposition of In_2S_3 Thin Films by Chemical Spray Pyrolysis. 2012.
145. **Mari Sepp**. Functions of the Basic Helix-Loop-Helix Transcription Factor TCF4 in Health and Disease. 2012.
146. **Anna Suhhova**. Detection of the Effect of Weak Stressors on Human Resting Electroencephalographic Signal. 2012.
147. **Aram Kazarjan**. Development and Production of Extruded Food and Feed Products Containing Probiotic Microorganisms. 2012.
148. **Rivo Uiboupin**. Application of Remote Sensing Methods for the Investigation of Spatio-Temporal Variability of Sea Surface Temperature and Chlorophyll Fields in the Gulf of Finland. 2013.
149. **Tiina Kriščiunaite**. A Study of Milk Coagulability. 2013.
150. **Tuuli Levandi**. Comparative Study of Cereal Varieties by Analytical Separation Methods and Chemometrics. 2013.
151. **Natalja Kabanova**. Development of a Microcalorimetric Method for the Study of Fermentation Processes. 2013.
152. **Himani Khanduri**. Magnetic Properties of Functional Oxides. 2013.
153. **Julia Smirnova**. Investigation of Properties and Reaction Mechanisms of Redox-Active Proteins by ESI MS. 2013.
154. **Mervi Sepp**. Estimation of Diffusion Restrictions in Cardiomyocytes Using Kinetic Measurements. 2013.
155. **Kersti Jääger**. Differentiation and Heterogeneity of Mesenchymal Stem Cells. 2013.
156. **Victor Alari**. Multi-Scale Wind Wave Modeling in the Baltic Sea. 2013.
157. **Taavi Päll**. Studies of CD44 Hyaluronan Binding Domain as Novel Angiogenesis Inhibitor. 2013.
158. **Allan Niidu**. Synthesis of Cyclopentane and Tetrahydrofuran Derivatives. 2013.
159. **Julia Geller**. Detection and Genetic Characterization of *Borrelia* Species Circulating in Tick Population in Estonia. 2013.
160. **Irina Stulova**. The Effects of Milk Composition and Treatment on the Growth of Lactic Acid Bacteria. 2013.
161. **Jana Holmar**. Optical Method for Uric Acid Removal Assessment During Dialysis. 2013.
162. **Kerti Ausmees**. Synthesis of Heterobicyclo[3.2.0]heptane Derivatives *via* Multicomponent Cascade Reaction. 2013.
163. **Minna Varikmaa**. Structural and Functional Studies of Mitochondrial Respiration Regulation in Muscle Cells. 2013.
164. **Indrek Koppel**. Transcriptional Mechanisms of BDNF Gene Regulation. 2014.
165. **Kristjan Pilt**. Optical Pulse Wave Signal Analysis for Determination of Early Arterial Ageing in Diabetic Patients. 2014.
166. **Andres Anier**. Estimation of the Complexity of the Electroencephalogram for Brain Monitoring in Intensive Care. 2014.